

AN ABSTRACT OF THE THESIS OF

James Richard Jewett for the degree of DOCTOR OF PHILOSOPHY

in CHEMISTRY presented on August 12, 1976

Title: A QUANTITATIVE DESCRIPTION OF THE SILVER/AQUEOUS  
CYANIDE ELECTROLYTE INTERFACE AND THE EFFECT  
OF THE INTERFACE ON THE RATE OF ELECTRODEPOSITION OF SILVER

Abstract approved: Redacted for Privacy  
Dr. Harry Freund

A computer-interfaced potentiostat was constructed to obtain measurements of double layer capacitance with a relative precision of 1% by means of a potential step technique. Minima in double layer capacitance vs. potential curves were observed with this instrument for a polycrystalline silver surface in dilute solutions of sodium fluoride. These measurements indicate that the potential of zero charge for silver in the absence of specific adsorption is about -0.94 V vs. SCE.

The amounts of specific adsorption at the silver surface were calculated over a range of potentials for the double layer capacitance curves for several solutions containing fluoride and cyanide. Cyanide is strongly adsorbed at attainable electrode potentials, but fluoride is adsorbed only weakly. The potentials of the inner and outer Helmholtz

planes were also calculated as functions of potential for these systems.

An equation based on absolute rate theory was developed to express the rate of metal deposition as a function of electrode potential and double layer parameters. This equation, which assumes that the reaction rate is limited only in the charge-transfer step, predicts a linear relation between  $\ln(i_F/a_{Ms})$  (where  $i_F$  is the partial faradaic current in the cathodic direction and  $a_{Ms}$  is the activity of the electroactive metal complex in the solution), the cell potential, the amount of specific adsorption, and the potential of the inner Helmholtz layer.

This prediction was confirmed by comparing the measured double layer quantities to exchange currents for the deposition of silver from cyanide solutions. These data provided a means for calculating a value of  $-350 \text{ Å}^2/\text{ion}$  for the coefficient of interaction  $B_{\ddagger\text{CN}}$  between the activated complex of the charge-transfer step and specifically adsorbed cyanide, and a value of 0.26 for the transfer coefficient  $\alpha$ .  $\text{Ag}(\text{CN})_4^{3-}$  was identified as the electroactive species.

The deposition rate of silver from cyanide solutions was measured at large overpotentials from cell current transients produced by potentiostatic steps. Comparison of these measurements to the double layer quantities was not as clear-cut as for the exchange current measurements because the deposition reaction becomes limited by mass transfer before the double layer attains a stable composition.

A Quantitative Description of the Silver /Aqueous Cyanide  
Electrolyte Interface and the Effect of the Interface on  
the Rate of Electrodeposition of Silver

by

James Richard Jewett

A THESIS

submitted to

Oregon State University

in partial fulfillment of  
the requirements for the  
degree of

Doctor of Philosophy

June 1977

APPROVED:

*Redacted for Privacy*

\_\_\_\_\_  
Professor of Chemistry

in charge of major

*Redacted for Privacy*

\_\_\_\_\_  
Chairman of Department of Chemistry

*Redacted for Privacy*

\_\_\_\_\_  
Dean of Graduate School

Date thesis is presented Aug 12 - 1976

Typed by Clover Redfern for James Richard Jewett

## ACKNOWLEDGMENT

This work would not have been completed without the unfailing support of my wife Pat and my son Tim. I am extremely grateful to them for graciously enduring a period of personal hardship in which they often placed my ambitions ahead of their own needs. Many thanks are due to Pat's and my parents, who have given us encouragement during some very discouraging times.

I am very appreciative to Dr. Freund for his advice and constructive criticism. I also wish to thank other professors in the chemistry department, including Drs. Decius, Fredericks, Hawkes, Ingle, Piepmeier, and Scott, for their helpful discussions. The technical assistance provided by Gerald Allison and John Archibald through the chemistry department shops is gratefully acknowledged.

J. R. J.

## TABLE OF CONTENTS

<u>Chapter</u>	<u>Page</u>
I. INTRODUCTION	1
II. THEORY	3
2. 1. The Nature of the Metal/Electrolyte Interface	3
2. 2. The Rate Equation for a Metal Deposition Reaction	6
2. 3. Determination of double layer quantities	21
2. 4. Double layer capacitance measurements	29
2. 5. Silver deposition rate measurements	50
III. EXPERIMENTAL	60
3. 1. Double Layer Capacitance Measurements	60
3. 2. Deposition Rate Measurements	99
IV. RESULTS	108
4. 1. Estimation of the Potential of Zero Charge	108
4. 2. Determination of Double Layer Quantities	115
4. 3. Rate of Silver Deposition	132
V. DISCUSSION	138
5. 1. Composition of Silver-Containing Solutions	138
5. 2. Effect of the Double Layer on Exchange Currents	151
5. 3. Effect of the Double Layer on Currents at High Polarization	169
VI. SUMMARY	175
BIBLIOGRAPHY	176
APPENDICES	180
Appendix 1. Definitions of Symbols	180
Appendix 2. Derivation of Equations for Potentiostat	188
Appendix 3. Programs for Control and Interpretation of the Capacitance Measurements	197
Part 1. Program CAP	197
Part 2. Program PLT	205
Part 3. Program CCPVE	211
Part 4. Subroutine Package for CAP	218
Part 5. Subroutine Package for PLT and CCPVE	235
Appendix 4. Program CHARGE	255
Appendix 5. Program Z2	259
Appendix 6. Program COMPN	266

## LIST OF TABLES

<u>Table</u>	<u>Page</u>
3. 1. 1. Functions performed by the program modules.	81
4. 1. 1. Measurement parameters used for dilute sodium fluoride solutions.	109
4. 2. 1. Crystallographic radii and inner layer capacities for some ions.	124
5. 1. 1. Solution compositions calculated from different estimates of $K_3$ and $K_4$ .	140
5. 1. 2. Equilibrium constant values determined by various authors.	151
5. 2. 1. Composition of solutions in reference (48) calculated by program COMPN.	156
5. 2. 2. Values of $\alpha$ and $B_{\dagger\text{CN}}$ for various choices of $z$ .	167
5. 3. 1. Data summary for high polarization measurements.	170

## LIST OF FIGURES

<u>Figure</u>	<u>Page</u>
2. 1. 1. Diagram of the double layer.	4
2. 2. 1. A stylized plot of standard electrochemical free energy vs. reaction coordinate for a charge-transfer step.	14
2. 2. 2. The potentials of the phases in a typical measurement cell.	18
2. 4. 1. Electrical analogs for a three-electrode cell.	30
2. 4. 2. Scheme of the dependence of calculated quantities on the independently measured ones.	41
2. 5. 1. Model for the frequency-dependent behavior of the current-to-voltage converter.	56
3. 1. 1. Block diagram of the double layer capacitance measurement system, detailing the grounding and shielding.	61
3. 1. 2. Cell potential vs. time and current vs. time plots for one capacitance measurement cycle.	62
3. 1. 3. Potentiostat portion of the interface circuit.	64
3. 1. 4. Current-to-voltage converter portion of the interface circuit.	65
3. 1. 5. Transient buffer portion of the interface circuit.	66
3. 1. 6. Transient amplifier portion of the interface circuit.	67
3. 1. 7. DC amplifier portion of the interface circuit.	68
3. 1. 8. Pictorial diagram of the electrode dropper.	77
3. 1. 9. Schematic diagram of the electrode dropper interface circuit.	78
3. 1. 10. A conversation with CAP.	83



<u>Figure</u>	<u>Page</u>
3. 1. 11. A typical plot of cell current vs. time produced by CCPVE.	91
3. 1. 12. A typical plot of the least-squares residual vs. time produced by CCPVE.	93
3. 1. 13. A typical plot of specific double layer capacitance vs. cell potential produced by CCPVE.	94
3. 2. 1. Block diagram of the deposition transient measurement apparatus.	100
3. 2. 2. Schematic diagram of the blanking circuit.	102
3. 2. 3. Pictorial diagram of the deposition transient measurement cell.	105
4. 1. 1. The potential of the capacitance minimum in 0.00500 M sodium fluoride solution vs. the time waited at -0.6 V for various times of polarization at -1.7 V.	110
4. 1. 2. The potential of the capacitance minimum in 0.0100 M sodium fluoride solution vs. the time waited at -0.48 V for various times of polarization at -1.69 V.	111
4. 1. 3. The potential of the capacitance minimum in 0.0200 M sodium fluoride solutions vs. the time waited at -0.8 V for various times of polarization at -1.7 V.	112
4. 2. 1. Specific double layer capacitance vs. electrode potential for 0.942 M sodium fluoride solutions.	117
4. 2. 2. Specific double layer capacitance vs. electrode potential for a solution containing 0.0162 M sodium cyanide and 0.926 M sodium fluoride.	118
4. 2. 3. Specific double layer capacitance vs. electrode potential for a solution containing 0.1880 M sodium cyanide and 0.754 M sodium fluoride.	119
4. 2. 4. Specific double layer capacitance vs. electrode potential for 0.942 M sodium cyanide solution.	120

<u>Figure</u>	<u>Page</u>
4. 2. 5. Double layer charge vs. electrode potential for solutions of sodium fluoride and sodium cyanide.	127
4. 2. 6. Amount of specific adsorption vs. cell potential for solutions of sodium fluoride and sodium cyanide.	128
4. 2. 7. The potentials $\phi_1$ and $\phi_m$ plotted vs. electrode potential.	131
4. 3. 1. Cell current vs. square root of time for silver deposition transients in solution A.	133
4. 3. 2. Cell current vs. square root of time for silver deposition transients in solutions B and C.	134
4. 3. 3. Cell current vs. square root of time for silver deposition transients in solution D.	135
4. 3. 4. Cell current vs. square root of time for silver deposition transients in solution E.	136
4. 3. 5. Real component of the frequency domain cell impedance measured during a silver deposition transient plotted vs. $1/\sigma$ .	137
5. 1. 1. Cell potential vs. $\ln(c_{CN}^2/c_2)$ .	144
5. 1. 2. The simplex optimization of $K_3$ and $K_4$ .	147
5. 2. 1. $\ln(i_{ex})$ determined in reference (48) vs. $\ln(c_{CN})$ calculated by program COMPN.	157
5. 2. 2. Equilibrium potentials calculated for solutions in reference (48) vs. $\ln(c_{CN})$ calculated by program COMPN.	159
5. 2. 3. Potential of the inner Helmholtz layer vs. $\ln(c_{CN})$ at constant cell potential.	160
5. 2. 4. Specifically adsorbed charge vs. $\ln(c_{CN})$ at constant cell potential.	161

<u>Figure</u>	<u>Page</u>
5.2.5. Variation of the potential of the inner Helmholtz layer with $\ln(c_{\text{CN}})$ holding the electrode at the equilibrium potential.	162
5.2.6. Variation of the specifically adsorbed charge with $\ln(c_{\text{CN}})$ holding the electrode at the equilibrium potential.	163
 <u>Appendix</u>	
A2.1. Cell model to describe potentiostat operation.	189

# A QUANTITATIVE DESCRIPTION OF THE SILVER/AQUEOUS CYANIDE ELECTROLYTE INTERFACE AND THE EFFECT OF THE INTERFACE ON THE RATE OF ELECTRODEPOSITION OF SILVER

## I. INTRODUCTION

Although the practice of silver plating from cyanide baths dates from the mid-1800's (32, p. 7; 42, p. 180), and although silver has been used extensively as a reference electrode material in electrochemistry, surprisingly little work has been directed toward characterizing the reaction mechanism of silver deposition under conditions similar to those of commercial importance. Several papers (16, 17, 27, 33) from the 1950's discuss the mechanism of silver deposition, but those studies were carried out either in non-complexing media or at extremely low overvoltages, or both. The deposition rates at very low overvoltages were found to be largely determined by diffusion of deposited silver atoms into crystal sites on the silver surface. At reasonably high overvoltages ( $> 50$  mV) the rate was found to be entirely controlled by the charge-transfer step.

The deposition of silver from cyanide electrolytes has been investigated by Vielstich and Gerischer (48) under conditions of moderate polarization ( $< 50$  mV) and by Nechaev, et al. (1, 2, 36-39). The interpretations of Vielstich and Gerischer are questionable in the light of recently developed theory. This will be discussed later. The

studies by Nechaev, et al., were conducted in solutions and conditions similar to those used in commercial plating. These studies showed that the deposition rate varied in an unusual way which seemed to be related to the nature of the metal-solution interface. Although much information about the mechanism was obtained, their data were not sufficient to support a quantitative relationship of the rate of deposition to the composition of the interface. Through theory (44) developed since these papers, and by collection of accurate data concerning both the composition of the interface and the deposition rate of silver under the same (or similar) conditions, a quantitative relation may now be established.

## II. THEORY

### 2.1. The Nature of the Metal/Electrolyte Interface

The first step in understanding the ways in which reaction rates can be influenced by the interface is to understand the nature of the interface itself. Therefore, a short description of the interface is included here.

The electrode/solution interface is a region of electrical and chemical discontinuity. The ions in the solution are distributed at the interface in a way that reflects the abrupt change in the electric potential and in their chemical environment. An ion near the surface may retain its sheath of hydration, maintaining an identity essentially the same as an ion in the bulk of the solution, or it may shed part of its hydration in exchange for a direct chemical bond with the electrode surface. These ions are said to be specifically adsorbed. It happens that the energies of bonding to the metal and the energy of hydration are sufficiently close, especially for anions, that there is a significant partitioning between the two states (6, pp. 742-744). The potential applied across the interface has a large effect on this partitioning.

Consideration of these electric and chemical forces has produced the generally accepted model of the interface (called a double layer because of the separation of charge across it) which is displayed in Figure 2.1.1. Points at distances less than  $x_2$  from

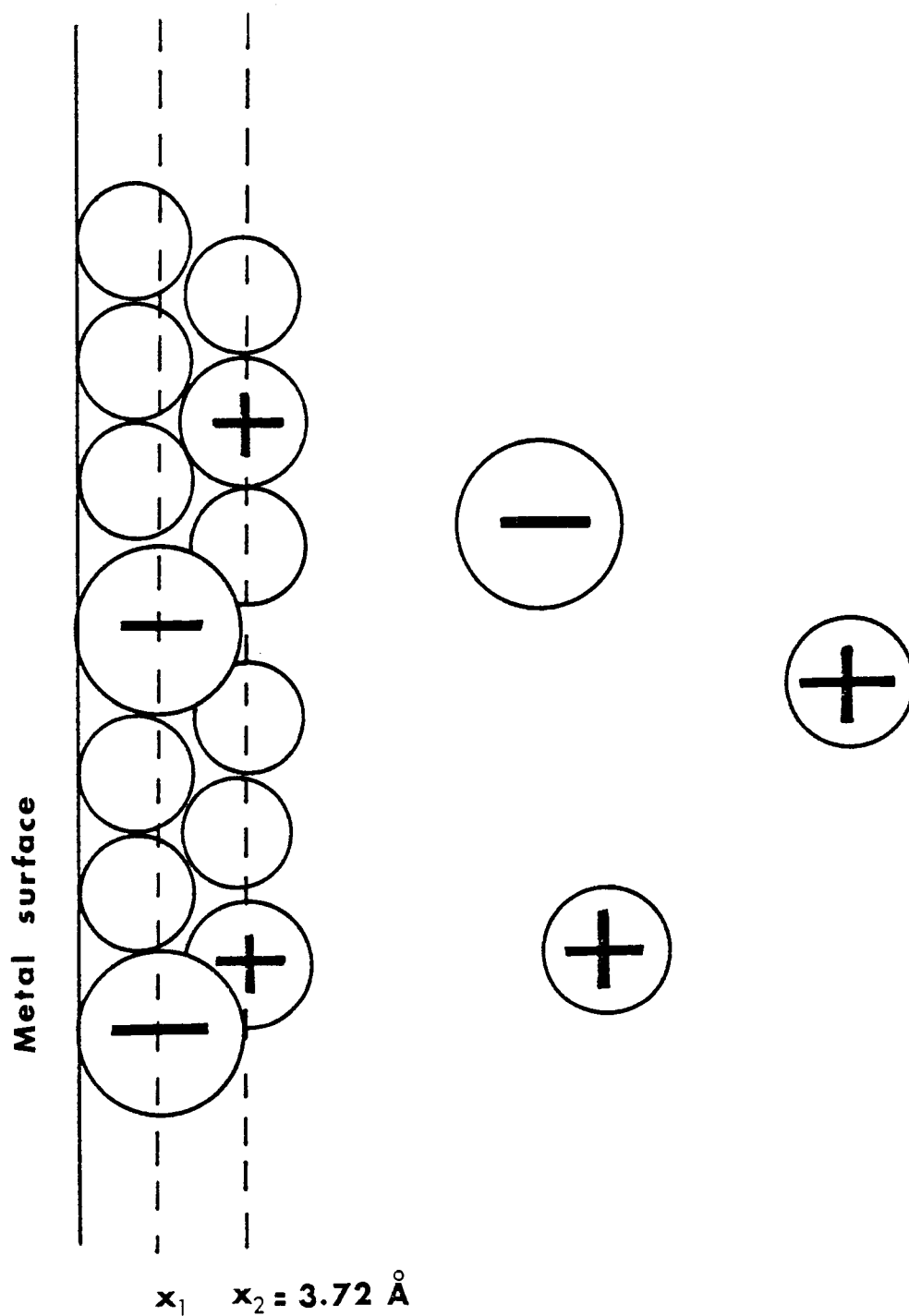


Figure 2. 1. 1. Diagram of the double layer. Blank circles are water molecules.

the electrode are said to be in the Helmholtz, or compact, layer.

Those at distances of  $x_2$  or greater are in the diffuse layer.

Giving rigorous definition to the planes at distances  $x_1$  and  $x_2$ , the inner and outer Helmholtz planes, respectively, has been much discussed. The properties of the double layer can be explained via any of several definitions. The definitions proposed by Devanathan (13) are shown in Figure 2.1.1, and will be used here because they simplify the quantitative determination of the components of the double layer. In Devanathan's model,  $x_1$  is the distance at which the specifically adsorbed ions reside. The model allows only one type of ion to be specifically adsorbed under any given set of conditions, and  $x_1$  is taken to be its crystallographic radius. The distance  $x_2$  is considered to be the distance of closest approach for the ions which retain their waters of hydration. It is taken to be equal to the distance at which the second layer of water resides, assuming hexagonal close-packing of water molecules near the electrode. In other words, non-specifically adsorbed ions, positive or negative, are considered to occupy voids which would otherwise be filled with water molecules. Adoption of this view results in assigning  $x_2 = 3.72 \text{ \AA}$  for all aqueous solutions.

The layering of the charge at the interface and the redistribution of the charge with changes in the interfacial potential give the double layer the characteristics of a capacitor. Unlike ordinary capacitors,

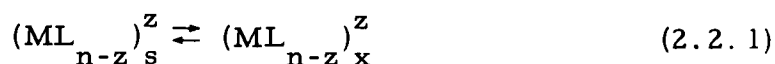


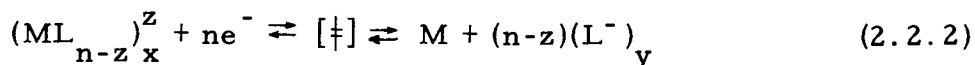
however, since the double layer charge is not fixed to just two sheets spaced at a constant distance, and since chemical as well as electrostatic forces are important, the capacitance of the double layer is strongly dependent on the applied potential. This capacitance is one of the more easily measured properties of the double layer, and studies of this property are responsible for much of the current knowledge of the structure of double layers.

## 2.2. The Rate Equation for a Metal Deposition Reaction

Application of the principles of absolute rate theory to electrochemical reaction rate studies has been practiced for many years (19) but the equations appropriate for a given circumstance are not often developed in a rigorous way. Many times the theory is developed with a simplified model reaction which is not readily adapted to more complicated reactions. Often certain potentially important aspects concerning the effects due to double layer structure have been omitted. As a result, in order to set the framework for this discussion, the rate law for deposition reactions will be developed here from the fundamental equations of absolute rate theory.

The reaction is considered to proceed according to the following steps:





Step 2.2.1 represents the equilibrium adsorption of a metal complex in the solution (denoted by subscript  $s$ ) onto a site at distance  $x$  from the electrode surface. The  $z$ -valent complex is composed of a metal atom in the  $n$  oxidation state and has  $n-z$  ligands, each bearing one negative charge. Step 2.2.2, the charge-transfer step, considered here to be rate-determining, shows the equilibrium of the adsorbed complex and the electrons on the metal with the activated complex, which decomposes irreversibly to the electrode metal and the ligands adsorbed at distance  $y$  from the electrode. These steps are preceded by preliminary homogeneous reactions in solution which might in some cases be rate-determining, but modification could be made for these later, if necessary. The reaction is assumed to be fast enough that the reverse rate can be ignored.

The premise of absolute rate theory that the step which forms the activated complex is in equilibrium (i. e., is microscopically reversible) permits equating the electrochemical potential of the activated complex with that of the reactants:

$$\bar{\mu}^\ddagger = \bar{\mu}_{\text{Mx}} + n\bar{\mu}_e. \quad (2.2.3)$$

In this equation the subscript  $Mx$  refers to the metal complex at distance  $x$  from the electrode. (A complete symbol table is included as Appendix 1.) Each of the electrochemical potentials may be separated into a standard electrochemical potential and a term expressing deviation from the standard chemical state:

$$\bar{\mu}^\ddagger = \bar{\mu}^{o\ddagger} + RT \ln a^\ddagger, \quad (2.2.4)$$

$$\bar{\mu}_{Mx} = \bar{\mu}_{Mx}^o + RT \ln a_{Mx}, \quad (2.2.5)$$

and

$$\bar{\mu}_e = \bar{\mu}_e^o. \quad (2.2.6)$$

The two activities indicated are activities of surface species, and are defined in terms of surface concentrations ( $\text{mol}/\text{cm}^2$ ). The last relation indicates that the chemical state of the electrons is invariant; this is a reflection of the fact that the electrode is of a constant composition. Effects due to electric potential remain in the standard electrochemical potentials ( $\bar{\mu}^o$ ).

Substitution of Equations 2.2.4 through 2.2.6 into 2.2.3, then solving for  $a^\ddagger$  gives

$$a^\ddagger = a_{Mx} \exp[-\bar{\Delta G}_c^{o\ddagger}/RT], \quad (2.2.7)$$

where

$$\bar{\Delta G}_c^{o\ddagger} \equiv \bar{\mu}^{o\ddagger} - \bar{\mu}_{Mx}^o - n\bar{\mu}_e^o \quad (2.2.8)$$

is the standard electrochemical free energy of activation for the charge-transfer step.

Since, according to absolute rate theory, the reaction proceeds at a rate proportional to the concentration of the activated complex,  $c^\ddagger$ , rather than activity, the activity coefficient is introduced (44):

$$\gamma^\ddagger \equiv a^\ddagger / c^\ddagger . \quad (2.2.9)$$

Just as the activity coefficient of a bulk species is affected by its chemical environment, e. g., ionic strength, so the activity coefficient of a surface species responds to the environment at the surface, e. g., the amount and types of other adsorbed species. Elimination of  $a^\ddagger$  between Equations 2.2.7 and 2.2.9 yields

$$c^\ddagger = \frac{a_{Mx}}{\gamma^\ddagger} \exp\left[ \frac{-\overline{\Delta G}_c^{o\ddagger}}{RT} \right] . \quad (2.2.10)$$

It is convenient to express the surface activity  $a_{Mx}$  in terms of the bulk solution activity  $a_{Ms}$ . Because the adsorption step is considered to be in equilibrium,

$$\overline{\mu}_{Mx} = \overline{\mu}_{Ms} . \quad (2.2.11)$$

Each of these quantities may be separated into a chemical and electrical contribution (24):

$$\mu_{Mx}^{\circ} + RT \ln a_{Mx} + zF\phi_x = \mu_{Ms}^{\circ} + RT \ln a_{Ms} . \quad (2.2.12)$$

In this equation the  $\mu^{\circ}$  quantities (without a bar) are standard chemical potentials. The reference for electric potential for the system is taken to be the potential of the bulk of the solution. Thus the electric contribution to the electrochemical potential of a species in the solution is zero, and  $\phi_x$ , the potential of the layer at which the reacting species lie, is taken with respect to the solution. Defining the standard chemical free energy of adsorption for the reactant as

$$\Delta G_{Mx}^{\circ} \equiv \mu_{Mx}^{\circ} - \mu_{Ms}^{\circ} , \quad (2.2.13)$$

Equation 2.2.12 may be solved to yield

$$a_{Mx} = a_{Ms} \exp\left[\frac{-\Delta G_{Mx}^{\circ} - zF\phi_x}{RT}\right] . \quad (2.2.14)$$

Thus, Equation 2.2.10 becomes

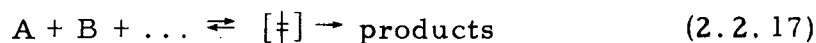
$$c^{\ddagger} = \frac{a_{Ms}}{\gamma^{\ddagger}} \exp\left[\frac{-\Delta G_c^{\circ\ddagger} - \Delta G_{Mx}^{\circ}}{RT}\right] \exp[-zf\phi_x] , \quad (2.2.15)$$

where

$$f = F/RT . \quad (2.2.16)$$

There are two steps in converting the terms in Equation 2.2.15 to experimentally measurable quantities. First, the concentration of activated complex  $c^\ddagger$  (upon which the reaction rate depends) must be related to a faradaic current density; secondly,  $\overline{\Delta G}_c^{o\ddagger}$  must be related to the cell potential and measurable properties of the double layer.

Absolute rate theory (19, pp. 187-190) asserts that the velocity of the chemical reaction



is

$$v = k_r c_A c_B \dots, \quad (2.2.18)$$

where

$$k_r = \tau \frac{kT}{h} K^\ddagger \quad (2.2.19)$$

and

$$K^\ddagger = \frac{c^\ddagger}{c_A c_B \dots} \quad (2.2.20)$$

The transmission coefficient  $\tau$  is the probability that the activated complex decomposes into the products of interest rather than into other species;  $\tau$  is usually equal to unity. Combination of these equation leads to

$$v = \tau \frac{kT}{h} c^\ddagger. \quad (2.2.21)$$

Considering the units in this equation in the case that the activated complex is a surface species,  $c^\ddagger$  must be in  $\text{mol cm}^{-2}$ . The units for  $v$  then work out to be  $\text{mol cm}^{-2} \text{sec}^{-1}$ , which are units of a material flux. Since each mole of reaction proceeds via  $nF$  coulombs of electricity, this material flux can be expressed in terms of an electric current density:

$$i_F = nFv \quad (\text{amp cm}^{-2}). \quad (2.2.22)$$

Combining this with Equation 2.2.21 gives the desired relation of faradaic current density to  $c^\ddagger$ ,

$$i_F = nF\tau \frac{kT}{h} c^\ddagger, \quad (2.2.23)$$

which may be substituted into 2.2.15 to give

$$i_F = nF\tau \frac{kT}{h} \frac{a_{Ms}}{\gamma^\ddagger} \exp\left[\frac{-\overline{\Delta G}_c^{o\ddagger} - \Delta G_{Mx}^o}{RT}\right] \exp[-zf\phi_x]. \quad (2.2.24)$$

Thus, the current due to metal deposition is related to the activity of the electroactive species in solution, which may be experimentally determined. The other variables in the equation,  $\gamma^\ddagger$  and  $\overline{\Delta G}_c^{o\ddagger}$ , must now be related to measurable quantities.

The "electrical part" of  $\overline{\Delta G}_c^{o\ddagger}$  may be isolated. A common method for doing this employs a stylized plot of standard

electrochemical free energy vs. reaction coordinate for the charge-transfer step 2.2.2 as is shown in Figure 2.2.1. In this figure, the lumped standard electrochemical free energy of the reactants, i.e.,

$$\bar{\mu}_{Mx}^0 + n\bar{\mu}_e^0, \quad (2.2.25)$$

is represented by the level at the minimum of curve R. Curve R' represents the energy of the reactants under a different set of electrical conditions (which would result from a change in potential across the interface). Curve P represents a similar quantity for the products of the reaction,

$$\bar{\mu}_m^0 + (n-z)\bar{\mu}_{Ly}^0. \quad (2.2.26)$$

The standard electrochemical free energy of reaction is the difference between the energies of the products and reactants, which is

$$\Delta\bar{G}_c^0 = \bar{\mu}_m^0 + (n-z)\bar{\mu}_{Ly}^0 - \bar{\mu}_{Mx}^0 - n\bar{\mu}_e^0 \quad (2.2.27)$$

for curves P and R, or  $(\Delta\bar{G}_c^0)'$  for curves P' and R'.

Thus a simple change in the free energy of the rate-determining step from  $\Delta\bar{G}_c^0$  to  $(\Delta\bar{G}_c^0)'$  without a change in the essential nature of reactant or products is represented on the reaction plot by a relative shift in the energy levels of products and reactants without a change in



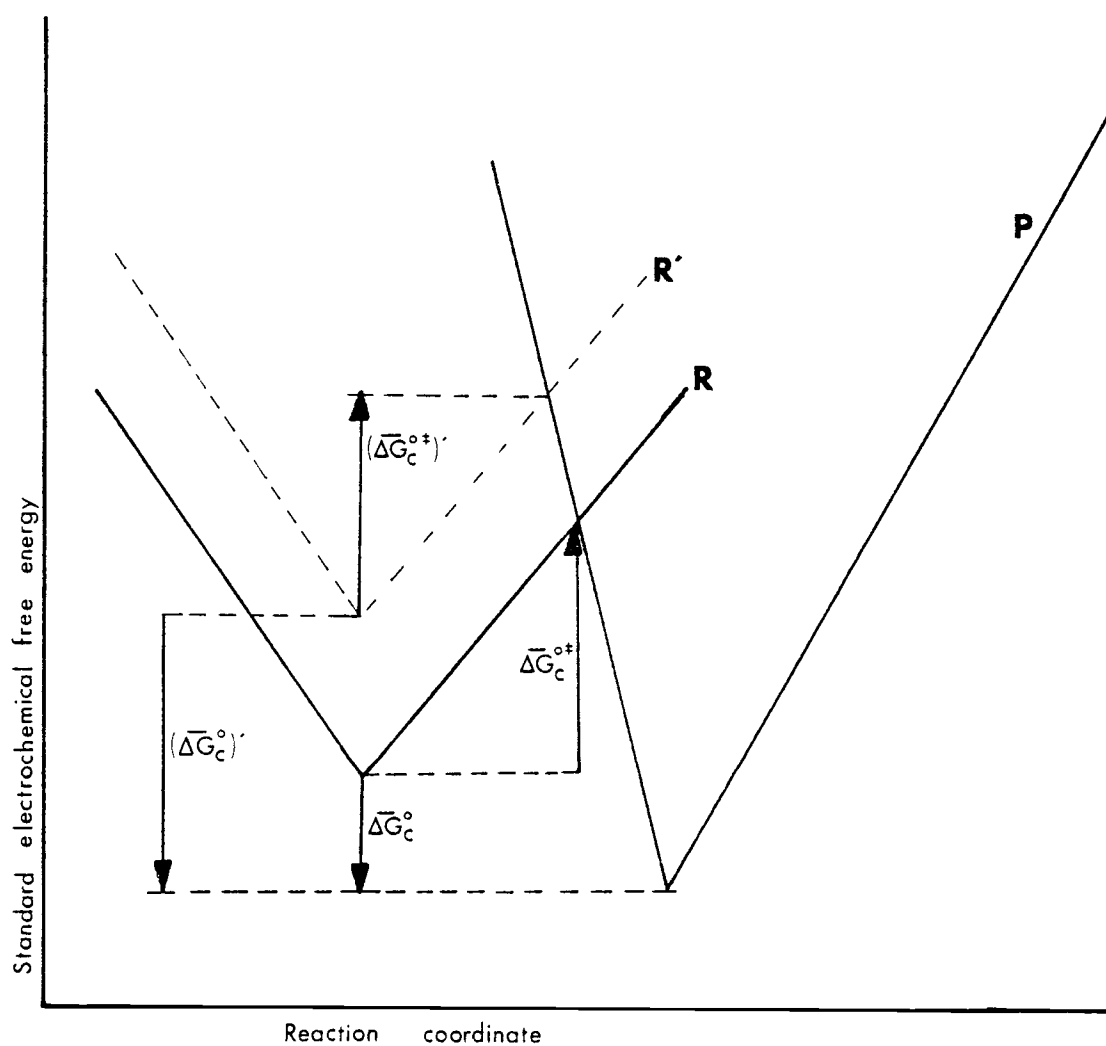


Figure 2.2.1. A stylized plot of standard electrochemical free energy vs. reaction coordinate for a charge-transfer step. Curve P is for the products; curves R and R' are for the reactants under two different electric conditions.

the shape of the curve. (This is shown in the figure by a change in levels for the reactants, but the change could be in either the reactants or products, or both.) Geometrical considerations (6, pp. 917-926; 9, pp. 98-99; 43, p. 30) show that only a fraction of this free energy change appears in the change in activation energy. Thus

$$(\overline{\Delta G}_c^{o\dagger})' - \overline{\Delta G}_c^{o\dagger} = \alpha [(\overline{\Delta G}_c^o)' - \overline{\Delta G}_c^o] , \quad (2.2.28)$$

where

$$0 < \alpha < 1. \quad (2.2.29)$$

The fraction  $\alpha$  is called the transfer coefficient.

If the primed quantities are assumed to apply at some standard state of polarization, then a constant may be defined,

$$\Delta G_c^{o\dagger} \equiv (\overline{\Delta G}_c^{o\dagger})' - \alpha (\overline{\Delta G}_c^o)' , \quad (2.2.30)$$

which permits the rewriting of Equation 2.2.28 as

$$\overline{\Delta G}_c^{o\dagger} = \Delta G_c^{o\dagger} + \alpha \overline{\Delta G}_c^o . \quad (2.2.31)$$

The symbol for the constant is written without a bar because it is not variable with electrical conditions. For this reason it may be called the standard chemical free energy of activation, although the idea that it represents the standard free energy of activation in the absence of

electrical effects is fallacious, since the standard state of polarization may be chosen at will for its definition.

To separate the chemical and electric effects in  $\overline{\Delta G}_c^0$ , again taking the bulk of the solution as the reference point for electric potentials, the pertinent electrochemical potentials are given as

$$\bar{\mu}_m^0 = \mu_m^0, \quad (2.2.32)$$

$$\bar{\mu}_{Ly}^0 = \mu_{Ly}^0 - F\phi_y, \quad (2.2.33)$$

$$\bar{\mu}_{Mx}^0 = \mu_{Mx}^0 + zF\phi_x, \quad (2.2.34)$$

and

$$\bar{\mu}_e^0 = \mu_e^0 - F\phi_m. \quad (2.2.35)$$

(Note that 2.2.34 is consistent with 2.2.12.) Then

$$\overline{\Delta G}_c^0 = \Delta G_c^0 - (n-z)F\phi_y - zF\phi_x + nF\phi_m, \quad (2.2.36)$$

where

$$\Delta G_c^0 \equiv \mu_m^0 + (n-z)\mu_{Ly}^0 - \mu_{Mx}^0 - n\mu_e^0. \quad (2.2.37)$$

Equation 2.2.36 may be substituted into 2.2.31 and 2.2.31 into 2.2.24 to yield

$$i_F = nF\tau \frac{kT}{h} \frac{a_{Ms}}{\gamma^\dagger} \exp\left[\frac{-\Delta G_c^{0\dagger} - \Delta G_{Mx}^0 - a\Delta G_c^0}{RT}\right] \\ \times \exp[-anf\phi_m] \exp[a(n-z)f\phi_y - (1-a)zf\phi_x], \quad (2.2.38)$$

thus replacing  $\overline{\Delta G}_c^{o\dagger}$  with constants and potentials at particular sites in the double layer.

In order to relate these potential differences to measurable potentials, the potentials of the various phases in a typical measurement cell should be considered. These are shown in Figure 2.2.2. The sum of the interfacial potentials in the figure is the externally measurable cell potential:

$$\begin{aligned}
 E_{\text{cell}} &= \phi_{\text{lead 1}} - \phi_{\text{lead 2}} \\
 &= (\phi_{\text{lead 1}} - \phi_m) + \phi_m + I_{\text{cell}} R_u + (\phi_s - \phi_{\text{KCl}}) \\
 &\quad + (\phi_{\text{KCl}} - \phi_{\text{Hg}}) + (\phi_{\text{Hg}} - \phi_{\text{lead 2}})
 \end{aligned}
 \tag{2.2.39}$$

In this equation,  $\phi_m$  is referenced to the potential of the solution just outside the double layer. The term  $I_{\text{cell}} R_u$  is the ohmic potential drop through the solution resistance  $R_u$ .  $I_{\text{cell}}$  is taken to be positive for anodic current.

The metal/metal junctions are in pseudoequilibrium because of the high reversibility of the exchange of electrons between them. Thus  $\phi_{\text{lead 1}} - \phi_m$  and  $\phi_{\text{Hg}} - \phi_{\text{lead 2}}$  are constants. The junction potential  $\phi_s - \phi_{\text{KCl}}$  between the test electrolyte and the filling solution of the reference electrode is kept practically constant by proper choice of test solutions. The interfacial potential  $\phi_{\text{KCl}} - \phi_{\text{Hg}}$  in the reference electrode is constant because of the reversible

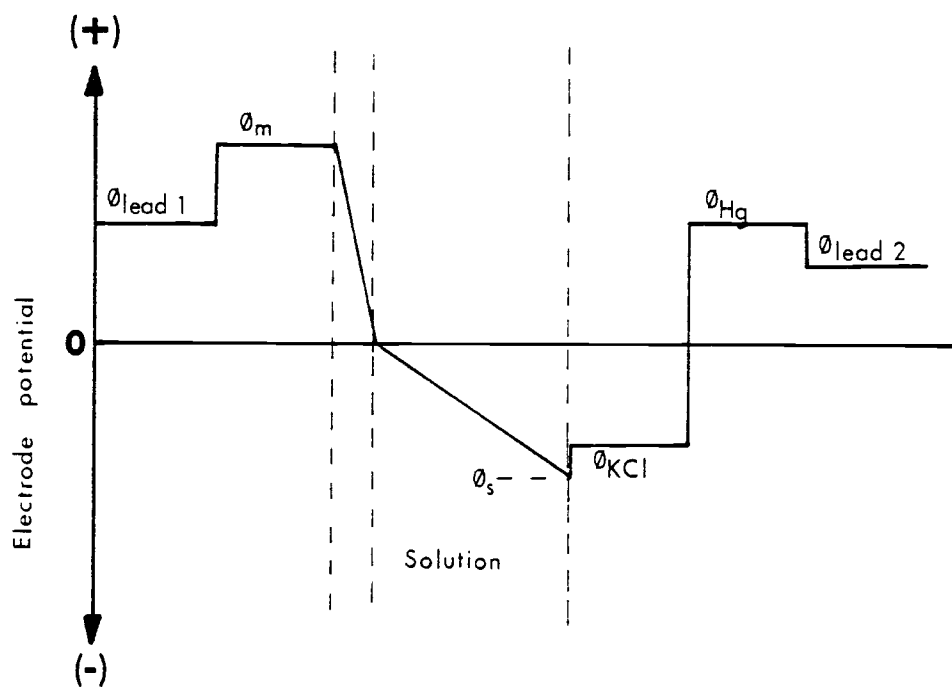


Figure 2.2.2. The potentials of the phases in a typical measurement cell (using an SCE). The phases shown are, from left to right, the test electrode lead, the test electrode metal, the interface being studied, the test electrolyte, the reference electrode electrolyte, the reference electrode metal, and the reference electrode lead. The potential of the solution immediately next to the studied interface is taken as the zero reference potential. Note the ohmic drop through the solution resistance. (The directions and magnitudes of the interfacial potential differences shown in the figure are arbitrary; they are not meant to approximate the actual potentials which exist.)

nature of the reference electrode reaction and the fact that the measurement system allows virtually no current to pass at this interface. We therefore define a constant

$$\phi_{\text{ref}} \equiv (\phi_{\text{lead 1}} - \phi_{\text{m}}) + (\phi_{\text{s}} - \phi_{\text{KCl}}) + (\phi_{\text{KCl}} - \phi_{\text{Hg}}) + (\phi_{\text{Hg}} - \phi_{\text{lead 2}}), \quad (2.2.40)$$

and rewrite 2.2.39 as

$$E_{\text{cell}} = \phi_{\text{m}} + I_{\text{cell}} R_{\text{u}} + \phi_{\text{ref}}. \quad (2.2.41)$$

It is convenient to define a symbol for the cell potential corrected for ohmic drop:

$$E \equiv E_{\text{cell}} - I_{\text{cell}} R_{\text{u}} = \phi_{\text{m}} + \phi_{\text{ref}}. \quad (2.2.42)$$

The quantity  $E$  will be referred to as the "electrode potential."

Substitution of  $\phi_{\text{m}}$  from 2.2.42 into 2.2.38 gives

$$i_{\text{F}} = nF\tau \frac{kT}{h} \frac{a_{\text{Ms}}}{\gamma_{\text{f}}} \exp\left[\frac{-\Delta G_{\text{c}}^{\text{of}} - \Delta G_{\text{Mx}}^{\text{o}} - a\Delta G_{\text{c}}^{\text{o}} + anF\phi_{\text{ref}}}{RT}\right] \\ \times \exp[-anfE] \exp[a(n-z)f\phi_{\text{y}} - (1-a)zf\phi_{\text{x}}]. \quad (2.2.43)$$

This equation shows that the rate of reaction may be affected both chemically and electrically by quantities related to the double layer.

The chemical composition of the double layer may have an effect on

$\gamma^\ddagger$ , and the double layer potentials  $\phi_x$  and  $\phi_y$  modify the influence of the cell potential.

A quantitative relation between  $\gamma^\ddagger$  and the composition of the double layer was proposed by Parsons (44), who assumed that specifically adsorbed ions on an electrode behave as a virial gas bound to only two dimensions. The relation he established is

$$\gamma^\ddagger = \exp \sum_j 2B_{\ddagger j} \Gamma_j, \quad (2.2.44)$$

where  $\Gamma_j$  is the amount of specific adsorption of ionic species  $j$  in (e.g.) ions/cm<sup>2</sup>. The quantities  $B_{\ddagger j}$  are second virial coefficients which are measures of the interactions between species  $j$  and the activated complex. Parsons states that the interparticle interactions should be largely coulombic in nature. Therefore the values of the  $B_{\ddagger j}$  should be positive when the activated complex and species  $j$  have the same charge, and negative when they do not. Writing 2.2.43 in a logarithmic form and making substitution from 2.2.44 yields:

$$\ln\left(\frac{i_F}{a_{Ms}}\right) = \left[ \ln\left(\frac{nF\tau kT}{h}\right) + \left( \frac{-\Delta G_c^{o\ddagger} - \Delta G_{Mx}^o - \alpha \Delta G_c^o + \alpha nF\phi_{ref}}{RT} \right) \right] \\ - \sum_j 2B_{\ddagger j} \Gamma_j - \alpha nFE + \alpha(n-z)f\phi_y - (1-\alpha)zf\phi_x, \quad (2.2.45)$$

Thus the faradaic current density  $i_F$  is related quantitatively to the experimentally measurable quantities  $a_{Ms}$ ,  $E$ ,  $\Gamma_j$ ,  $\phi_x$ , and  $\phi_y$ .

An important objective of this work is to investigate the applicability of this equation to the silver deposition reaction in aqueous cyanide-containing solutions. In the next section, the evaluation of the quantities in this equation which are related to the double layer, namely  $\Gamma_j$ ,  $\phi_x$ , and  $\phi_y$  is discussed.

### 2.3. Determination of Double Layer Quantities

By application of fundamental electrostatic theory to the model of the double layer previously discussed, Devanathan (13) developed a set of equations for determining the amount of specific adsorption at an interface. Although there are several sign errors in the development (Equations 2, 4, and 6 of ref. (13)) they do not affect the result for the double layer capacitance  $C_{dl}$ :

$$\frac{1}{C_{dl}} = \frac{1}{K_{m-1}} + \left( \frac{1}{K_{1-2}} + \frac{1}{C_{2-s}} \right) \left( 1 - \frac{dq_1}{dq} \right), \quad (2.3.1)$$

where  $K_{m-1}$  is the electrostatic capacity for the region from the electrode to  $x_1$ ,  $K_{1-2}$  is the electrostatic capacity for the region from  $x_1$  to  $x_2$ ,  $C_{2-s}$  is the capacitance of the diffuse double layer,  $q$  is the total excess charge on the solution-side of the double layer, and  $q_1$  is the charge due to specifically adsorbed



ions. The specifically adsorbed charge is related to the amount of specific adsorption by

$$\Gamma_j = q_1 / z_j e_o , \quad (2.3.2)$$

where  $z_j$  is the charge on the specifically adsorbed ion  $j$ , and the assumption that there is only one specifically adsorbed ion is invoked.

The inner layer capacities are given by the electrostatic formulae:

$$K_{m-1} = D_{m-2} \epsilon_o' / x_1 \quad (2.3.3)$$

and

$$K_{1-2} = D_{m-2} \epsilon_o' / (x_2 - x_1) , \quad (2.3.4)$$

where  $\epsilon_o'$  is the rationalized permittivity of free space, equal to  $8.85 \times 10^{-14}$  farad  $\text{cm}^{-1}$ , and  $D_{m-2}$  is the dielectric constant of the inner layer (assumed to be constant throughout the layer). On the basis of the double layer model just described,  $D_{m-2}$  is estimated to be 7.2.

Evaluation of the diffuse double layer capacitance is well-known; it is based upon the Boltzmann distribution of the ions in that layer. For an aqueous solution of a 1-1 electrolyte, the equation for the diffuse double layer capacitance is

$$C_{2-s} = (e_o A / kT) [1 + (q - q_1)^2 / 4A]^{1/2}, \quad (2.3.5)$$

where  $e_o$  is the charge of a proton,

$$A \equiv 2D_{2-s} \epsilon_o' RTc, \quad (2.3.6)$$

and  $c$  is the total electrolyte concentration.  $D_{2-s}$  is equal to the dielectric constant of bulk water because the potential gradients in the diffuse double layer are not great enough to cause much electrostriction. Substitution of the appropriate constants into Equation 2.3.5 gives

$$C_{2-s} = (19.46 \frac{\mu F}{\mu C}) [(137.8 \frac{(\mu C)^2 \ell}{cm^4 mol}) c + (q - q_1)^2]^{1/2} \quad (2.3.7)$$

Since all the other quantities in Equation 2.3.1 are known or are measurable, it can be solved for  $dq_1/dq$ :

$$\frac{dq_1}{dq} = 1 - \frac{(1/C_{dl}) - (1/K_{m-1})}{(1/K_{1-2}) + (1/C_{2-s})}. \quad (2.3.8)$$

Thus, in order to determine  $q_1$ , an integration with respect to  $q$  must be performed. This requires that  $q$  be known and that a constant of integration be established.

To determine  $q$ , it is first necessary to establish the potential of zero charge ( $E_{zc}$ ). This is easily done for dilute solutions of ions which are specifically adsorbed only weakly at this potential, since in these solutions, the double layer capacitance vs. electrode potential curve goes through a minimum at  $E_{zc}$ . This is due to the fact that the diffuse double layer capacitance goes through a distinct minimum at  $E_{zc}$ , becoming small enough that it dominates and determines the overall measured capacitance. (Refer to Equations 2.3.1 and 2.3.7, setting  $q_1 = 0$ .) A significant amount of specific adsorption will cause  $C_{2-s}$  to reach its minimum at some potential other than  $E_{zc}$ . If specific ionic adsorption occurs, the amount of it may logically be expected to depend on the concentration of the ion in the solution. Therefore, if the capacitance minima are the same for a range of electrolyte concentrations less than, e.g., 0.02 M, it is taken as proof that the minimum coincides with  $E_{zc}$ , and that specific adsorption occurs to only a small extent for that electrolyte.

The double layer charge at any electrode potential  $E_x$  for any concentration of that electrolyte may now be found by integrating the experimentally measured values of  $C_{dl}$  for that solution from  $E_{zc}$  to  $E_x$ :

$$q(E_x) = - \int_{E_{zc}}^{E_x} C_{dl} dE . \quad (2.3.9)$$

This equation comes directly from the definition of  $C_{dl}$ .

Suppose that it is now desired to determine the double layer charge at given potentials in a solution containing anions which may be specifically adsorbed at the electrode. If the charge at a single potential in this solution may be established, then the charge at all other potentials can be found by integration of the double layer capacitance in a way similar to that indicated in Equation 2.3.9. In order to find this first point, the double layer of the solution with specific adsorption will be compared to the double layer of another solution. This second solution will be the same as the first with respect to concentration and cation, but the anion in the second must not be specifically adsorbed to any significant extent.

As Grahame and Soderberg (22) have pointed out, if the electrode potential is made sufficiently cathodic, all specifically adsorbed ions can be driven from the inner layer. If any ions are present in the inner layer at this very negative potential, they are cations, which are identical in the two solutions. The identity of anions present in the diffuse double layer is immaterial, since they act simply as point charges. Therefore, at this very negative potential,  $E_{neg}$ , the double layers of the two electrolytes should behave identically. That is, they have the same capacitance, double layer charge, and amount of specific adsorption. Since the double layer charge in the solution without specific adsorption may be determined at this potential (by

Equation 2.3.9), it is also known for the solution with specific adsorption.

The double layer charge at any potential  $E_x$  in the solution with specific adsorption can now be given by an equation of the same form as 2.3.9 but with different limits of integration:

$$q(E_x) = - \int_{E_{neg}}^{E_x} C_{dl} dE + q(E_{neg}) . \quad (2.3.10)$$

(Of course, in this equation,  $C_{dl}$  is measured in the solution with specific adsorption.)

The purpose for evaluating the double layer charge  $q$  was to make calculation of the amount of specific adsorption possible. Basic rules of integral calculus give

$$q_1(E_x) = q_1(E_{start}) + \int_{q(E_{start})}^{q(E_x)} \left( \frac{dq_1}{dq} \right) dq. \quad (2.3.11)$$

The specifically adsorbed charge  $q_1$  must thus be determined if  $q_1(E_{start})$  and  $dq_1/dq$  are known. Evaluation of these will be discussed next.

The value of the derivative  $dq_1/dq$  may be taken from Equation 2.3.8. However, evaluation of  $C_{2-s}$  in that equation requires that  $q_1$  be known, (see Equation 2.3.7) thus forcing one to

estimate  $C_{2-s}$ . This estimate does not have to be very precise, since  $C_{2-s}$  has such a small effect; it is most easily performed by assuming  $q_1 = 0$ . After  $q_1$  is calculated for all the necessary potentials in this way, the process may be reiterated, calculating  $C_{2-s}$  from the values of  $q_1$  determined the first time. The iterations may be repeated until no further significant change occurs in the calculated values.

Evaluation of a constant of integration for 2.3.11 requires re-examination of Devanathan's concept of the double layer. His view permits only one species of ion to be specifically adsorbed at one time. Therefore, at the potential at which the specifically adsorbed charge goes through zero, no ions may be adsorbed. It is then reasonable to suppose that the amount of specific adsorption at this point does not change substantially with potential, i. e., that

$$dq_1/dq \approx 0. \quad (2.3.12)$$

Equation 2.3.1 shows that for reasonably concentrated solutions, where  $C_{2-s}$  does not have a great effect, this condition produces a minimum in the  $C_{dl}$  vs.  $E$  curve which is independent of electrolyte type and concentration. (This minimum is not to be confused with the diffuse double layer capacitance minimum which occurs near  $E_{zc}$  in dilute solutions.) Since minima which meet these criteria occur in

the double layer capacitance curves for mercury/aqueous potassium halide interfaces, Devanathan chose the potential  $E_{\text{start}}$  to be at these minima, and assigned  $q_1(E_{\text{start}}) = 0$ .

Having determined  $q$  and  $q_1$ , the potential of the outer Helmholtz plane may be evaluated (13) as

$$\phi_2 = (2kT/e_o) \sinh^{-1}[(q_1 - q)/2A], \quad (2.3.13)$$

the potential of the inner Helmholtz plane as

$$\phi_1 = (q_1 - q)/K_{1-2} + \phi_2, \quad (2.3.14)$$

and the net potential difference across the interface as

$$\phi_m = \phi_1 - q/K_{m-1}. \quad (2.3.15)$$

The procedures just described for calculating the double layer quantities  $q$ ,  $q_1$ ,  $\phi_1$ ,  $\phi_2$ , and  $\phi_m$  were applied by Devanathan (13) to mercury/aqueous potassium halide interfaces. The results were in good agreement with previous data, which were based on electrocapillary (surface tension) measurements. Devanathan's method is inherently more precise than the electrocapillary method; it indicates that a slight amount of specific adsorption of cations does occur at highly cathodic potentials, whereas it had been generally assumed before that cationic adsorption for all but the larger cations (e. g. ,

cerium and tetraalkylammonium ions) was immeasurably small.

#### 2.4. Double Layer Capacitance Measurements

To measure the double layer capacitance, a potential step is applied to the interface using a three-electrode cell. A suitable electrical analog for studying electrical transients in such a cell is shown in Figure 2.4. 1a. This model shows the double layer capacitances, faradiac resistances, and solution resistances associated with each electrode. The batteries representing the interfacial potentials have been omitted, since the DC levels will not be of importance in these measurements.

The potential between the reference and test electrodes in a three-electrode cell is controlled electronically by passing an appropriate amount of current from the auxiliary to the test electrode. No current is passed through the reference electrode; its potential is sensed by a high-impedance device. This results in the fact that no transient potential differences develop between the reference electrode and the solution node. The components between these two points may then be omitted from the model. In addition, since the electronic potentiostat provides whatever current is necessary to maintain the desired potential difference between the reference electrode (or solution node) and the test electrode, the elements connecting the auxiliary electrode to the solution node do not affect the cell current



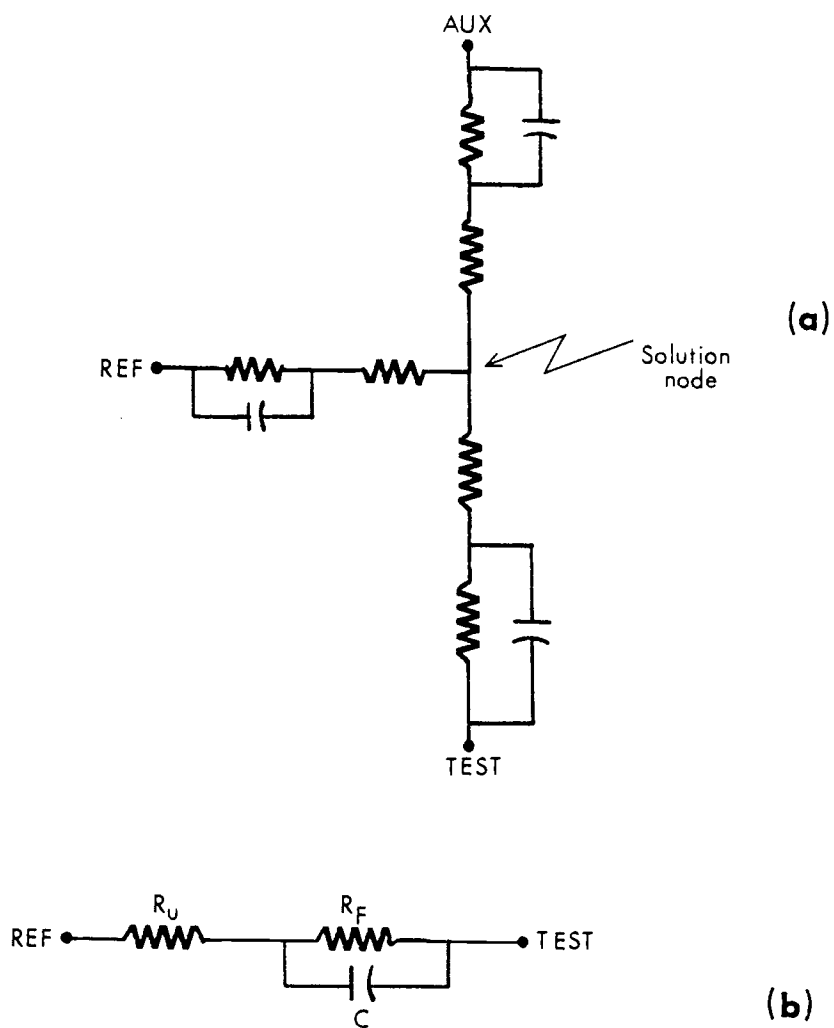


Figure 2.4.1. Electrical analogs for a three-electrode cell. (a) The full model, showing the solution resistance, the faradaic resistance, and the double layer capacitance for each electrode. (b) The model which is simplified by elimination of components which do not affect the cell current.

and may be omitted. The simplified model which results is shown in Figure 2.4. 1b.

Assuming an initial steady state, if the potential across this cell model were changed suddenly from  $V_1$  to  $V_1 + V_2$ , the current would change abruptly from

$$I_b = V_1 / (R_u + R_F) , \quad (2.4.1)$$

and eventually settle to a value

$$I_b + I_s = (V_1 + V_2) / (R_u + R_F) . \quad (2.4.2)$$

The quantity  $I_s$  is thus defined to be the difference between the final and initial currents:

$$I_s = V_2 / (R_u + R_F) . \quad (2.4.3)$$

Since  $R_F$ , which is due to various (often unknown) reactions, normally varies with electrode potential, there is not a direct correspondence between the potential  $V_1$  of the cell model from which the chemical batteries have been removed and the potential  $E_{\text{cell}}$  of an actual cell. However, for sufficiently small  $V_2$ ,  $R_F$  may be assumed to be nearly constant over the range of the potential step. Since  $V_2$  is a change in the potential across the model, it can be identified with a change of the same magnitude in the cell potential.

### The Cell Current as a Function of Time

Referring to Figure 2.4.1b, let  $I_{\text{cell}}$  be the current through  $R_u$ ,  $I_C$  the current through  $C$ , and  $I_F$  the current through  $R_F$ . Then

$$I_{\text{cell}} = I_C + I_F . \quad (2.4.4)$$

Letting  $V_C$  be the potential across  $C$ ,

$$I_C = C \frac{dV_C}{dt} . \quad (2.4.5)$$

From the model, it can be seen that after the cell potential is changed from  $V_1$  to  $V_1 + V_2$ ,

$$I_{\text{cell}} = (V_1 + V_2 - V_C) / R_u , \quad (2.4.6)$$

and

$$I_F = V_C / R_F . \quad (2.4.7)$$

Substitution of 2.4.5 through 2.4.7 into 2.4.4 yields

$$\frac{V_1 + V_2 - V_C}{R_u} = C \frac{dV_C}{dt} + \frac{V_C}{R_F} , \quad (2.4.8)$$

which rearranges to

$$\frac{dV_C}{dt} = \frac{V_1 + V_2}{R_u C} - \frac{V_C}{C} \left( \frac{1}{R_u} + \frac{1}{R_F} \right) . \quad (2.4.9)$$

Taking the Laplace transform,

$$\mathcal{L}\left(\frac{dV_C}{dt}\right) = \frac{V_1 + V_2}{k_1} \mathcal{L}(1) - \frac{1}{k_2} \mathcal{L}(V_C), \quad (2.4.10)$$

where

$$k_1 = R_u C, \quad (2.4.11)$$

$$k_2 = R_u R_F C / (R_u + R_F), \quad (2.4.12)$$

and  $\mathcal{L}$  is the Laplace operator. Using properties of the Laplace operator and the fact that at  $t = 0$

$$V_C = V_1 R_F / (R_u + R_F), \quad (2.4.13)$$

the result is

$$s \mathcal{L}(V_C) - \frac{V_1 R_F}{R_u + R_F} = \frac{V_1 + V_2}{k_1 s} - \frac{1}{k_2} \mathcal{L}(V_C), \quad (2.4.14)$$

which may be rearranged to give

$$\mathcal{L}(V_C) = \frac{V_1 + V_2}{k_1 s(s + 1/k_2)} + \frac{V_1 k_2}{k_1(s + 1/k_2)}. \quad (2.4.15)$$

Taking the inverse Laplace transform yields

$$V_C = (V_1 + V_2) \left(\frac{k_2}{k_1}\right) (1 - e^{-t/k_2}) + \left(\frac{k_2}{k_1}\right) V_1. \quad (2.4.16)$$

Substituting 2.4.16 into 2.4.6 gives

$$I_{\text{cell}} = \frac{V_1 + V_2}{R_u + R_F} + \frac{V_2 R_F e^{-t/k_2}}{R_u (R_u + R_F)} . \quad (2.4.17)$$

Substitution of Equation 2.4.2 gives

$$I_{\text{cell}} = I_b + I_s + \frac{R_F V_2 \exp(-t/k_2)}{R_u (R_u + R_F)} . \quad (2.4.18)$$

If the electrode is practically ideally polarized, i.e., if  $R_F$  is much greater than  $R_u$ , then  $I_b$  and  $I_s$  are relatively small compared to the cell current for times on the order of a few half-lives of the transient, and Equation 2.4.18 reduces to

$$I_{\text{cell}} \approx \frac{V_2}{R_u} \exp(-t/k_1) . \quad (2.4.19)$$

#### Evaluation of Cell Parameters from the Cell Current

$R_F$ ,  $R_u$ , and  $C$  can all be evaluated from Equation 2.4.18 using a linear least-squares technique, if the currents before and after the step are measured at several times, and if the step potential  $V_2$  is known. Writing Equation 2.4.18 in the linear form,

$$\ln(I_{\text{cell}} - I_b - I_s) = \ln \left[ \frac{V_2 R_F}{R_u (R_u + R_F)} \right] - \frac{t}{k_2} . \quad (2.4.20)$$

If  $I_b$  and  $I_s$  can be determined and  $I_{cell}$  measured at several times, the left-hand side may be plotted vs.  $t$  to yield an intercept

$$B = \ln \left[ \frac{V_2 R_F}{R_u (R_u + R_F)} \right] \quad (2.4.21)$$

and slope

$$M = - \frac{R_u + R_F}{R_u R_F C} . \quad (2.4.22)$$

The values of  $I_b$  and  $I_{cell}$  may be measured directly; evaluation of  $I_s$  is discussed below.

$R_F$ ,  $R_u$  and  $C$  may be determined from the values for  $V_2$ ,  $M$ ,  $B$ , and  $I_s$ . From Equation 2.4.3,

$$V_2 = I_s (R_u + R_F) . \quad (2.4.23)$$

Substituting 2.4.23 into 2.4.21 and rearranging gives

$$R_F = R_u e^B / I_s . \quad (2.4.24)$$

Substituting 2.4.24 into 2.4.23 and rearranging gives

$$R_u = V_2 / (I_s + e^B) . \quad (2.4.25)$$

Then, combining 2.4.24 and 2.4.25,

$$R_F = V_2 e^B / (I_s + e^B) / I_s . \quad (2.4.26)$$

From Equation 2.4.22

$$C = -M(R_u + R_F) / (R_u R_F) . \quad (2.4.27)$$

Combining with Equations 2.4.25 and 2.4.26 gives

$$C = -(I_s + e^B)^2 / (M e^B V_2) . \quad (2.4.28)$$

In our scheme,  $I_s$  is not found directly by observation at times much larger than the transient time constant, since other processes may supercede at longer times. Instead, it is estimated from three of the current measurements during the decay by the following method. For three data points of the form

$$[I_k, t_1 + (k-1)\Delta t], \quad k = 1, 2, 3$$

taken at uniform intervals  $\Delta t$ , we may write three equations of the form

$$\ln(I_k - I_b - I_s) = B + M[t_1 + (k-1)\Delta t], \quad k = 1, 2, 3. \quad (2.4.29)$$

By subtracting the second equation from the first, and the third from the second, one gets

$$\ln\left[\frac{I_1 - I_b - I_s}{I_2 - I_b - I_s}\right] = \ln\left[\frac{I_2 - I_b - I_s}{I_3 - I_b - I_s}\right] = M\Delta t. \quad (2.4.30)$$

The left-hand and center members of this equation yield

$$I_s = \frac{I_1 I_3 - I_2^2}{I_1 I_3 - 2I_2} - I_b. \quad (2.4.31)$$

(A similar equation is given in (11, p. 12).)

The evaluation of  $B$  and  $M$  is carried out with a numerical, weighted least-squares method. The ordinate values are weighted unequally because they do not all have equal uncertainties. Letting the ordinate values be

$$Y_j \equiv \ln(I_j - I_b - I_s), \quad (2.4.32)$$

and assuming all the current measurements to have the same uncertainty  $\sigma_I$ , application of the equation for propagation of errors (discussed more fully in the next subsection) gives

$$\begin{aligned} \sigma_{Y_j}^2 = & \sigma_I^2 \left(\frac{\partial Y_j}{\partial I_j}\right)^2 + \sigma_{I_b}^2 \left(\frac{\partial Y_j}{\partial I_b}\right)^2 + \sigma_{I_s}^2 \left(\frac{\partial Y_j}{\partial I_s}\right)^2 + \sigma_{I_b I_s}^2 \left(\frac{\partial Y_j}{\partial I_b}\right) \left(\frac{\partial Y_j}{\partial I_s}\right) \\ & + 2\sigma_{I_j I_s}^2 \left(\frac{\partial Y_j}{\partial I_j}\right) \left(\frac{\partial Y_j}{\partial I_s}\right). \end{aligned} \quad (2.4.33)$$

After using 2.4.32 to evaluate the partial derivatives, 2.4.33 becomes



$$\sigma_{Y_j}^2 = \left[ \frac{1}{I_j - I_b - I_s} \right]^2 [\sigma_I^2 + \sigma_{I_b}^2 + \sigma_{I_s}^2 + 2\sigma_{I_b I_s} - 2\sigma_{I_j I_s}] . \quad (2.4.34)$$

Statistical considerations dictate that the weights be in inverse proportion to the variances, (23, p. 98) so for each data point  $(I_j, t_j)$ , the weight for the corresponding  $Y_j$  may be expressed as

$$w_j = \frac{(I_j - I_b - I_s)^2}{\sigma_I^2 + \sigma_{I_b}^2 + \sigma_{I_s}^2 + 2\sigma_{I_b I_s} - 2\sigma_{I_j I_s}} . \quad (2.4.35)$$

The denominator of this equation consists of constants except for the last term. It was shown on several real data sets that the last term was considerably smaller than the others. This fact makes it possible to estimate the weights more simply as

$$w_j = (I_j - I_b - I_s)^2 . \quad (2.4.36)$$

This simplification normally has an effect of only a percent or two on the relative weights, and the effect on the calculated capacitance is imperceptible.

The equations for the intercept and slope are standard statistical formulae (23, p. 96):

$$B = \left[ \sum_j w_j t_j^2 \sum_j w_j Y_j - \sum_j w_j t_j \sum_j w_j t_j Y_j \right] / D \quad (2.4.37)$$

and

$$M = \left[ \sum_j w_j \sum_j w_j t_j Y_j - \sum_j w_j t_j \sum_j w_j Y_j \right] / D, \quad (2.4.38)$$

where

$$D = \sum_j w_j \sum_j w_j t_j^2 - \left[ \sum_j w_j t_j \right]^2. \quad (2.4.39)$$

Thus, from the  $(I_j, t_j)$  data,  $I_s$  can be determined, then the slope  $B$  and intercept  $M$  of  $\ln(I_j - I_b - I_s)$  vs.  $t_j$  may be found.

$R_u$ ,  $R_F$ , and  $C$  are given as functions of  $V_2$ ,  $I_s$ ,  $B$ , and  $M$  by Equations 2.4.25, 2.4.26, and 2.4.28, respectively.

#### The Variances in the Measurements of $R_u$ , $R_F$ , and $C$

Since the calculations are quite complex, the variances to be expected in the calculated quantities are not readily apparent. Equations have therefore been developed using the ideas of "propagation of errors" to provide estimates of the errors involved in assigning values to  $R_u$ ,  $R_F$ , and  $C$ .

In one experiment, measurements of the current are made before the step is applied ( $I_{bj}$ ) and after the step ( $I_j$ ) at known times  $t_j$ . The value of the step potential  $V_2$  is established in

another experiment. Thus, all the just-named quantities are independently evaluated, i. e., there is no basis to relate their "indeterminate" errors (46, pp. 43-49) to one another. Figure 2.4.2 shows the dependence among these quantities and the other quantities of concern. When a quantity  $y$  is functionally dependent on other quantities  $x_j$ , its variance may be expressed as a function of the variances of the others (3, p. 59):

$$\sigma_y^2 = \sum_j \left( \frac{\partial y}{\partial x_j} \right)^2 \sigma_{x_j}^2. \quad (2.4.40)$$

If the  $x_j$  are not all independently acquired, then covariance terms of the form

$$2 \left( \frac{\partial y}{\partial x_j} \right) \left( \frac{\partial y}{\partial x_k} \right) \sigma_{x_j x_k}^2$$

must be added into the summation.

Equation 2.4.28 shows that  $C$  is a function of  $I_s$ ,  $B$ ,  $M$  and  $V_2$ . Since  $I_s$ ,  $B$ , and  $M$  are derived from the same data, propagation of errors for  $C$  will involve covariances between these.

Defining

$$I_o \equiv e^B, \quad (2.4.41)$$

one can write

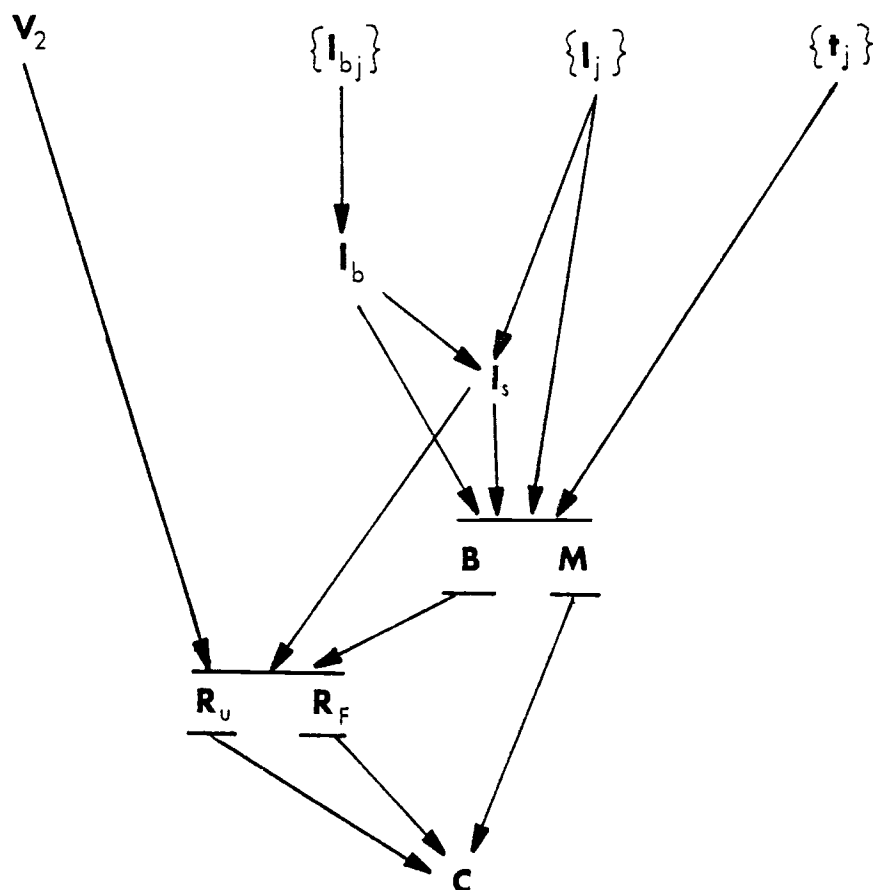


Figure 2.4.2. Scheme of the dependence of calculated quantities on the independently measured ones. Braces indicate a set of values.

$$\begin{aligned}
\sigma_C^2 = & \sigma_{I_s}^2 \left( \frac{\partial C}{\partial I_s} \right)^2 + \sigma_{I_o}^2 \left( \frac{\partial C}{\partial I_o} \right)^2 + \sigma_M^2 \left( \frac{\partial C}{\partial M} \right)^2 + \sigma_{V_2}^2 \left( \frac{\partial C}{\partial V_2} \right)^2 \\
& + 2\sigma_{I_s I_o}^2 \left( \frac{\partial C}{\partial I_s} \right) \left( \frac{\partial C}{\partial I_o} \right) + 2\sigma_{I_s M}^2 \left( \frac{\partial C}{\partial I_s} \right) \left( \frac{\partial C}{\partial M} \right) \\
& + 2\sigma_{I_o M}^2 \left( \frac{\partial C}{\partial I_o} \right) \left( \frac{\partial C}{\partial M} \right) .
\end{aligned} \tag{2.4.42}$$

The partial derivatives may be evaluated from Equation 2.4.28:

$$\frac{\partial C}{\partial I_s} = \frac{-2(I_s + I_o)}{M I_o V_2} , \tag{2.4.43}$$

$$\frac{\partial C}{\partial I_o} = [(I_s / I_o)^2 - 1] / (M V_2) , \tag{2.4.44}$$

$$\frac{\partial C}{\partial M} = -C / M , \tag{2.4.45}$$

$$\frac{\partial C}{\partial V_2} = -C / V_2 . \tag{2.4.46}$$

The variances and covariances in Equation 2.4.42 may be determined ultimately from the noise in the current measurements. Each will be taken in turn.

1. From a propagation of errors on Equation 2.4.31,

$$\sigma_{I_s}^2 = \sigma_{I_b}^2 \left( \frac{\partial I_s}{\partial I_b} \right)^2 + \sum_{k=1}^3 \sigma_{I_k}^2 \left( \frac{\partial I_s}{\partial I_k} \right)^2 . \tag{2.4.47}$$

The partial derivatives are, from Equation 2.4.31,

$$\frac{\partial I_s}{\partial I_b} = -1, \quad (2.4.48)$$

$$\frac{\partial I_s}{\partial I_1} = \frac{I_3 - I_s}{I_1 + I_3 - 2I_2}, \quad (2.4.49)$$

$$\frac{\partial I_s}{\partial I_2} = 2 \left[ \frac{I_s - I_2}{I_1 + I_3 - 2I_2} \right], \quad (2.4.50)$$

and

$$\frac{\partial I_s}{\partial I_3} = \frac{I_1 - I_s}{I_1 + I_3 - 2I_2}. \quad (2.4.51)$$

In the experimental scheme to be employed, several measurements of the current are made immediately before application of the step. These measurements are averaged to yield  $I_b$ . If it is assumed that all currents are to be measured with the same uncertainty, the usual equation for the variance in each measurement (23, pp. 9-10) is

$$\sigma_I^2 \equiv \sigma_{I_j}^2 = \sigma_{I_{bj}}^2 = \left[ \sum_{j=1}^N I_{bj}^2 - \left( \sum_{j=1}^N I_{bj} \right)^2 / N \right] / (N-1), \quad (2.4.52)$$

where  $I_{bj}$  refers to the individual measurements made before application of the step and  $N$  is the number of these measurements.

This equation is based on the premise that each measurement may take any value which can be represented on a number line. However, these measurements are to be made with an analog-to-digital converter, the resolution of which is finite, i. e., it may assume only a finite number of values. This situation results in the fact that the minimum uncertainty possible corresponds to one-half of the least significant bit of the converter. A convenient, though not strictly correct, method to deal with the limitation is to consider the resolution  $d$  of the analog-to-digital converter as another source of noise in the measurement, then write

$$\sigma_I^2 = \left[ \sum_{j=1}^N I_{bj}^2 - \left( \sum_{j=1}^N I_{bj} \right)^2 / N \right] / (N-1) + d^2 . \quad (2.4.53)$$

The value of  $d$  can be estimated to be the amount of current corresponding to one-half the least significant bit.

Since the residual current is evaluated as a function of the  $N$  measurements before the step:

$$I_b = \left[ \sum_{j=1}^N I_{bj} \right] / N , \quad (2.4.54)$$

propagation of errors gives

$$\sigma_{I_b}^2 = \sum_{j=1}^N \sigma_I^2 \left( \frac{\partial I_b}{\partial I_{bj}} \right)^2 = \frac{\sigma_I^2}{N} . \quad (2.4.55)$$

But since the uncertainty must be at least one-half the least significant bit, the variance due to resolution is added back in:

$$\sigma_{I_b}^2 = \sigma_I^2 / N + d^2 . \quad (2.4.56)$$

Substituting 2.4.48 through 2.4.51 and 2.4.55 into 2.4.47,

$$\sigma_{I_s}^2 = \sigma_I^2 \left[ \frac{1}{N} + \frac{(I_1 - I_s)^2 + 4(I_2 - I_s)^2 + (I_3 - I_s)^2}{(I_1 + I_3 - 2I_2)^2} \right] + d^2 . \quad (2.4.57)$$

2. From the definition of  $I_o$ , Equation 2.4.41,

$$\sigma_{I_o}^2 = I_o^2 \sigma_B^2 . \quad (2.4.58)$$

It can be shown (23, pp. 99-100) that

$$\sigma_B^2 = \frac{S^2}{\sum w_j} \left[ 1 + \left( \sum w_j t_j \right)^2 / D \right] , \quad (2.4.59)$$

where the summations are over all the points obtained for the decay  
and



$$S^2 = \left[ \sum w_j Y_j^2 - \frac{(\sum w_j Y_j)^2}{\sum w_j} - \frac{M^2 D}{\sum w_j} \right] / (N-2) . \quad (2.4.60)$$

Substitution of Equations 2.4.59 and 2.4.60 into 2.4.58 provides the means for evaluating  $\sigma_{I_o}^2$ .

3. The value of  $\sigma_M^2$  can be estimated by (23, p. 98)

$$\sigma_M^2 = \left[ S^2 \sum w_j \right] / D . \quad (2.4.61)$$

4. The uncertainty in  $V_2$  originates in the potentiostat calibration procedure (discussed in the experimental section). The relative standard error given from this procedure is

$$\sigma_{V_2} / V_2 = 2 \times 10^{-4} . \quad (2.4.62)$$

5. The values of  $I_s$  and  $I_o$  are both dependent on the three currents used for  $I_s$ . The covariance between  $I_s$  and  $I_o$  can be estimated as (3, p. 161)

$$\sigma_{I_s I_o}^2 = \sum_{k=1}^3 \sigma_{I_k}^2 \left( \frac{\partial I_s}{\partial I_k} \right) \left( \frac{\partial I_o}{\partial I_k} \right) . \quad (2.4.63)$$

Using the chain rule,

$$\sigma_{I_s I_o}^2 = \sum_{k=1}^3 \sigma_I^2 \left( \frac{\partial I_s}{\partial I_k} \right) \left( \frac{\partial I_o}{\partial B} \right) \left( \frac{\partial B}{\partial Y_k} \right) \left( \frac{\partial Y_k}{\partial I_k} \right). \quad (2.4.64)$$

The partials  $\partial I_s / \partial I_k$  are given by Equations 2.4.49 through 2.4.51.

From Equation 2.4.41

$$\frac{\partial I_o}{\partial B} = I_o, \quad (2.4.65)$$

from Equation 2.4.37

$$\frac{\partial B}{\partial Y_k} = w_k \left[ \sum_{j=1}^N w_j t_j^2 - t_k \sum_{j=1}^N w_j t_j \right] / D, \quad (2.4.66)$$

and from Equation 2.4.32

$$\frac{\partial Y_k}{\partial I_k} = 1 / (I_k - I_b - I_s). \quad (2.4.67)$$

The result is

$$\sigma_{I_s I_o}^2 = \frac{\sigma_{I_o}^2}{D(I_1 - 2I_2 + I_3)} [Z_1 - 2Z_2 + Z_3], \quad (2.4.68)$$

where

$$Z_k = \left[ \frac{(I_{4-k} - I_s) w_k}{I_k - I_b - I_s} \right] \left[ \sum_{j=1}^N w_j t_j^2 - t_k \sum_{j=1}^N w_j t_j \right]. \quad (2.4.69)$$

6. The values of  $I_s$  and  $M$  are dependent on the same three current measurements, so

$$\sigma_{I_s M}^2 = \sum_{k=1}^3 \left( \frac{\partial I_s}{\partial I_k} \right) \left( \frac{\partial M}{\partial I_k} \right) \sigma_I^2, \quad (2.4.70)$$

or, expanding on the chain rule,

$$\sigma_{I_s M}^2 = \sigma_I^2 \sum_{k=1}^3 \left( \frac{\partial I_s}{\partial I_k} \right) \left( \frac{\partial M}{\partial Y_k} \right) \left( \frac{\partial Y_k}{\partial I_k} \right). \quad (2.4.71)$$

The center partial may be evaluated from Equation 2.4.38 to be

$$\frac{\partial M}{\partial Y_k} = w_k \left[ t_k \sum_{j=1}^N w_j - \sum_{j=1}^N w_j t_j \right] / D. \quad (2.4.72)$$

Combining Equations 2.4.49 through 2.4.51, 2.4.67, 2.4.71, and 2.4.72 yields

$$\sigma_{I_s M}^2 = \left[ \frac{\sigma_I^2}{D(I_1 - 2I_2 - I_3)} \right] [Z_1^* - 2Z_2^* + Z_3^*], \quad (2.4.73)$$

where

$$Z_k^* = \left[ \frac{(I_{4-k} - I_s) w_k}{I_k - I_b - I_s} \right] \left[ t_k \sum_{j=1}^N w_j - \sum_{j=1}^N w_j t_j \right]. \quad (2.4.74)$$

7. The values estimated for  $I_o$  and  $M$  are dependent on all the current measurements, so

$$\sigma_{I_o M}^2 = \sigma_I^2 \sum_{j=1}^N \left( \frac{\partial I_o}{\partial I_j} \right) \left( \frac{\partial M}{\partial I_j} \right). \quad (2.4.75)$$

Combining Equations 2.4.65 through 2.4.67 and 2.4.72 with 2.4.75 yields the result

$$\sigma_{I_o M}^2 = -I_o \sigma_I^2 \left[ \sum_j w_j t_j \right] / D^2. \quad (2.4.76)$$

Now  $\sigma_C^2$  may be estimated by substituting Equations 2.4.43 through 2.4.46, 2.4.57 through 2.4.62, 2.4.68, 2.4.69, 2.4.73, 2.4.74, and 2.4.76 into 2.4.42. In practice, it was found that the covariance terms were entirely negligible, so they were not included in the routine error calculations.

By applying the propagation of errors formula to Equation 2.4.25, the variance in  $R_u$  is found to be

$$\sigma_{R_u}^2 = \left( \frac{\partial R_u}{\partial V_2} \right)^2 \sigma_{V_2}^2 + \left( \frac{\partial R_u}{\partial I_s} \right)^2 \sigma_{I_s}^2 + \left( \frac{\partial R_u}{\partial B} \right)^2 \sigma_B^2. \quad (2.4.77)$$

Evaluation of the partial derivatives gives

$$\sigma_{R_u}^2 = \frac{\sigma_{V_2}^2}{(I_s + I_o)^2} + \left[ \frac{V_2^2 (\sigma_{I_s}^2 + \sigma_{I_o}^2)}{(I_s + I_o)^4} \right] . \quad (2.4.78)$$

If the approximation  $I_s \ll I_o$  is made, then

$$\left( \frac{\sigma_{R_u}}{R_u} \right)^2 \approx \left( \frac{\sigma_{V_2}}{V_2} \right)^2 + \left( \frac{\sigma_{I_s}}{I_s} \right)^2 + \left( \frac{\sigma_{I_o}}{I_o} \right)^2 . \quad (2.4.79)$$

If  $I_s$  is significant with respect to  $I_o$ , then this equation is an overapproximation.

Application of propagation of errors to Equation 2.4.24 yields

$$\left( \frac{\sigma_{R_F}}{R_F} \right)^2 = \left( \frac{\sigma_{R_u}}{R_u} \right)^2 + \left( \frac{\sigma_{I_o}}{I_o} \right)^2 + \left( \frac{\sigma_{I_s}}{I_s} \right)^2 . \quad (2.4.80)$$

This completes the equations necessary to estimate the uncertainties in  $C_{dl}$ ,  $R_u$ , and  $R_F$ .

## 2.5. Silver Deposition Rate Measurements

Silver deposition in cyanide solution is quite a fast reaction (48), and the steady-state reaction rate is entirely controlled by diffusion of the silver species to the electrode at overpotentials where the partial current due to the reverse reaction (dissolution) can be ignored (i.e., at overpotentials greater than 100 mV). Since it is

desired to establish the reaction rate in the absence of any significant reverse reaction or diffusion control, a transient method was selected. As a compromise between simplicity of experiment and ease of interpretation, the potential-step method was chosen.

In this method the cell potential is controlled. The potential is initially adjusted to the equilibrium value, i. e., so that the current is zero. The experiment is initiated by changing the cell potential in a single step to a new value cathodic of the equilibrium potential. The cell current is then measured as a function of time. Thus, the experiment is quite similar to the double layer capacitance measurement experiment, except that the object is to obtain the faradaic current with accuracy, rather than the capacitative current.

In order to minimize the time when the capacitance current is significant, the uncompensated resistance is made as small as possible. This can be accomplished by placing the reference electrode in a Luggin capillary whose tip is close to the electrode.

Gerischer and Vielstich (18) developed the equation describing the change of the faradaic current with time where the rise time of the electrode potential is negligible:

$$i_F(t) = i_F(0) \exp(\lambda^2 t) \operatorname{erfc}(\lambda t^{1/2}), \quad (2.5.1)$$

where

$$\lambda = \frac{i_{ex}}{nF} \left\{ \frac{\exp[anf\eta]}{C_R D_R^{1/2}} + \frac{\exp[-(1-a)nf\eta]}{C_O D_O^{1/2}} \right\} \quad (2.5.2)$$

and

$$\eta = E - E_{eq} . \quad (2.5.3)$$

At short times where  $\lambda t^{1/2} \ll 1$ , this reduces to

$$i_F(t) \approx i_F(0) [1 - 2\lambda \pi^{-1/2} t^{1/2}] . \quad (2.5.4)$$

Thus, a plot of  $i_{cell}$  vs.  $t^{1/2}$  at sufficiently short times (but long enough that  $i_C \ll i_F$ ) is a straight line, the intercept of which is  $i_F(0)$ , the faradaic current density in the absence of diffusion control.

Of course, in an actual experiment, the electrode potential rises at a finite rate, so the true faradaic current at time zero is really zero. The meaning of  $i_F(0)$ , as used here is the value obtained for the faradaic current by extrapolation to  $t = 0$  from times when the electrode potential has reached a constant value.

Equation 2.5.4 has been examined closely by several authors.

They point out that mere observation of a linear segment in an  $i_{cell}$  vs.  $t^{1/2}$  curve does not necessarily mean that extrapolation of that segment to  $t = 0$  will yield the correct value of  $i_F(0)$ .

Oldham and Osteryoung (41) showed that in order to keep the error in the intercept within 1%, the currents from which the extrapolation is

made must be at least 0.9 of the value at the intercept. Steeper extrapolations will produce values less than  $i_F(0)$ . They have provided a graphical method for correction of the intercept values to get  $i_F(0)$ . Lingane and Christie (30) and Niki, et al. (40), have proposed more complex procedures to evaluate the initial faradaic current without restricting the data to small times.

A small, but significant, potential error occurs during the passage of these large currents through the uncompensated cell resistance. This error can be corrected using values of  $R_u$  based on the high-frequency behavior of the cell. The data for this determination can be collected during the early part of the transient, where the cell current is mainly due to double layer charging. At these short times, the cell model shown in Figure 2.4.1b roughly applies, and the impedance of the double layer capacitance is low enough that its effect dominates over  $R_F$ .

Since the potentiostat rise time is significant in this time frame, a rather complicated form of the cell current occurs. However, as Pilla (45) has shown, Laplace transformation permits a relatively simple solution. For short times or high frequencies (fast changes in signal) the real component of the Laplace transform of the cell impedance is

$$Z(\sigma) \equiv \mathcal{L}(E_{\text{cell}}) / \mathcal{L}(I_{\text{cell}}) = R_u + 1/\sigma C, \quad (2.5.5)$$



where  $\sigma$  is the real component of the Laplace variable  $s$ . Thus, a plot of  $Z(\sigma)$  vs.  $1/\sigma$  has the value  $R_u$  at the intercept. The slope is  $1/C$ ; thus, if  $C$  changes significantly with the change in  $E_{\text{cell}}$ , the line may not be quite straight; however,  $R_u$  is normally a constant and should be given by the intercept.

The real components of the transforms of the cell potential and cell current in Equation 2.5.5 may be determined from  $(E_{\text{cell}}, I_{\text{cell}})$  data points and the definition of the real Laplace transform,

$$\mathcal{L}(X) = \int_0^{\infty} X \exp(-\sigma t) dt, \quad (2.5.6)$$

where  $X$  is a time function. Pilla carried out the integration via a summation formula

$$\begin{aligned} \mathcal{L}(X) = & \frac{X(t_1)}{\sigma t_1} [1 - (1 + \sigma t_1) \exp(-\sigma t_1)] \\ & + \sum_{j=2}^N \frac{[X(t_j) \exp(-\sigma t_j) - X(t_{j-1}) \exp(-\sigma t_{j-1})][t_j - t_{j-1}]}{\ln[X(t_j) \exp(-\sigma t_j) / X(t_{j-1}) \exp(-\sigma t_{j-1})]} \\ & + \frac{X(t_N) \exp(-\sigma t_N)}{\sigma}, \end{aligned} \quad (2.5.7)$$

in which the function is assumed to be exponential in form over each interval. In this formula, the  $t_j$  are times, not necessarily at

uniform intervals, at which the function is measured; by the time  $t_N$  the function must be essentially constant.

The response time of the current-to-voltage converter is appreciable at these short times, so its output voltage must be corrected to obtain a true measure of the cell current. The current-to-voltage converter amplifier may be considered to have the input characteristic of a parallel resistor and capacitor between the two inputs, and the voltage transfer characteristic of a low-pass filter with high gain. Figure 2.5.1 diagrams this model of the amplifier.

The cell current divides into three paths at the amplifier input according to

$$I_{\text{cell}} = \frac{V_{\text{in}} - V_{\text{out}}}{R_f} + \frac{V_{\text{in}}}{R_{\text{in}}} + C_{\text{in}} \frac{dV_{\text{in}}}{dt}, \quad (2.5.8)$$

where the meanings of the symbols are shown in the figure. The output current of the amplifier is

$$\frac{V_{\text{out}} - V_{\text{in}}}{R_f} = \frac{-GV_{\text{in}} - V_{\text{out}}}{R_{\text{out}}} - C_{\text{out}} \frac{dV_{\text{out}}}{dt}. \quad (2.5.9)$$

These two equations may be converted to the Laplace frequency domain to give

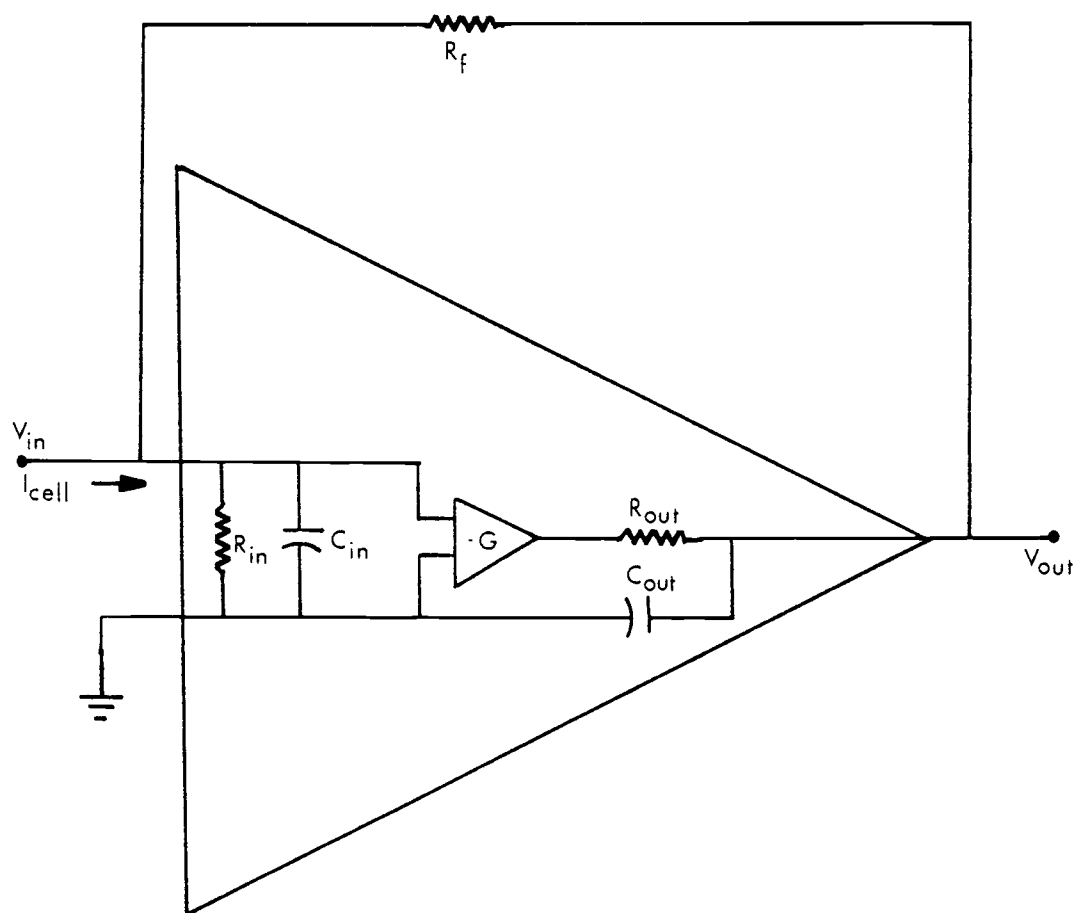


Figure 2.5.1. Model for the frequency-dependent behavior of the current-to-voltage converter.  $G$  is the DC open-loop gain of the operational amplifier.

$$\begin{aligned}
R_{in} R_f \mathcal{L}(I_{cell}) = & -R_{in} \mathcal{L}(V_{out}) + (R_{in} + R_f + s R_f R_{in} C_{in}) \mathcal{L}(V_{in}) \\
& - R_f R_{in} C_{in} V_{in}(0^+)
\end{aligned} \tag{2.5.10}$$

and

$$\begin{aligned}
(R_{out} + R_f + s R_f R_{out} C_{out}) \mathcal{L}(V_{out}) = & (R_{out} - R_f G) \mathcal{L}(V_{in}) \\
& + R_f R_{out} C_{out} V_{out}(0^+) .
\end{aligned} \tag{2.5.11}$$

Since both  $V_{in}$  and  $V_{out}$  are zero before the cell potential is stepped, and because  $C_{in}$  and  $C_{out}$  prevent  $V_{in}$  and  $V_{out}$  from changing instantaneously, the last term in each of the last two equations may be dropped.  $V_{in}$  may be eliminated between the two equations to give the transfer function of the current-to-voltage converter,

$$\begin{aligned}
T(s) = \mathcal{L}(V_{out}) / \mathcal{L}(I_{cell}) & \tag{2.5.12} \\
= \frac{R_{in} R_f (R_{out} - G R_f)}{(R_{out} + R_f + s R_f R_{out} C_{out})(R_{in} + R_f + s R_f R_{in} C_{in}) + R_{in} (R_f G - R_{out})} .
\end{aligned}$$

When  $s$  is small enough, the DC transfer function is given to be

$$T(\sim 0) = -R_f / \left( 1 + \frac{1}{G} + \frac{R_f}{R_{in} G} + \frac{R_{out}}{R_f G} + \frac{R_{out}}{R_{in} G} \right) . \tag{2.5.13}$$

When reasonable limitations are placed on  $R_{in}$ ,  $R_{out}$ , and  $R_f$ , this

reduces to simply

$$T(\sim 0) = -R_f . \quad (2.5.14)$$

Comparison of Equations 2.5.12 and 2.5.14 show that

$$T(s) = T(\sim 0)/D(s) , \quad (2.5.15)$$

where  $D(s)$  represents the modification of the DC transfer function due to the frequency response characteristics of the operational amplifier.

$D(s)$  may be calculated from the  $(E_{\text{cell}}(t), I_{\text{cell}}(t))$  data collected for a step potential applied to a dummy cell composed of just a known resistor (for  $R_u$ ). For this cell, the current transform is

$$\mathcal{L}(I_{\text{cell}}) = -\mathcal{L}(E_{\text{cell}})/R_u , \quad (2.5.16)$$

so

$$D(s) = \frac{T(\sim 0)}{T(s)} = \frac{-R_f \mathcal{L}(I_{\text{cell}})}{\mathcal{L}(V_{\text{out}})} = \frac{R_f \mathcal{L}(E_{\text{cell}})}{R_u \mathcal{L}(V_{\text{out}})} . \quad (2.5.17)$$

$D(s)$  depends on  $R_f$ , so  $D(s)$  must be calculated for each of the current-to-voltage converter sensitivities used in the deposition rate measurements.

Combination of Equations 2.5.12, 2.5.14, and 2.5.15 shows that  $\mathcal{L}(I_{\text{cell}})$  may be calculated as

$$\mathcal{L}(I_{\text{cell}}) = -D(s) \mathcal{L}(V_{\text{out}})/R_f \quad (2.5.18)$$

The method for determination of the uncompensated cell resistance may now be summarized. Measurements of the current-to-voltage converter output and of the cell potential down to very small times after application of the step potential are transformed to the real Laplace domain using Equation 2.5.7 for several values of  $\sigma$ . These transforms are used to calculate the frequency domain cell impedance  $Z(\sigma)$  by Equations 2.5.5 and 2.5.18.  $Z(\sigma)$  is plotted against  $1/\sigma$ , the plot is extrapolated linearly to  $1/\sigma = 0$ , and the value of  $R_u$  is taken from the intercept.

### III. EXPERIMENTAL

#### 3.1. Double Layer Capacitance Measurements

The double layer capacitance measurements were controlled by a computer, which was interfaced to the test cell via an instrument consisting of a potentiostat and a special-purpose current-to-voltage converter. This system is block diagrammed in Figure 3.1.1. The computer is programmed to perform the experiment described as follows. The initial potential is set, and a predetermined length of time is passed to ensure a constant-current condition. The residual current is measured a selectable number of times at a selectable rate, a small step potential is added to the initial potential, and the resulting decay-current is monitored the same number of times and at the same rate as for the residual current. The step potential is then removed. A typical data-acquisition cycle is shown in Figure 3.1.2. The cycle may be repeated up to 32 times with a delay between each iteration (usually set to 10 to 20 times the decay-current measuring period) so that the current becomes constant before each step. The current measurements for each iteration are added to the corresponding measurements for the previous ones. The accumulated values are each divided by the number of iterations before performing any calculations with them. The effect of this "ensemble averaging" is to reduce the effect of high- and mid-range-frequency noise.

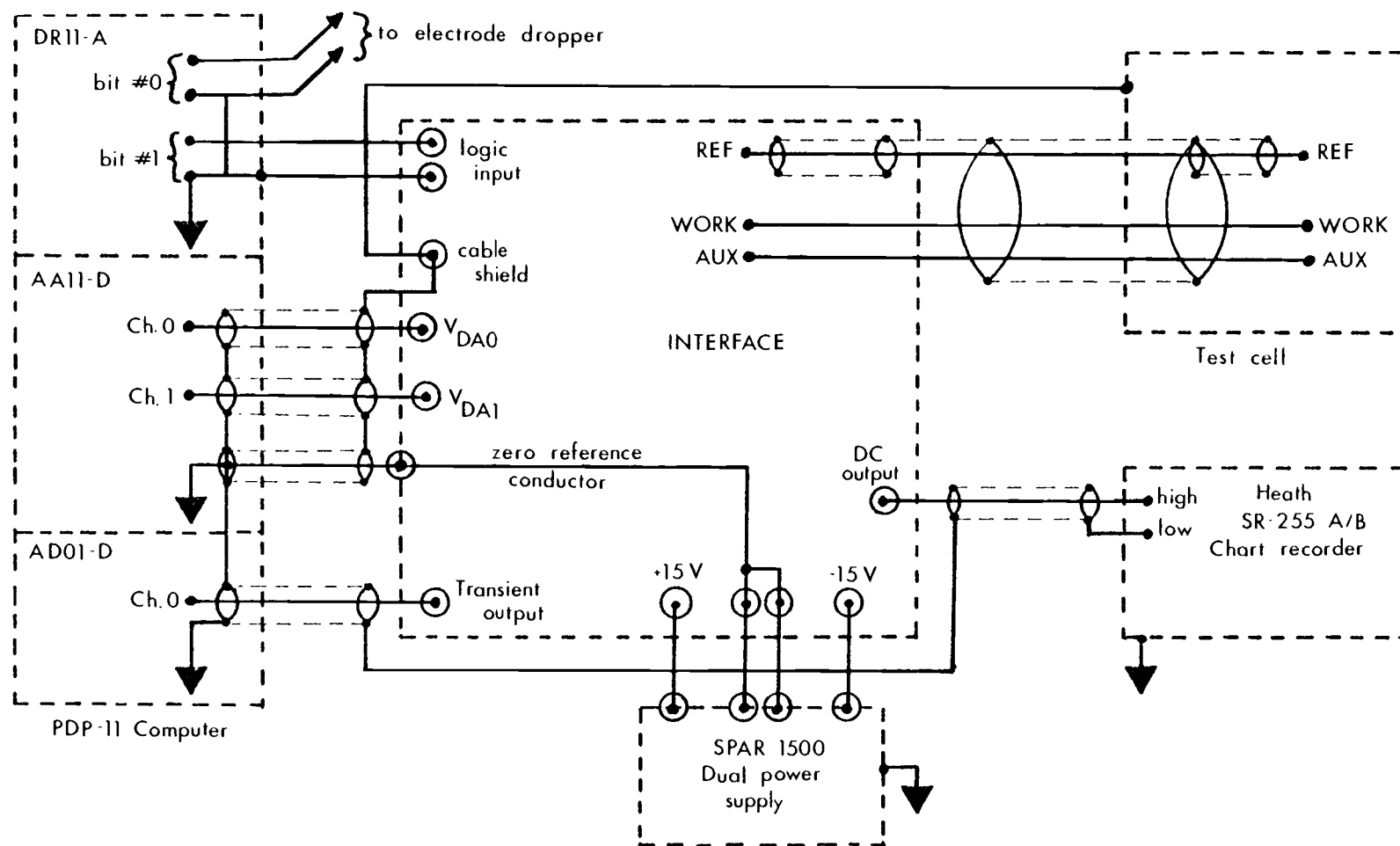


Figure 3. 1. 1. Block diagram of the double layer capacitance measurement system, detailing the grounding and shielding.



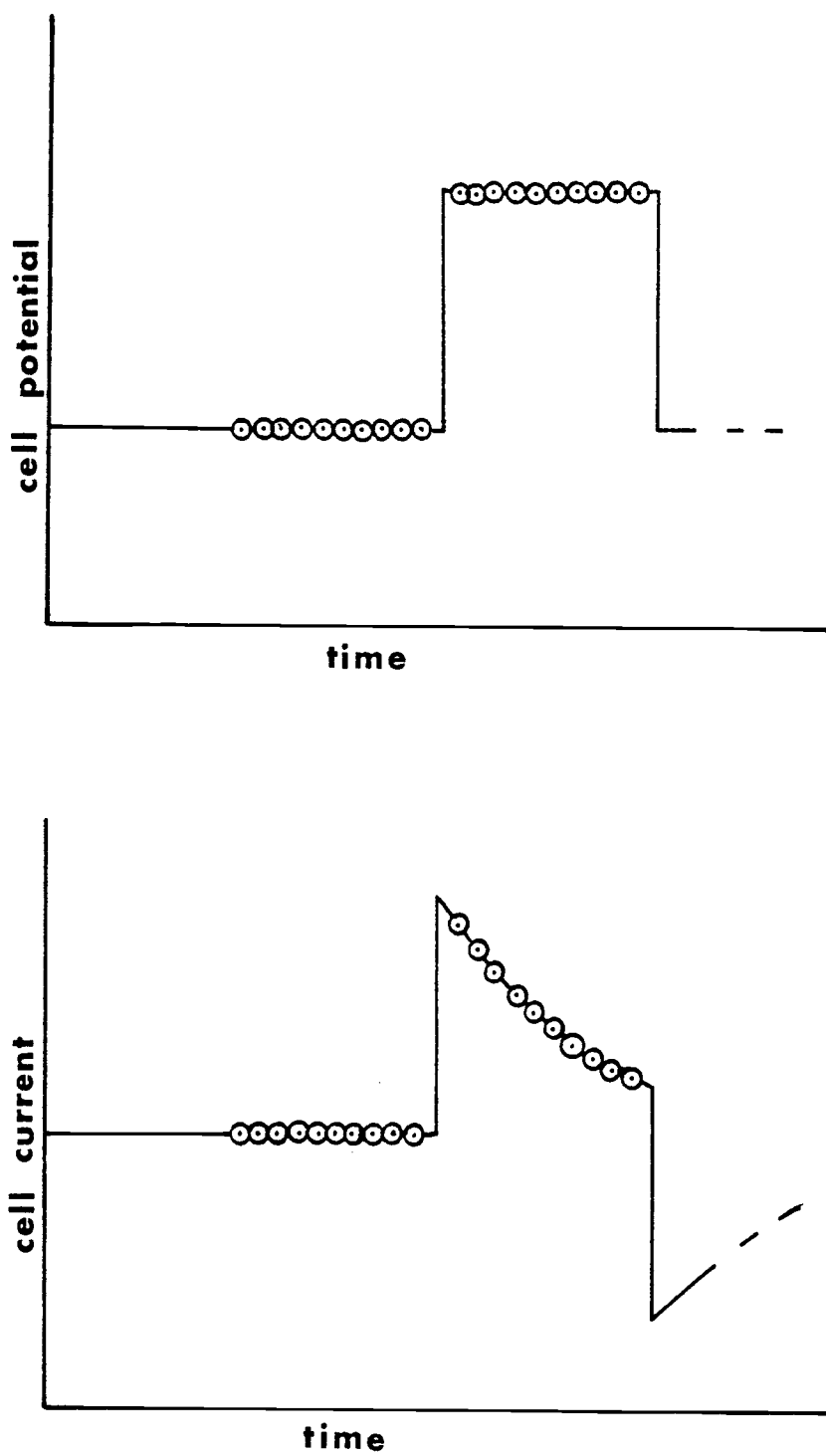


Figure 3. 1. 2. Cell potential vs. time and current vs. time plots for one capacitance measurement cycle. The circles indicate the points at which the current is measured.

The computer program allows for several of these measurements to be executed in sequence. The timing and potentials involved in each measurement are independent of the other measurements. Before the sequence of measurements is started, the test electrode is automatically immersed into the electrolyte; it is removed at the end of the sequence.

### Instrumentation

The circuits of the potentiostatic interface are diagrammed in Figures 3.1.3 through 3.1.7. The potentiostat and current-to-voltage converter sections (Figures 3.1.3 and 3.1.4) are of conventional design. The input signals, one for the initial potential and one for the step, are taken from the two digital-to-analog converters (DACs) of the computer. The cell selector switch permits the instrument to control either a dummy cell consisting of electrical components mounted on the front of the instrument with dual banana plugs or the chemical test cell which is connected at the rear of the instrument. The DC potential offset error of this system can easily be set to  $0 \pm 100 \mu\text{V}$  with the two ten-turn balancing potentiometers. The maximum current output for the potentiostat is 20 mA; the current-to-voltage converter will handle up to 5 mA.

The speed with which successive capacitance measurements can be made is improved considerably by the way in which the

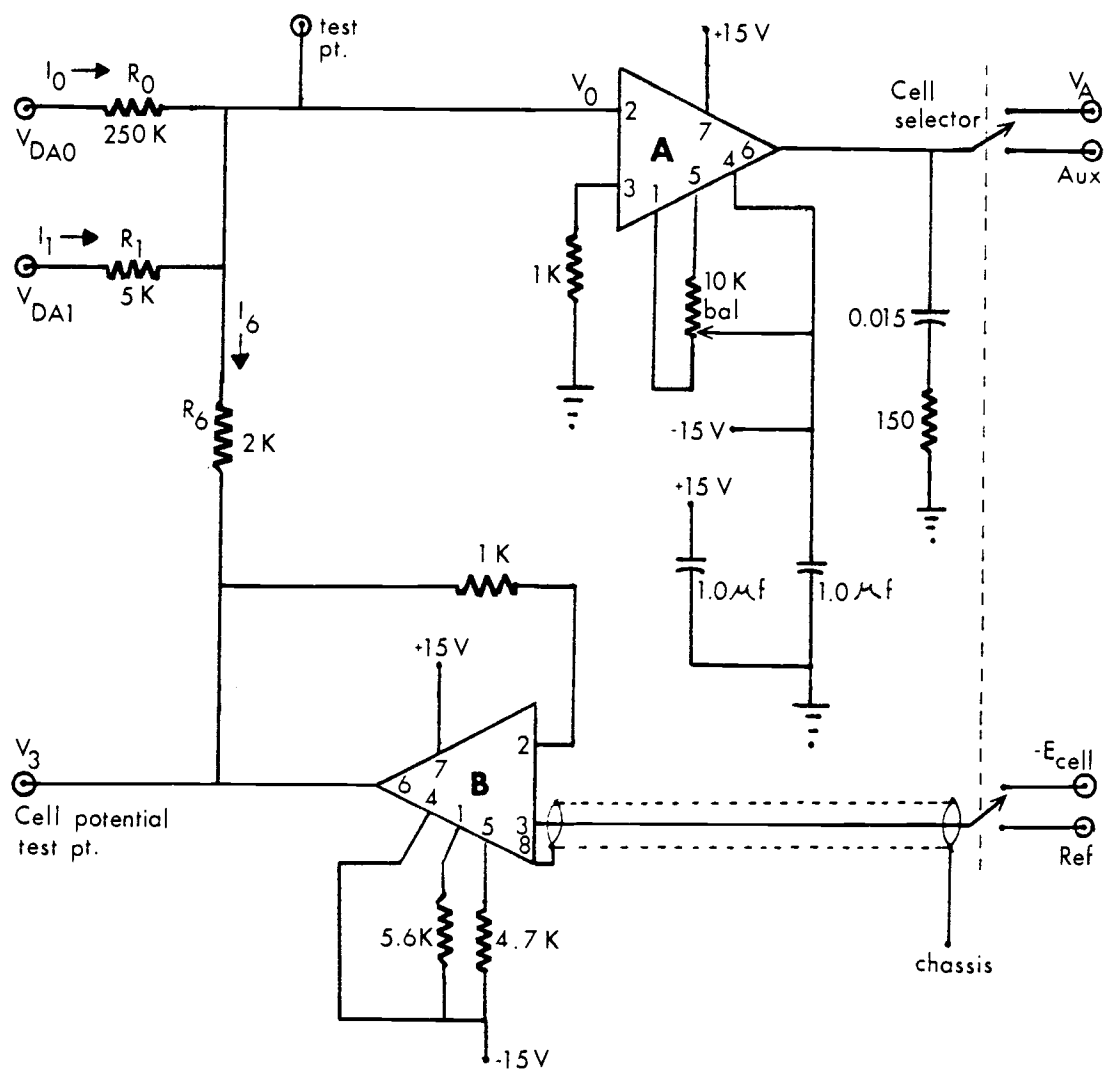


Figure 3.1.3. Potentiostat portion of the interface circuit.  
 Amplifier A: Fairchild 741EHC. Amplifier B: Burr-Brown 3522K.

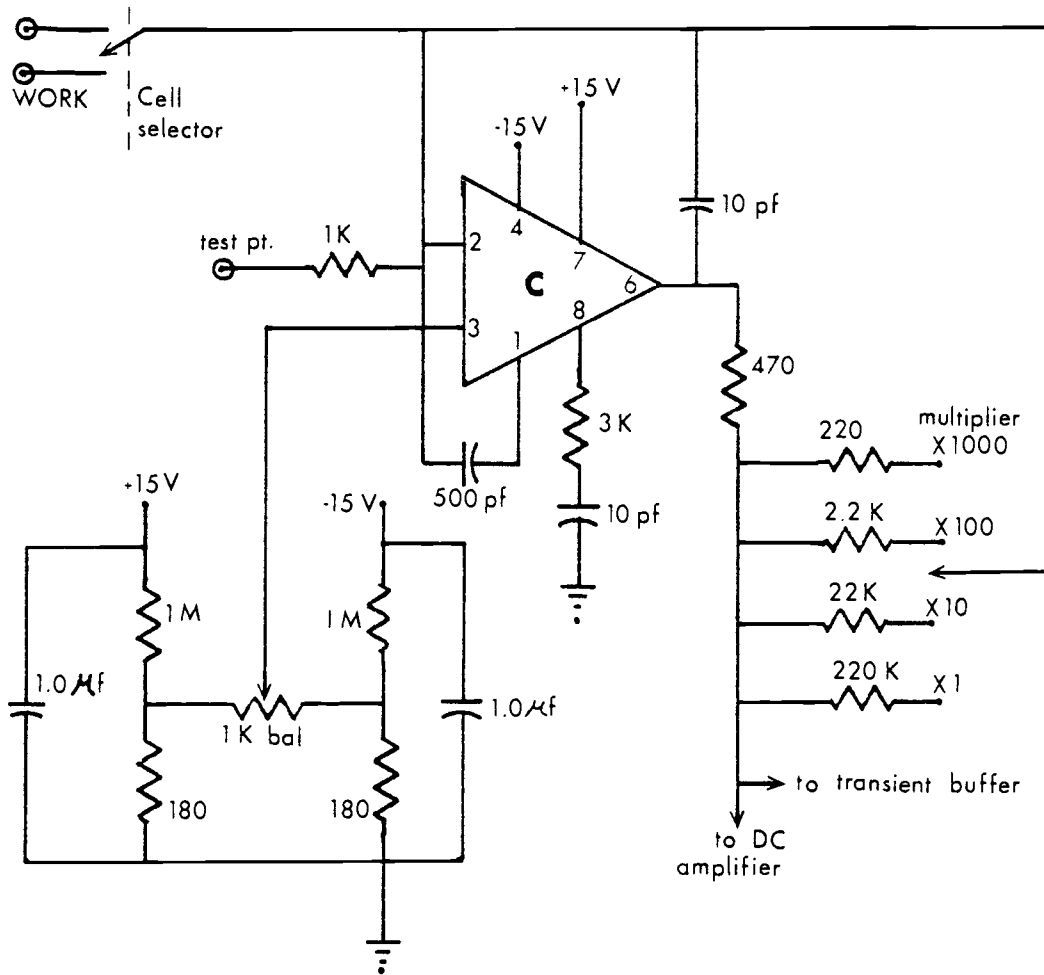


Figure 3. 1. 4. Current-to-voltage converter portion of the interface circuit. Amplifier C: Fairchild LM108H.



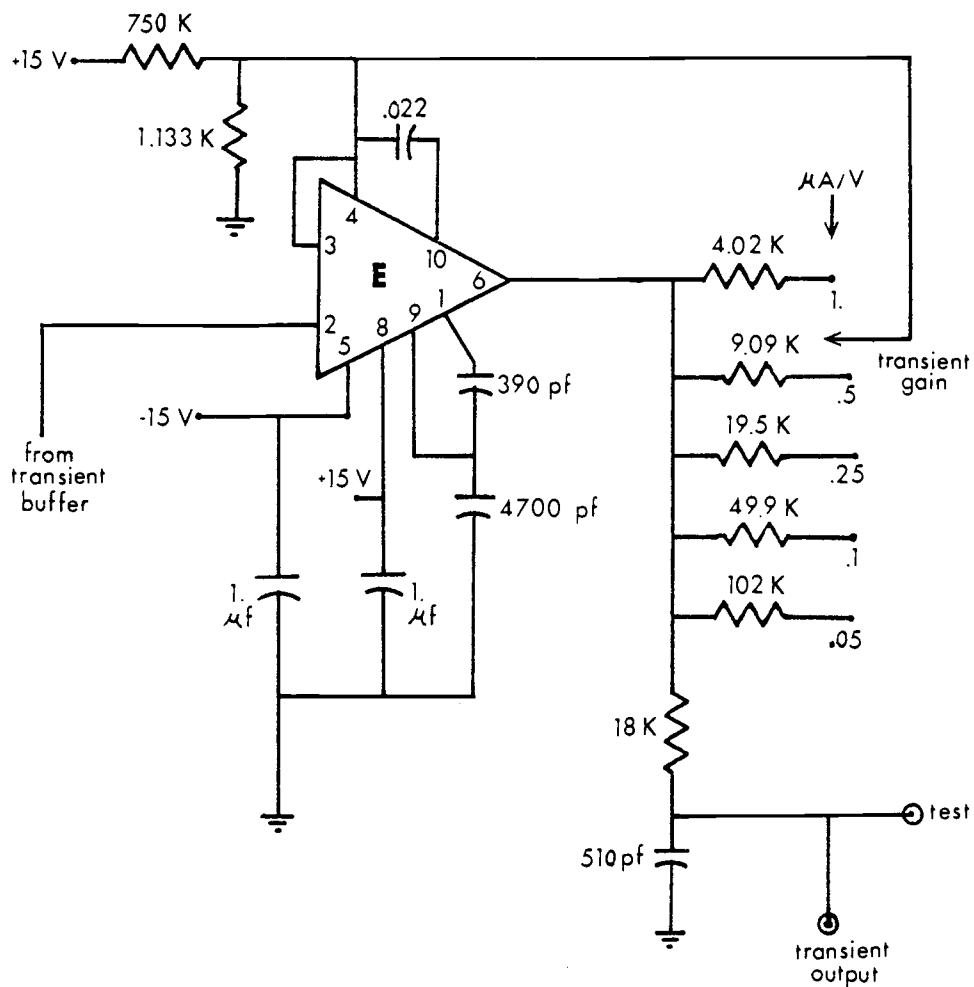


Figure 3.1.6. Transient amplifier portion of the interface circuit.  
Amplifier E: Analog Devices AD 505K.

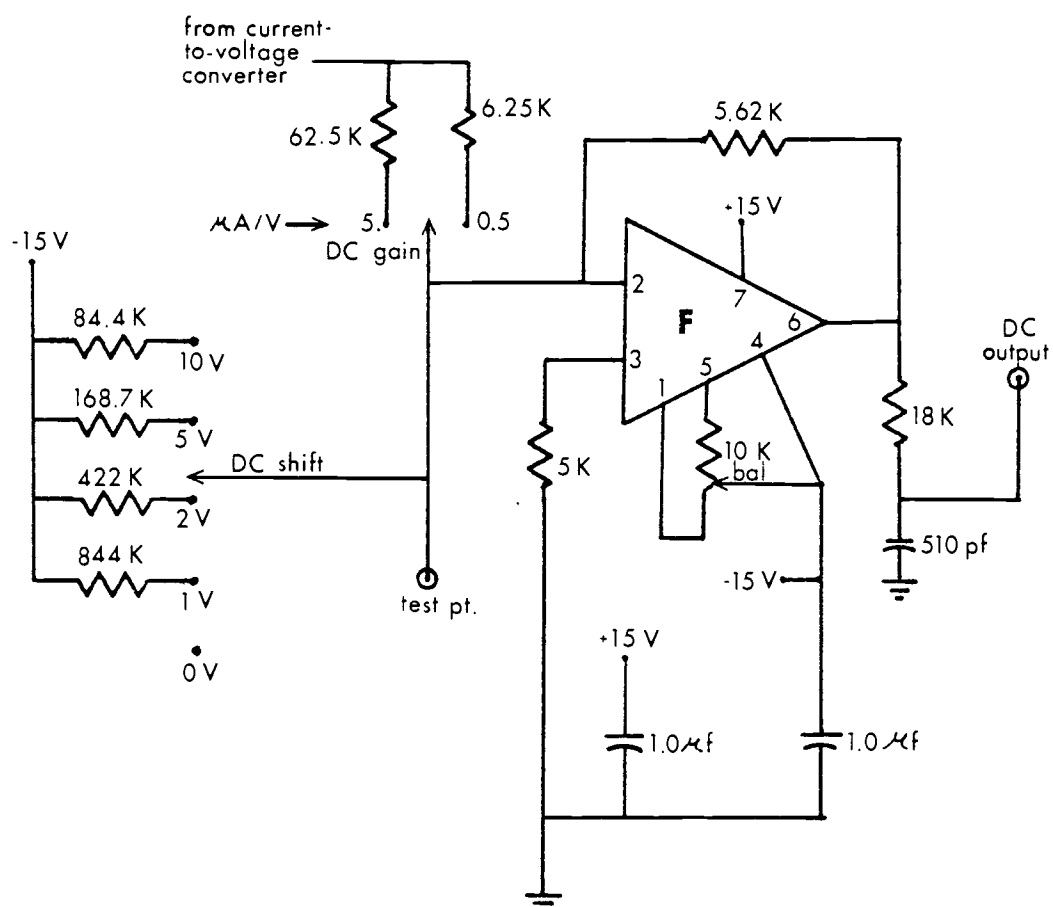


Figure 3. 1. 7. DC amplifier portion of the interface circuit.  
Amplifier F: Fairchild 741EHC.

current-to-voltage converter output is handled. This voltage is fed through a capacitor (Figure 3.1.5) to the input of a high impedance buffer amplifier (input current less than 2 pA), the output of which is amplified further (Figure 3.1.6), then sent to the analog-to-digital converter (ADC) of the computer. Normally, the input of the buffer amplifier is connected to a source of about +20 mV. Just before the residual current measurements are made, this source is disconnected by means of an FET switch which is controlled by the computer via an optocoupler. The input of the buffer amplifier is then free to rise and fall with the output of the current-to-voltage converter, but always offset by whatever potential difference was across the capacitor when the switching occurred. The switch is returned to the normal state after the last measurement is made on each transient. The transient amplifier is designed to amplify only the difference between the buffer output and the +20 mV initial level. By selecting the various feedback resistors on the current-to-voltage amplifier and the transient amplifier, the output sensitivity for the transient current can be changed from 0.05  $\mu\text{A/V}$  to 1 mA/V with three sensitivities available in each decade.

This design permits a considerable amount of residual cell current to flow without driving the transient signal offscale. The level of the residual current has no effect on the capacitance measurements, although it cannot change appreciably during each iteration of the step



voltage. Thus, measurements at different cell potentials can be made in quick succession without having to make any adjustment for the different residual currents which may flow.

Since the transient system does not display the full cell current, another amplifier (Figure 3.1.7) was included for this purpose. This amplifier permits a limited amount of gain adjustment and includes a DC shift network to permit the display of anodic current on a positive scale. The output of this amplifier was connected to a strip chart recorder (Model SR-255 A/B, Heath Company, Benton Harbor, Mich.) to obtain a record of cell current during the capacitance measurements. Both the DC and transient amplifier have 10  $\mu$ s filters at their outputs to reduce high-frequency noise.

Power for the operational amplifiers in this instrument was taken from a variable-voltage dual power supply (Model 1500, Spar Electronics, Inc., San Diego, Calif.) set to  $\pm 15$  V. In order to reduce "cross-talk" between sections, 1.0  $\mu$ f "decoupling" capacitors were placed between each power lead and the zero reference conductor (signal ground) at the point where power was brought into each section of the instrument.

The computer was a PDP-11/20 (Digital Equipment Corporation (DEC), Maynard, Mass.) equipped with a DEC AA11-D digital-to-analog converter (DAC), a DEC AD01-D analog-to-digital converter (ADC), a DEC KW11-P programmable interval clock, and two DEC

DR11-A general device interfaces for input and output of digital information. Other features of the computing system are 8K words of core memory, high-speed paper tape reader and punch, and a graphics terminal (Model T-4002, Tektronix, Inc., Beaverton, Ore.) equipped with a hard-copy unit (Model 4601, Tektronix).

The DAC has two outputs, each with a range of  $\pm 10$  V, and output impedance specified at less than one ohm. The 12-bit buffer (including sign bit) yields a resolution of 5 mV.

The ADC is a ten-bit unipolar serial-approximations converter with a range of 10 V and a rated accuracy of 0.1%. Conversion time is specified to be 22  $\mu$ s including addressing time; input impedance is 1000 megohms in parallel with 20 pf.

The interval clock employs a crystal oscillator and operates under program control; count rates of 100 KHz, 10 KHz, and line frequency may be established. The clock has interrupt capability, i. e., it may interrupt a running program to initiate another process (for instance, the acquisition of data) after a given number of counts.

Since this general purpose computer was used in several other research projects, being wheeled between laboratories as necessary, an interface panel was designed for it, so that electrical connections could be made quickly and easily. The panel uses BNC jacks for the analog signals so that connections could be made with coaxial cables;

the digital signals are presented at multi-pin jacks for connecting flat multi-conductor cables.

The two channels of the DAC, connected to the two inputs to the potentiostat, provide a DC bias potential (initial potential) and the step potential required for the capacitance measurement. The DC equation describing the potentiostat control, developed in Appendix 2, is

$$E_{\text{cell}} = R_6 \left[ \frac{V_{\text{DA0}}}{R_0} + \frac{V_{\text{DA1}}}{R_1} \right] \quad (3.3.1)$$

where the meanings of the symbols are indicated in Figure 3.1.3.

(This equation applies only for signals which change much more slowly than the time constants of the potentiostat circuits.)

Since the initial potentials and the step potentials desired will always be within the ranges  $\pm 5$  V and  $\pm 100$  mV, respectively, and the DAC outputs have a  $\pm 10$  V range, the resistor ratios  $R_6/R_0$  and  $R_6/R_1$  were chosen to be about 0.5 and 0.01, respectively. This design allows the potentials to be set as precisely as possible, while maintaining adequate range.

It was not necessary to know the individual resistances for  $R_0$ ,  $R_1$ , and  $R_6$ , as calibration was easily handled by insertion of appropriate calibration factors in the controlling program. These calibration factors were determined by placing randomly chosen

numbers in the 12-bit DAC output registers and carefully measuring the potential produced at the cell potential test point (Figure 3.1.3).

These potential measurements were made with a voltage reference source (VRS Model EU-80A, Heath Co., Bonton Harbor, Mich.) and a digital microvoltmeter (Model 8200A, John Fluke Manufacturing Co., Inc., Seattle, Wash.). The VRS input was connected between the cell potential test point and the zero reference conductor; the microvoltmeter was connected to the VRS output. With the VRS in the difference mode, and adjusting its dials to obtain zero output, the cell potential is displayed on its face. This procedure was used to take advantage of the 0.1% stability of the VRS voltage. (This degree of stability could not be obtained with the microvoltmeter.) Ten of these measurements were made for each channel of the DAC, keeping the channel not being tested set to zero.

The data for each channel was fitted to a linear least-squares line. The calibration factors were determined from the slopes of the lines to be  $452.1 \pm 0.1$  DAC counts/volt for the initial potential and  $22.282 \pm 0.005$  DAC counts/millivolt for the step potential, where the tolerances given are the standard deviations in the slopes calculated in the least-squares computation. The intercepts were close enough to zero ( $< 0.5$  mV) to be ignored.

The measurements were made with only negative potentials for  $V_{DA0}$  and only positive potentials for  $V_{DA1}$  because it was found that there was a significant non-linearity at the zero-crossing in the outputs of both DACs. This was satisfactory for the experiments being conducted, since only negative cell potentials and positive-going steps were used. A few of these measurements were repeated each day that the system was used; the calibration did not change over the several months of use.

A major problem in interfacing the potentiostat was in eliminating various types of noise introduced into the potentiostat by the computer. Analog noise in the computer ground conductors may easily be a tenth of a volt without impairing the operation of the computer; however, if this noise is allowed into the potentiostat circuit, the low-level signals there may easily be obscured. Accordingly, the grounding and shielding of the system (Figure 3.1.1) is important. To prevent unnecessary currents through the zero reference conductor, it was connected to the shield at the DAC ground terminal in the computer. The instrument shield was "segmented" from the shields of the cell and of the cables going to the computer (35, pp. 48-49), i. e., it was connected not to the cable shields, but to the shielded zero reference conductor from the DAC where the conductor enters the potentiostat shield. This technique provides the potentiostat with the best approximation of the zero reference potential, thus reducing

capacitative coupling of the shield potentials into the highly sensitive feedback elements. The cell lead was a shielded three-conductor cable. The shield of the lead was connected to the potentiostat shield to protect the high-impedance input to amplifier B from picking up ambient electric fields.

Provided that the interface power supply was turned on for several hours in advance, and the computer for at least five minutes, the four balance potentiometers were found to need adjustment very infrequently; nevertheless, the power supply voltages were checked and corrected to 15 V ( $\pm 0.01$  V) every few weeks, and the DC balance of the instrument was normally checked with the Fluke microvoltmeter within a few hours before the capacitance measurements were conducted. The balancing procedure is as follows:

- 1) The instrument was connected to a dummy cell or to the reference and auxiliary electrodes of a real cell.
- 2) The DAC outputs of the computer were set to zero volts.
- 3) The transient buffer switch (Figure 3.1.5) was set to the normal state (bit #1 of the DR11-A set to 1).
- 4) The test point in the potentiostat circuit (Figure 3.1.3) was monitored and adjusted to  $0 \pm 100 \mu\text{V}$  if necessary with the balance potentiometer of amplifier A.
- 5) The current-to-voltage converter test point (Figure 3.1.4) was monitored and adjusted to  $0 \pm 100 \mu\text{V}$  if necessary with

the balance potentiometer for amplifier C.

- 6) The transient amplifier test point (Figure 3.1.6) was monitored. With the transient sensitivity set to  $0.05 \mu\text{A/V}$ , the test point was set to  $+20 \pm 1 \text{ mV}$ .
- 7) The DC amplifier test point (Figure 3.1.7) was monitored and adjusted if necessary to  $0 \pm 100 \mu\text{V}$  with the balance potentiometer of amplifier F.

The one part of the cell-to-computer interface which remains to be discussed is the electrode dropper, a device for automatically immersing the test electrode at the beginning of the series of measurements and removing it at the end. This device employs a solenoid under computer control. Figure 3.1.8 is a pictorial diagram of the device. The electrode body (a  $3/8$ " diameter Teflon rod) is mounted on the lower end of the Teflon rod of the dropper with a small piece of rubber tubing. When the solenoid is activated, the electrode is lifted from the solution; when deactivated, the electrode is dropped into the solution.

Figure 3.1.9 shows the circuit for switching the solenoid current. A TTL low at bit #0 of the DR11-A forward-biases Q1, cutting off the base current to Q2. Thus, the solenoid is deactivated and the electrode is down. A logic high at the input to this circuit causes the emitter of Q1 to have a higher potential than that of the collector. This results in reverse operation of Q1, which provides

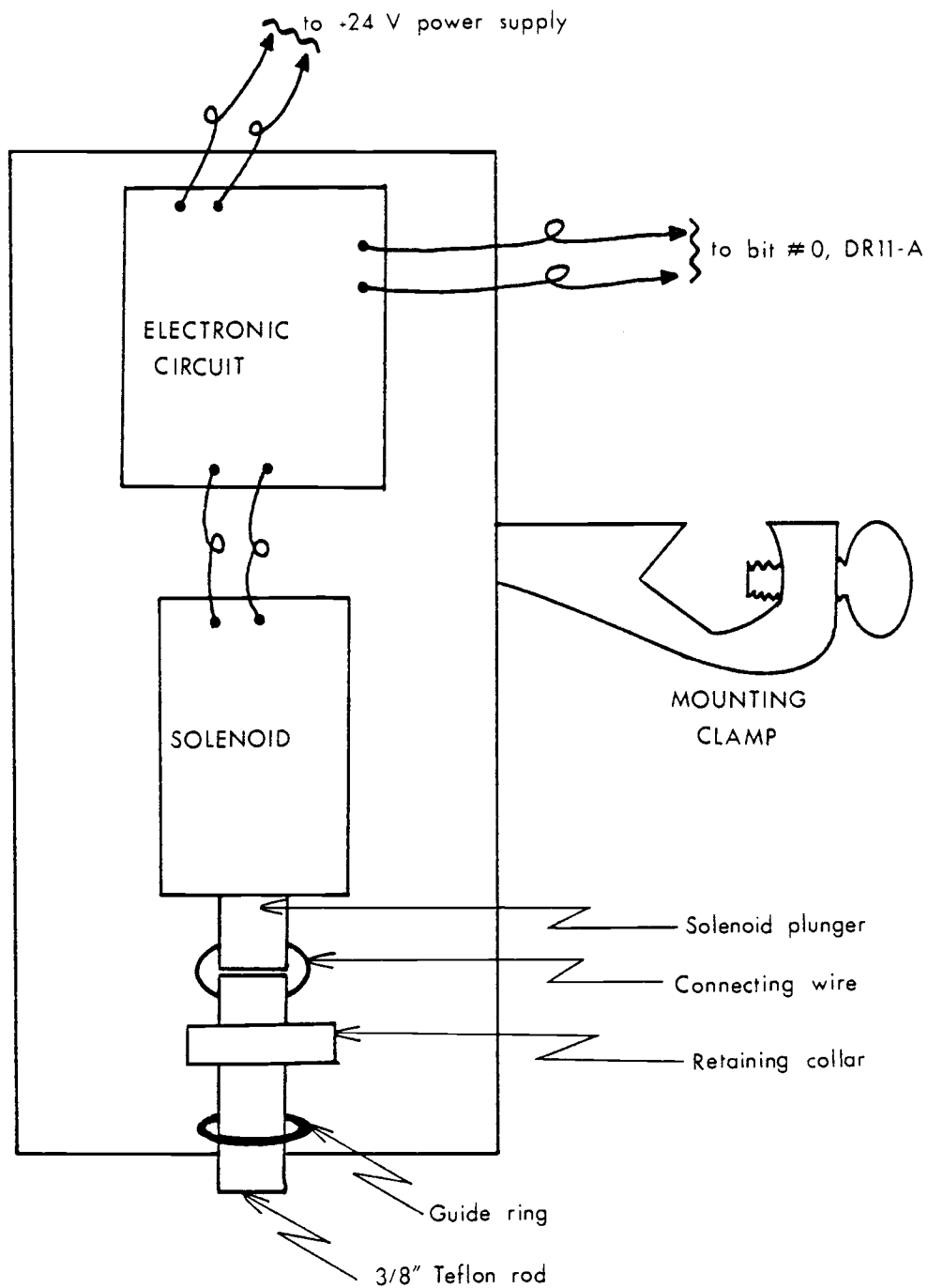


Figure 3.1.8. Pictorial diagram of the electrode dropper.



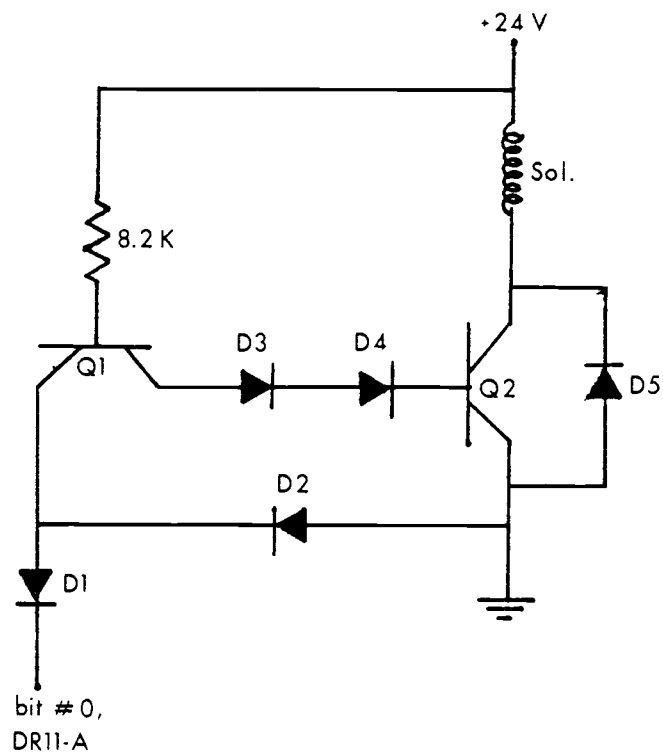


Figure 3.1.9. Schematic diagram of the electrode dropper interface circuit. Q1: SE8541. Q2: 2N4237. D1, D2, D3, D4, D5: silicon signal diodes. Sol.: Deltrol Model D30 solenoid, 80 ohm.

base current for Q2. In this condition the solenoid is on, and the electrode is up. Power for this circuit is obtained from another Spar deluxe dual power supply with the two outputs connected in series to make a total of 24 V.

### Programming

Programs were written to enable the PDP-11 to control the potential-step measurement, to acquire the data, and to calculate desired quantities from the data. Functions such as punching the data onto paper tape and plotting the data on the Tektronix graphic terminal were also included in the programs.

Programs were written in two languages, BASIC and PAL-11. BASIC is a relatively high-level language designed to facilitate computations with floating-point numbers on small computers. Input and output routines for the teletype (or Tektronix terminal) are part of the BASIC program. The BASIC language is similar in level to FORTRAN; many statements in BASIC have analogous statements in FORTRAN. However, there are fundamental differences in their operation. A FORTRAN program is compiled in its entirety before execution; a BASIC program is compiled and executed line-by-line. An object program cannot be obtained. The BASIC package contains a run-time editing feature. The result of these differences is that FORTRAN is

quicker in execution, but that BASIC makes program changes much easier.

PAL-11 is the DEC assembly language for the PDP-11. After a PAL-11 program is written it is compiled by the PAL-11 compiler which produces a paper tape containing the equivalent binary instructions (machine language). This binary (object) program is loaded into core memory and executed.

Both types of programming were used since it was desired to have both the convenient computational capability of BASIC and the capability of assembly language for accessing particular computer addresses. Whereas BASIC automatically chooses arbitrary locations for storing numbers, experimental control and the taking of data necessitate that particular locations, such as control and status registers and data buffers of the input-output devices, be accessed individually.

Three program packages, named CAP, PLT, and CCPVE, were written to obtain and interpret the capacitance data. All are quite similar in construction; each consists of a BASIC program with subroutines written in PAL. The functions performed by these packages are contained in program modules, which are indicated in Table

3.1.1. The operator may indicate which module is to be performed by typing the corresponding module number. Generally speaking, CAP contains the modules necessary to specify how the measurements are

Table 3.1.1. Functions performed by the program modules.

Module Number	Program	Function
0	CAP	Make a series of capacitance measurements.
1	CAP	Print the sequence numbers of capacitance measurements containing offscale data.
2	all	List the data on the graphics terminal.
3	CAP	Punch the parameters for the measurement onto paper tape.
4	PLT	Plot current vs. time.
5	PLT	Plot $\ln(I_j - I_s - I_b)$ vs. $t_j$ .
6	PLT	Plot residuals of the current measurements from the least-squares line vs. time.
7	all	Calculate $C$ , $R_u$ , and $R_F$ . (In CCPVE, the printing of results is optional.)
8	CAP	Punch the data onto paper tape.
9	all	Input the measurement parameters from the keyboard and/or from paper tape. (Abbreviated in PLT and CCPVE for input from tape only.)
11	all	Input old data from paper tape.
12	all	List the measurement parameters.
13	all	Input the value of the effective overall feedback resistor for the current-to-voltage converter.
14	all	Input the maximum and minimum times for the data to be used in the calculation of module 7.
15	CCPVE	Calculate, list, and plot the specific capacitances and standard errors of the specific capacitances.
16	CCPVE	Input the electrode area and its uncertainty.

to be made, to take the data, to list it, and to calculate the capacitances according to the method previously discussed, PLT contains the modules necessary to make diagnostic plots of the data points for a capacitance measurement, and CCPVE calculates the specific double layer capacitances for a series of measurements and plots them vs. cell potential. Appendix 3 contains listings of each of these program packages.

### Operation of the Programs

Figure 3. 1. 10 is a demonstration of the use of CAP. The parts typed in by the operator have been underscored. The following remarks are keyed to the labelled points on Figure 3. 1. 10.

A. The BASIC program is loaded into the computer memory using the high-speed paper-tape reader and the program announces itself.

B. BASIC is instructed to halt so that the machine-language subroutines may be loaded using the high-speed paper-tape reader. After the loading, BASIC is automatically restarted and announces that it is "ready."

C. This command causes the BASIC-language program CAP to be loaded from the high-speed paper-tape reader.

D. The line containing the potentiostat calibration factors is listed to assure that the most recent calibration factors are present.

Figure 3. 1. 10. A conversation with CAP.

**A** PDP-11 BASIC, VERSION 007A  
**B** #0 H  
 READY  
**C** OLD  
 READY  
**D** LIST3300  
 3300LETK1=452.1:IFM>4THENLETK1=22.202  
 READY  
**E** RUN  
 SUPERVERSION(11-6-73)  
**F** CHOOSE?9  
**G** NO. SETS TO READ?  
**H** DONE,DELETE,CHANGE,ADD;0,1,2,3?3  
**I** SEQ?1  
**J** ?-1  
?7  
?1  
? .015  
?10  
? .0015  
?10  
?1  
**K** ERROR AT PARAM \*?6  
**L** SEQ?  
**M** NO. SETS TO READ?  
**N** DONE,DELETE,CHANGE,ADD;0,1,2,3?  
**O** CHOOSE?3  
**P** BEGIN,END SEG \*?1,B  
**Q** CHOOSE?  
**R** GO,LIFT WHEN DONE?  
**S** CHOOSE?2

```

BEGIN,END SEG *21,1
RUN * 1 TIME IN SEC
INIT. -.3997788 U START 1
STEP 7.001167 MU ITER .015
MAX OUT 1.25 U DECAY .0015
RF
ERROR 123 AT LINE 1420
0 OHM
NO. ITER. 10 NO. PTS. 10
TIME VOLTS
.00015 .3027344E-1
.0003 .2990723E-1
.00045 .2905273E-1
.0006 .2893066E-1
.00075 .0279541
.0009 .0279541
.00105 .2807617E-1
.0012 .2746582E-1
.00135 .2819824E-1
.0015 .2868652E-1
.00015 .8479004
.0003 .6987305
.00045 .576416
.0006 .4769287
.00075 .394043
.0009 .3278809
.00105 .2735596
.0012 .2301025
.00135 .1923828
.0015 .1621094

```



T CHOOSE?13

200100

U CHOOSE?14

2.9

V CHOOSE?8

X CHOOSE?7

BEGIN,END SEG •1.1

		TIME IN SEC	
RUN •	1		1
INIT.	-.9997788 V	START	.015
STEP	7.001167 MV	ITER	.0015
MAX OUT	1.25 V	DECAY	
RF	200100 OHM		
NO. ITER.	10	NO. PTS.	10

FOR DATA BETWEEN 0 AND 9 SEC

	RES CURR	GAMMA	
	.1431779E-6	.1240026E-7	10
STD. DEVS.	2.352695 %	194.3703 %	.5000873E-5
			.3112523E-1 %

TAU= .740607E-3 SEC

RUNC= 1396.524 OHMS +/- .4836922 %

RFAR= 562837.9 OHMS +/- 194.3709 %

CAP = .5316376E-6 UF +/- .9662633 %

Y CHOOSE?

If re-calibration is required, this line could be changed by simply retyping it, including the line number, at this point.

E. The program is started and announces itself (the "super-version" of CAP).

F. Module #9 is selected to input the parameters for a measurement.

G. Since no parameters are to be read from paper tape, a zero is indicated by typing a "carriage return."

H. Typing a "0" (a carriage return has the effect of a zero) here would terminate the execution of module #9. A "1" would indicate that the next parameter set(s) on the tape being read are to be skipped. A following question would ask for the number of sets to skip. A "2" would cause the next parameter set(s) to be read in with changes. Questions would follow to determine which parameters are to be changed, and in how many sets they are to be changed. The "3" which is entered requires that all the parameters in the set be entered from the keyboard.

I. The sequence number of the current parameter set is entered.

J. The measurement control parameters are entered in the following order:

- 1) Initial cell potential (volts),
- 2) Step potential (mV),

- 3) Initial delay time before the first step (sec),
- 4) Time to wait between iterations of the measurement cycle (sec),
- 5) Number of iterations of the measurement cycle,
- 6) The length of time that the data is to be taken after application of the step potential (sec),
- 7) The number of current measurements to be obtained both before and after application of the step potential,
- 8) Maximum allowable output to the ADC in volts. This causes the full scale sensitivity of the ADC to be set to 1.25 V, 2.5 V, 5.0 V, or 10.0 V, whichever is smallest but larger than the number entered. (In this case, the 1.25 V scale would be selected.)

K. A negative number indicates that no errors have been committed in entering the parameters. Entering a (positive) parameter number allows that parameter to be changed.

L. Another set of measurement parameters is requested, but entering a sequence number of zero terminates this request.

M. No parameter sets are to be read from paper tape.

N. All desired parameters have been entered, so execution of module #9 is terminated. (Up to 25 sets of parameters could have been entered.)

O. Module #3 causes the parameters to be saved on paper tape.

P. The sequence numbers of the parameter sets to be punched are requested. The numbers are inclusive. Entering "1,8" would cause the first through the eighth sets to be punched, if there were that many. If not, it punches all the sets. In this case, only one set is punched, since only one had been entered.

Q. Choosing module #0 indicates that double layer capacitance measurements are to be executed according to the parameters entered in module #9.

R. Any response causes the measurements to be executed. A "1" would cause the electrode to be raised out of the solution upon completion of all the capacitance measurements. A "carriage return" causes the electrode to remain in the solution at the potential for the last measurement. The data are stored in place of the parameters, so module #9 must be re-executed before more measurements can be made.

S. Module #2 lists the data.

T. The error in the data heading above indicates that the feedback resistance had not been entered. Module #13 allows this to be done.

U. Module #14 allows the operator to specify the time range (after application of the step) over which the data are to be considered valid. Thus, any offscale data may be omitted from the calculations. In this case, the entry permits data from zero to nine seconds after

the step to be used (i. e. , all the data).

V. Module #8 causes all the data taken in the last execution of module #0 to be punched onto paper tape.

X. Module #7 calculates the double layer capacitance and other quantities relating to the measurement. ("Res curr" refers to  $I_b$ , "gamma" to  $I_s$ , "I0" to  $I_o$ , and "tau" to  $k_2$ . The other abbreviations should be self-evident.)

Y. Program CAP does not terminate by itself. However, its operation may be interrupted at any time by hitting the "DLE" key on the Tektronix terminal or the "control P" if the teletype is being used. Following the interruption with the statement "GO TO 185" causes the program to print "CHOOSE?" so that another module may be executed. Stored variables are not lost in this interrupt-and-restart procedure.

A paper tape containing the appropriate parameters must be placed in the tape reader before execution of modules #1, 2, 7, 8, and 12. A parameter tape is required for module #9 as well, unless input is entirely from the keyboard. If a tape is not in the reader, the computer halts; it may be restarted by placing the proper tape in the reader and pressing the "continue" switch on the computer console.

The programs PLT and CCPVE operate in much the same way as CAP. PLT contains only the segments necessary for the plotting (vs. time) of the current,  $\ln(I_j - I_s - I_b)$ , or the residuals from the linear least-squares fit. Figure 3.1.11 is a sample of the current vs.

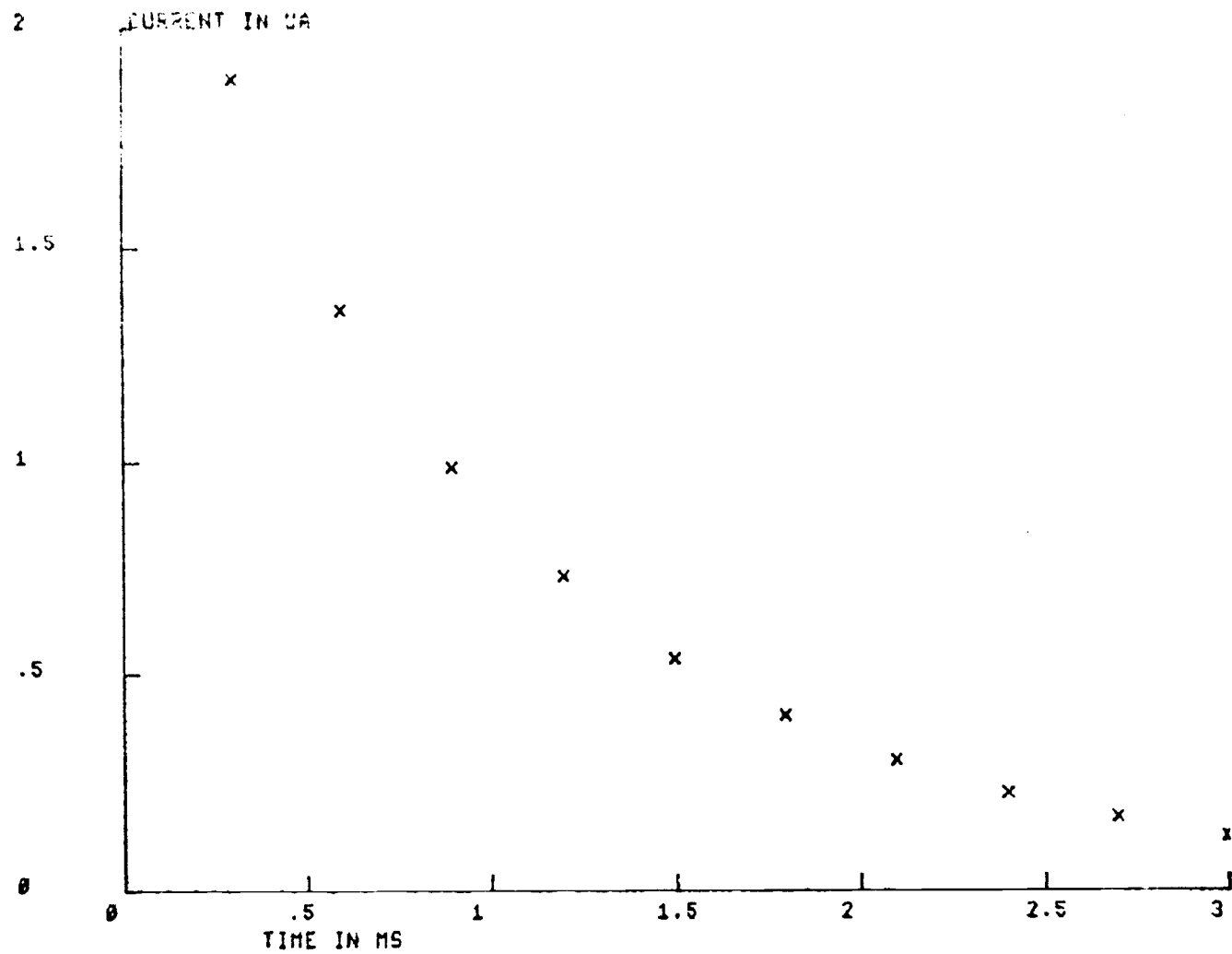


Figure 3. 1. 11. A typical plot of cell current vs. time produced by CCPVE.

time plot produced by PLT, and Figure 3. 1. 12 shows a least-squares residual plot. CCPVE contains only the segments necessary to plot  $C_{dl}$  vs.  $E_{cell}$ ; Figure 3. 1. 13 is an example of this type of plot.

### The Cell and Electrodes

The cell used for the capacitance measurements was a three-chamber type made of Pyrex glass; the chambers are connected via medium-porosity glass frits. The reference and auxiliary electrodes were placed together in one of the outer arms when concentrated electrolytes were studied, and in opposite arms for dilute electrolytes. The working electrode was inserted into the center chamber. (The different placement of the reference electrode was to make  $R_u$  of a size to produce a cell time constant of one millisecond or so in the solutions used.) The solution levels in the arms were kept lower than in the center chamber to prevent contamination of the electrolyte in the center chamber.

The cell was water-jacketed by means of a Plexiglas box through the top of which each arm of the cell was sealed. Water from a bath maintained at  $25.0 \pm 0.2$  C by a Cole-Parmer "Tempunit" and a cold-water coil was circulated through the jacket at about three liters per minute by a centrifugal pump with a magnetically driven impeller. A Delrin cover with holes for the test electrode and deaerating capillary reduced the likelihood of foreign material falling

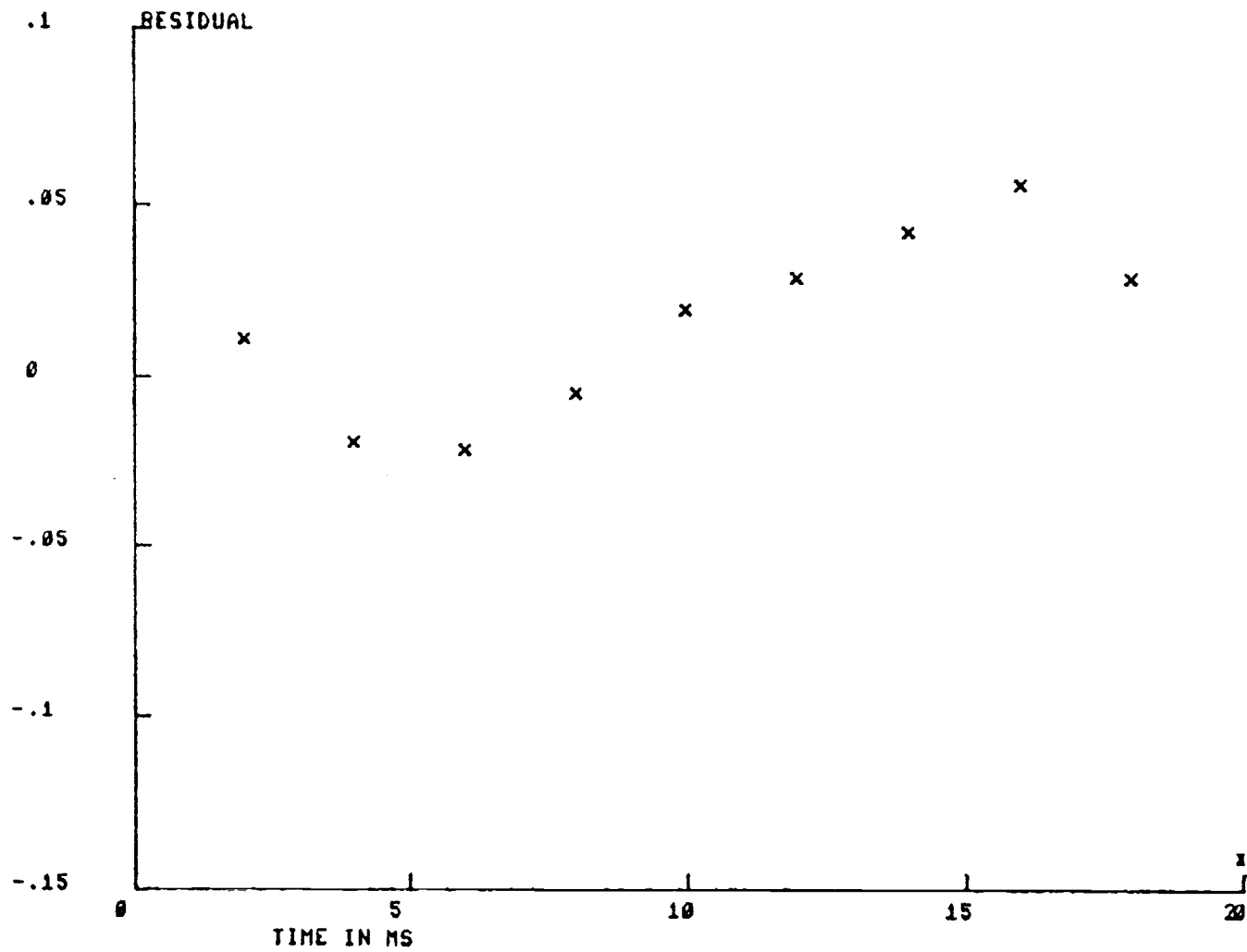


Figure 3. 1. 12. A typical plot of the least-squares residual vs. time produced by CCPVE.



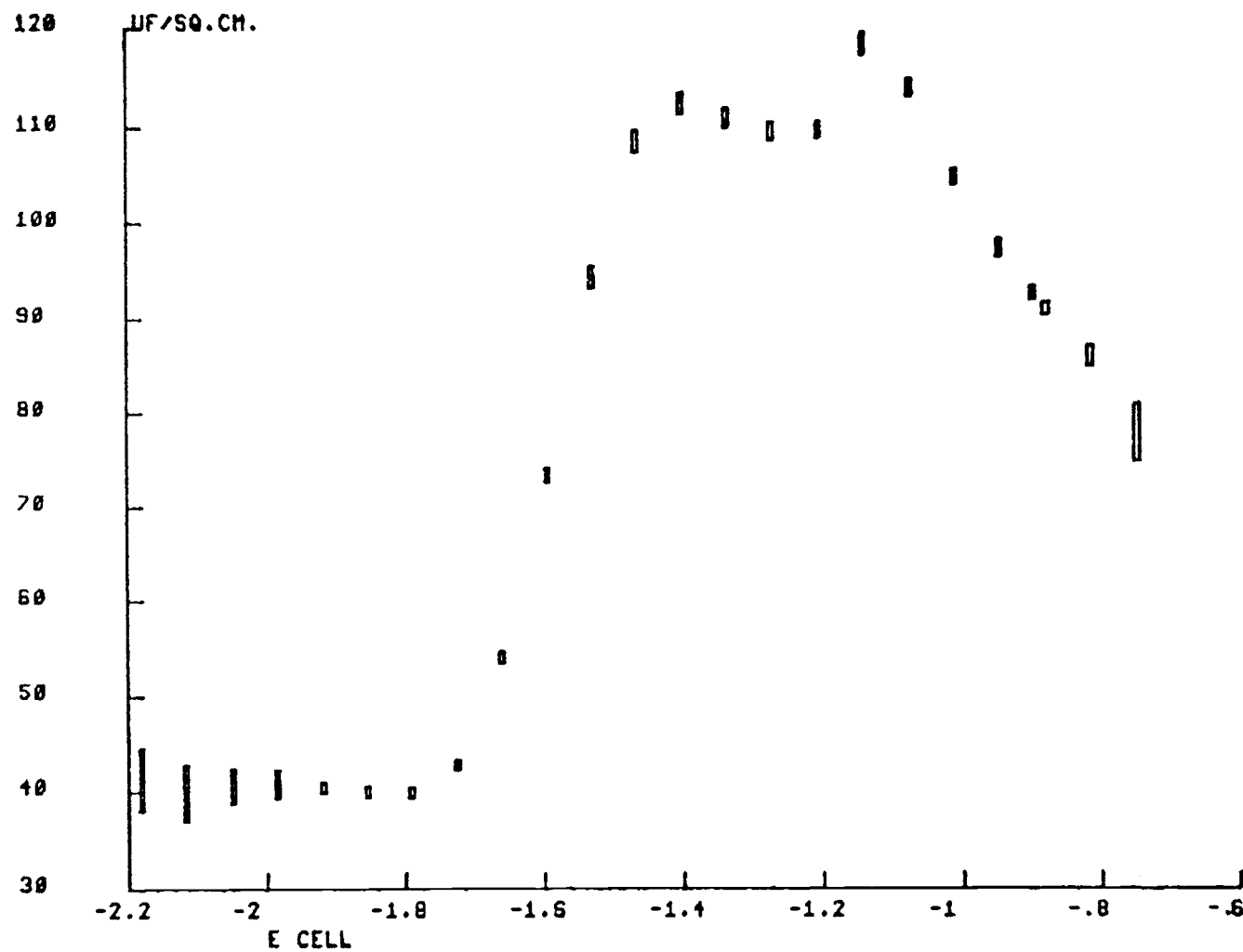


Figure 3.1.13. A typical plot of specific double layer capacitance vs. cell potential produced by CCPVE.

into the center chamber of the cell and lowered the rate at which air might mix with the nitrogen atmosphere over the solution.

Electrostatic shielding for the cell was provided by placing the cell and its water-jacket in a shield consisting of a box lined with copper wire screen. The shield was connected to the computer interface as shown in Figure 3. 1. 1. Sixty-hertz noise introduced through the water bath was eliminated by adding a large amount of sodium sulfate to the bath and connecting the bath to the cell shield by means of a one-foot piece of 1/8" diameter copper rod sealed through the Plexiglas water-jacket.

The working electrode used for the capacitance measurements was designed for use in the deposition transient measurements as well. It consisted of the cross-section of a 1/8-inch diameter silver wire ( $0.0792 \text{ cm}^2$  area) surrounded at a distance of about 0.005 inch by a copper ring, the purpose of the ring being to prevent non-perpendicular diffusion at the edges of the electrode in the deposition transient measurements. The ring was insulated from the disc by means of a Teflon sleeve. The ring and the disc were press-fitted together into a Teflon-rod body to form a flush, water-tight mount. The surfaces of both metals were ground to a rough finish with sandpaper, then with wet 500-mesh alumina first on smooth glass, then on cotton gauze. The final polishing stage was with "Gamal" (Fisher Scientific Company) gamma alumina particles of less than 0.1 micron

diameter in water on cotton felt.

Before the capacitance measurements were obtained, both the ring and disc were silver-plated at a current density of about  $5 \text{ mA/cm}^2$  using vigorous bubbling of nitrogen in a plating bath consisting of approximately 0.25 M AgCN, 0.35 M NaCN, 0.5 M  $\text{Na}_2\text{CO}_3$ , and 1.0 M NaCl. Under these conditions, the plating cell potential oscillated between about -0.87 V and -0.67 V vs. SCE with a period of about 30 sec. The reason for this oscillation was not investigated.

The measurements were performed on an electrode which had been cycled repeatedly through this plating and polishing on Gamal. (The rough grinding operations were performed only infrequently, when the electrode was new, and when the repeatedly plated surfaces of the ring and disc had nearly grown together.) After several cycles, a moderately reflective surface was formed. The final step of the electrode preparation was always the plating step, followed by a rinse with the glass-distilled water. The electrode was then immersed in the test solution, and the measurements were started.

The reference electrode was a ceramic-tip saturated calomel electrode (SCE) made by A.H. Thomas Company. Its lead was replaced with a phono jack mounted on top of the electrode so that the shielded cell lead from the potentiostat could be connected close to the electrode. This modification reduced the noise in the current

measurements considerably. A coil of platinum wire served as the auxiliary electrode.

### Solutions

Capacitance measurements were conducted in solutions containing amounts of sodium cyanide ranging from 0.0162 M to 0.942 M. In each of these solutions, an amount of sodium fluoride was included to bring the total electrolyte strength to 0.942 M. Measurements were also conducted in dilute sodium fluoride solutions (0.00500 M, 0.0100 M, and 0.0200 M). The concentrated solutions were prepared from reagent grade salts (sodium cyanide, Mallinckrodt #7616; sodium fluoride, B & A #2250) and water distilled in a Corning AG-3 all-glass still. The dilute solutions were prepared from "ultrapure" sodium fluoride (Alfa #87629) and water freshly distilled in the Corning still, then redistilled in a two-stage still made from standard taper glassware (joints assembled without lubricant). Each stage of this still employed a 50-cm Vigreux column; potassium permanganate was added to the first stage still pot. The solutions were filtered through a bed of powdered alumina (B & A #1236) which had been fired to 400 C for a few hours. All solutions were stored in Pyrex; they were usually used within a few days of preparation.

## Procedure

The cell was cleaned with chromic acid cleaning solution and rinsed thoroughly with the glass-distilled water. Then the center compartment was filled with the solution in which the measurements were to be made. The solution was then thermostatted and sparged for at least one hour with "prepure" nitrogen (Grade 4.5, Airco, Inc., Murray Hill, N.J.). The nitrogen was passed through a column of activated charcoal and introduced into the electrolyte by means of a disposable capillary pipet.

The potentiostat system was balanced, the program CAP was started, and the parameters were read in from a previously prepared paper tape using module #9. All the double layer capacitance measurements were conducted using ten iterations of the step potential, making ten measurements of the cell current during each step. The 1.25 V ADC sensitivity was used for all measurements. The values of the other parameters will be given in the results.

The auxiliary and reference electrodes were placed into the cell and connected to the potentiostat. The sparging was stopped. The test electrode was repolished and replated, rinsed, placed into the electrode dropper, and connected to the potentiostat. The computer-controlled measurement sequence and the strip-chart recorder for recording the cell current were then started simultaneously. The

measurement parameters invariably started with a waiting period at -1.7 V followed by another period at a potential anodic of the potential of zero charge. A stream of nitrogen bubbles was directed against the electrode at each of these potentials to wash away any small bubbles which might be present on the electrode surface. After the series was completed, the current measurements were checked to see if all were on scale (module #1), then stored on punched paper tape (module #8).

Several series of measurements were usually collected in one session. Sparging with nitrogen was resumed between the series. Before each series the electrode was repolished and replated.

### 3.2. Deposition Rate Measurements

#### Measurement Apparatus

The apparatus for making the deposition rate measurements is block diagrammed in Figure 3.2.1. The cell potential was controlled by means of a potentiostat (Model 173, Princeton Applied Research Corp., Princeton, N.J.) with a plug-in module (Model 179, Princeton Applied Research) to monitor the cell current. This potentiostat contains two potential sources, either one of which may be selected to be applied to the cell.

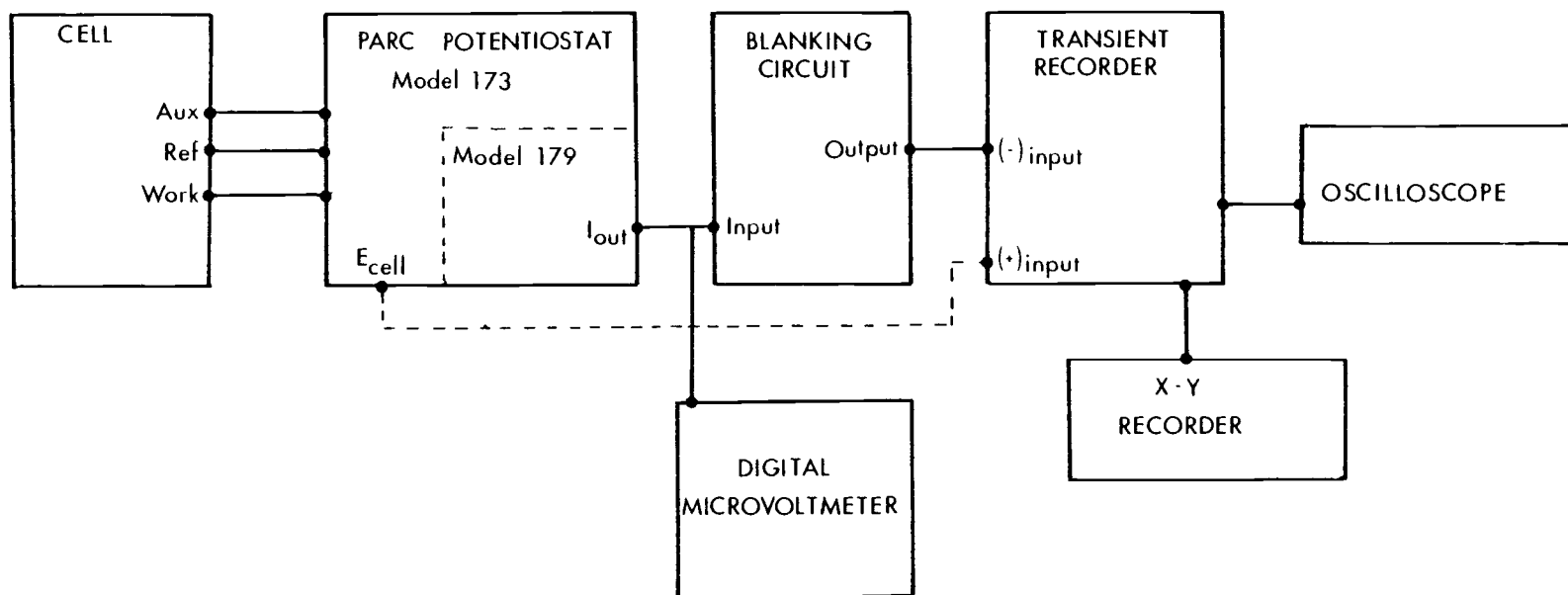


Figure 3.2.1. Block diagram of the deposition transient measurement apparatus.

The voltage at the point labelled " $I_{out}$ " on the Model 179 is proportional to the cell current, and is monitored with the Fluke digital microvoltmeter mentioned before. The voltage at " $I_{out}$ " is fed through a blanking circuit to the inverting input of a transient recorder (Model 610, Biomation Corporation, Cupertino, Cal.). The blanking circuit was necessary to prevent the transient recorder input amplifier from becoming saturated by the large capacitance spike when attempting to observe the relatively small signal later in the transient. The output of the blanking circuit normally is the same as the input. However, when the input rises above a set level, the output drops to nearly zero. Figure 3.2.2 is a schematic of the blanking circuit. The  $\pm 12.4$  V supply voltage for this circuit is obtained by using four Zener diodes to reduce the  $\pm 24$  V supply which is available at the accessory socket of the potentiostat.

The transient recorder, when triggered, records the input signal into a 128 word x 6 bit digital memory. The time interval over which the first 100 words of the memory are filled can be varied from 10  $\mu$ s to 5 sec by factors of 1, 2, and 5. The contents of the memory are repetitively displayed on the oscilloscope. When the "plot" button on the transient recorder is pushed, the memory is played out onto the X-Y recorder (Model F-80, Hewlett-Packard, Palo Alto, Cal.) at a rate of ten words per second. The trigger input of the transient recorder was connected to an output on the potentiostat which changes



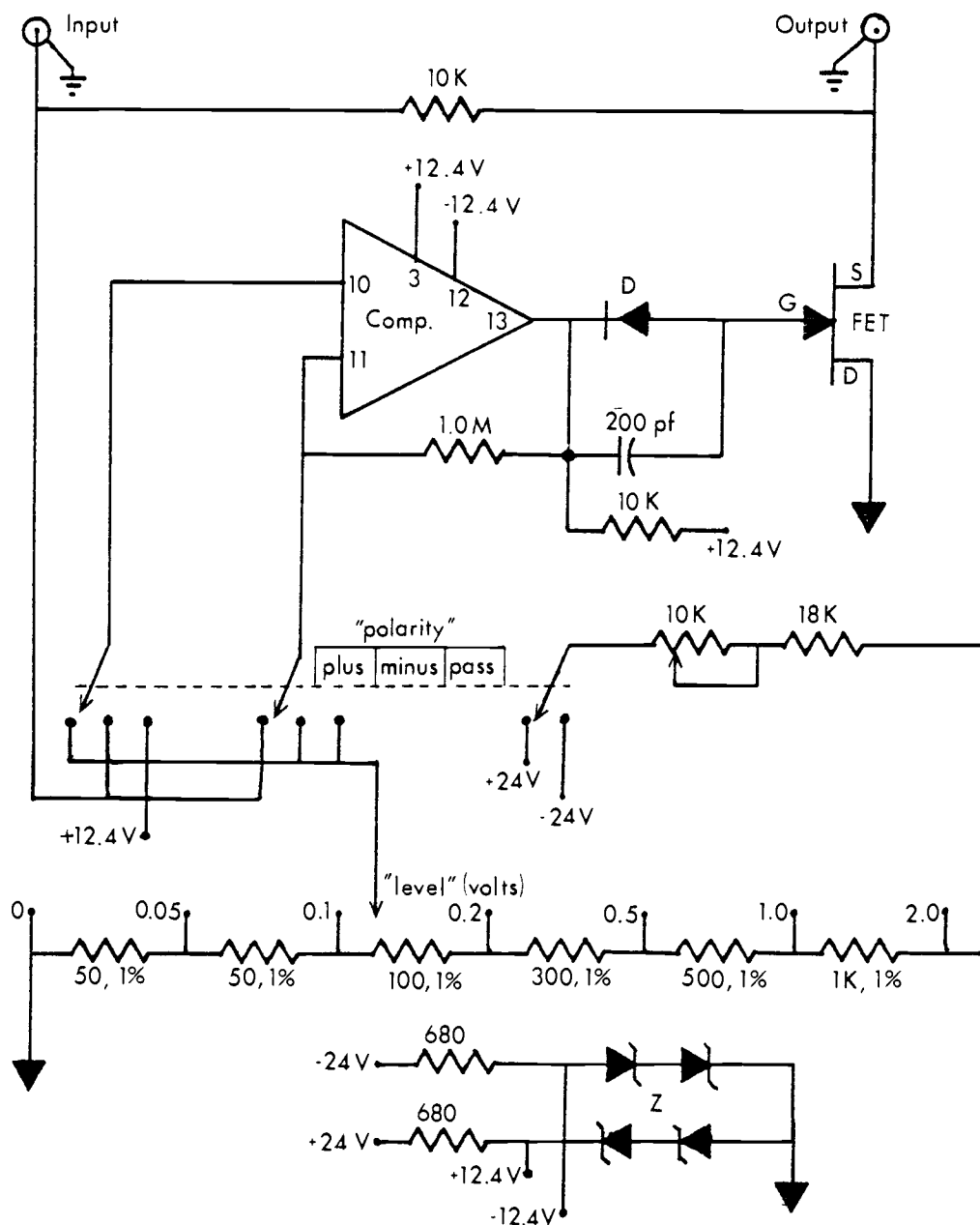


Figure 3.2.2. Schematic diagram of the blanking circuit. Comp.: 1/4 of a Fairchild LM399. D: 1N456. FET: 2N5457. Z: 1N4735.

state when the potentiostat is switched from one of its potential sources to the other. Thus, when the step potential was applied by switching between the two sources, the transient was recorded.

### Cell and Electrodes

The measurement cell was the same as for the double layer capacitance measurements, although only the center compartment was used. The cell was maintained at  $25.0 \pm 0.2$  C in the same way as described previously.

The working electrode was the same as for the other measurements and was prepared in the same way. Again, only the disc part of the electrode was connected to the test electrode lead of the potentiostat. The ring, however, was connected to the ground clip of the potentiostat. Since the potentiostat holds the test electrode at a virtual ground, the ring has the same potential as the disc. Thus, diffusion of solution species to the ring is the same as that to the disc, thereby eliminating any non-perpendicular diffusion which might otherwise occur at the edge of the disc. The auxiliary electrode supplies current for both the disc and the ring, but only the current drawn by the disc is measured, the rest being drawn to ground through the ring.

The reference electrode was the same commercial ceramic-tip SCE as described before. For the deposition rate measurements,

however, the reference electrode was placed in a tube drawn out to a fine J-shaped capillary, (a "Luggin" capillary) the end of which was placed within a millimeter or so of the surface of the disc. The tube was filled with the test electrolyte.

The auxiliary electrode was made of a 19-gauge platinum wire wound into a one-centimeter helix which was placed around the Luggin capillary tip. This close placement of the auxiliary electrode produced a low total cell resistance, which enhanced the rise-time of the potentiostat. The slight amount of product (presumably oxygen) produced at the auxiliary electrode has no effect on the measurements.

All three electrodes were held in the cell in a fixed geometric arrangement by means of a specially designed cell lid made of Delrin plastic. Figure 3.2.3 shows this. The auxiliary electrode passes through a notch in the cell lid next to the Luggin capillary. Both the Luggin capillary and the auxiliary electrode are prevented from moving by two tight-fitting notched Teflon rings (parts F in the figure). The test electrode is held in a snug Delrin collar which may be moved horizontally in a slot in the cell lid and fixed into position with screws. Vertical positioning of the working electrode is provided by slipping the tight-fitting Teflon ring (part G in the figure) to the desired position.

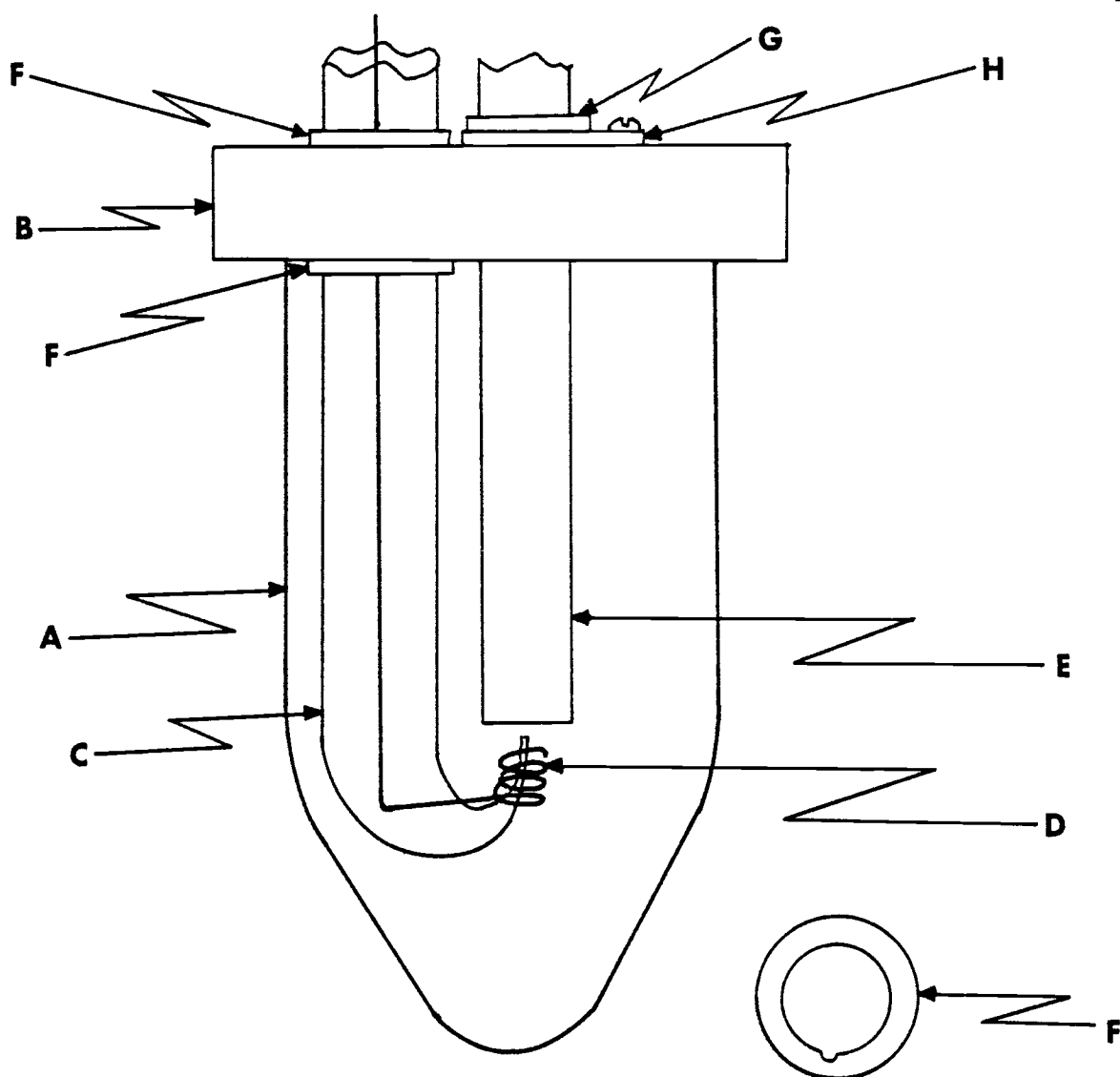


Figure 3.2.3. Pictorial diagram of the deposition transient measurement cell. A: Pyrex cell. B: Delrin cell lid. C: Pyrex Luggin capillary. D: Platinum auxiliary electrode. E: Ring-disc working electrode with Teflon body. F: Notched Teflon retaining rings. G: Teflon ring. H: Movable Delrin collar.

## Solutions

The deposition current transients were measured in solutions containing 0.03 M AgCN and amounts of NaCN ranging from 0.05 M to 1.0 M. The ionic strength was adjusted to 1.0 by addition of NaF. The solutions were prepared from pure AgCN (B & A #2182), reagent grade NaCN (Mallinckrodt #7616), reagent grade NaF (B & A #2250), and water distilled in the Corning AG-3 all-glass still. Some solutions were filtered through alumina as for the capacitance measurement solutions, but it is doubtful that this has any effect. All solutions were stored in glass; they were usually used within a few days of preparation. Immediately before the measurements the solutions were sparged for at least one hour with prepure nitrogen which was first passed through activated charcoal.

## Procedure

After sparging the test solution, the electrode was prepared and positioned in the solution close to the Luggin capillary. The disc electrode was connected to the working lead of the potentiostat, and the ring to the ground lead.

The potentiostat was switched to the "external cell" position and the cell potential was adjusted to make the voltage at  $I_{out}$  equal to zero. Then a stream of the nitrogen was directed across the face

of the electrode to clear it of any tiny bubbles which might be present.

Immediately afterwards, the potentiostat potential sources were switched momentarily to produce the cathodic potential step, and the transient signal was played out onto the recorder. Measurements of the current transient were carried out repeatedly, using recording spans of 10  $\mu$ s, 20  $\mu$ s, 50  $\mu$ s, 100  $\mu$ s, etc. to about 1.0 sec. after which time the signal was nearly constant. The electrode was bubbled with nitrogen before each transient was recorded. The transient recorder sensitivity was adjusted to display the last half of each scan as a deflection of at least half scale (insofar as possible). For measurements of the currents after the signal peak, the level of the blanking circuit was set to coincide with the full-scale sensitivity of the transient recorder. For signals before the peak, the blanking circuit was set to the "pass" position. After about every eight scans, the electrode was repolished and replated.

After the current transients were recorded, the input to the transient recorder was disconnected, and the " $E_{\text{cell}}$ " output of the potentiostat was connected to the non-inverting input. Transient recordings of the cell potential were then made, using successive time spans from 10  $\mu$ s to a time at which the signal became constant.

## IV. RESULTS

### 4.1. Estimation of the Potential of Zero Charge

The double layer capacitance of the silver electrode was measured over a range of potentials in dilute sodium fluoride solutions in order to estimate the potential of zero charge in the absence of specific adsorption. After the electrode was prepared for these measurements, it was prepolarized at  $-1.7$  V vs. SCE for a measured period of time, then at a "waiting" potential which ranged from  $-0.48$  V in some experiments to  $-0.8$  V in others for another period of time. The prepolarization scheme was followed by a cathodic "scan" of measurements, i. e., the measurements were collected at uniform time intervals over a series of uniformly spaced cell potentials, each potential being a few millivolts cathodic of the previous one. More information about the measurement parameters is given in Table 4.1.1.

The standard errors reported by program CCPVE for the capacitances in these measurements were between 1% and 2%. Plots constructed by program PLT of the least-squares residuals for randomly selected capacitance measurements revealed a sinusoidal variation with the time after the step, indicating that the major source of the standard error is a lack of fit of the measurements to the model, rather than random noise. A minimum in the capacitance vs. cell

potential curve always occurred in these measurements. The potentials of the minima could be determined to within  $\pm 10$  mV from the plots.

Table 4.1.1. Measurement parameters used for dilute sodium fluoride solutions.

Parameter	Concentration		
	0.00500 M	0.0100 M	0.0200 M
Waiting potential	-0.6 V	-0.48 V	-0.8 V
Step potential	10.0 mV	8.0 mV	5.0 mV 5.4 mV
Time between measurements	2 sec	2 sec	1 sec
Potential change between measurements	20 mV	35 mV	10 mV
Approximate cell time constant	7.5 ms	5.5 ms	2.5 ms

As stated in Section 2.3 the potential of zero charge may be identified with the potential of the capacitance minimum obtained for a dilute solution of a non-specifically adsorbed electrolyte. The potential of zero charge of a clean polycrystalline silver surface has been measured by others in this way (25, 29, 47); those workers obtained values ranging from -0.94 V to -0.97 V vs. SCE. However, in this work, as shown in Figures 4.1.1 through 4.1.3, the potential of the minimum was found to depend greatly on the prepolarization history of the electrode. The plots show that the potential of the minimum always drifts to more anodic potentials as the electrode stands in the



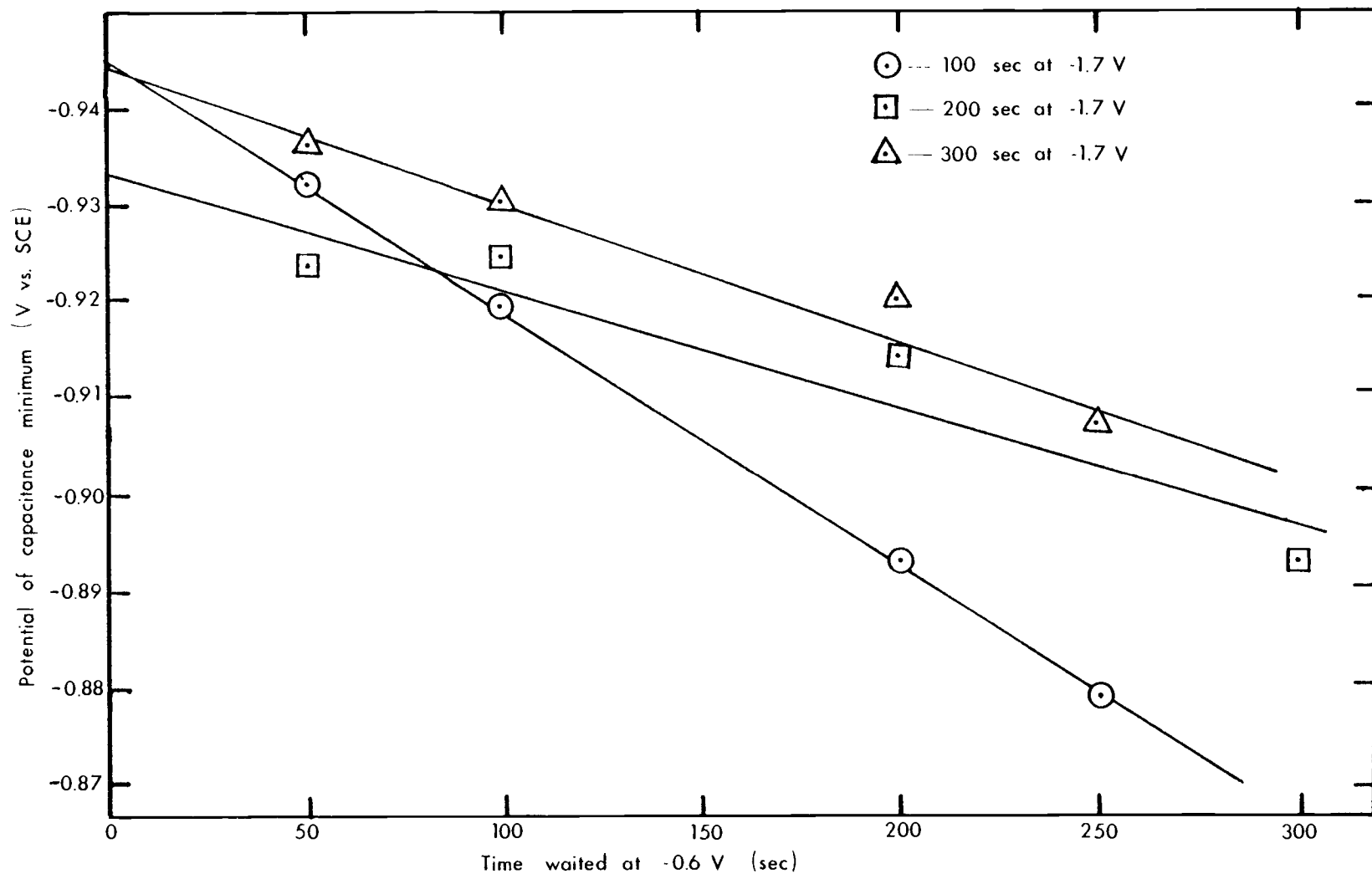


Figure 4. 1. 1. The potential of the capacitance minimum in 0.00500 M sodium fluoride solution vs. the time waited at -0.6 V for various times of polarization at -1.7 V.

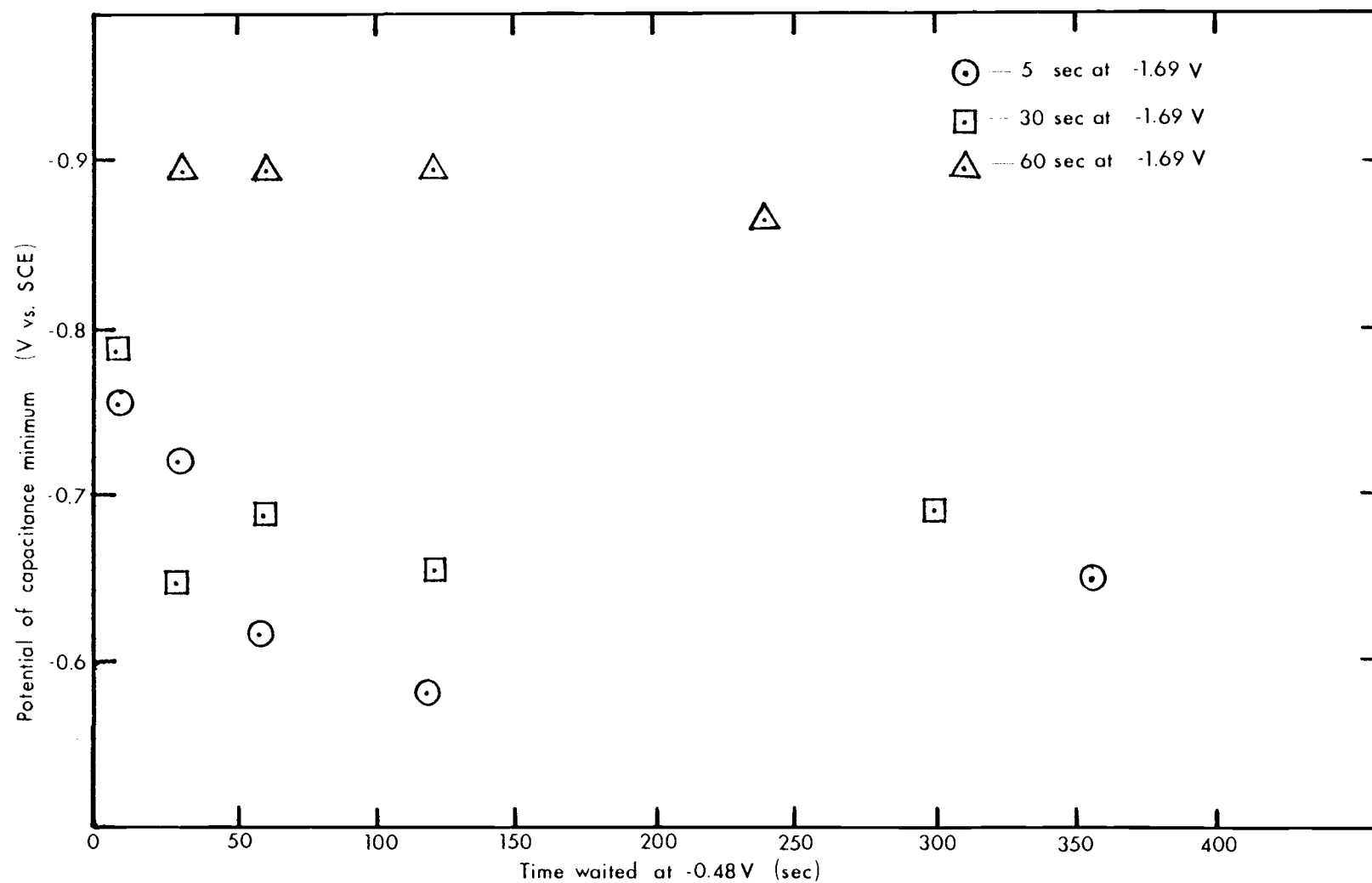


Figure 4. 1. 2. The potential of the capacitance minimum in 0. 0100 M sodium fluoride solution vs. the time waited at -0. 48 V for various times of polarization at -1. 69 V.

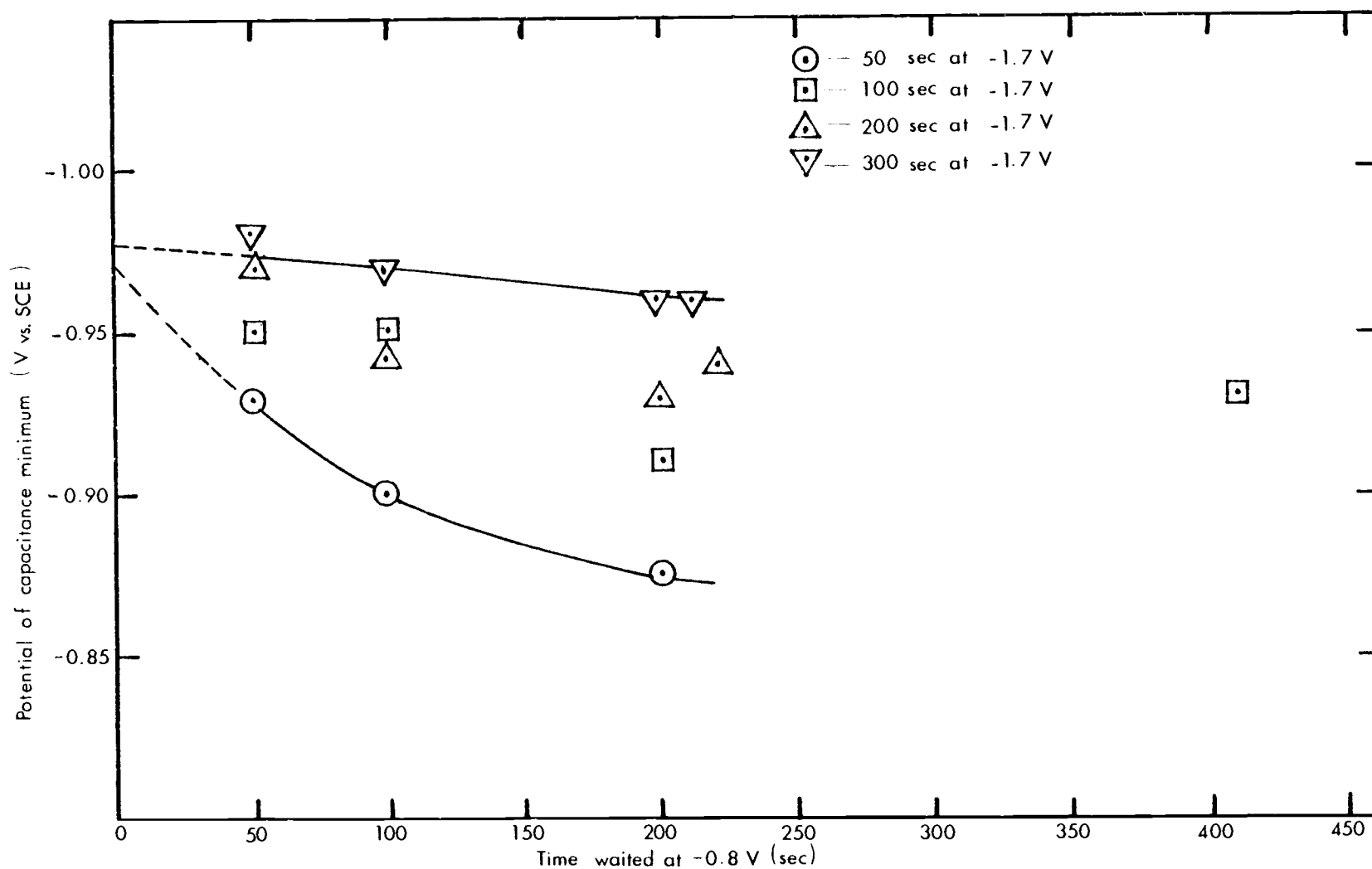


Figure 4. 1. 3. The potential of the capacitance minimum in 0. 0200 M sodium fluoride solution vs. the time waited at -0. 8 V for various times of polarization at -1. 7 V.

solution at moderate potentials anodic of the minimum. This drift is reduced substantially, but not eliminated, by prepolarization at  $-1.7$  V for at least 100 sec.

Other workers have also reported cathodic electrode pretreatment to be necessary for obtaining reproducible capacitance measurements (29, 47). This cathodic prepolarization is thought to drive off or chemically reduce specifically adsorbed impurities (which might be anions, uncharged organic molecules, or adsorbed oxygen). The generated hydrogen, which is adsorbed at the electrode, is evidently desorbed quite rapidly as the electrode is returned to more moderate values. This premise is supported experimentally by the fact that if capacitance measurements are made in an anodic scan from  $-1.7$  V, the measured values are much higher than measured on a cathodic scan, but quickly descend toward the values usually obtained. Adsorption and desorption of neutral substances are normally accompanied by high electrode capacitances (9, p. 70-71).

The anodic drift of the potential of the minimum may be due to adsorption of organic impurities from the solution. Impurities have been suggested as the cause of instability in similar measurements at mercury electrodes (12, 20, 21). The adsorption of a variety of substituted aliphatic substances has been shown to cause anodic shifts in the potential of zero charge by as much as  $0.2$  to  $0.3$  V (4).

However, some of the minima recorded in our experiments occurred at potentials too anodic to be explained in this way. These minima may involve surfaces containing adsorbed oxygen. The early measurements (8, 28) of the potential of zero charge of silver produced various values much more anodic than those already mentioned; in a more recent paper (5) a value of  $-0.69$  V vs. SCE was reported, and it was mentioned that the surface may have contained adsorbed oxygen. In our experiments, the most rapid changes of the potential of the minima (Figure 4. 1. 2) occurred after the shortest cathodic polarizations (5 sec and 30 sec). These measurements were conducted with the most anodic "rest" potential used in any of the experiments; this may have resulted in the adsorption of additional oxygen, which would account for the large anodic drift in those measurements.

In light of the foregoing suppositions, it would be reasonable to believe that the  $t = 0$  intercepts of the curves in Figures 4. 1. 1 through 4. 1. 3 should be the best estimates of the potential of zero charge of a clean silver surface, and that the curves obtained with the larger cathodic polarization times are the more reliable. For these reasons, the value of the potential of zero charge was assigned to be  $-0.94$  V, based on the six series of measurements for which the polarization times were at least 100 sec. The intercepts of these curves range from  $-0.93$  V to  $-0.98$  V. Since the difference between the results for the  $0.00500$  M solution and for the  $0.0200$  M solution

is quite small, and may be due just to the uncertainty of the measurements, fluoride may be assumed to be only weakly adsorbed. An error of a few tens of millivolts in the potential of zero charge will not produce any serious error in the double layer quantities to be calculated, because they are based mainly on changes in the double layer charge, rather than the actual value of charge.

#### 4.2. Determination of Double Layer Quantities

##### Capacitance in Sodium Fluoride-Sodium Cyanide Solutions

The double layer capacitance was measured in four solutions containing 0.00 M, 0.0162 M, 0.1880 M, and 0.942 M, respectively, of sodium cyanide and an amount of sodium fluoride sufficient to make the total electrolyte concentration equal to 0.942 M in each case. The capacitance was measured over as wide a range of cell potentials as possible, the anodic end of the range being determined by the onset of anodic dissolution of the electrode, and the cathodic end by the onset of hydrogen evolution. An increase in the rate of hydrogen evolution results in a decrease of  $R_F$ . When  $R_F$  becomes too small, it effectively short-circuits the double layer capacitance, making measurements of the latter impossible.

The measurements in these solutions were also executed in a cathodic "scan." The successive cell potentials were 65 mV apart;

the delay between measurements was 2.5 sec. Two different sets of parameters were used, with their cell bias potentials offset from each other by 30 mV, so that in two runs, the capacitances would be measured at intervals of no more than 35 mV apart. Each "scan" of measurements was preceded by a prepolarization at -1.7 V for 30 sec, then at a potential anodic of  $E_{zc}$  for another 30 sec. This latter potential was -0.8 V for the 0.942 M sodium fluoride solution, -0.95 V for the 0.942 M sodium cyanide solution, and -0.90 V for the other two. The step potentials were in the range of 5 to 8 mV; the measurement periods were maintained at about three to four times the cell time constants, which varied from about 0.2 ms to 0.9 ms.

Figures 4.2.1 through 4.2.4 show the results of these measurements. The potentials on this plot are electrode potentials, i. e., the cell potentials have been corrected for ohmic drop (which is appreciable at highly cathodic potentials) according to Equation 2.2.42. The standard errors calculated for the capacitance measurements are with few exceptions, less than 1%. The points on these plots represent several repetitions of the measurement sequence, replating the electrode before each run. The good repeatability which occurred in most cases indicates that the plating procedure produces an electrode of the same roughness (same microscopic area) each time, and that the composition of the double layer is well-defined. The most variability between repeated runs occurred in the region of

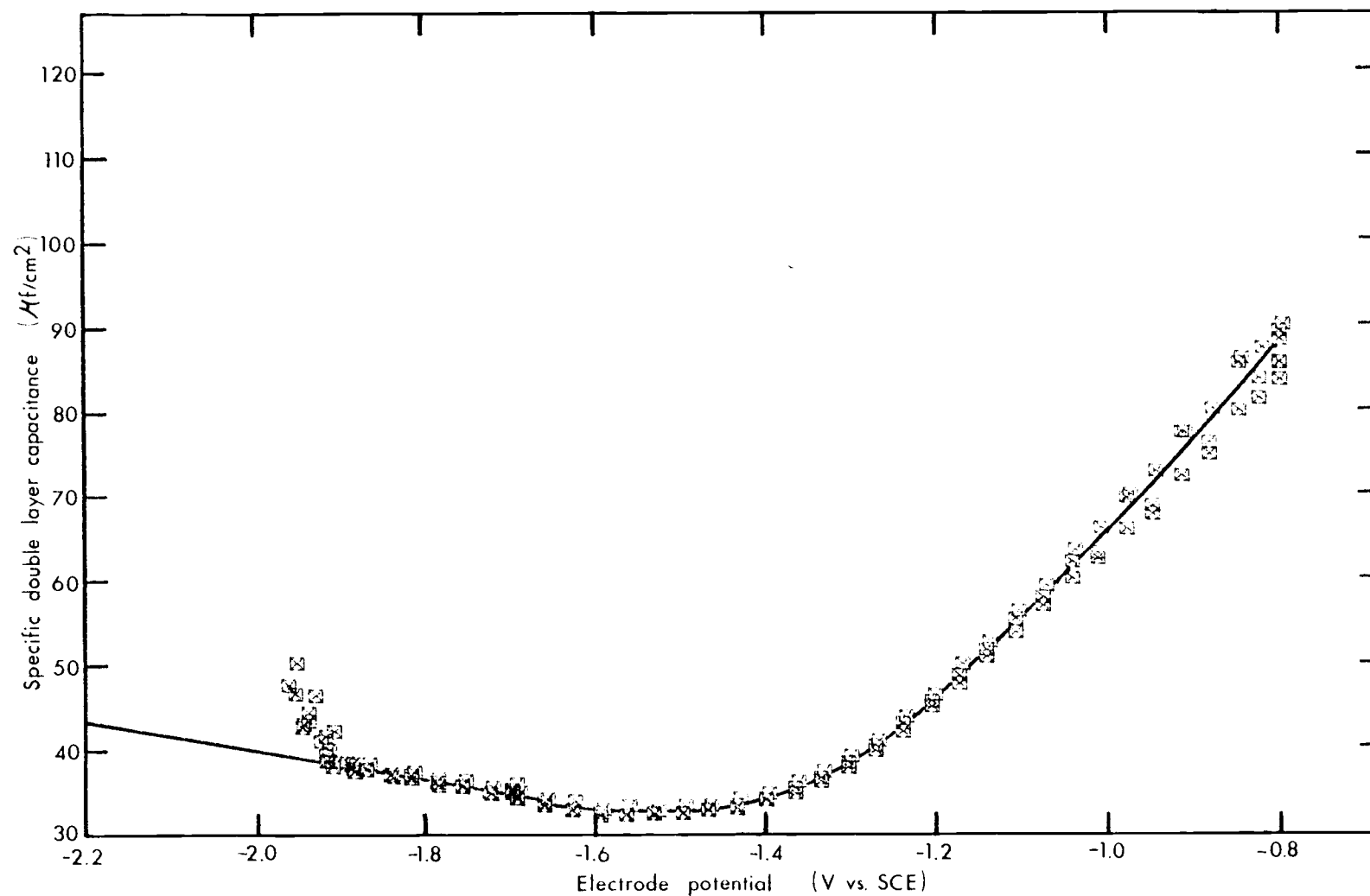


Figure 4.2.1. Specific double layer capacitance (referred to the macroscopic electrode area) vs. electrode potential for 0.942 M sodium fluoride solution.



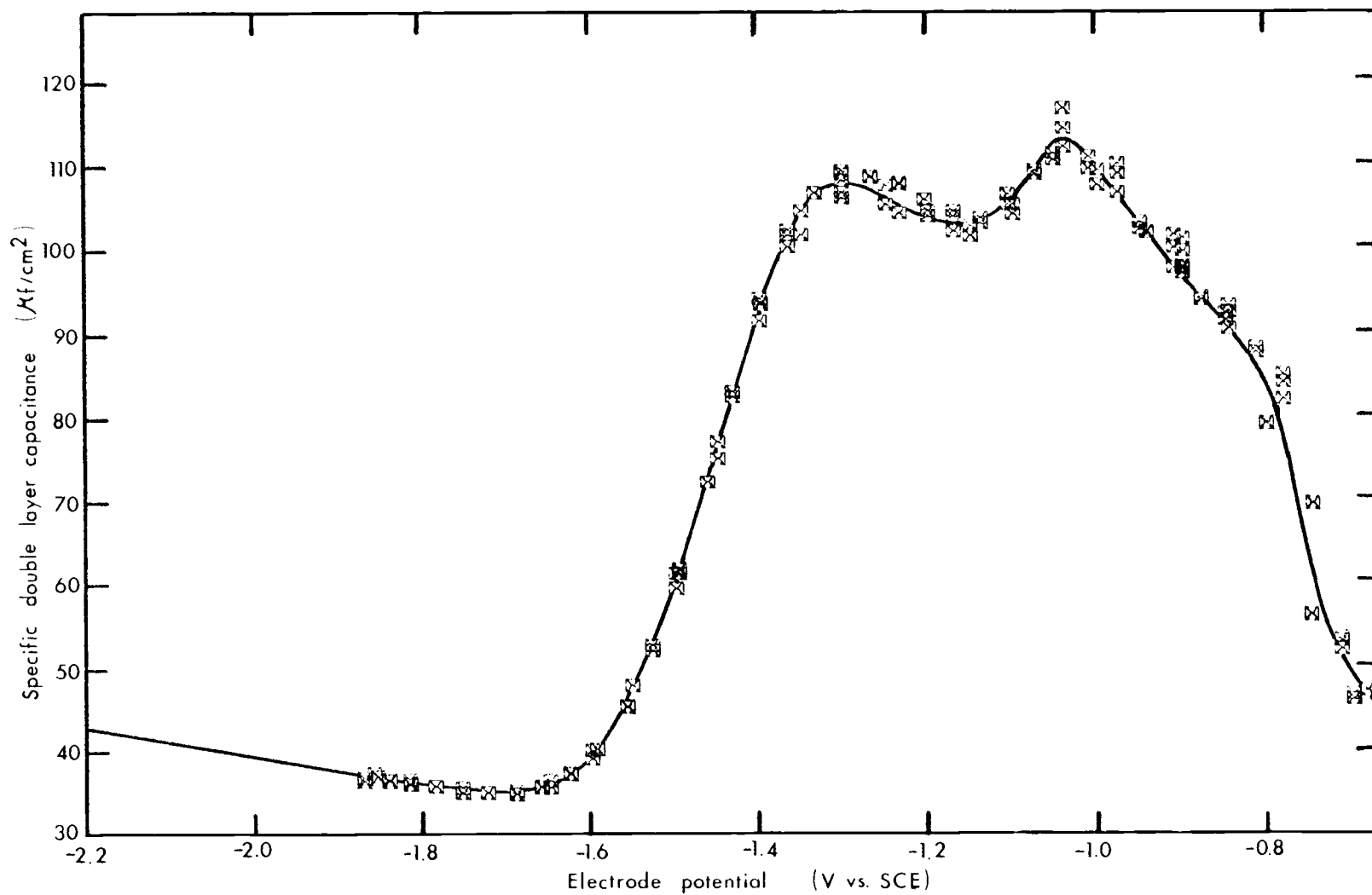


Figure 4.2.2. Specific double layer capacitance (referred to the macroscopic electrode area) vs. electrode potential for a solution containing 0.0162 M sodium cyanide and 0.926 M sodium fluoride.

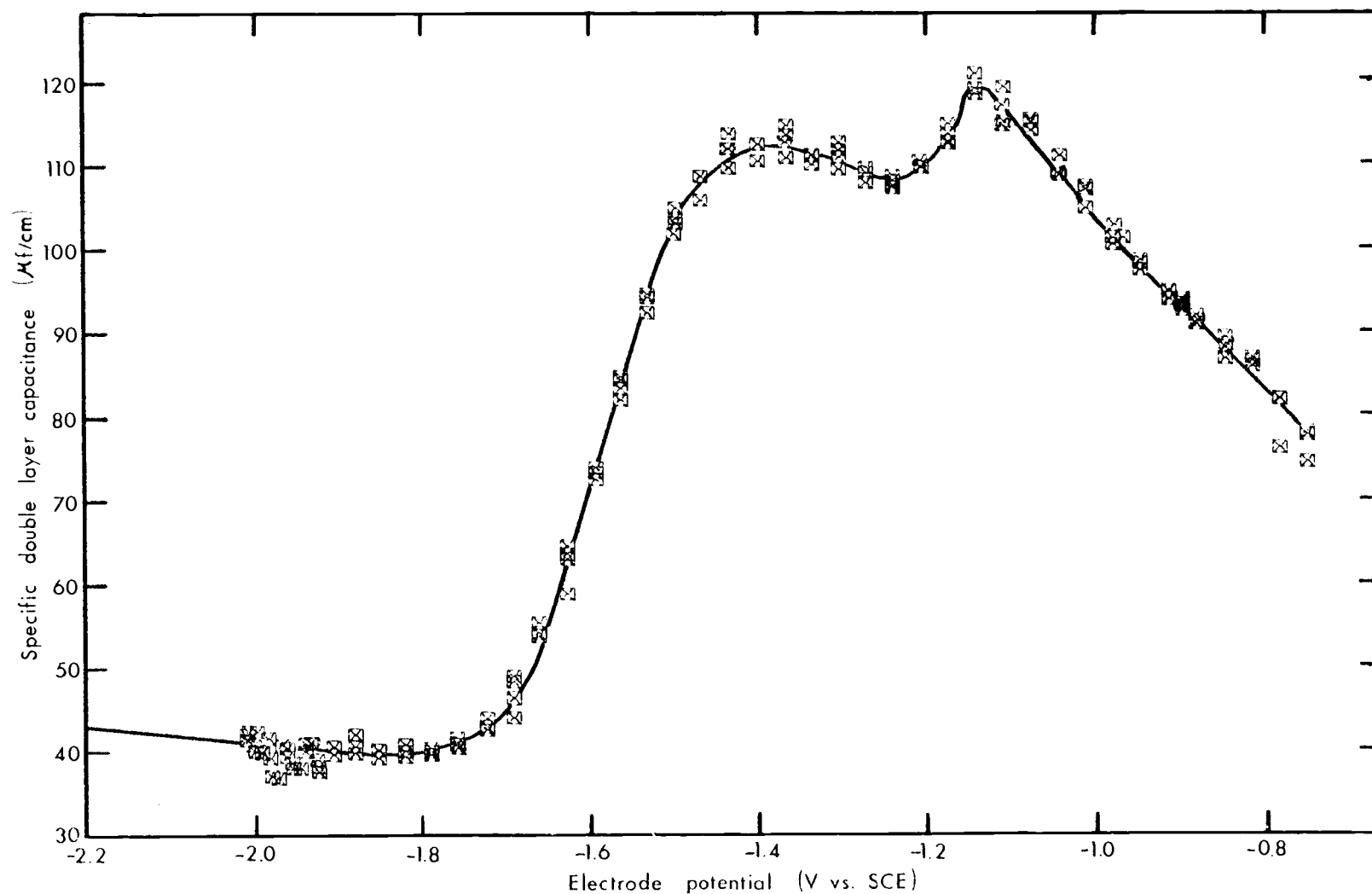


Figure 4.2.3. Specific double layer capacitance (referred to the macroscopic electrode area) vs. electrode potential for a solution containing 0.1880 M sodium cyanide and 0.754 M sodium fluoride.

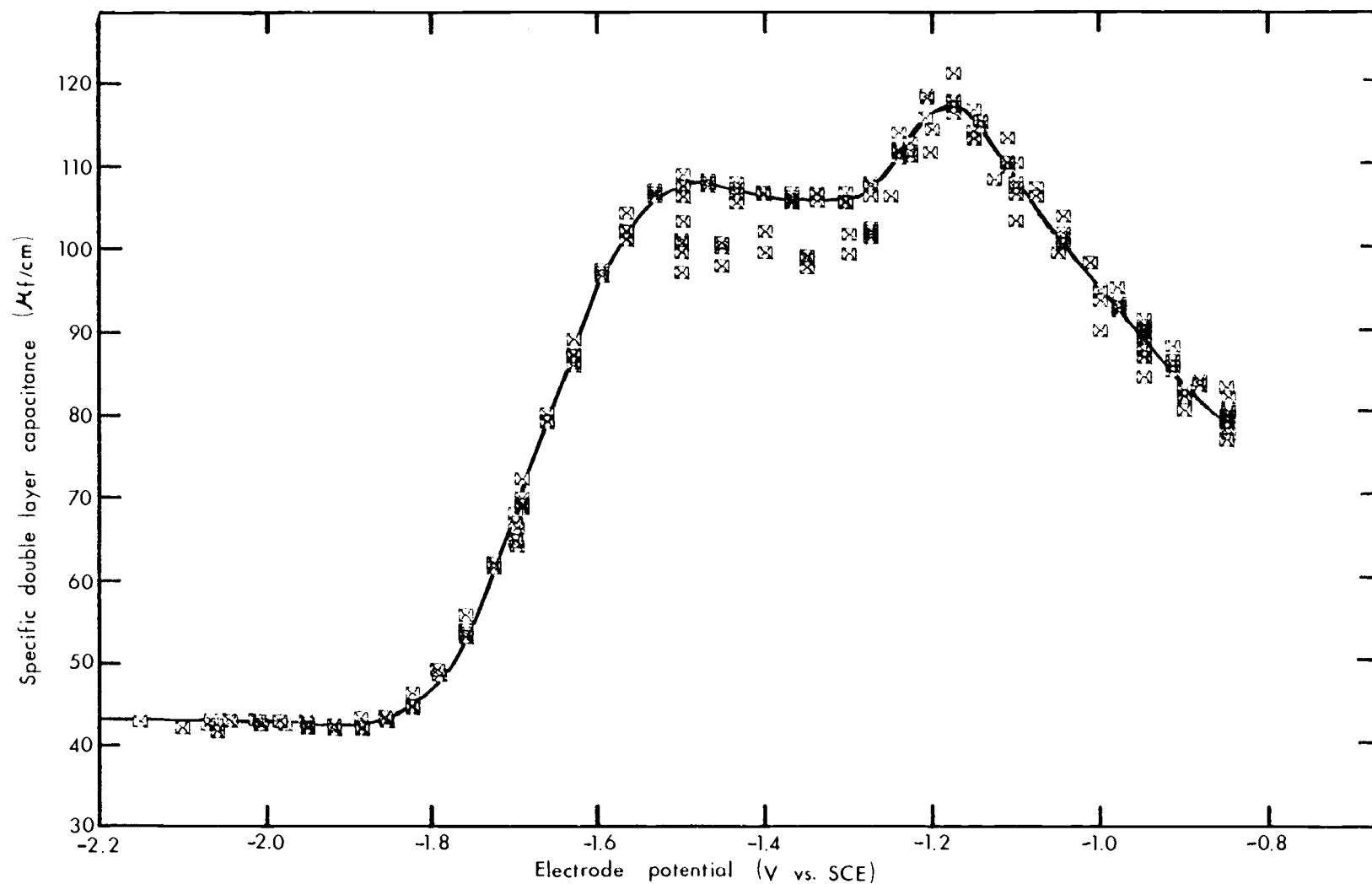


Figure 4. 2. 4. Specific double layer capacitance (referred to the macroscopic electrode area) vs. electrode potential for 0. 942 M sodium cyanide solution.

the cathodic hump in the solutions containing 0.1880 M and 0.942 M sodium cyanide.

### Calculation of Double Layer Quantities

As stated before, Devanathan's assumption holds that  $dq_1/dq$  is zero at the minima of the  $C_{dl}$  vs.  $E$  curves. Accordingly, for this point, Equation 2.3.1 becomes

$$\frac{1}{C_{dl}} = \frac{1}{K_{m-1}} + \frac{1}{K_{1-2}} + \frac{1}{C_{2-s}} \quad (4.2.1)$$

Combining this with Equations 2.3.2 and 2.3.4 gives

$$\frac{1}{C_{dl}} = \frac{X_2}{D_{m-2}\epsilon'_o} + \frac{1}{C_{2-s}} = \frac{1}{17.1 \mu f/cm^2} + \frac{1}{C_{2-s}} \quad (4.2.2)$$

If the double layer at silver is anything like that at mercury, the double layer charge will be fairly positive, making  $C_{2-s}$  quite large compared to  $(1/K_{m-1}) + (1/K_{1-2})$ . In this case the diffuse layer capacitance will be of only secondary importance. In light of this, the electrode charge at the capacitance minimum in the sodium fluoride solution was tentatively assigned to be  $13 \mu C/cm^2$ , the same as Devanathan's estimate for mercury. Then, using the assumption that  $q_1 = 0$  at the minimum, Equation 2.3.7 gives

$C_{2-s} = 336 \mu f/cm^2$ . Thus  $C_{dl}$  can be estimated from Equation

4.2.2 to be  $16.3 \mu\text{f}/\text{cm}^2$ .

The measured minimum of  $32.6 \mu\text{f}/\text{cm}^2$  for the sodium fluoride solution is not unreasonable compared to the calculated value, if it is remembered that the solid silver electrode, unlike mercury, is likely to be microscopically rough. The electrode roughness factor may be defined as

$$\begin{aligned}\rho &= \frac{\text{microscopic area of electrode}}{\text{macroscopic area of electrode}} \\ &= \frac{\text{microscopic area of electrode}}{C} \cdot \frac{C}{\text{macroscopic area of electrode}} \\ &= \frac{C_{dl} \text{ (with respect to measured area)}}{C_{dl} \text{ (with respect to actual area)}}.\end{aligned}$$

Therefore, it is estimated that

$$\rho \approx \frac{32.6}{16.3} = 2.00.$$

This value compares favorably with other estimates of the roughness of a similarly prepared silver electrode (33, 47).

The double layer charge density  $q$  (with respect to the microscopic area) was calculated at 20-mV intervals for the 0.942 M sodium fluoride solution according to Equation 2.3.9. The capacitances for this calculation were taken at 20-mV intervals along the line drawn in Figure 4.2.1. (Ten-mV intervals were used at points

along the plot where curvature was most extreme.) Each value of capacitance along this curve was divided by the roughness factor to convert it to terms of microscopic area. The integration of Equation 2.3.9 was performed by summation, assuming the  $C_{dl}$  vs.  $E$  curve to be linear in each 20-mV interval. As discussed previously, the potential of zero charge for this solution, at which potential the integration is begun, was assumed to be -0.94 V vs. SCE. This calculation produced a value of  $14.2 \mu\text{C}/\text{cm}^2$  (in terms of microscopic area) for the double layer charge at the capacitance minimum. For this charge, Equation 2.3.7 gives  $C_{2-s} = 354 \mu\text{f}/\text{cm}^2$ . Substitution of this value into Equation 4.2.1 does not change the previously estimated value of  $16.3 \mu\text{f}/\text{cm}^2$  for the true specific double layer capacitance at this point.

Now,  $q_1$  may be determined via Equation 2.3.11. Program CHARGE was written to perform the calculations for  $q$  and  $q_1$  simultaneously. The integrals of Equations 2.3.10 and 2.3.11 were evaluated by summation. Input to the program includes  $\rho$ ,  $K_{m-1}$ , and  $K_{1-2}$  for both the cation and anion, the total electrolyte concentration, and a list of ordered pairs  $(E, C_{dl})$ . The list itself must be ordered according to potential. The values of  $q$  and  $q_1$  (in  $\mu\text{C}/\text{cm}^2$  of microscopic area) for the first potential in the list must also be included in the input data to initiate the integrations. The program uses values of the inner layer capacities corresponding to

the cation when  $q_1$  is positive; otherwise, those for the anion are used. When both fluoride and cyanide were present, the value for cyanide was used, assuming that it was more strongly adsorbed than fluoride. Table 4.2.1 gives these values and the ionic radii upon which they are based. A listing of program CHARGE is included as Appendix 4.

Table 4.2.1. Crystallographic radii and inner layer capacities for some ions.

Ion	Crystallographic Radius (Å)	$K_{m-1}$ ( $\mu\text{f}/\text{cm}^2$ )	$K_{1-2}$ ( $\mu\text{f}/\text{cm}^2$ )
$\text{Na}^+$	0.95 <sup>(1)</sup>	67.1	23.0
$\text{F}^-$	1.36 <sup>(1)</sup>	46.9	27.0
$\text{CN}^-$	1.8 <sup>(2)</sup>	35.4	33.2

(1) From ref. (10, p. 45).

(2) From ref. (26). This is the effective length of the ion. It may also be considered to be the effective radius when the ion is freely rotating.

The results of program CHARGE for the sodium fluoride solution, assuming  $q_1$  to be zero at the minimum (-1.56 V), are given in Figures 4.2.5 and 4.2.6. The latter figure shows that there is a slight amount of sodium ion adsorption at very cathodic potentials and a small but significant amount of fluoride adsorption at the anodic extreme. The rather wide region about -1.56 V in which  $q_1$  is

essentially zero indicates that the assumption of  $dq_1/dq = 0$  was a good one.

Unlike the data handled by Devanathan (13) for the mercury interfaces, the cathodic minima in Figures 4.2.1 through 4.2.4 do not all have the same capacitance value. Instead, the capacitance at the minimum rises with cyanide concentration. Therefore, Equation 4.2.1 cannot apply at the minima of all the curves; Equation 2.3.1 implies that the value of  $dq_1/dq$  at the minimum must become larger as the cyanide concentration is increased. Thus, in order to get the constants of integration from Equations 2.3.10 and 2.3.11, it was necessary to find a potential  $E_{\text{neg}}$  which was cathodic enough to dispel all adsorbed anions, making the double layers of all the solutions identical.

Although the onset of hydrogen evolution prevented measurement of the double layer capacitance out to a potential at which the capacitance values were the same in all solutions, measurements could be taken close enough to this point that a reasonable extrapolation could be performed. As shown in Figures 4.2.1 through 4.2.4 all of the capacitance vs. cell potential curves were extrapolated to  $(-2.2 \text{ V}, 43.0 \text{ } \mu\text{f}/\text{cm}^2)$ . At this point, the values of  $q$  and  $q_1$  in the 0.942 M solution of sodium fluoride, and therefore in the other solutions, were found to be  $26.2 \text{ } \mu\text{C}/\text{cm}^2$  and  $2.06 \text{ } \mu\text{C}/\text{cm}^2$ , respectively. (As a check on the criticality of the extrapolation, the curves



were also extended to  $(-2.0 \text{ V}, 42.4 \mu\text{f}/\text{cm}^2)$ . The amounts of specific adsorption calculated from the two different assignments were virtually identical.) The sharp rise in capacitance at potentials more cathodic than  $-1.9 \text{ V}$  for the  $0.942 \text{ M}$  sodium fluoride solution is probably due to hydrogen adsorption. The measurements on this sharp rise were therefore ignored when the extrapolation was made.

Program CHARGE was then used to calculate  $q$  and  $q_1$  at 20-mV intervals for the cyanide-containing solutions. Figures 4.2.5 and 4.2.6 show the results of these calculations.

The fractional surface coverage can be calculated from the  $q_1$  values if the effective area covered by a single ion is known. Assuming that cyanide ions have freedom to rotate at the surface (i.e., they are not oriented) and that at complete coverage they are hexagonally close packed, the radius of cyanide ion given in Table 4.2.1 leads to an effective area for each ion of  $11.2 \text{ \AA}^2$ . On this basis, complete coverage with cyanide ions corresponds to  $q_1 = 143 \mu\text{C}/\text{cm}^2$ . Thus the data plotted in Figure 4.2.1 correspond to surface coverages of as high as 40%.

The microscopic basis for the double hump in the capacitance curves (Figures 4.2.2 through 4.2.4) is not certain. The implication of this feature, according to Equation 2.3.8, is that there is a slackening of the rate of adsorption as the electrode potential is changed. This may be due to the tendency of the cyanide dipoles to

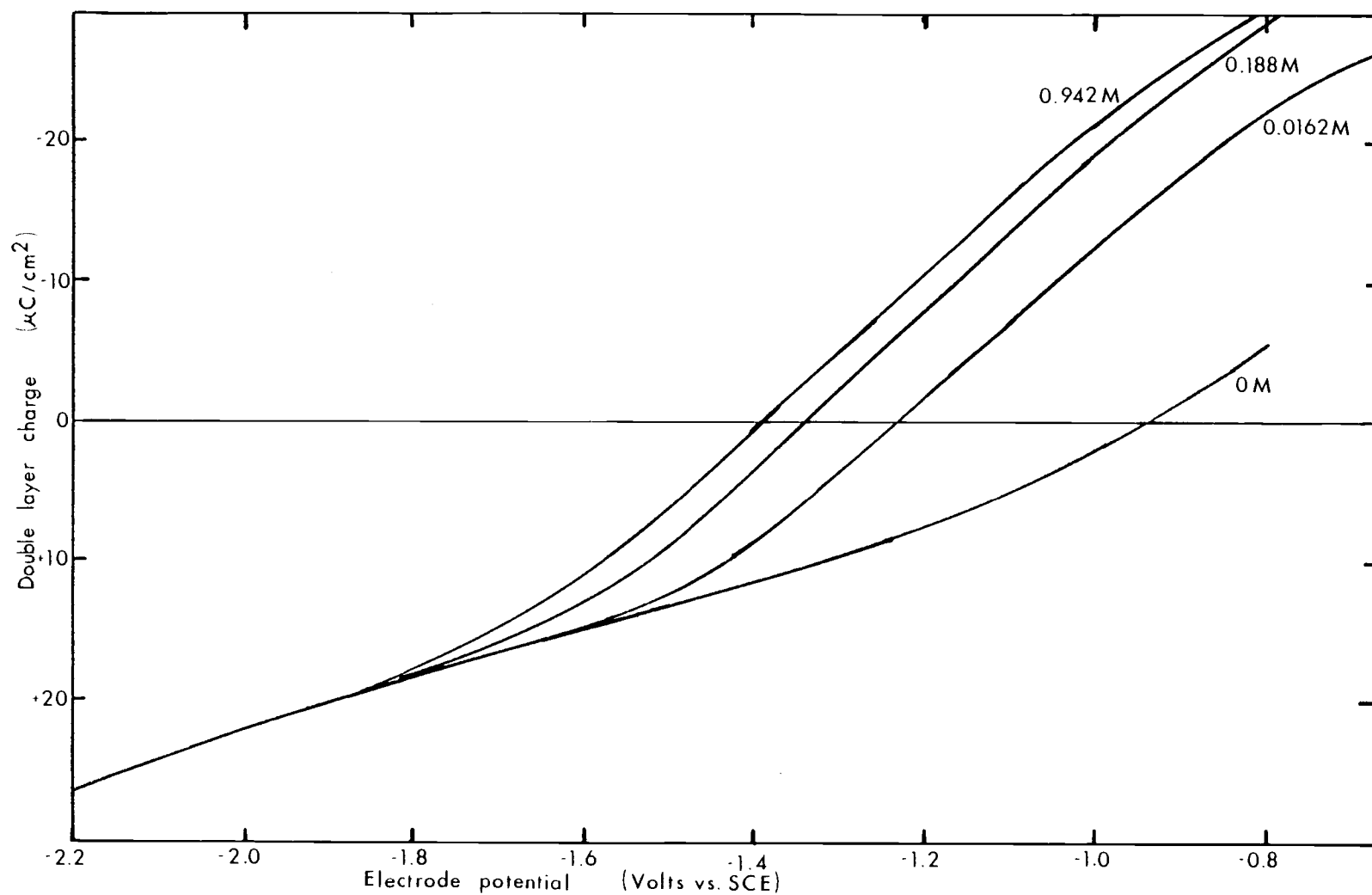


Figure 4.2.5. Double layer charge vs. electrode potential for solutions of sodium fluoride and sodium cyanide. Total electrolyte strength is 0.942 M for each solution. Sodium cyanide concentration is marked on each curve.

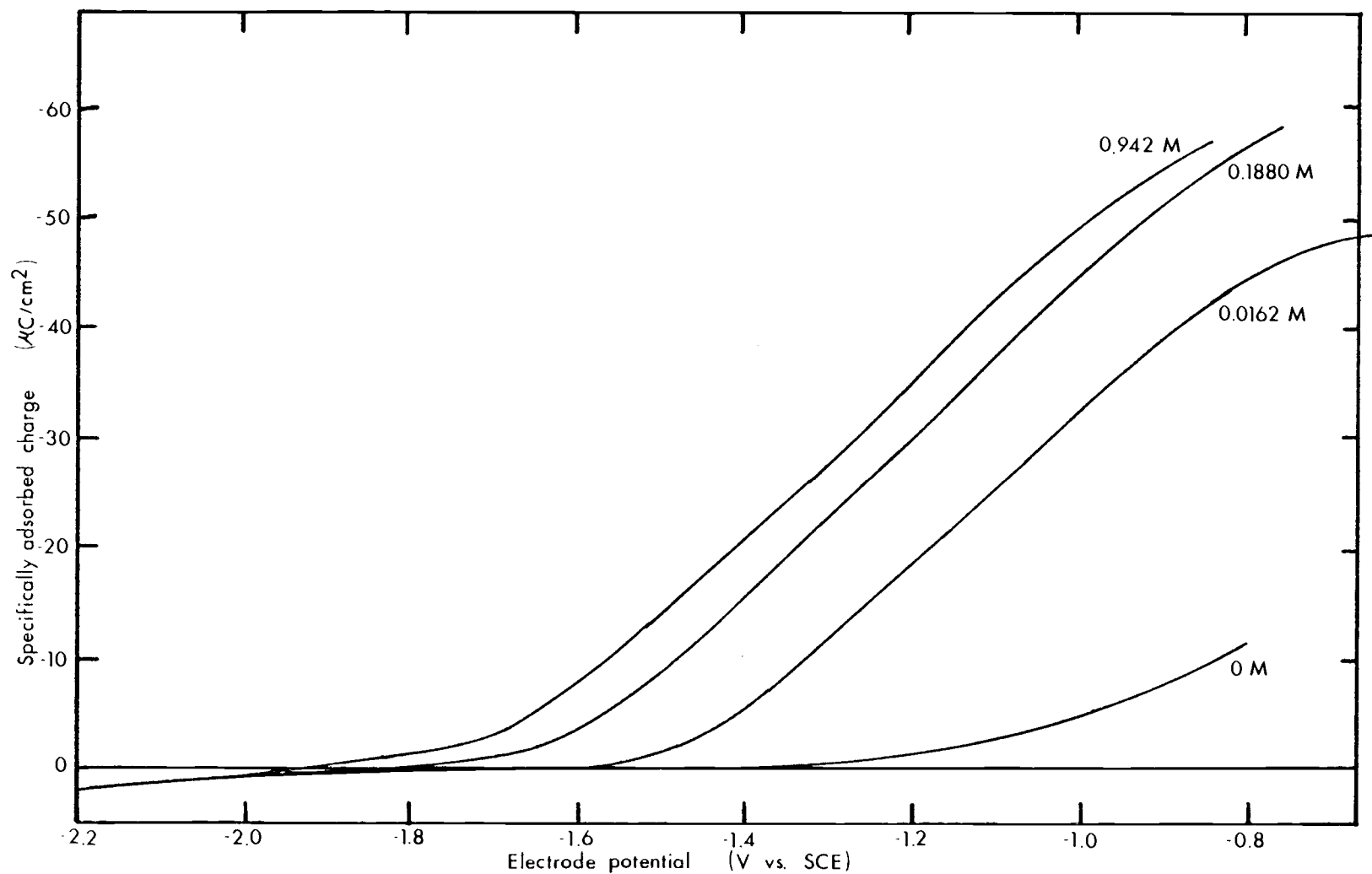


Figure 4.2.6. Amount of specific adsorption vs. electrode potential for solutions of sodium fluoride and sodium cyanide. Total electrolyte strength is 0.942 M for each solution. Sodium cyanide concentration is marked on each curve.

invert as the double layer charge passes through a critical value. (Comparison of Figures 4.2.2 through 4.2.4 to Figure 4.2.5 shows that the measured double layer charge is +2 to +5  $\mu\text{C}/\text{cm}^2$  at the dips.) The inability to orient in any particular direction at this value of charge would result in a lesser amount of attraction than would occur otherwise.

The electric dipole moment of the cyanide ion is not known, but it can be compared to carbon monoxide, for which the dipole moment is very small, about 0.1 Debye (31). Cyanide has the same number of electrons as carbon monoxide; the only formal difference in charge between the two is that the nitrogen in cyanide has one less proton than the oxygen in carbon monoxide. However, this difference in charge distribution causes the electrons to be farther away from nitrogen in cyanide than they are from oxygen in carbon monoxide, so that the total difference in dipole moments between the two species should be quite small. Thus, if there is a tendency of the cyanide to orient, it is slight. However, the observed effect is quite small, too; the inflections produced in the  $q_1$  vs.  $E$  curves (Figure 4.2.6) are hardly noticeable.

Only one other study has been found in which the specific adsorption of cyanide has been determined. In that work (49) the adsorption of cyanide on mercury was calculated from surface tension data. As mentioned in Section 2.3, this method is inherently less

precise than the double layer capacitance method, so that, if a small irregularity did occur in the specific adsorption curve, it would not have been observed.

The potentials  $\phi_2$  and  $\phi_1$  of the outer and inner Helmholtz layers, respectively, were calculated by Equations 2.3.13 and 2.3.14 at intervals of cell potential for each of the solutions. Values of  $\phi_2$  were small and negative (about -70 mV), as expected, varying no more than 25 mV over the entire range of cell potentials studied in the cyanide solutions (about 1.5 V). The values of  $\phi_1$ , shown in Figure 4.2.7 followed the general trends shown by Devanathan (13) for halides at mercury. All values were negative. The curves all coincide at their cathodic ends, representing the region of sodium ion adsorption. The values in the cyanide adsorption region were more negative for higher cyanide concentration. A discontinuity exists at potentials corresponding to  $q_1 = 0$ ; this is a reflection of the fact that the inner Helmholtz plane is not defined when there is no specific adsorption.

Values of  $\phi_m$ , calculated with Equation 2.3.15, are also shown in Figure 4.2.7. The points for all the solutions adhere very closely to a single straight line with unity slope. Devanathan states that this is good evidence that his double layer model is valid, since no direct potential measurements are used to determine  $\phi_m$ . If substantial deviations did occur, it would mean that there was an

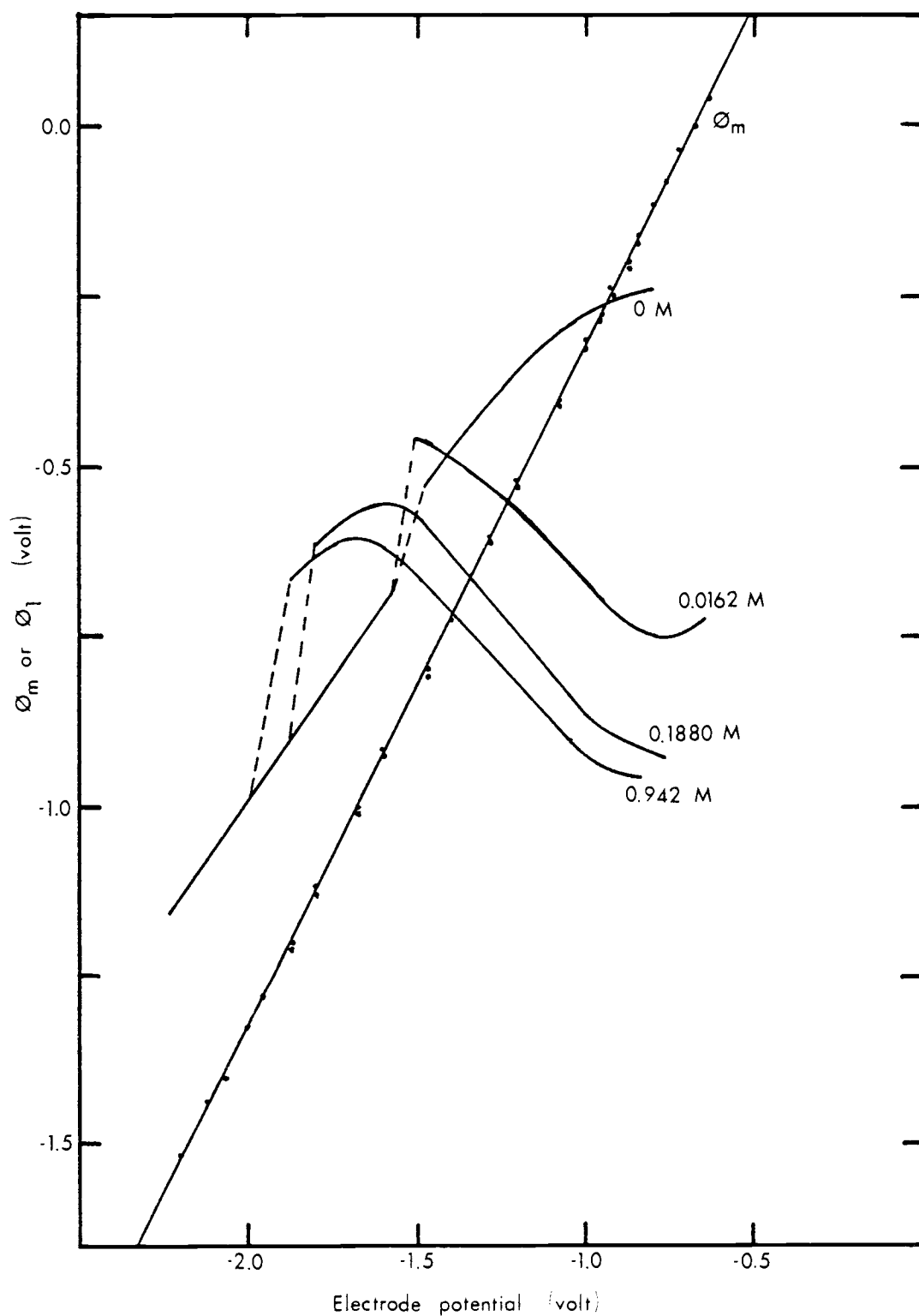


Figure 4.2.7. The potentials  $\phi_l$  and  $\phi_m$  vs. electrode potential. The cyanide concentration is marked on each of the  $\phi_l$  curves. The straight line drawn through the  $\phi_m$  points has unity slope.

error in the model, or that changes in the cell potential affect potentials at interfaces other than the one being studied.

#### 4.3. Rate of Silver Deposition

Fourteen cell current transients were measured for solutions of five different cyanide concentrations (solutions labelled A through E) using potentiostatic steps from the equilibrium potential large enough to permit the reverse reaction rate to be ignored. In Figures 4.3.1 through 4.3.4 the cell currents taken from the X-Y recordings are plotted vs. the square root of the time after the step. Only the measurements necessary to show the linear part of the curves are shown in these figures; the points immediately after the step, which contain mostly capacitative current are not included.

The electrode potential was corrected for ohmic drop in the solution by the procedure described in Section 2.5. Program Z2 (listed in Appendix 5) was written to perform the calculations required to evaluate  $Z(\sigma)$ . Data points  $(E_{\text{cell}}, V_{\text{out}})$  for input to this program were obtained for the chemical cell from the X-Y chart recordings at 1  $\mu\text{s}$  intervals for the first 12  $\mu\text{s}$ , then at 18 points per decade of time up to one sec, or until the signal became constant. Data points for the potentiostat response to the resistor dummy cell were measured at the same points in time as for the chemical cell. Figure 4.3.5 is a typical plot of  $Z(\sigma)$  vs.  $1/\sigma$ .

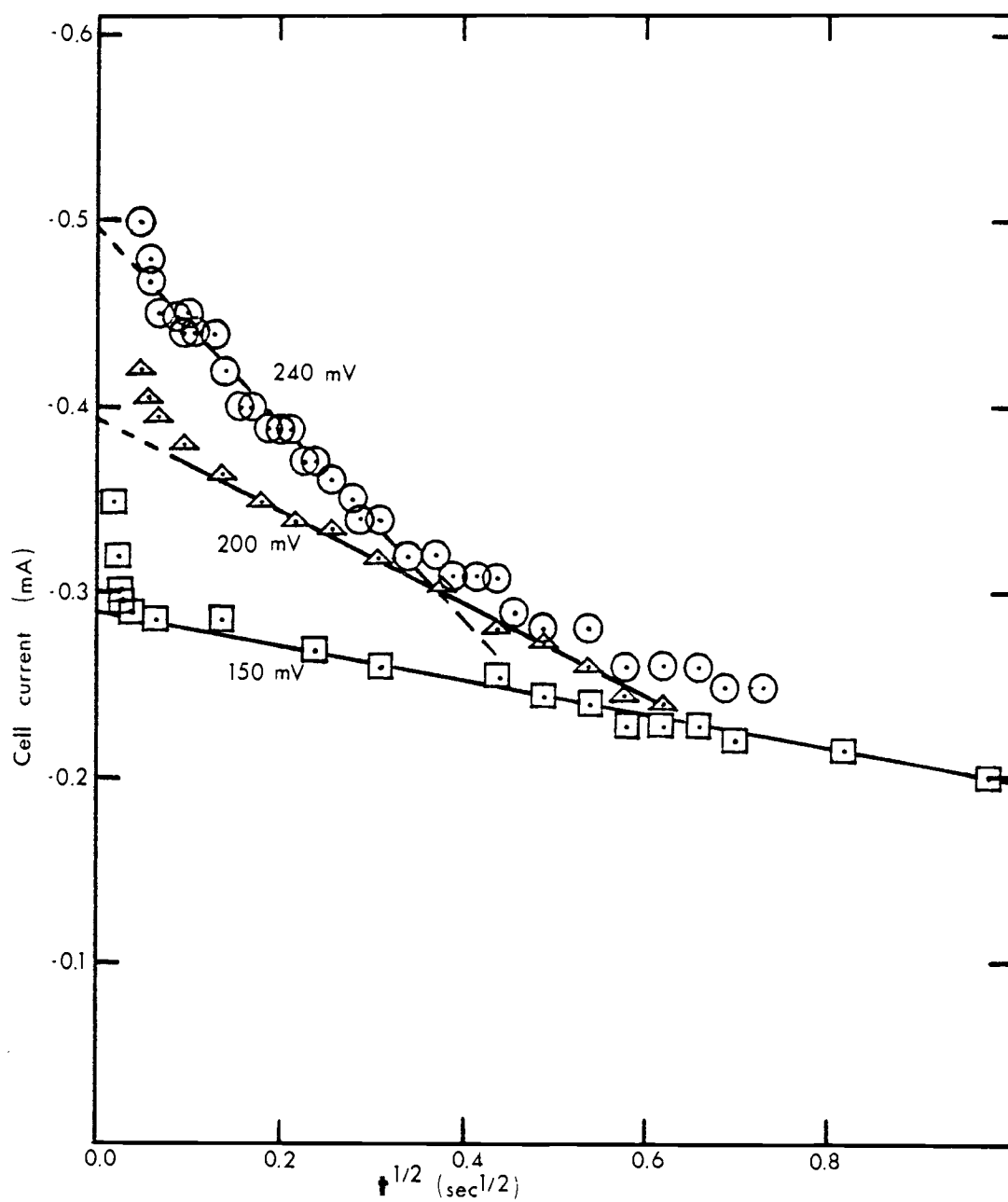


Figure 4.3.1. Cell current vs. square root of time for silver deposition transients in solution A. Cathodic step potential indicated on each curve.



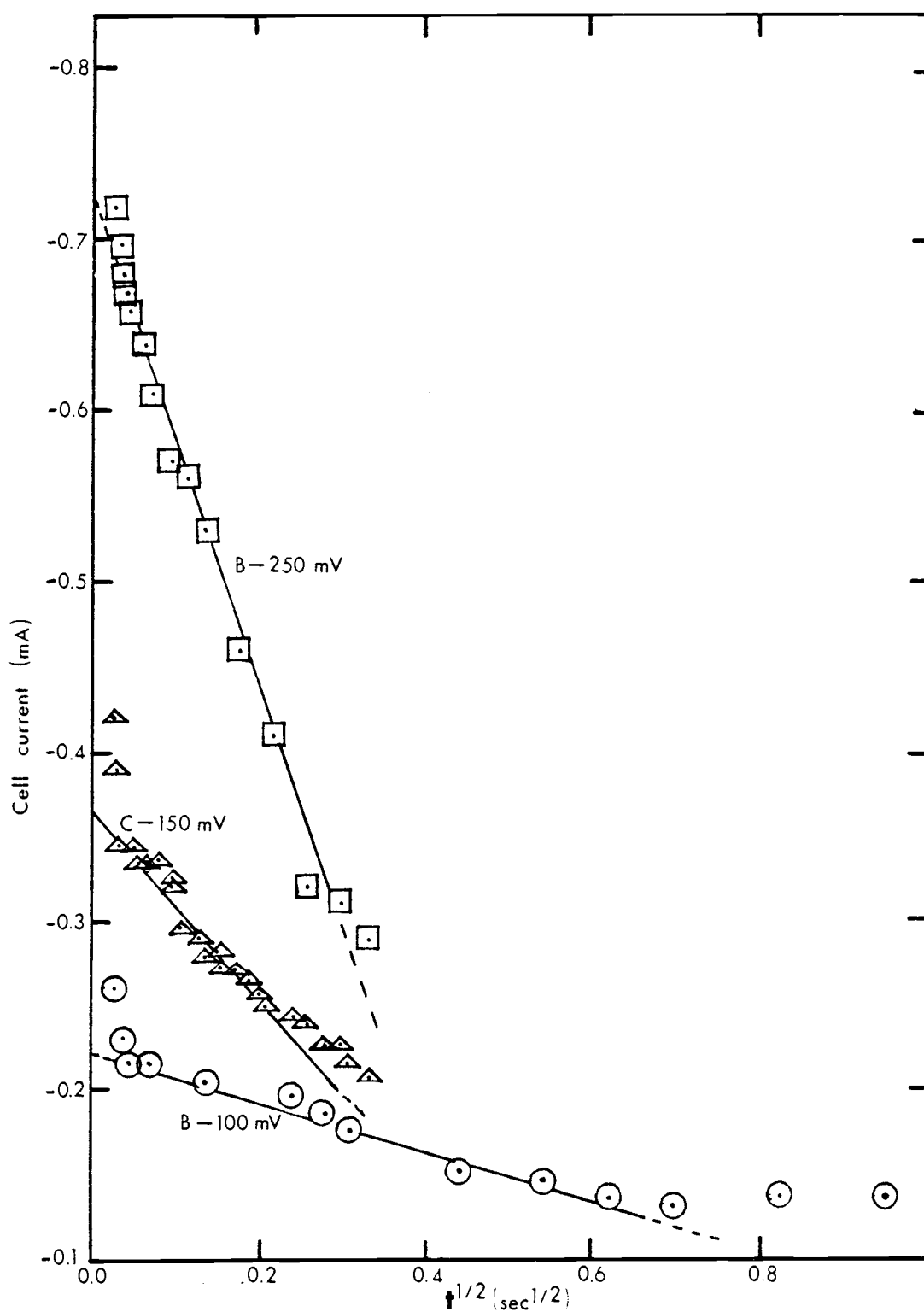


Figure 4.3.2. Cell current vs. square root of time for silver deposition transients in solutions B and C. Cathodic step potential indicated on each curve.

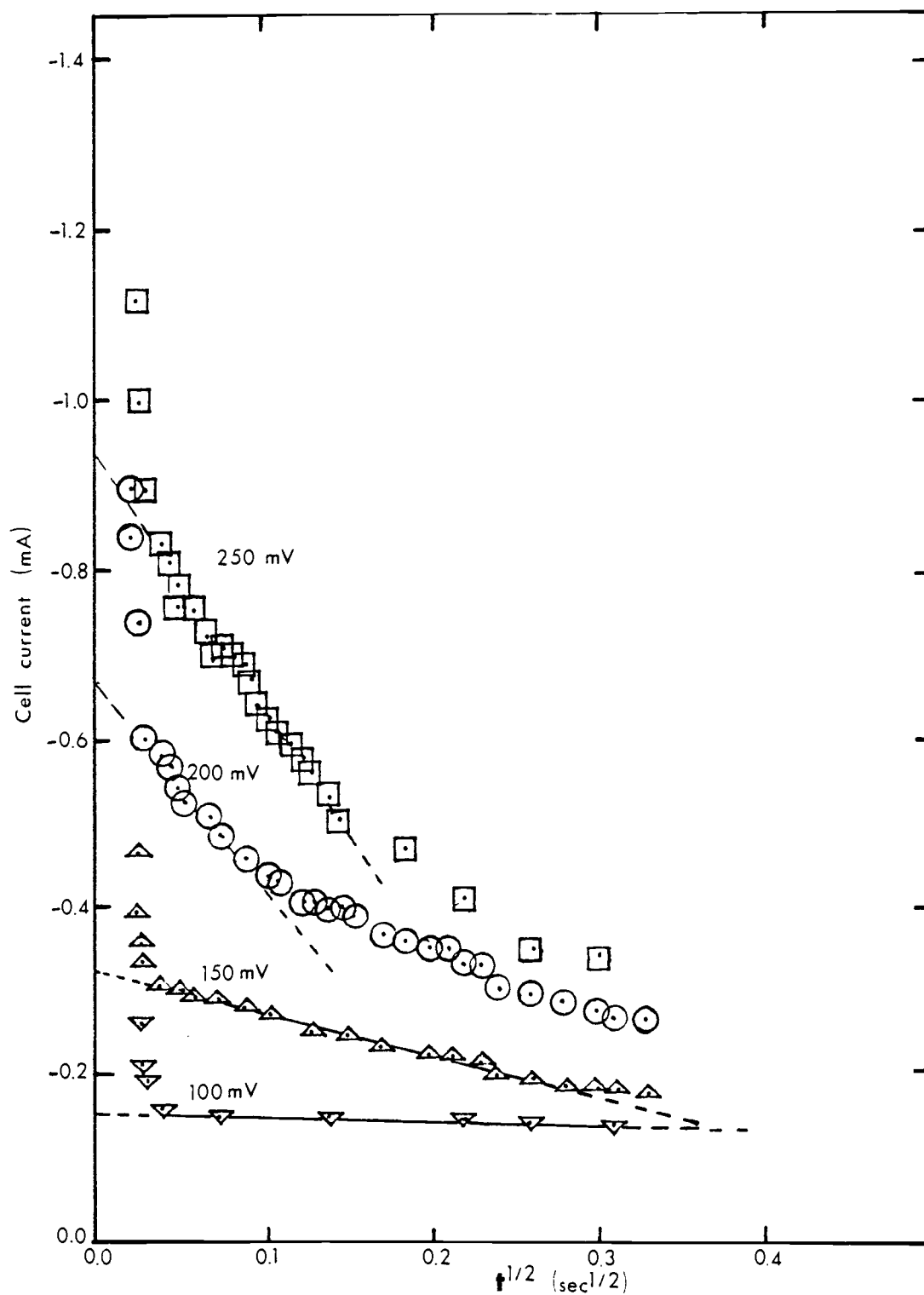


Figure 4.3.3. Cell current vs. square root of time for silver deposition transients in solution D. Cathodic step potential indicated on each curve.

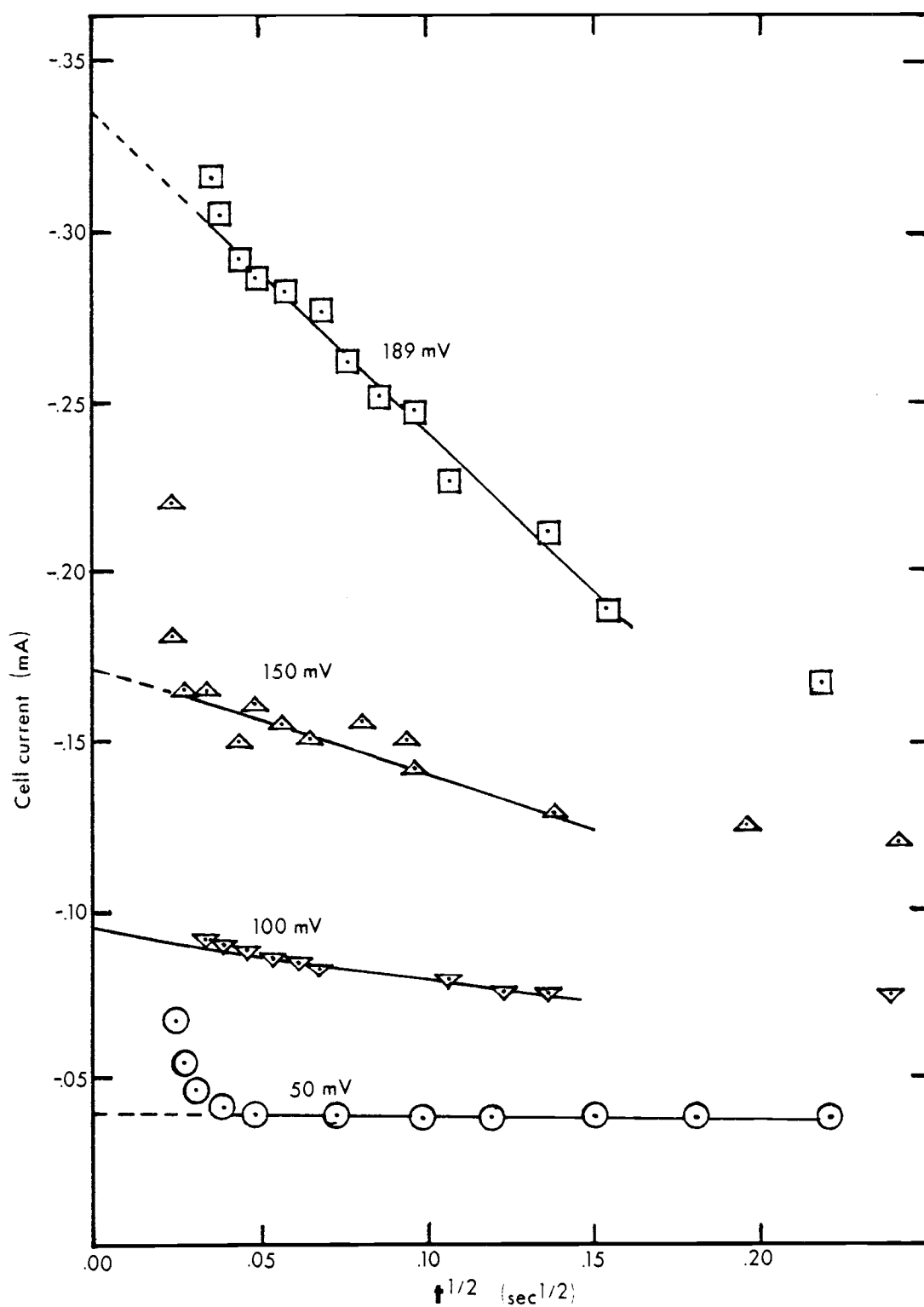


Figure 4. 3. 4. Cell current vs. square root of time for silver deposition transients in solution E. Cathodic step potential indicated on each curve.

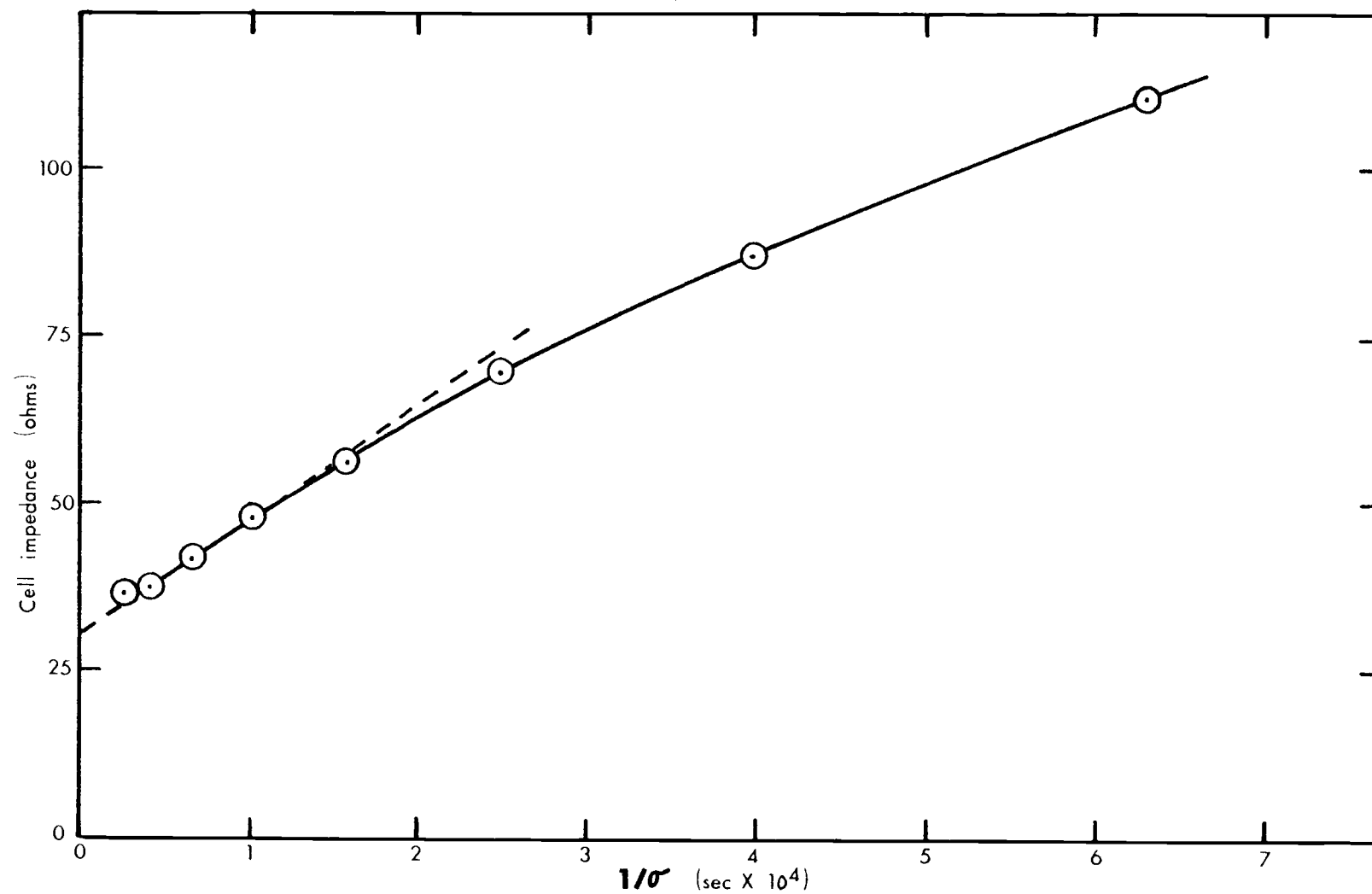


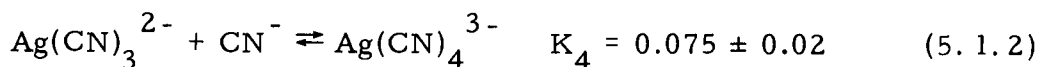
Figure 4. 3. 5. Real component of the frequency domain cell impedance measured during a silver deposition transient plotted vs.  $1/\sigma$ .

## V. DISCUSSION

### 5. 1. Composition of Silver-Containing Solutions

In this chapter, the information concerning the double layer composition will be related to the deposition rate of silver through Equation 2.2.45. This equation states that  $\ln[i_F/a_{Ms}]$  is proportional to the cell potential and various double layer parameters. Thus, it is necessary to know the activity of the electroactive species in the silver-bearing solutions. Actually, since constant ionic strength has been employed, knowledge of the concentration of the electroactive species is sufficient, and the activity coefficient may be lumped into the constant term in Equation 2.2.45. The cyanide concentration must also be known so that the amount of specific adsorption can be determined.

Jones and Penneman (26) have reported values for the stepwise formation constants of tricyanoargentate and tetracyanoargentate:



These constants were calculated on the basis of concentrations determined by infrared adsorption spectroscopy over a range of

solution compositions and ionic strengths. The stated uncertainties are the average deviations in the values determined for the various solutions. In order to calculate the ionic activities, activity coefficients were assumed to follow the Debye-Hueckel equation, even though the ionic strengths of the solutions were quite high, exceeding 5.0 in some cases. The usefulness of the constants is diminished by this fact, and by the large reported uncertainties. However, if the Debye-Hueckel equation is used to evaluate concentrations from these values of the equilibrium constants, much of the effect due to the wrong choice of activity coefficients should be reversed, resulting in reasonable values for the concentrations.

The determination of concentrations from the equilibrium constants was accomplished via an iterative calculation. Program COMPN (listed in Appendix 6) was written to perform the calculations. The program uses estimated values of the concentrations as input, and revises the concentrations by trial and error, maintaining mass balance, until the concentrations satisfy the values of the equilibrium constants. The solution compositions determined in this way are given in Table 5.1.1.

The concentrations determined from Jones and Penneman's equilibrium constants were improved by relating them to the experimentally determined equilibrium potentials observed during the deposition rate experiments. A Nernst equation for the (arbitrarily

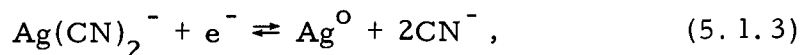
Table 5.1.1. Solution compositions calculated from different estimates of  $K_3$  and  $K_4$ . \*

Solution	$c_{CN}$	$c_2$	$c_3$	$c_4$
A	$\frac{.01619}{.01465}$	$\frac{.0262}{.0247}$	$\frac{.00378}{.00534}$	$\frac{1.7 \times 10^{-5}}{7.4 \times 10^{-6}}$
B	$\frac{.1907}{.1893}$	$\frac{.01072}{.00780}$	$\frac{.01828}{.0219}$	$\frac{9.9 \times 10^{-4}}{4.0 \times 10^{-4}}$
C	$\frac{.2543}{.2524}$	$\frac{.00874}{.00622}$	$\frac{.01983}{.0232}$	$\frac{.00143}{5.6 \times 10^{-4}}$
D	$\frac{.3376}{.3367}$	$\frac{.00710}{.00496}$	$\frac{.0214}{.0247}$	$\frac{.00204}{7.9 \times 10^{-4}}$
E	$\frac{.9368}{.9426}$	$\frac{.00259}{.001864}$	$\frac{.0217}{.0260}$	$\frac{.00579}{.00234}$

\* Entries in the table are in the form:  

$$\left[ \frac{\text{value calculated from } K_3 \text{ and } K_4 \text{ found in ref. (26)}}{\text{value calculated from } K_3^c \text{ and } K_4^c \text{ found in this work}} \right].$$
  
 Units are mol/l.

assumed) half-reaction,



can be written as

$$E_{\text{eq}} = E_2^0 - \frac{1}{f} \ln \left[ \frac{c_{\text{CN}}^2}{c_2} \right] - \frac{1}{f} \ln \left[ \frac{\gamma_{\text{CN}}^2}{\gamma_2} \right], \quad (5.1.4)$$

where the subscript 2 indicates  $\text{Ag}(\text{CN})_2^-$ . ( $E_2^0$  is the standard electrode potential for Reaction 5.1.3 which is written in terms of  $\text{Ag}(\text{CN})_2^-$ .) Since all solutions used for the deposition rate measurements had the same ionic strength, the activity coefficients for each ion should be the same in all of them. It is then possible to lump the activity coefficients and the standard electrode potential into a formal electrode potential,  $E_2^f$ , such that

$$E_{\text{eq}} = E_2^f - \frac{1}{f} \ln \left( \frac{c_{\text{CN}}^2}{c_2} \right). \quad (5.1.5)$$

Thus, if correct assignments have been made for  $c_{\text{CN}}$  and  $c_2$ , a plot of  $E_{\text{eq}}$  vs.  $\ln(c_{\text{CN}}^2/c_2)$  should be a straight line with a slope of  $-1/f$ .

The residual current which flows without any silver present in the solution is a possible source of bias in the measurement of  $E_{\text{eq}}$ .



The residual currents at  $E_{eq}$  cannot be measured directly because, in the absence of silver in solution, the electrode would dissolve at the equilibrium potential for the silver-bearing solution. However, residual currents measured in solutions without silver at more cathodic potentials than the equilibrium potentials were cathodic, and decreased with decreasing cyanide concentration and with increasing electrode potential. Thus, solution E, which has the highest cyanide concentration and the most negative equilibrium potential, is presumed to have the highest residual current flowing at its equilibrium potential. This presumption is supported by the fact that  $E_{eq}$  for this solution was the most unstable. During the deposition transient measurements for this solution composition, the first electrode surface used in each portion of the solution was the most anodic, and drifted cathodically 3 to 4 mV during the several minutes that it was used. Successive replatings of the electrode each gave more cathodic potentials and showed less drift.

If a cathodic residual current is flowing while an equilibrium potential measurement is attempted, the observed potential will be anodic of the true equilibrium potential, since the reaction of interest is required to supply anodic current to offset the residual current. Thus, an interpretation of the observed behavior is that the residual current decreases over the time that the experiments were conducted, and approaches some constant value. This could be due to depletion

of the substances in the solution responsible for the residual current. The drift cannot be explained by a change in silver concentration, since an anodic current would increase the silver concentration, causing an anodic drift of potential, according to Equation 5.1.5.

This interpretation of the drift indicates that the later, more cathodic, measurements are nearest to the true equilibrium potential values. In Figure 5.1.1, this assumption was used to plot the equilibrium potentials against values of  $\ln(c_{\text{CN}}^2/c_2)$  determined on the basis of Jones and Penneman's estimates for the equilibrium constants. The points on this plot (circles on Figure 5.1.1) are nearly on a straight line, but there is a definite concave upward curvature. To remove the curvature, an attempt was made to home in on a better value of  $K_3$  by trial and error. For each trial value of  $K_3$ , the solution compositions were calculated by program COMPN, the deviations of the  $E_{\text{eq}}$  vs.  $\ln(c_{\text{CN}}^2/c_2)$  points about a straight line were found, and a new value of  $K_3$  was chosen to reduce the amount of curvature of the line. Since, for the last few trials, the curvature could not be easily seen on a graph, it was necessary to use least-squares programming to determine the line and the deviations of the points from the line.

It became apparent that adjustment of the  $K_3$  value alone would not produce a straight line of the correct slope. A value of  $K_3 = 7.6$  gave the best value for the slope, but curvature was still

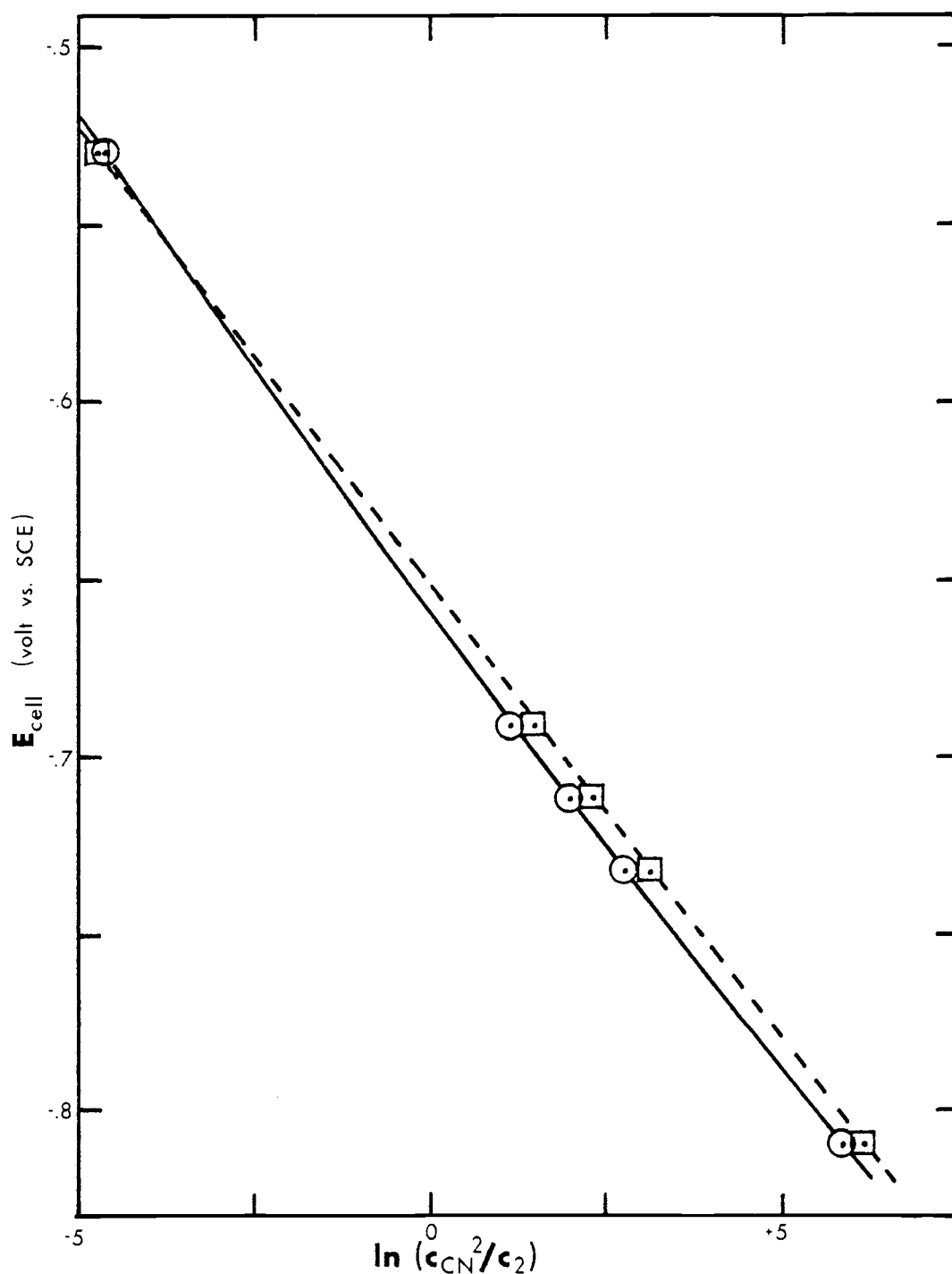


Figure 5.1.1. Cell potential vs.  $\ln(c_{\text{CN}}^2/c_2)$ . Circles are based on  $K_3$  and  $K_4$  given in ref. (26). Squares are based on  $K_3 = 7.6$  and  $K_4 = 0.0746$ . Solid curve goes through circles. Dashed line has slope of  $1/f$ . Concentrations in mol/l.

somewhat apparent from examination of the residuals of the data points from the least-squares straight line.

The values of  $K_3$  and  $K_4$  were further improved using a simplex method. From Equation 5.1.5, it may be stated that

$$(E_{eq})_j = E_2^f - L_j/f + \epsilon_j, \quad (5.1.6)$$

where the subscripts  $j$  identify a particular solution composition, the last term on the RHS represents the deviation of the measured value of  $(E_{eq})_j$  from the value predicted by Equation 5.1.5, and

$$L_j \equiv \ln[(c_{CN})_j^2 / (c_2)_j]. \quad (5.1.7)$$

For a series of  $N$  measurements of  $E_{eq}$  at  $N$  different solution compositions, the degree to which the measurements diverge from the predictions may be expressed as

$$S \equiv \sum_{j=1}^N \epsilon_j^2, \quad (5.1.8)$$

which, from Equation 5.1.6, can be written as

$$S = \sum_{j=1}^N [(E_{eq})_j - E_2^f + L_j/f]^2. \quad (5.1.9)$$

The object of the simplex method is to find values for the adjustable parameters in this equation,  $E_2^f$ ,  $K_3$ , and  $K_4$ , for which  $S$  is a minimum.

The  $L_i$  may be calculated on the basis of a given estimate of  $K_3$  and  $K_4$ , and a value of  $E_2^f$  may be chosen to minimize  $S$  by setting the partial derivative of Equation 5.1.9 with respect to  $E_2^f$  equal to zero,

$$\partial S / \partial E_2^f = -2 \sum_{j=1}^N [(E_{eq})_j - E_2^f + L_j / f] = 0, \quad (5.1.10)$$

and solving:

$$E_2^f = \frac{1}{N} \left[ \sum_{j=1}^N (E_{eq})_j + \frac{1}{f} \sum_{j=1}^N L_j \right]. \quad (5.1.11)$$

This value for  $E_2^f$  may be used to calculate  $S$  via Equation 5.1.9.

The simplex method, detailed in Figure 5.1.2, was implemented to find values for  $K_3$  and  $K_4$  which give the smallest  $S$  value. For each of several choices of  $K_3$  and  $K_4$ ,  $S$  was evaluated in the manner just described. The three initial choices are at the corners of the simplex labelled #1. Where a back-reflection was indicated, reflection of the second highest point was used (#3, #9, #11). Succeeding simplexes were formed by reflecting the point with the highest  $S$  value through the opposite side of the current simplex.

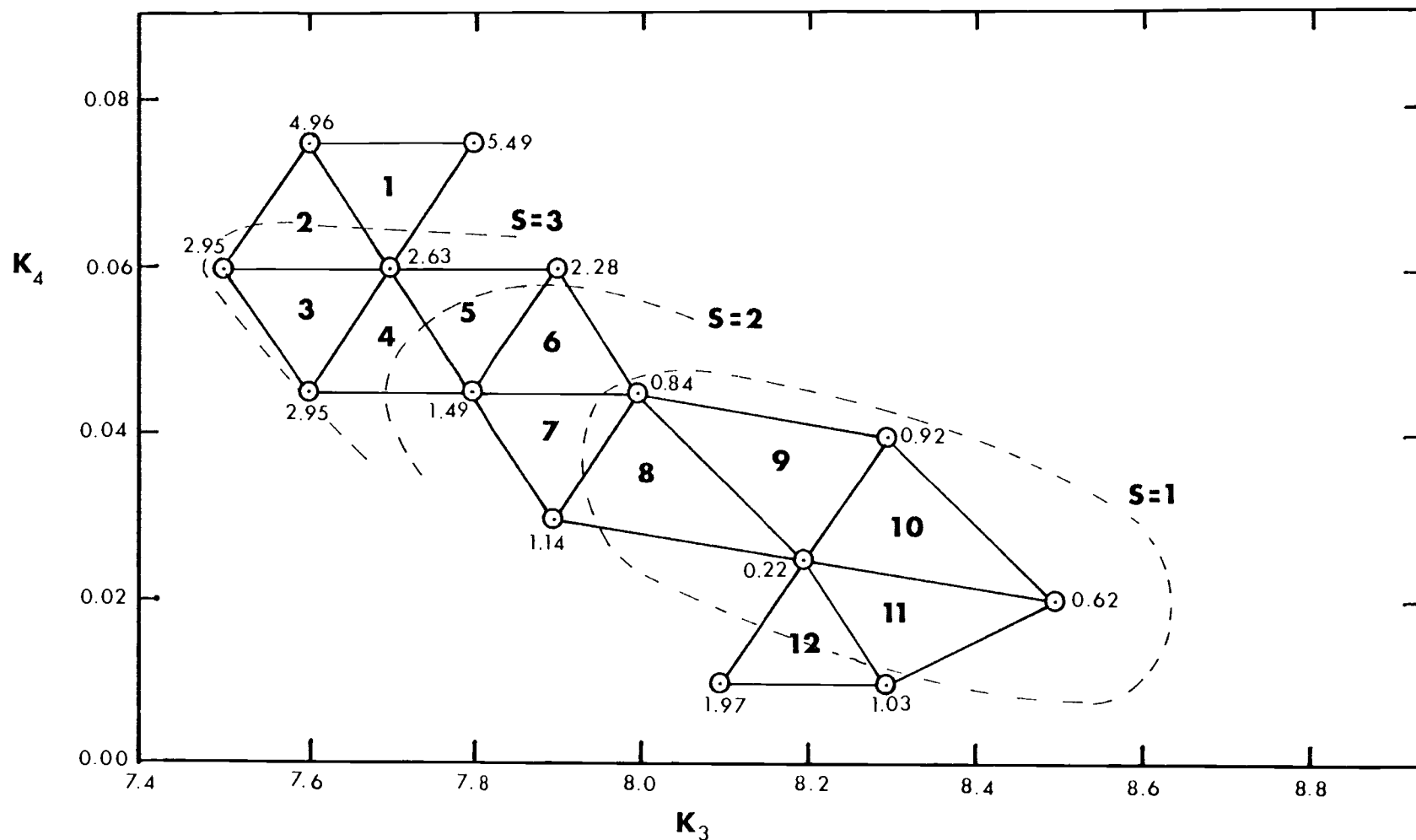


Figure 5. 1. 2. The simplex optimization of  $K_3$  and  $K_4$ . The numbers printed in the centers of the simplexes indicate the order in which they were constructed. The number next to each point is the  $S$  value in volts<sup>2</sup>  $\times 10^6$ . The dashed lines are "iso- $S$ " contours and are labelled with the corresponding  $S$  values.

At one point in the procedure (simplex #8) the distance of the reflection was doubled in order to approach the minimum  $S$  value more quickly. The values of  $K_3$  and  $K_4$  which produced the smallest value of  $S$  were 8.2 and 0.025, respectively.

The uncertainty in these values may be derived from the uncertainty in the potential measurements. The potential can be read from the potentiostat to 1 mV, i. e., to  $\pm 0.5$  mV. Since repetitive measurements of the equilibrium potentials were nearly all the same (except for the one solution mentioned previously) this error is estimated to be two or three standard deviations. Thus, a generous estimate of  $\sigma_{E_{eq}}$  is about 0.25 mV. According to Equation 5.1.5, this would correspond to an error in the concentration quotients of about 1%.

The usual estimate of standard deviation gives

$$\sigma_{E_{eq}}^2 \approx S/(N-1). \quad (5.1.12)$$

Thus, a reasonable estimate of  $S$  for the group of five measurements, based on the standard deviation in  $E_{eq}$  is

$$S = (N-1)\sigma_{E_{eq}}^2 = 0.25 \times 10^{-6} \text{ volt}^2. \quad (5.1.13)$$

The value of  $S$  corresponding to two standard deviations is

$$S = (N-1)(2\sigma_{E_{eq}})^2 = 1.00 \times 10^{-6} \text{ volt}^2. \quad (5.1.14)$$

The "iso-S" line for  $S = 1$  on Figure 5.1.2 therefore encompasses the values of  $K_3$  and  $K_4$  which correspond to an error of  $\pm 0.5$  mV in the potential measurements. On the basis of this perimeter, the values of  $K_3$  and  $K_4$  may be established to be  $8.3 \pm 0.3$  and  $0.025 \pm 0.015$ , respectively.

As stated before, these values are based on the assumption that the Debye-Hueckel equation applies for these solutions. Since this assumption is probably a poor one, and since the measurements were made at only one ionic strength, the determined values of  $K_3$  and  $K_4$  probably apply only at this ionic strength, and should be expressed in terms of concentrations, rather than the inaccurately assumed activities. We thus write the concentration equilibrium constants as

$$\begin{aligned} K_3^c &\equiv \frac{c_3}{c_2 c_{CN}} = K_3 \cdot \frac{\gamma_2 \gamma_{CN}}{\gamma_3} \\ &= 8.3 \left[ \frac{(.685)(.573)}{.220} \right] = 14.8 \pm 0.5 \end{aligned} \quad (5.1.15)$$

and

$$\begin{aligned} K_4^c &\equiv \frac{c_4}{c_3 c_{CN}} = K_4 \cdot \frac{\gamma_3 \gamma_{CN}}{\gamma_4} \\ &= 0.025 \left[ \frac{(.220)(.573)}{.0332} \right] = 0.10 \pm 0.06 \end{aligned} \quad (5.1.16)$$



where values of the activity coefficients have been calculated and used in program COMPN.

In Table 5. 1. 2, the equilibrium constants calculated in this work are compared with the results of other workers. Direct comparisons of the values in the table are difficult because of differences in conditions. However, it is interesting to note that none of Jones and Penneman's experimental determinations of  $K_3^c$  (from which the average value reported in Table 5. 1. 2 is taken) were as high as the one determined in this work. Our determination of  $K_3^c$  is also higher than that found by Bodlander and Eberlein (7). On the other hand, our values for  $K_4$  and  $K_4^c$  are lower than Jones and Penneman's. The values for  $K_3$  determined here and by Zsaka and Petri (50) compare quite well. Because of rather large variations in these results, and because the values calculated in this work apply specifically to the solutions of interest, the values reported by others were not considered in determination of the solution compositions. To demonstrate the effect of proper choice of the equilibrium constants, the solution compositions calculated on the basis of the constants determined here are compared with those determined from the values of Jones and Penneman in Table 5. 1. 1.

Table 5.1.2. Equilibrium constant values determined by various authors.

Source	$K_3$	$K_4$	$K_3^c$	$K_4^c$	T	Medium	Method
This work	8.3	0.025	14.8	0.10	25 C	$\mu = 1.0$	equ. ptl.
Ref. (26)	5.0	0.075	9.3	0.28	21 C	variable	I. R.
Ref. (7)	-	-	7.8	-	-	variable	equ. ptl.
Ref. (50)	8.9	-	-	-	20.5 C	-	equ. ptl.

### 5.2. Effect of the Double Layer on Exchange Currents

There are two separate sets of data available which concern the rate of deposition of silver from cyanide solution. These are the group of 14 current transients collected in this work and the data collected by Vielstich and Gerischer (48), mentioned on page 1. In addition, there is the large body of information collected by Nechaev, et al. (1, 2, 36-39), but in those papers other surface-active agents ( $\text{CO}_3^{2-}$ ,  $\text{HCO}_3^-$ , HCN) were present, and the reaction rates were partially limited by mass transport. Because of these complications, the results of that investigation will not be examined further.

Of these three sets, the data obtained by Vielstich and Gerischer proved to be the most amenable to treatment via Equation 2.2.45. In that work the deposition rate was measured in much the same way as was done here. Their instrumentation was relatively primitive, however, (by today's standards) limiting their studies to

small-to-moderate over-potentials (up to about 40 mV). From their measurements of initial currents resulting from various potentiostatic steps, both anodic and cathodic, the exchange current was determined. A series of ten exchange current determinations were performed in which the total silver content was held at 0.005 M and the cyanide concentration was varied from about 0.03 M to 0.7 M. The ionic strength was held to 1.0 by adding potassium chloride. Their published plot of exchange current vs.  $\ln c_{\text{CN}}$  consisted of two fairly straight branches, one at each end of the range of cyanide concentrations. The transition from one branch to the other occurred in the region between 0.1 M and 0.2 M cyanide.

Vielstich and Gerischer explained this behavior in terms of a change in electroactive species from  $\text{Ag}(\text{CN})_2^-$  to  $\text{AgCN}$  as the cyanide concentration is decreased. Double layer effects were not considered. It is the intent of the following to show (via Equation 2.2.45) how changes in the double layer may also explain the observations of Vielstich and Gerischer.

In both the present work and that of Vielstich and Gerischer, the assumption is made that the electrode reaction rate is determined by the electron transfer step. On the other hand, Mehl and Bockris (33) have found that the rate of silver deposition from perchlorate solution, a non-complexing medium, is limited by diffusion of adsorbed silver atoms across the surface into crystalline growth sites. This surface

diffusion rate was determined to be about  $10 \text{ mA/cm}^2$  at the equilibrium potential, independent of silver concentration, with its effect becoming less significant as the electrode diverges from the equilibrium potential. Since surface diffusion should not be affected by solution parameters, it should be about the same when cyanide solutions are used. Since the exchange currents measured by Vielstich and Gerischer are around  $1 \text{ mA/cm}^2$ , considerably lower than found for perchlorate solutions, and since most of their measurements were made at appreciable displacements from equilibrium, the effect of surface diffusion should be minimal. The deposition currents measured in this work should be unaffected by surface diffusion because of the high polarizations employed. Thus, the reaction rate should be entirely controlled by the electron transfer step, and Equation 2.2.45 should apply.

In that equation the potential  $\phi_y$  of the layer of adsorbed ligands may be identified with  $\phi_1$ , since the silver concentration is quite small in these solutions, and its effect on the double layer should therefore be minimal. The potential  $\phi_x$  of the region in which the discharging species resides is assigned to be zero, since the silver complexes have radii (26) of about  $4.8 \text{ \AA}$ , well into the diffuse layer. Making these substitutions, and realizing that the exchange current is equal to the cathodic partial current at the equilibrium potential, Equation 2.2.45 may be written as

$$\ln(i_{\text{ex}}/c_{\text{Ms}}) = \text{const}_1 - \alpha f E_{\text{eq}} + \alpha(1-z)f\phi_1 + 2(B_{\text{CN}}/e_o)q_1, \quad (5.2.1)$$

where it has been recognized that  $n = 1$  for the silver deposition reaction, and that the use of constant ionic strength makes it possible to use  $c_{\text{Ms}}$  for  $a_{\text{Ms}}$  if the constant activity coefficient is included with the other constants in the equation. The specifically adsorbed charge  $q_1$  (due to cyanide) is substituted for  $\Gamma_{\text{CN}}$  via Equation 2.3.2. The Nernst equation for the electrode reaction, written in terms of the electroactive species, is

$$E_{\text{eq}} = E_M^f - \frac{1}{f} \ln[(c_{\text{CN}})^{1-z}/c_{\text{Ms}}]. \quad (5.2.2)$$

(In accordance with Reaction 2.2.2, the electroactive species has  $1-z$  ligands.) This equation may be solved for  $c_{\text{Ms}}$  and substituted into Equation 5.2.1 to yield

$$\begin{aligned} \ln i_{\text{ex}} = & \text{const}_2 + (1-z) \ln c_{\text{CN}} + (1-\alpha)fE_{\text{eq}} \\ & + \alpha(1-z)f\phi_1 + (2B_{\text{CN}}/e_o)q_1 \end{aligned} \quad (5.2.3)$$

where  $E_M^f$  has been absorbed into the constant. Differentiation gives

$$\begin{aligned} \frac{d \ln i_{\text{ex}}}{d \ln c_{\text{CN}}} = (1-z) + (1-\alpha)f \frac{dE_{\text{eq}}}{d \ln c_{\text{CN}}} + \alpha(1-z)f \frac{d\phi_1}{d \ln c_{\text{CN}}} \\ + \frac{2B_{\text{CN}}}{e_o} \cdot \frac{dq_1}{d \ln c_{\text{CN}}} . \end{aligned} \quad (5.2.4)$$

Gerischer (15) derived a similar equation, but the aspects of the double layer influence (the last two terms of the RHS) were not included. It should be possible to evaluate from experimental data all of the derivatives in this equation. The validity of Equations 5.2.4 and 2.2.45 may be investigated on the basis of these values.

Vielstich and Gerischer have constructed a plot of  $\ln i_{\text{ex}}$  vs.  $\ln c_{\text{CN}}$  from which they evaluated  $d \ln i_{\text{ex}} / d \ln c_{\text{CN}}$ . However, in that work it was assumed that  $\text{Ag}(\text{CN})_3^{2-}$  was the only silver species present in the solution; it has been shown in the previous chapter that this assumption is incorrect. For this reason, the coordinates of the ten  $\ln i_{\text{ex}}$  vs.  $\ln c_{\text{CN}}$  points were carefully obtained with a measuring magnifier from the published figure, and the solution compositions were re-determined using the program COMPN and the equilibrium constants determined in the previous chapter. It was assumed that the silver was added to these solutions as silver chloride, and that the plotted values of  $c_{\text{CN}}$  in the published figure were based on the assumption that all the silver was present as  $\text{Ag}(\text{CN})_3^{2-}$ . The calculated solution compositions are

listed in Table 5.2.1. The resulting  $\ln i_{\text{ex}}$  vs.  $\ln c_{\text{CN}}$  graph is shown in Figure 5.2.1. The slope of this curve at low cyanide concentrations was determined to be -0.30, based on the five data points in that region; the slope at high cyanide concentration is +0.49, based on four points.

Table 5.2.1. Composition of solutions in reference (48) calculated by program COMPN.\*

Solution I. D.	$c_{\text{CN}}$	$c_2$	$c_3$	$c_4$
1	.0324	.00339	.001608	$4.78 \times 10^{-6}$
2	.0421	.00309	.001905	$7.36 \times 10^{-6}$
3	.0596	.00266	.00233	$1.274 \times 10^{-5}$
4	.0763	.00235	.00263	$1.845 \times 10^{-5}$
5	.1079	.001924	.00305	$3.02 \times 10^{-5}$
6	.1614	.001470	.00348	$5.16 \times 10^{-5}$
7	.231	.001121	.00380	$8.06 \times 10^{-5}$
8	.370	.000762	.00412	.0001391
9	.590	.000495	.00425	.000232
10	.720	.00426	.00434	.000289

\* Entries in mol/l.

The equilibrium potentials were calculated for each point from a Nernst equation. For this purpose a value for the formal potential  $E_2^f$  was determined from other data in reference (48) to be about -0.65 V vs. normal calomel electrode. The equilibrium potentials

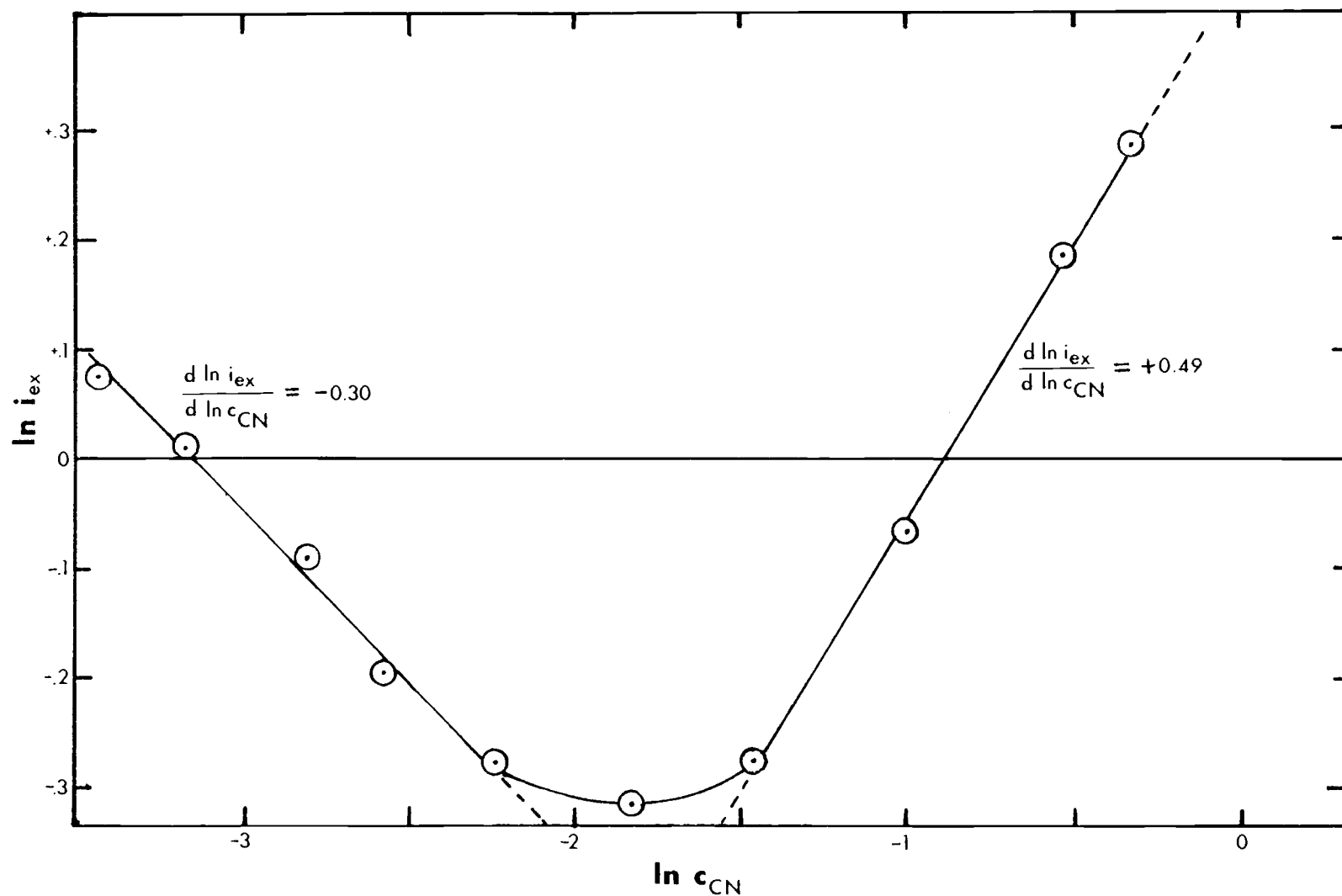


Figure 5.2.1.  $\ln(i_{ex})$  determined in reference (48) vs.  $\ln(c_{CN})$  calculated by program COMPN. Units of  $i_{ex}$  are  $\text{mA}/\text{cm}^2$ ; units for  $c_{CN}$  are  $\text{mol/l}$ .



are plotted against  $\ln c_{\text{CN}}$  in Figure 5.2.2.

The double layer data obtained in the present work were used to determine  $\phi_1$  and  $q_1$  for each of Vielstich and Gerischer's ten points. In order to find these quantities at various cyanide concentrations, graphs of  $\phi_1$  and  $q_1$  vs.  $\ln c_{\text{CN}}$  were constructed by reading values of  $\phi_1$  and  $q_1$  from each curve in Figures 4.2.6 and 4.2.7 at each of the equilibrium potentials for Vielstich and Gerischer's solutions. These values were then replotted against  $\ln c_{\text{CN}}$  at constant potential. Some extrapolation was necessary in these operations, but the error incurred should not be large.

Representative curves for  $\phi_1$  vs.  $\ln c_{\text{CN}}$  and for  $q_1$  vs.  $\ln c_{\text{CN}}$  at various potentials are shown in Figures 5.2.3 and 5.2.4. The values of  $\phi_1$  and  $q_1$  were read from these curves for each of the ten points. These values are plotted against the logarithm of the cyanide concentration in the silver-containing solutions in Figures 5.2.5 and 5.2.6. The difference between these figures and Figures 5.2.3 and 5.2.4 is, of course, that the cell potential is held constant in the former but is allowed to follow the equilibrium potential in the latter.

Values of  $d\phi_1/d \ln c_{\text{CN}}$  and  $dq_1/d \ln c_{\text{CN}}$  were determined for high and low cyanide concentrations from the fairly straight portions on these graphs. In each case, five points were used to estimate the values at low cyanide concentration, and four points for high

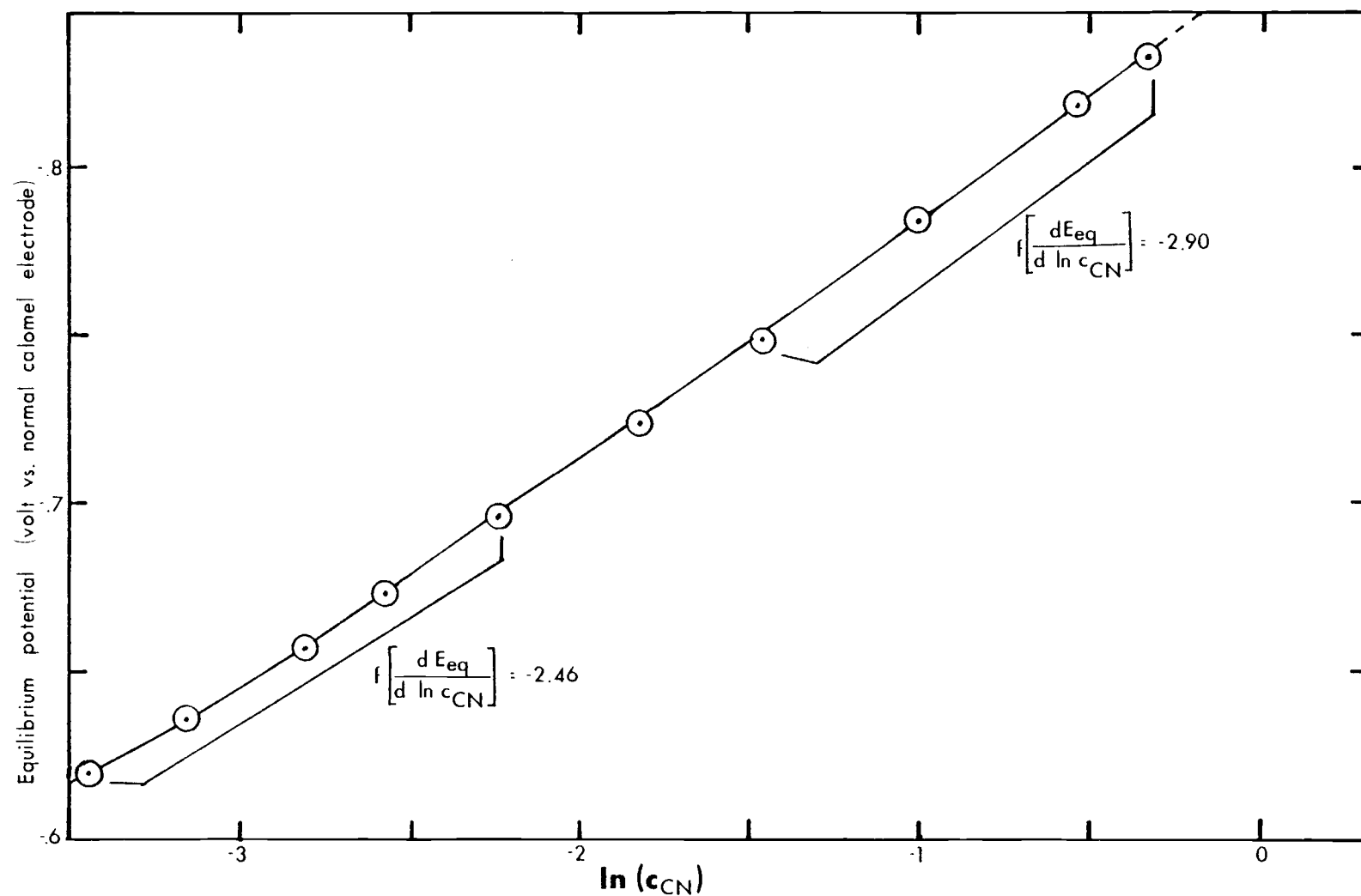


Figure 5.2.2. Equilibrium potentials calculated for solutions in reference (48) vs.  $\ln(c_{CN})$  calculated by program COMPN. Units of  $c_{CN}$  are mol/l.

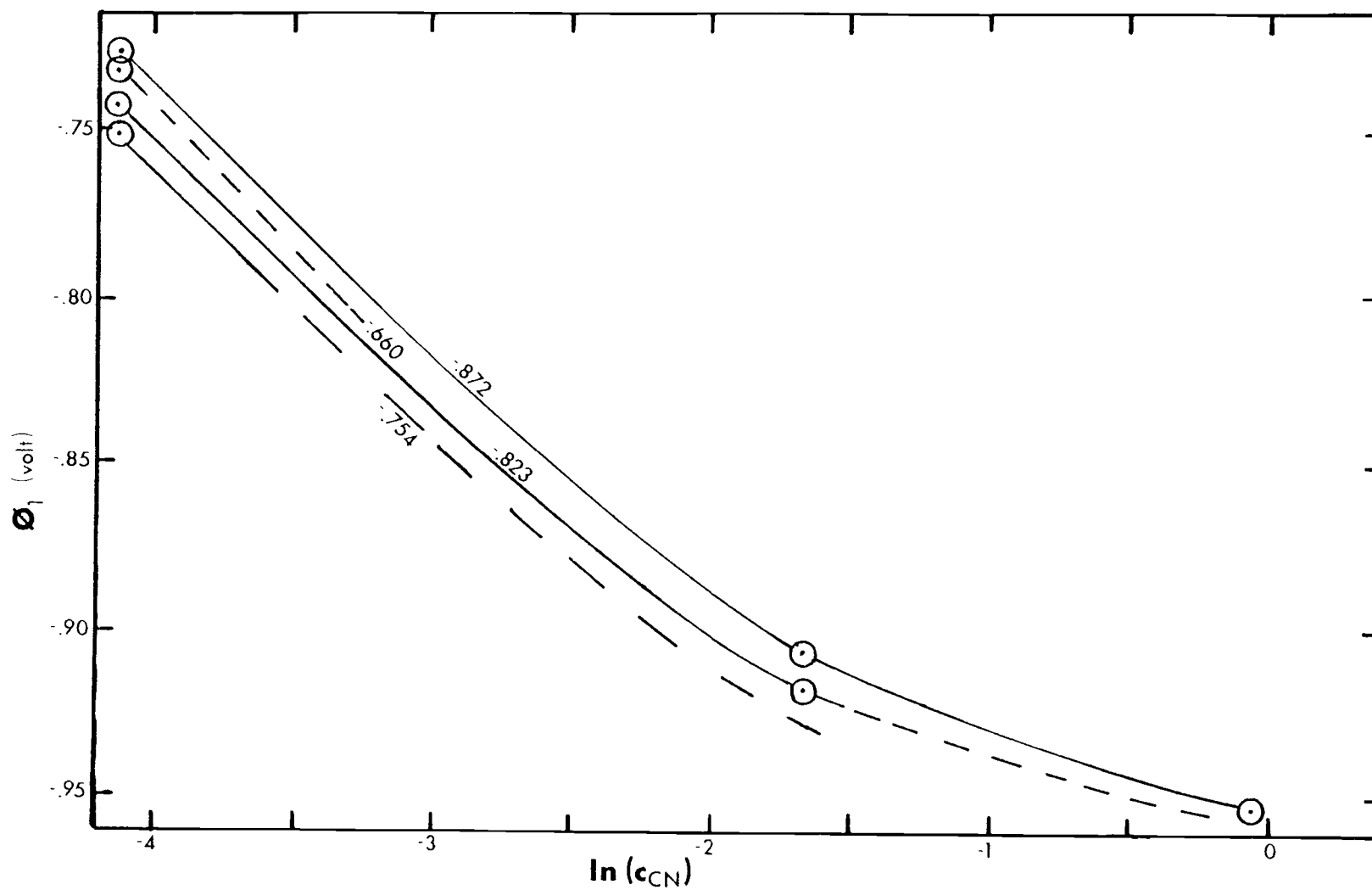


Figure 5.2.3. Potential of the inner Helmholtz layer vs.  $\ln(c_{CN})$  at constant cell potential. Units of  $c_{CN}$  are mol/l. Cell potential indicated on each curve.

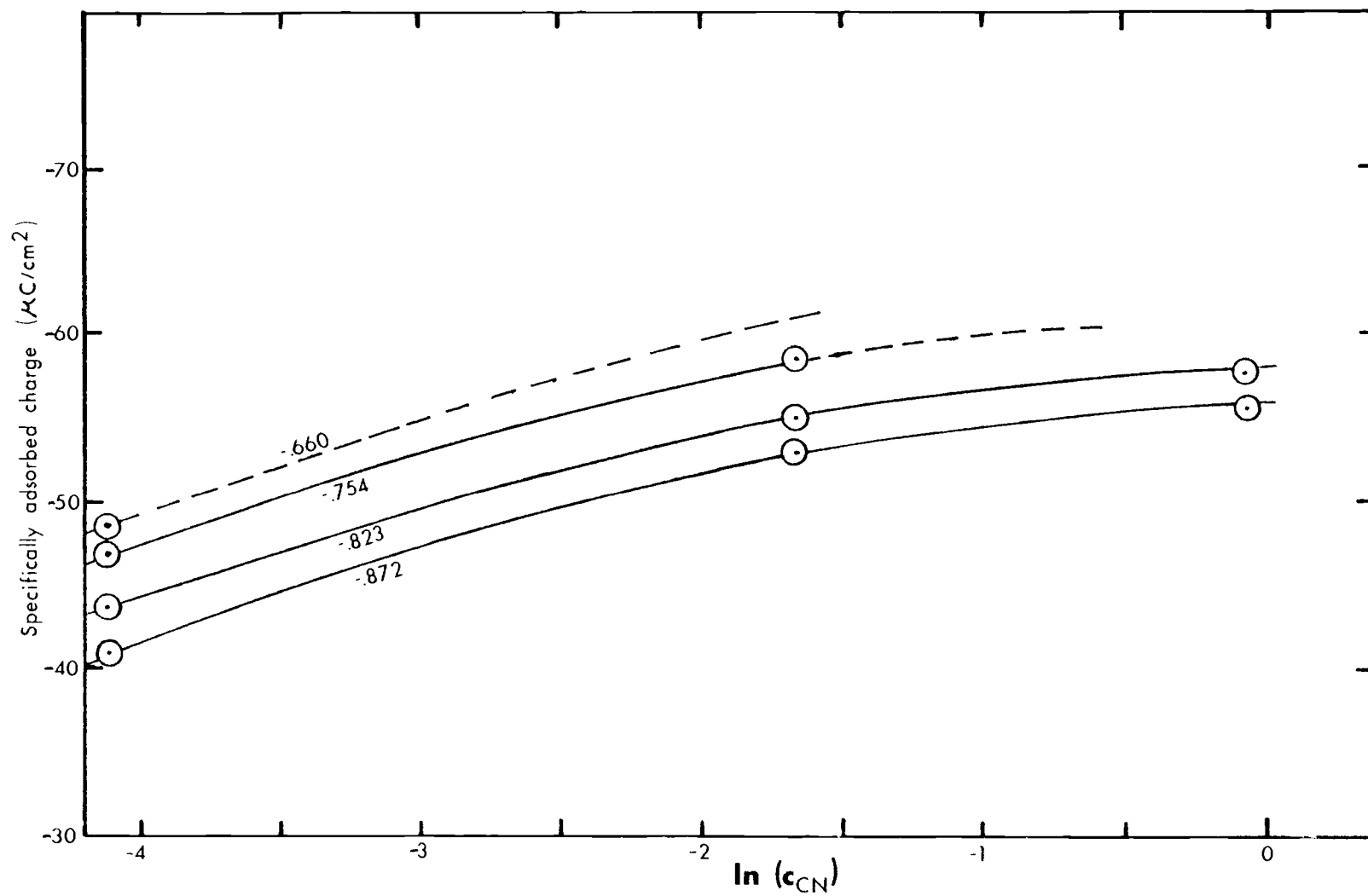


Figure 5.2.4. Specifically adsorbed charge vs.  $\ln(c_{\text{CN}})$  at constant cell potential. Units of  $c_{\text{CN}}$  are mol/l. Cell potential indicated on each curve.

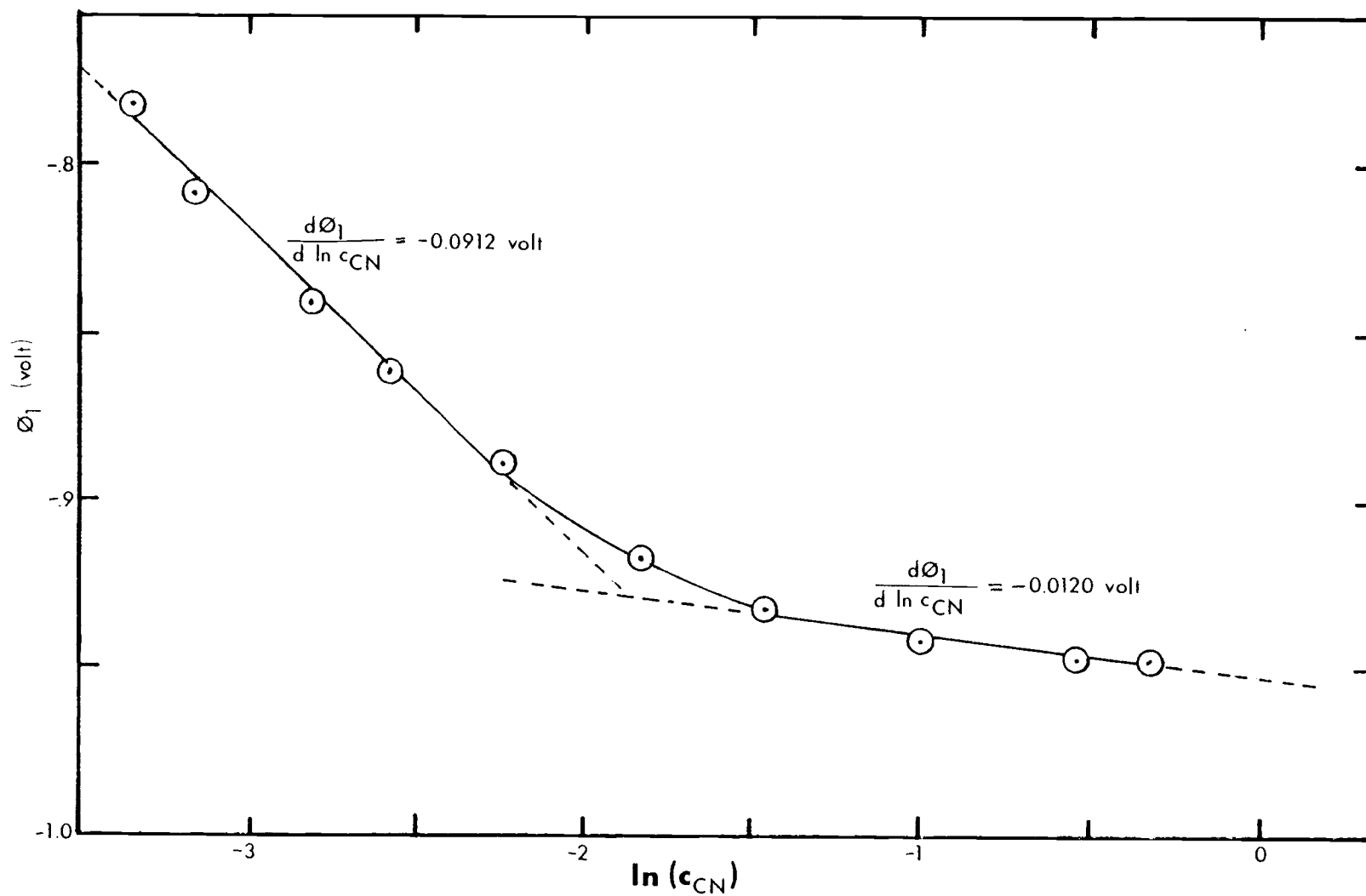


Figure 5.2.5. Variation of the potential of the inner Helmholtz layer with  $\ln(c_{CN})$ , holding the electrode at the equilibrium potential. Units of  $c_{CN}$  are mol/l.

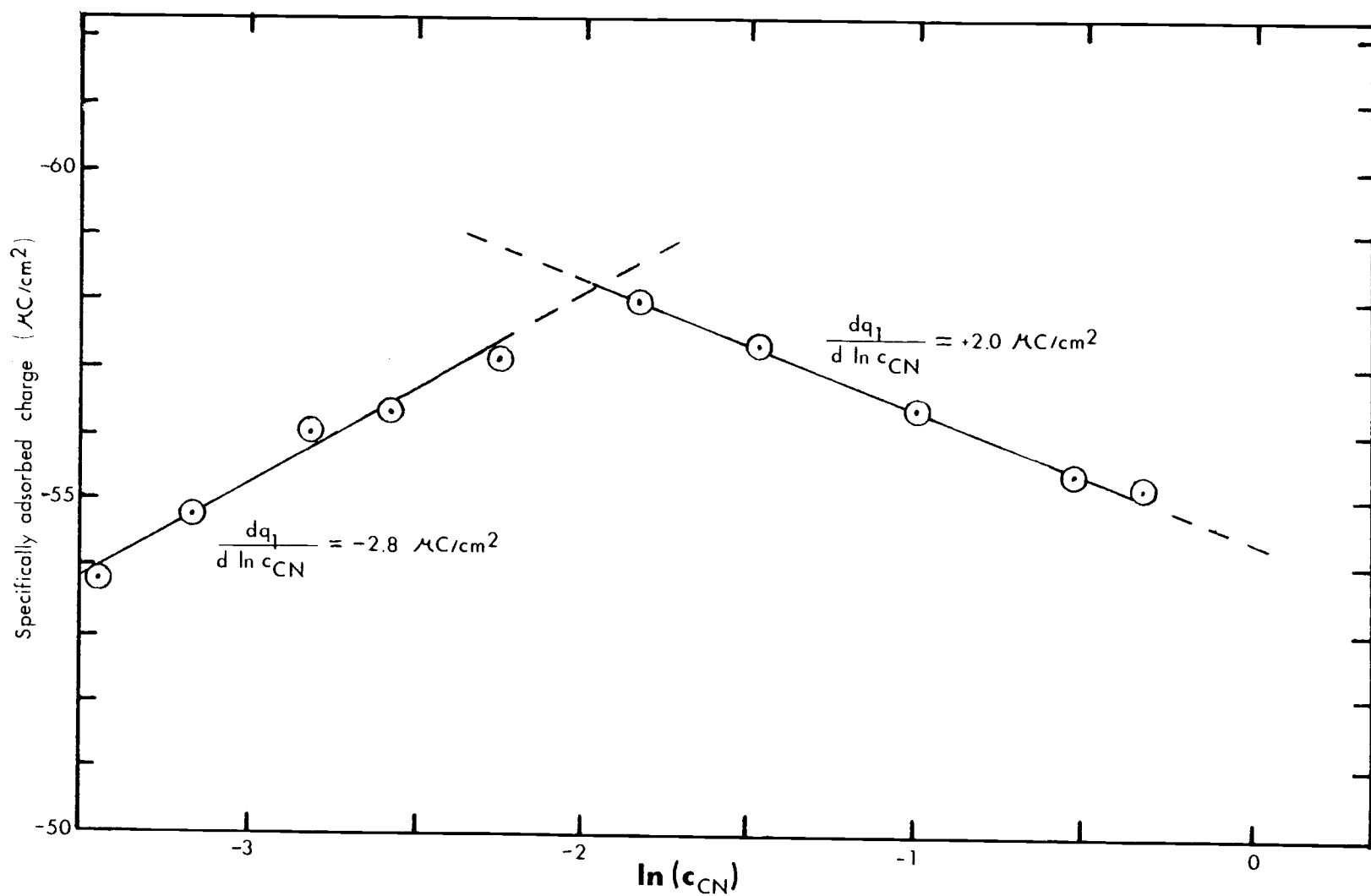


Figure 5.2.6. Variation of the specifically adsorbed charge with  $\ln(c_{\text{CN}})$ , holding the electrode at the equilibrium potential. Units of  $c_{\text{CN}}$  are mol/l.

cyanide concentration. The values of the slopes are indicated on the graphs.

There are two differences which must be considered between Vielstich and Gerischer's solutions and the ones used for the double layer measurements. Vielstich and Gerischer used potassium for the cations, whereas sodium was used in this work; Vielstich and Gerischer used chloride to maintain ionic strength, whereas fluoride was used in this work. The first difference should be of no concern, since there are no specifically adsorbed cations in either case. However, the replacement of chloride with fluoride makes it necessary to assume that chloride adsorbs only to a very small extent (compared to cyanide) or that the effect of adsorbed chloride on the reaction rate is small. Evidence to support this assumption is cited at the end of this section.

Instead of using the slope measured from Figure 5.2.2 to estimate  $dE_{eq}/d \ln c_{CN}$  directly, an algebraic method was used. The method is based on the fact that the total amount of silver was the same throughout the series of solutions, i. e. ,

$$0 = \frac{dc_2}{dc_{CN}} + \frac{dc_3}{dc_{CN}} + \frac{dc_4}{dc_{CN}}, \quad (5.2.5)$$

and on the fact that the ionic strength was held constant. This last fact permits concentration equilibrium constants to be employed,

so that

$$c_4 = K_4^c c_{CN} c_3 \quad (5.2.6)$$

and

$$c_3 = K_3^c c_{CN} c_2 . \quad (5.2.7)$$

These two equations may be differentiated, and the equilibrium constants eliminated by substitution to give

$$\frac{dc_4}{dc_{CN}} = \frac{c_4}{c_{CN}} + \frac{c_4}{c_3} \cdot \frac{dc_3}{dc_{CN}} \quad (5.2.8)$$

and

$$\frac{dc_3}{dc_{CN}} = \frac{c_3}{c_{CN}} + \frac{c_3}{c_2} \cdot \frac{dc_2}{dc_{CN}} . \quad (5.2.9)$$

Substitution of these into Equation 5.2.5 and rearrangement gives

$$\frac{dc_2}{dc_{CN}} = - \frac{c_2}{c_{CN}} \cdot \frac{c_3 + 2c_4}{(Ag)_T} , \quad (5.2.10)$$

where  $(Ag)_T$  has been substituted for  $c_2 + c_3 + c_4$ .

To relate this derivative to equilibrium potentials, the Nernst Equation 5.1.5 may be differentiated to give

$$f \frac{dE_{eq}}{d \ln c_{CN}} = -2 + \frac{c_{CN}}{c_2} \cdot \frac{dc_2}{dc_{CN}} . \quad (5.2.11)$$

Substituting Equation 5.2.10 into this results in



$$f \frac{dE_{eq}}{d \ln c_{CN}} = -2 - \frac{c_3 + 2c_4}{(Ag)_T} \quad (5.2.12)$$

The concentrations calculated for the solutions (Table 5.2.1) were put into this equation. The average values of  $f(dE_{eq}/d \ln c_{CN})$  for the four highest and the five lowest cyanide concentrations are indicated in Figure 5.2.2.

The values of the derivatives given in Figures 5.2.1, 5.2.2, 5.2.5, and 5.2.6 may now be substituted into Equation 5.2.4 to give two equations which may be arranged in the form:

$$1.16 + z = (3.55z - 1.09)\alpha - (5.6 \mu C/cm^2)(B_{\dagger CN}/e_o) \quad (5.2.13a)$$

for low cyanide concentration, and

$$2.39 + z = (0.47z + 2.43)\alpha + (4.0 \mu C/cm^2)(B_{\dagger CN}/e_o) \quad (5.2.13b)$$

for high cyanide concentration. These equations can be solved simultaneously for  $\alpha$  and  $B_{\dagger CN}$  if various values of  $z$  are assumed.

Table 5.2.2 shows that, for the three choices of  $z$  corresponding to species present in the solution (-1, -2, and -3), both -2 and -3 give values for  $\alpha$  between zero and one. Thus either of these choices would reasonably explain the data of Vielstich and Gerischer. However, since the  $\alpha$  value for  $z = -2$  is so close to zero, representing a very extreme geometry in the reaction curve

(Figure 2.2.1), it is not likely that  $\text{Ag}(\text{CN})_3^{2-}$  is the electroactive species. One might also consider values of  $z$  more negative than -3, since these also give  $\alpha$  values between zero and one; however, it is quite unlikely that silver would coordinate with more than four ligands, even briefly at the interface. This leaves  $\text{Ag}(\text{CN})_4^{3-}$  (with  $z = -3$ ) as the only likely electroactive species. Thus,  $\alpha$  is taken (from Table 5.2.2) to be 0.26. The fact that this value is much lower than the values reported by Vielstich and Gerischer for both high and low cyanide concentrations is of no consequence, since those experimental observations are confounded by the effects of simultaneous changes in the electrode potential and specific adsorption.

Table 5.2.2. Values of  $\alpha$  and  $B_{\ddagger\text{CN}}$  for various choices of  $z$ .

$z$	$\alpha$	$B_{\ddagger\text{CN}}/e_0$ ( $\text{cm}^2/\mu\text{C}$ )	$B_{\ddagger\text{CN}}$ ( $\text{\AA}^2/\text{ion}$ )
-1	-1.11	+0.891	+1430
-2	+0.05	+0.079	+126
-3	+0.26	-0.219	-350
-4	+0.35	-0.451	-722

The value of  $B_{\ddagger\text{CN}}$  which results from Equations 5.2.13 with  $z = -3$  is  $-350 \text{ \AA}^2/\text{ion}$ . The magnitude of this number is certainly reasonable when compared to values reported by Parsons (44) for the effects of halides on hydrogen evolution and by Eriksrud (14) for the

effects of halides on cobalt reduction; however, the sign of the number is surprising. Parsons (44) has suggested that the major type of interaction between the adsorbed ions and the activated complex should be electrostatic in nature, and that, on this basis, a negative value for the interaction coefficient indicates that the interacting particles are of opposite signs. This line of reasoning thus implies that the activated complex in silver deposition has a positive charge. One way of interpreting this is that there is very little cyanide associated with the activated complex, i. e., that the activated complex is very much like a naked adsorbed silver ion.

The fact that each of the curves in Figures 5.2.1, 5.2.5, and 5.2.6 have two straight portions corresponding to the same ranges of cyanide concentration, coupled with the reasonable values obtained for  $\alpha$  and  $B_{\ddagger\text{CN}}$ , is very convincing evidence that Equations 5.2.4 and 2.2.45 are appropriate descriptors of the rate of silver deposition in cyanide solution. This fact also supports the assumption previously made that chloride is not specifically adsorbed in the presence of cyanide or does not affect the reaction rate. In addition, the use of these equations does not require that the extremely dilute species AgCN be identified as the electroactive species, as the interpretation of Vielstich and Gerischer did require.

### 5.3. Effect of the Double Layer on Currents at High Polarization

By using the same reasoning employed in writing Equation 5.2.1, Equation 2.2.45 may be written for the deposition currents obtained at high polarization in solutions A through E as:

$$\ln[i_F(0)/c_{Ms}] = \text{const}_1 - \alpha f[E - (1-z)\phi_1] + 2(B_{\ddagger CN}/e_o)q_1. \quad (5.3.1)$$

All but one of the constants in this equation have been determined from the analysis of the data of Vielstich and Gerischer. Substitution of these yields

$$\begin{aligned} \ln[i_F(0)/c_4] = \text{const}_1 - (10.13 \text{ volt}^{-1})(E - 4\phi_1) \\ + (-0.438 \text{ cm}^2/\mu\text{C})q_1. \end{aligned} \quad (5.3.2)$$

The quantities associated with the 14 measurements at high polarization which are pertinent to this equation are given in Table 5.3.1. The values of  $c_4$  used to calculate  $\ln[i_F(0)/c_4]$  are based on the equilibrium constants determined in this work. (See Table 5.1.1.)

The double layer quantities  $\phi_1$  and  $q_1$  were determined in the same way as for the solutions of Vielstich and Gerischer, i.e., by using curves similar to Figures 5.2.3 and 5.2.4 of  $\phi_1$  and  $q_1$  vs.  $\ln c_{CN}$  at constant electrode potential. For the solutions of lower cyanide concentration in this series, the amount of silver is not

Table 5.3.1. Data summary for high polarization measurements.

Sol'n. I. D.	$-i_F(0)$ mA/cm <sup>2</sup>	$E_{eq} - E_{cell}$ volt	$-E_{cell}$ volt vs. SCE	$-E$ volt vs. SCE	$\ln[i_F(0)/c_4]$ Arg. in: A cm/mol	$-q_1$ $\mu C/cm^2$	$-\phi_1$ volt	$E - 4\phi_1$ volt	$\epsilon^{(a)}$	$\epsilon^{(b)}$
A1	3.71	.150	.680	.668	13.125	55.6	.811	2.576	-1.189	+0.926
A2	4.99	.200	.730	.714	13.421	53.8	.822	2.574	-0.036	+1.990
A3	6.25	.240	.770	.750	13.647	52.6	.831	2.574	+0.788	+2.742
B1	2.79	.100	.791	.784	8.850	58.0	.930	2.936	+0.654	-0.754
B2	9.17	.250	.941	.919	10.040	50.2	.898	2.673	+0.389	+1.189
C	4.65	.150	.861	.848	9.024	54.8	.929	2.868	+1.042	+0.133
D1	2.05	.100	.832	.827	7.861	56.3	.940	2.933	+0.452	-1.028
D2	4.08	.150	.882	.872	8.550	54.2	.931	2.852	+0.542	-0.240
D3	8.5	.200	.932	.913	9.284	52.0	.921	2.771	+0.727	+0.637
D4	12.0	.250	.982	.953	9.628	49.4	.908	2.679	+0.498	+1.188
E1	.503	.050	.859	.858	5.370	56.2	.957	2.970	-1.238	-3.101
E2	1.174	.100	.906	.904	6.218	54.1	.950	2.896	-0.846	-2.083
E3	2.15	.150	.957	.953	6.823	51.6	.939	2.803	-0.884	-1.325
E4	4.24	.189	1.000	.994	7.502	49.2	.926	2.710	-0.898	+0.537

(a) Deviation from the least squares plane through the points.

(b) Deviation from the prediction based on the values of  $\alpha$  and  $B_{\ddagger CN}$  for the data of ref. (48).

negligible in computing the double layer quantities. However, since the outer spheres of the silver complexes consist of cyanide, it seems reasonable to suppose that the adsorption of these species is somewhat the same as for cyanide itself. For these reasons the values on the abscissas of the  $\phi_1$  vs.  $\ln c_{\text{CN}}$  and  $q_1$  vs.  $\ln c_{\text{CN}}$  plots were taken to be  $\ln[c_{\text{CN}} + (\text{Ag})_T]$  rather than  $\ln c_{\text{CN}}$ . Whereas this is probably not a very accurate approximation for the effect of adsorbed silver species, it is certainly better than completely ignoring it.

Adherence of the high polarization data to Equations 5.3.1 and 5.3.2 was tested in two ways. The first method involved the construction of a three-dimensional model in which  $\ln[i_F(0)/c_4]$  was plotted against  $q_1$  and  $E - 4\phi_1$ . If the data follow the equations, all the points must fall into a plane. The second method involved the use of linear least squares regression analysis of the same three quantities.

The deviations of the  $\ln[i_F(0)/c_4]$  values from the least squares plane are given in Table 5.3.1. Their magnitudes are disconcertingly large, producing a multiple correlation coefficient squared of only 0.90, i.e., only 0.90 of the variations (34, p. 91) in the  $\ln[i_F(0)/c_4]$  values is due to the variations of  $q_1$  and  $E - 4\phi_1$ . The partial slopes of the least squares plane yield  $\alpha = 0.52 \pm 0.05$  and  $B_{\ddagger\text{CN}}/e_o = -0.25 \pm 0.05$  where the indicated tolerances are one standard deviation. Because the adherence of this data to Equation 5.3.1 is not nearly as good as that of Vielstich and Gerischer's data

to Equation 5.2.4, the  $\alpha$  and  $B_{\dagger\text{CN}}$  values found from Vielstich and Gerischer's data should be regarded as more correct.

To investigate the reasons for the poor adherence of the high polarization data, it was compared to predictions based on the results of the previous section. This comparison was performed by determining the deviations of the points from a plane which passes through the mean of the  $\{\ln[i_F(0)/c_4], q_1, E - 4\phi_1\}$  points and having a slope corresponding to the previously determined  $\alpha = 0.26$  and  $B_{\dagger\text{CN}}/e_o = -0.219$ . These deviations, given in Table 5.3.1, follow two clearly defined trends. (1) In each solution, as the polarization is increased, the deviation becomes more positive, and, (2) from one solution to the next, the deviations become more positive as the cyanide concentration is decreased.

These deviations can be explained as results of the fact that the double layer does not reach equilibrium within the times involved in the experiments. When the electrode is suddenly made more cathodic, a considerable amount of cyanide is dispelled into the adjacent solution, producing a local excess which dissipates through processes which are at least partly diffusive in nature, and, therefore, occur over a time which is significant within the time frame of the experiment. In addition, faradaic production of cyanide tends to maintain the local excess.

The sudden reduction of the amount of specific adsorption, (increase in  $q_1$ ) does not affect the total double layer charge  $q$  immediately, since the expelled charge remains in the diffuse double layer for a while. The local excess of cyanide will have the same effect on the specific adsorption as a high bulk cyanide concentration would have. Thus,  $q_1$  will be more negative than for an equilibrium double layer. The diffuse double layer potential  $\phi_2$  will become less because of the excess cyanide, but this should not be too great an effect at times when  $i_{\text{cell}} \approx i_F$ , because the high field will quickly spread the charge. (Equation 2.3.13 for  $\phi_2$  becomes inoperative in this situation because it is based on an assumption of equilibrium in the double layer structure.)

The effect on  $\phi_1$  may be judged through examination of Equation 2.3.14. Immediately after the step, both the total double layer charge  $q$  and the specifically adsorbed charge  $q_1$  will be more negative than for a stable double layer at the same potential. These effects tend to cancel, so the difference in the expected and actual values of  $\phi_1$  is probably not too large.

Thus, the only major difference between the calculated values of the double layer (Table 5.3.1) and those which are actually likely to exist during the deposition current measurements is that  $q_1$  is more negative than expected. Equation 5.3.2 shows that this would produce a higher current than predicted. This deduction is consistent



with the observations that for each solution the deviations from the predictions based on Vielstich and Gerischer's data are more positive as the step is made larger. These non-equilibrium double layer effects are not present in the data of Vielstich and Gerischer because small step potentials were used, and the results were extrapolated to zero overvoltage to get the exchange currents.

The other observation regarding the deviations from the Vielstich-and-Gerischer-based predictions, that of a general positive trend as the cyanide concentration is decreased, may be attributed to the much greater effect of the desorbed cyanide in the dilute cyanide solutions. As the surface cyanide concentration is increased through possibly several orders of magnitude, the amount of the electroactive species  $\text{Ag}(\text{CN})_4^{3-}$  is also increased. Thus, the calculated  $\ln[i_F(0)/c_4]$  values are larger than actually exist in all cases, but more so in the solutions of lower cyanide concentration.

This discussion demonstrates that any method developed to calculate  $q_1$ ,  $\phi_1$ , and the concentrations of the various solution species adjacent to the double layer at times soon after a large potential step would necessarily be quite complex. It would require simultaneous consideration of the mass transport of all solution species under the influences of both electric and concentration gradients, homogeneous reaction rates among the silver complexes, as well as the detailed considerations of the double layer structure which have already been discussed. Such a treatment is probably possible, but is beyond the scope of the present work.

## VI. SUMMARY

Several characteristic quantities of the double layer at a silver electrode in cyanide and fluoride solutions, namely the amount of specific adsorption and the potentials of the inner and outer Helmholtz layers, have been determined from double layer capacitance data obtained by means of a specially constructed, computer-controlled potentiostat. The calculations are based on a method proposed by Devanathan (13) for investigating aqueous interfaces at mercury. It was found that the silver interface is qualitatively similar to that of mercury.

An equation based on absolute rate theory (19) and on a detailed model of the double layer (13) was developed to relate the double layer structure to the rate of electrodeposition of silver from cyanide electrolytes. The equation was found to provide quite acceptable correlation between the structure of the double layer and the exchange current data of Vielstich and Gerischer (48). Deposition currents obtained at high polarization in this work did not correlate to the calculated double layer quantities nearly as well as the data of Vielstich and Gerischer did. This was explained in terms of slow mass transport processes connected with the sudden changes in the double layer which are produced by the applied potentiostatic step.

## BIBLIOGRAPHY

1. Bek, R. Yu., E. A. Nechaev, and N. T. Kudryavtsev, *Soviet Electrochem.*, 3, 999-1001 (1967).
2. Bek, R. Yu., E. A. Nechaev, and N. T. Kudryavtsev, *Soviet Electrochem.*, 3, 1316-1318 (1967).
3. Bevington, Philip R., "Data Reduction and Error Analysis for the Physical Sciences," McGraw-Hill, New York, 1969.
4. Blomgren, E., J. O'M. Bockris, and C. Jesch, *J. Phys. Chem.*, 65, 2000-2010 (1961).
5. Bockris, J. O'M., S. D. Argade, and E. Gileadi, *Electrochim. Acta*, 14, 1259-1283 (1969).
6. Bockris, J. O'M., and A. K. N. Reddy, "Modern Electrochemistry," Vol. 2, Plenum Press, New York, 1970.
7. Bodlander, G., and W. Eberlein, *Z. anorg. Chem.*, 41, 193 (1904). Cited in: "Stability Constants of Metal-Ion Complexes, with Solubility Products of Inorganic Substances," Special publication No. 7, Chemical Society, London, 1958. P. 35.
8. Borisova, T. I., in "Transactions of the Conference on Electrochemistry," Moscow, 1953, p. 386. Cited in: D. I. Leikis, *Proceedings of the Academy of the USSR, Physical Chemistry Section*, 135, 1199-1201 (1960).
9. Conway, B. E., "Theory and Principles of Electrode Processes," Ronald Press, New York, 1965.
10. Cotton, F. Albert, and Geoffrey Wilkinson, "Advanced Inorganic Chemistry. A Comprehensive Text," 2nd ed., Wiley, New York, 1966.
11. Davis, Dale Stroble, "Nomography and Empirical Equations," Reinhold, New York, 1962.
12. Delahay, P., R. deLevie, and A. -M. Giuliani, *Electrochim. Acta*, 11, 1141-1146 (1966).

13. Devanathan, M. A. V., *Trans. Faraday Soc.*, 50, 373-385 (1954).
14. Eriksrud, Elisabeth, *J. Electroanal. Chem.*, 45, 411-418 (1973).
15. Gerischer, H., *Z. phys. Chem.*, 202, 292 (1953). Cited in: W. Vielstich and H. Gerischer, *Z. phys. Chem., N.F.*, 4, 10 (1955).
16. Gerischer, Heinz, and Ragnar P. Tischer, *Z. Elektrochem.*, 58, 819-827 (1954).
17. Gerischer, Heinz, and Wolf Vielstich, *Z. Electrochem.*, 56, 380-386 (1952).
18. Gerischer, H., and W. Vielstich, *Z. phys. Chem., N.F.*, 3, 16-33 (1955).
19. Glasstone, S., K.J. Laidler, and H. Eyring, "The Theory of Rate Processes," McGraw-Hill, New York, 1946.
20. Grahame, David C., *J. Am. Chem. Soc.*, 68, 301-310 (1946).
21. Grahame, David C., "Thermodynamic Properties of the Electrical Double Layer. I. Differential Capacity of Mercury in Aqueous Sodium Fluoride Solutions at 25°C," Technical Report Number 14 to the Office of Naval Research, Feb. 18, 1954.
22. Grahame, David C., and Barbara A. Soderberg, *J. Chem. Phys.*, 22, 449-460 (1954).
23. Guest, P.G., "Numerical Methods of Curve-Fitting," Cambridge Press, London, 1961.
24. Gugenheim, E. A., *J. Phys. Chem.*, 33, 842-849 (1929).
25. Hampson, N. A., D. Larkin, and J.R. Morley, *J. Electrochem. Soc.*, 114, 817-818 (1967).
26. Jones, Llewellyn H., and Robert A. Penneman, *J. Chem. Phys.*, 22, 965-970 (1954).
27. Kaischew, R., B. Mutaftshiew, and D. Nenow, *Z. phys. Chem.*, 205, 341-348 (1956).

28. Kheifets, V.L., and B.S. Krasikov, Dokl. Akad. Nauk SSSR, 109, 586 (1956). Cited in D.I. Leikis, Proceedings of the Academy of Sciences of the USSR, Physical Chemistry Section, 135, 1199-1201 (1960).
29. Leikis, D.I., Proceedings of the Academy of Sciences of the USSR, Physical Chemistry Section, 135, 1199-1201 (1960).
30. Lingane, Peter James, and Joseph H. Christie, J. Electroanal. Chem., 10, 284-294 (1965).
31. McClellan, A.L., "Tables of Experimental Dipole Moments," Freeman, San Francisco, 1963.
32. McDonald, Donald, in "Silver: Economics, Metallurgy and Use," Allison Butts, ed., with the collaboration of Charles D. Coxe, Van Nostrand, Princeton, 1967. Pp. 1-15.
33. Mehl, Wolfgang, and John O'M. Bockris, Can. J. Chem., 37, 190-204 (1959).
34. Morrison, Donald F., "Multivariate Statistical Methods," McGraw-Hill, New York, 1967.
35. Morrison, Ralph, "Grounding and Shielding Techniques in Instrumentation," Wiley, New York, 1967.
36. Nechaev, E.A., and R. Yu. Bek, Soviet Electrochem., 2, 138-142 (1966).
37. Nechaev, E.A., R. Yu. Bek, and N.T. Kudryavtsev, Soviet Electrochem., 1, 1187-1192 (1965).
38. Nechaev, E.A., R. Yu. Bek, and N.T. Kudryavtsev, Soviet Electrochem., 1, 1296-1301 (1965).
39. Nechaev, E.A., R. Yu. Bek, and N.T. Kudryavtsev, Soviet Electrochem., 4, 483-486 (1968).
40. Niki, K., et al., Electrochim. Acta, 16, 487-493 (1971).
41. Oldham, K.B., and R.A. Osteryoung, J. Electroanal. Chem., 10, 397-405 (1965).

42. Orr, M. A., in "Silver: Economics, Metallurgy and Use," Allison Butts, ed., with the collaboration of Charles D. Coxe, Van Nostrand, Princeton, 1967. Pp. 180-189.
43. Parsons, Roger, in "Advances in Electrochemistry and Electrochemical Engineering," Vol. 1, Paul Delahay, ed., Interscience, New York, 1961. Pp. 1-64.
44. Parsons, Roger, J. Electroanal. Chem., 21, 35-43 (1969).
45. Pilla, Arthur A., J. Electrochem. Soc., 117, 467-477 (1970).
46. Skoog, Douglas A., and Donald M. West, "Fundamentals of Analytical Chemistry," Holt, Rinehart, and Winston, New York, 1963.
47. Valette, Georges, C.R. Acad. Sci., Paris, 275, 167-170 (1972).
48. Vielstich, W., and H. Gerischer, Z. phys. Chem., N.F., 4, 10-23 (1955).
49. Wroblowa, H., Z. Kovac, and J. O'M. Bockris, Trans. Faraday Soc., 61, 1523-1548 (1965).
50. Zsako, J., and E. Petri, Rev. Roumaine Chim., 10, 571 (1965). Cited in: "Stability Constants of Metal-Ion Complexes," Special publication No. 25, Chemical Society, London, 1971. P. 55.

## APPENDIX 1

Definitions of Symbols

$a$	activity
$A$	$= 2D_{2-s} \epsilon_o' RTc$
$(Ag)_T$	total silver concentration
$B$	intercept of the linearized form of the capacitative current transient
$B_{\ddagger j}$	constant of interaction between species $j$ and the activated complex
$c$	with subscript--concentration; without subscript--electrolyte concentration
$C$	measured capacitance of the double layer ( $\mu f$ )
$C_A$	see Figure A2. 1
$C_{dl}$	specific double layer capacitance ( $\mu f/cm^2$ )
$C_{in}$	input capacitance of current-to-voltage converter
$C_{out}$	effective output capacitance of current-to-voltage converter
$C_{2-s}$	diffuse double layer capacitance
$d$	the uncertainty in the current measurement due to the resolution of the ADC
$D$	without subscript--the denominator in determining the least-squares slope and intercept for the linearized capacitative current transient; with subscript--diffusion coefficient
$D(s)$	ratio of the DC transfer function for the current-to-voltage converter to the transfer function at frequency $s$
$D_{m-2}$	dielectric constant of inner layer

$D_{2-s}$	dielectric constant of diffuse layer
$e$	base of natural logarithms
$e_o$	protonic charge ( $1.602 \times 10^{-19}$ coul)
$E$	electrode potential; i. e. , cell potential corrected for ohmic loss
$E_{\text{cell}}$	externally measured cell potential
$E_{\text{eq}}$	equilibrium potential
$E_M^f$	formal electrode potential for silver deposition written in terms of the electroactive species
$E_{\text{neg}}$	a value of the electrode potential at which the double layers of several solutions behave identically
$E_{\text{start}}$	electrode potential at the beginning of an integration
$E_x$	some arbitrary value of the electrode potential
$E_{\text{zc}}$	potential of zero charge
$E_2^f$	formal electrode potential for silver deposition written in terms of $\text{Ag}(\text{CN})_2^-$
$E_2^o$	standard electrode potential for silver deposition written in terms of $\text{Ag}(\text{CN})_2^-$
$f$	$= F/RT$ ( $38.96 \text{ volt}^{-1}$ at 25 C)
$F$	the Faraday (96487 coul/equ)
$G$	gain of an operational amplifier
$G_A$	gain of amplifier A, Figure 3. 1. 3
$G_B$	gain of amplifier B, Figure 3. 1. 3
$h$	Planck's constant
$i_{\text{cell}}$	cell current density



$i_{\text{ex}}$	exchange current density
$i_{\text{F}}$	faradaic current density
$I_{\text{b}}$	background (residual) current
$I_{\text{bj}}$	the $j$ th measurement of the residual current
$I_{\text{C}}$	capacitative cell current
$I_{\text{cell}}$	cell current
$I_{\text{F}}$	faradaic current
$I_{\text{j}}$ or $I_{\text{k}}$	cell current at $t_{\text{j}}$ or $t_{\text{k}}$
$I_{\text{o}}$	cell current evaluated at $t = 0$ in a capacitative current transient
$I_{\text{s}}$	additional residual current due to a potential step
$I_0, I_1, I_6$	see Figure 3.1.3
$j$	integer identifier
$k$	Boltzmann's constant or an integer identifier
$k_{\text{r}}$	rate constant for a reaction
$k_1$	cell time constant for capacitance measurement when $R_{\text{F}} \gg R_{\text{u}}$
$k_2$	cell time constant for capacitance measurement
$K_{\text{m-1}}$	electrostatic capacity of the space between the metal surface and the inner Helmholtz layer
$K_{1-2}$	electrostatic capacity between the inner and outer Helmholtz planes
$K_3$	stepwise formation constant for $\text{Ag}(\text{CN})_3^{2-}$
$K_3^{\text{c}}$	concentration formation constant for $\text{Ag}(\text{CN})_3^{2-}$

$K_4$	stepwise formation constant for $\text{Ag}(\text{CN})_4^{3-}$
$K_4^c$	concentration formation constant for $\text{Ag}(\text{CN})_4^{3-}$
$K^\ddagger$	equilibrium constant for the microscopically reversible activation step
$L_j$	$= \ln[(c_{\text{CN}})_j^2 / (c_2)_j]$
$\mathcal{L}$	Laplace operator
$M$	slope of the linearized form of the capacitive current transient
$n$	number of electrons involved in the charge-transfer step
$N$	number of times a measurement is made
$q$	net charge density on the solution-side of the double layer
$q_1$	charge density due to specifically adsorbed ions
$R$	gas constant (8.31 joule/deg/mol)
$R_A$	see Figure A2.1
$R_{\text{cell}}$	$= R_A + R_v + R_u + R_F$
$R_D^2$	$= R_0 R_1 + R_0 R_6 + R_1 R_6$
$R_f$	feedback resistance
$R_F$	faradaic resistance
$R_{\text{in}}$	input resistance of current-to-voltage converter
$R_{\text{out}}$	effective output resistance of the current-to-voltage converter
$R_u$	uncompensated solution resistance
$R_v$	see Figure A2.1
$R_0, R_1$	input resistors to the potentiostat control amplifier

$R_6$	feedback resistor for the control loop of the potentiostat
$s$	Laplace domain variable
$S$	sum of the deviations $\epsilon_j$
$S^2$	least squares variance
$t$	time after application of step potential
$T$	absolute temperature
$T(s)$	transfer function of the current-to-voltage converter
$v$	velocity of a chemical reaction
$V_A, V_B$	see Figure A2. 1
$V_C$	the potential across the double layer capacitance
$V_{DA0}$	input potential to the potentiostat to control the cell bias potential
$V_{DA1}$	input potential to the potentiostat to control the step potential
$V_{in}$	input voltage to the current-to-voltage converter
$V_{out}$	output potential of the current-to-voltage converter
$V_0$	see Figure 3. 1. 3
$V_1$	potential across the cell model before the step
$V_2$	the step potential
$V_3$	see Figure 3. 1. 3
$w_j$	weighting factor in the least squares analysis of the linearized capacitative current transient
$x_1$	distance of inner Helmholtz plane from the metal surface
$x_2$	distance of outer Helmholtz plane from the metal surface

$Y_j$	value of the ordinate in the linearized capacitive current transient at $t_j$
$z$	charge of the electroactive metal complex
$Z(\sigma)$	the Laplace-domain cell impedance
$z_j$	charge on ion $j$
$Z_k, Z_1, Z_2, Z_3$	variables used to calculate $\sigma_{I_s I_o}^2$
$Z_k^*, Z_1^*, Z_2^*, Z_3^*$	variables used to calculate $\sigma_{I_s M}^2$
$\alpha$	symmetry factor for the charge-transfer step
$\gamma$	activity coefficient
$\Gamma_j$	amount of specific adsorption ( $\text{mol}/\text{cm}^2$ ) of species $j$
$\Delta G_c^o$	standard free energy of the charge-transfer step
$\overline{\Delta G_c^o}$	standard electrochemical free energy of the charge-transfer step
$\Delta G_c^{o\ddagger}$	standard free energy of activation for the charge-transfer step
$\overline{\Delta G_c^{o\ddagger}}$	standard electrochemical free energy of activation for the charge-transfer step
$\Delta G_{Mx}^o$	standard free energy for adsorption of the electroactive metal complex from the solution to a distance $x$ from the metal surface
$\Delta t$	time interval between current measurements
$\epsilon_j$	deviation of a measured value of $(E_{eq})_j$ from the predicted value
$\epsilon_o'$	rationalized permittivity of free space ( $8.85 \times 10^{-14}$ farad/cm)
$\eta$	overvoltage; $= E - E_{eq}$

$\lambda$	time-independent function for determining the faradaic current after a step from equilibrium
$\mu$	chemical potential
$\bar{\mu}$	electrochemical potential
$\rho$	electrode roughness factor
$\sigma$	without a subscript--real component of the Laplace-domain variable $s$ ; with a subscript--standard deviation of the variable in the subscript
$\tau$	transmission coefficient
$\phi$	electric potential of a chemical phase with respect to the solution
$\phi_{\text{ref}}$	a constant potential which incorporates all the constant interfacial potentials in the measurement cell
$\phi_1$	potential of inner Helmholtz plane with respect to the solution
$\phi_2$	potential of outer Helmholtz plane with respect to the solution

#### Subscripts and Superscripts

CN	for cyanide
e	for electrons in the metal
Hg	for the metal of the reference electrode
j	integer identifier
k	integer identifier
KCl	for the reference electrode filling solution
L	for the ligand
m	for the electrode metal
M	for the electroactive metal complex

O	for the oxidized species
R	for the reduced species
s	for the bulk of the solution
x	at distance $x$ from the metal, where the electroactive species is adsorbed
y	at distance $y$ from the metal, where the ligand is adsorbed
2, 3, 4	(used with $a$ , $\gamma$ , and $c$ ) for $\text{Ag}(\text{CN})_2^-$ , $\text{Ag}(\text{CN})_3^{2-}$ , $\text{Ag}(\text{CN})_4^{3-}$ , respectively
o	at standard chemical conditions
‡	for activated complex

## APPENDIX 2

Derivation of Equations for Potentiostat

To describe the manner in which the potentiostat controls the cell potential, it is necessary to consider the nature of the cell itself. The cell model shown in Figure A2. 1 will be employed. This model was obtained from Figure 2. 4. 1a by omitting the components connecting the reference electrode to the solution node for the reasons cited on p. 29. In contrast to Figure 2. 4. 1b the components connecting the auxiliary electrode to the solution node are retained, since it is of interest here to understand how the potentiostat control works when these are present. Thus the circuit which will be described here is that of the cell model diagrammed in Figure A2. 1 connected to the potentiostat circuit shown in Figure 3. 1. 3. The symbols used in this appendix are given in those figures. The test electrode may be considered to be tied to ground, since it is connected to the summing point of the current-to-voltage converter.

To derive an equation for  $E_{\text{cell}}$  as a function of the potentiostat (and cell) components and the input voltages, ten equations are written which relate the potentials and currents in the circuit:

$$I_{\text{cell}} = \frac{V_C}{R_F} + C \frac{dV_C}{dt}, \quad (\text{A2. 1})$$

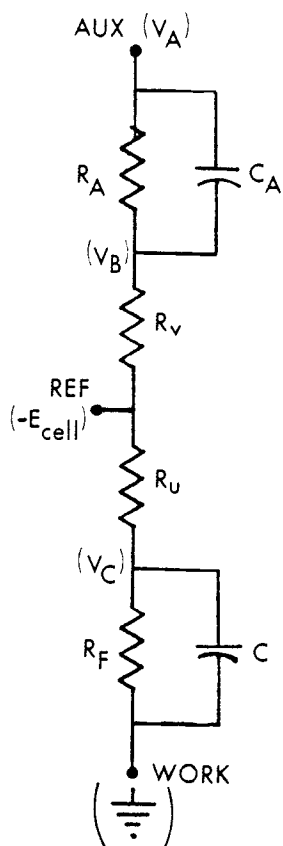


Figure A2. 1. Cell model to describe potentiostat operation.



$$I_{\text{cell}} = -(E_{\text{cell}} + V_C)/R_u, \quad (\text{A2. 2})$$

$$I_{\text{cell}} = (V_B + E_{\text{cell}})/R_v, \quad (\text{A2. 3})$$

$$I_{\text{cell}} = (V_A - V_B)/R_A + C_A \frac{d(V_A - V_B)}{dt}, \quad (\text{A2. 4})$$

$$V_A = -G_A V_0, \quad (\text{A2. 5})$$

$$I_6 = I_0 + I_1, \quad (\text{A2. 6})$$

$$I_0 = \frac{V_{DA0} - V_0}{R_0}, \quad (\text{A2. 7})$$

$$I_1 = \frac{V_{DA1} - V_0}{R_1}, \quad (\text{A2. 8})$$

$$I_6 = \frac{V_0 - V_3}{R_6}, \quad (\text{A2. 9})$$

and

$$V_3 = -G_B(E_{\text{cell}} + V_3). \quad (\text{A2. 10})$$

$V_C$  may be eliminated between Equations A2. 1 and A2. 2 to give

$$E_{\text{cell}} = -(R_u + R_F)I_{\text{cell}} + R_F C \frac{dV_C}{dt}. \quad (\text{A2. 11})$$

Equation A2. 4 may be substituted for  $I_{\text{cell}}$  to give

$$\begin{aligned}
E_{\text{cell}} = & \frac{(R_u + R_F)(V_B - V_A)}{R_A} + (R_u + R_F)C_A \frac{d(V_B - V_A)}{dt} \\
& + R_F C \frac{dV_C}{dt} .
\end{aligned} \tag{A2. 12}$$

$V_B$  may be eliminated from this equation by combining Equations A2. 3 and A2. 4 and rearranging to give

$$V_B = \frac{R_v V_A}{R_A + R_v} + \frac{R_A R_v C_A}{R_A + R_v} \frac{d(V_A - V_B)}{dt} - \frac{R_A E_{\text{cell}}}{R_A + R_v} , \tag{A2. 13}$$

which may be substituted into A2. 12 to give

$$\begin{aligned}
E_{\text{cell}} = & \frac{(R_u + R_F)R_v V_A}{R_A(R_A + R_v)} + \frac{(R_u + R_F)R_v C_A}{R_A + R_v} \frac{d(V_A - V_B)}{dt} \\
& - \frac{(R_u + R_F)E_{\text{cell}}}{R_A + R_v} - \frac{(R_u + R_F)V_A}{R_A} + (R_u + R_F)C_A \frac{d(V_B - V_A)}{dt} \\
& + R_F C \frac{dV_C}{dt} .
\end{aligned} \tag{A2. 14}$$

$E_{\text{cell}}$  may be extracted from the right-hand side and Equation A2. 5 used for  $V_A$  to yield

$$\begin{aligned}
E_{\text{cell}} = & \frac{(R_u + R_F)G_A V_0}{R_{\text{cell}}} - \frac{R_A C_A (R_u + R_F)}{R_{\text{cell}}} \frac{d(V_A - V_B)}{dt} + \frac{R_F C (R_A + R_v)}{R_{\text{cell}}} \frac{dV_C}{dt} ,
\end{aligned} \tag{A2. 15}$$

where

$$R_{\text{cell}} \equiv R_A + R_v + R_u + R_F. \quad (\text{A2. 16})$$

By combining Equations A2. 6 through A2. 9,  $V_0$  may be expressed as

$$V_0 = \frac{R_6}{R_D^2} (R_1 V_{DA0} + R_0 V_{DA1}) + \frac{R_0 R_1}{R_D^2} V_3, \quad (\text{A2. 17})$$

where

$$R_D^2 \equiv R_0 R_1 + R_0 R_6 + R_1 R_6. \quad (\text{A2. 18})$$

Equation A2. 10 may be rearranged to

$$V_3 = - \frac{G_B E_{\text{cell}}}{G_B + 1}. \quad (\text{A2. 19})$$

Substitution of A2. 19 into A2. 17 and the result into A2. 15 produces, upon rearrangement,

$$\begin{aligned} E_{\text{cell}} = & \left[ \frac{1+G_B}{R_{\text{cell}} R_D^2 (1+G_B) + (R_u + R_F) R_0 R_1 G_A G_B} \right] \\ & \times [G_A (R_u + R_F) R_6 (R_1 V_{DA0} + R_0 V_{DA1}) - R_D^2 R_A C_A (R_u + R_F) \\ & \times \frac{d(V_A - V_B)}{dt} + R_D^2 R_F C (R_A + R_v) \frac{dV_C}{dt}] . \end{aligned} \quad (\text{A2. 20})$$

Since  $G_B \gg 1$ , the quantity in the first set of brackets on the right-hand side of this equation reduces to

$$\left[ \frac{1}{R_{\text{cell}} R_D^2 + (R_u + R_F) R_0 R_1 G_A} \right] .$$

Under normal circumstances,  $G_A$  is sufficiently large that it is possible to ignore the first term in the denominator of this fraction as well as the terms containing derivatives in Equation A2.20. The criterion for simplifying the fraction in this way is

$$G_A \gg \left[ 1 + \frac{R_A + R_v}{R_u + R_F} \right] \left[ 1 + \frac{R_6}{R_0} + \frac{R_6}{R_1} \right] . \quad (\text{A2.21})$$

Substituting known values for the potentiostat resistors and a typical value of  $2 \times 10^5$  for  $G_A$ , this becomes

$$\frac{R_A + R_v}{R_u + R_F} \ll 1.3 \times 10^5 . \quad (\text{A2.22})$$

Assuming an allowed error of 1%, this is

$$\frac{R_A + R_v}{R_u + R_F} < 1300 . \quad (\text{A2.23})$$

The fraction on the left-hand side of this inequality may reasonably be assumed to be less than unity because of the comparative sizes of the

auxiliary and test electrodes and their placement in the cell. Thus, this criterion is easily met, and Equation A2.20 becomes

$$E_{\text{cell}} = \frac{R_6}{R_0 R_1} (R_1 V_{\text{DA0}} + R_0 V_{\text{DA1}}) + \frac{1}{G_A} \left[ 1 + \frac{R_6}{R_0} + \frac{R_6}{R_1} \right] \\ \times \left[ \frac{(R_A + R_v) R_F C}{R_u + R_F} \frac{dV_C}{dt} - R_A C_A \frac{d(V_A - V_B)}{dt} \right]. \quad (\text{A2.24})$$

In order to drop the last term of this equation it must be shown that it is insignificant with respect to the step potential. Assuming that it can be neglected, the step potential is given by

$$V_2 = \frac{R_6}{R_1} V_{\text{DA1}}. \quad (\text{A2.25})$$

Using Equation A2.4, the quantity in the last brackets of A2.24 may be written

$$\left[ \frac{(R_A + R_v) R_F C}{R_u + R_F} \frac{dV_C}{dt} - R_A I_{\text{cell}} + (V_A - V_B) \right]. \quad (\text{A2.26})$$

The worst case (where  $dV_C/dt$  and  $I_{\text{cell}}$  are largest) is immediately after the step, when (referring to equations in Section 2.4)

$$I_{\text{cell}} = I_b + I_s + I_o = I_b + \frac{V_2}{R_u} = I_b + C \frac{dV_C}{dt}. \quad (\text{A2.27})$$

Then, recognizing that  $V_A - V_B$  is essentially the same as before the step, A2.26 is

$$\left[ \frac{(R_A + R_v)R_F}{R_u + R_F} \frac{V_2}{R_u} - R_A I_{\text{cell}} + R_A I_b \right]. \quad (\text{A2.28})$$

Combining the last two terms by using A2.27, the limiting criterion may be stated as

$$V_2 \gg \frac{1.5}{2 \times 10^5} \left[ \frac{(R_A + R_v)R_F - (R_u + R_F)R_A}{R_u + R_F} \right] \frac{V_2}{R_u}, \quad (\text{A2.29})$$

which may be rearranged to

$$\frac{R_v}{R_u (R_u / R_F + 1)} \ll 1.3 \times 10^5. \quad (\text{A2.30})$$

The left-hand side is largest when its denominator is smallest, i.e., when  $R_u \ll R_F$ . It may then be seen that the limiting criterion (for 1% error) is

$$R_v < 1300 R_u. \quad (\text{A2.31})$$

This is actually easier to achieve than the previously discussed limit A2.23. Thus for any sensible arrangement of the test cell,

$$E_{\text{cell}} = R_6 \left( \frac{V_{\text{DA0}}}{R_0} + \frac{V_{\text{DA1}}}{R_1} \right) . \quad (\text{A2.32})$$

A limitation which has not been touched on here is that due to the response time of the potentiostat amplifiers. This is not a real problem, though, since the amplifiers are connected in configurations of unity gain or less, where their responses are rated at 1 MHz, which is much faster than the time constants of any cells studied.

### APPENDIX 3

#### Programs for Control and Interpretation of the Capacitance Measurements

##### Part 1

##### Program CAP

(written in BASIC language)



```

10DATA0,3,9,1,5,10,7,11,4
20DIMA(25),T(2),Z(11),U(1,2)
25LETLO=0:LETL1=0:LETK=16176
30PRINT"SUPERVERSION(11-6-73)"
185PRINT"CHOOSE":INPUT B1
190IFB1=0THENGOSUB210
191IFB1=1THENGOSUB240
192IFB1=2THENGOSUB240
193IFB1=3THENGOSUB1440
197IFB1=7THENGOSUB3100
198IFB1=8THENGOSUB1470
199IFB1=9THENGOSUB1490
201IFB1=11THENGOSUB3000
202IFB1=12THENGOSUB240
203IFB1=13THENINPUTR
204IFB1=14THENINPUTLO,L1
205GOTO185
210PRINT"GO,LIFT WHEN DONE":INPUTT:LETA=EXF(O,M)
220IFT=1THENLETA=EXF(1,E)
230RETURN
240GOSUB3030
250FORN=T(1)TOT(2)
260GOSUB3060
300IFB1>1THENGOSUB1400
310IFB1=12GOTO420
320LETA=A(N):IFB1=2THENPRINT"TIME","VOLTS"
330LETB2=0
340FORM1=1TO2
350FORM=1TOZ(11):LETA=A-2:LETT=EXF(A,R)
360IFB1=2THENPRINTZ(8)*M,T/Z(10)*Z(4)/1024:GOTO390
370IFT=0THENPRINTN:GOTO430
380IFT=1023*Z(10)THENPRINTN:GOTO430
390NEXTM
400NEXTM1
405IFB1=16GOTO430
420FORM=1TO8:PRINT:NEXTM

```

```

430NEXTV
435RETURN
440PRINT"BEGIN,END SEG #";:INPUTT(1),T(2)
450IFT(2)>V1THENLETT(2)=V1
460RETURN
470LETM=1:GOSUB530
480LETM=3:GOSUB950
490LETZ(4)=1.25*2+(3-Z(4)/8):LETM=5:GOSUB530
500LETM=7:LETZ(8)=Z(8)-8:GOSUB530
510LETZ(7)=Z(7)*Z(11):LETM=9:GOSUB950
520LETZ(8)=Z(7)/Z(11):RETURN
530LETT=Z(M):LETZ(M)=T/1E5
540IFZ(M+1)=67THENLETZ(M)=T/1E4
550IFZ(M+1)=69THENLETZ(M)=T/60
560RETURN
615LETY2=(Y1+Y3)/2
620IFABS(Y2-INT(Y2+1E-6))>3E-6THENLETY3=Y3-1:GOTO615
625LETM=Y1:GOSUB3280
630LETY1=T:LETM=Y2:GOSUB3280
635LETY2=T:LETM=Y3:GOSUB3280
640LETY3=T:LETG1=Y1+Y3-2*Y2
645LETG=(Y1*Y3-Y2+2)/G1
650LETS2=(Z(4)/2048)+2
655LETI2=(R1/Z(11)+S2)/R/R
665LETG0=((Y3-G)+2+(Y1-G)+2+4*(Y2-G)+2)/G1/G1
667LETG0=I2+(R1+S2)/R/R*G0
670PRINT:PRINT,"RES CURR","GAMMA"," IO"
675LETP2=0:LETT6=0:LETT7=0:LETY6=0:LETY7=0:LETT(2)=0:LETT5=0:LETT(1)=0

```

```

710FORM=1TOZ(11)
720GOSUB3280
730LETT(1)=T(1)+Z(8):IFT(1)<LOGOT0790
740IFT(1)>LIGOT0800
745GOSUB3280
750LETT5=T5+1:LETY=T-G:LETW=Y*Y:LETY=LOG(Y)
760LETT6=T6+W*T(1):LETY6=Y6+W*Y:LETP2=P2+W*T(1)*Y
770LETT7=T7+W*T(1)+2:LETY7=Y7+Y*Y*W:LETT(2)=T(2)+W
790NEXTM
800LETD=T(2)*T7-T6*T6:LETM1=(T(2)*P2-Y6*T6)/D:LETB=(T7*Y6-T6*P2)/D
810LETIO=EXP(B):PRINT,S/R,G,IO
820IFT5<6THENLETS2=0:GOT0840
830LETS2=(Y7-Y6*Y6/T(2)-M1*M1*D/T(2))*(T5-3)/T5/(T5-5)
835IFS2<0THENLETS2=0
840LETS3=IO+2*S2*(1+T6+2/D)/T(2)
845IFS=0THENLETS=1
850PRINT"STD. DEVS.",SQR(I2)/S*R*100;"%",
855PRINTSQR(GO)/G*100;"%",SQR(S3)/IO*100;"%"
860PRINT:PRINT"    TAU=";-1/M1;"SEC":LETC=(Z(9)/1E3)/(G+IO)
870LETV1=4E-8:LETS3=S3/IO+2
880LETB3=SQR(V1+GO/IO+2+S3)
890PRINT"    RUNC=";C;"OHMS +/-";B3*100;"%"
900LETC3=IO*C/G:LETB3=SQR(S3+B3*B3+GO/G/G)*100
910PRINT"    RFAR=";C3;"OHMS +/-";B3;"%"
920LETC3=-(G+IO)+2/M1/IO/Z(9)*1E3
925LETT=SQR(4*GQ/IO+2+S3+S2*T(2)/D/M1/M1+V1)*100
930PRINT"    CAP =" ;C3"UF +/-"T"%" :NEXTV
940RETURN
950GOSUB3300
960LETZ(M)=Z(M)/K1:RETURN
1400PRINT"RUN #",N,"    TIME IN SEC"
1405PRINT"INIT.",Z(3);"V","START",Z(1)
1410PRINT"STEP",Z(9);"MV","ITER",Z(5)
1415PRINT"MAX OUT",Z(4);"V","DECAY",Z(7)
1420PRINT"RF",R;"OHM":PRINT"NO. ITER.",Z(10),"NO. PTS.",Z(11)

```

```

1430RETURN
1440GOSUB440
1450FORN=T(1)TOT(2):LETT=EXF(A(N),T,11):NEXTN
1460RETURN
1470FORN=1TON1:LETT=EXF(K,T,0)
1480LETT=EXF(A(N),T,2*EXF(16154,R)):NEXTN
1485RETURN
1490LETT=EXF(0,1):LETN1=0
1500PRINT"NO. SETS TO READ":INPUTT:IFT=0GOTO1550
1510LETT(1)=N1+1:LETT(2)=T(1)+T-1
1520FORN1=T(1)TOT(2):LETT=EXF(K,T,0)
1530LETA(N1)=EXF(K,R):LETA=K:GOSUB2080
1535GOSUB2050
1540NEXTN1
1550PRINT"DONE, DELETE, CHANGE, ADD;0,1,2,3":INPUTT
1560IFT=1GOTO1610
1570IFT=2GOTO1632
1580IFT<>3THENRETURN
1590GOSUB1700
1600GOTO1500
1610PRINT"HOW MANY":INPUTN
1620LETT(1)=N+1:GOSUB3040
1630GOTO1500
1632PRINT"HOW MANY":INPUTN
1634LETT(1)=N1+1:LETT(2)=N1+N:PRINT"PARAM, VALUE"
1636FORP2=0TO2:INPUTU(0,P2),U(1,P2)
1637IFU(0,P2)=0GOTO1639
1638NEXTP2
1639FORN1=T(1)TOT(2)
1640LETT=EXF(K,T,0):LETA=K:GOSUB2080
1650GOSUB470
1660FORN=0TOP2:LETM=U(0,N)
1663GOSUB1800
1665LETZ(A)=U(1,N):NEXTN
1670GOSUB1830
1680LETA(N1)=EXF(K,R):GOSUB2050

```

```

1685NEXTN1
1690GOTO1500
1700RESTORE:PRINT"SEQ";
1710FORM=0T08:READT:INPUTZ(T):IFZ=0THENRETURN
1720NEXTM
1730LETN1=N1+1:GOSUB1770
1740GOSUB1830
1750LETA(N1)=EXF(K,R):GOSUB2050
1760GOTO1700
1770PRINT"ERROR AT PARAM #";:INPUTM:IFM<0THENRETURN
1780GOSUB1800
1790INPUTZ(A):GOTO1770
1800RESTORE
1810FORM1=0T0M:READA:NEXTM1
1820RETURN
1830LETM=1:GOSUB1930
1840LETM=3:GOSUB2020
1850IFZ(4)<0GOTO1880
1860FORM1=0T03:IFZ(4)<1.25*2*M1+3E-6GOTO1890
1870NEXTM1
1880LETM=4:GOSUB2000
1890LETZ(4)=24-8*M1:LETM=5:GOSUB1930
1900LETZ(7)=Z(7)/Z(11):LETM=7:GOSUB1930
1910LETZ(8)=Z(8)+8:LETM=9:GOSUB2020
1920RETURN
1930LEFT=Z(M):IFT<0GOTO1980
1940LETZ(M)=T*1E5+.1:LETZ(M+1)=65
1950IFT>.327THENLETZ(M)=T*1E4+.1:LETZ(M+1)=67
1960IFT>3.27THENLETZ(M)=T*60+.1:LETZ(M+1)=69
1970IFZ(M)<32700THENRETURN
1980GOSUB2000
1990GOTO1930
2000RESTORE
2003FORM1=0T08:READA:IFA=MGOTO2005
2004NEXTM1
2005PRINT"Z#"M1"OUT OF RANGE"

```

```

2010PRINT"NEW #";:INPUTZ(M):RETURN
2020GOSUB3300
2025LETZ(M)=INT(Z(M)*K1+.5)
2030IFABS(Z(M))>2047THENGOSUB2000
2040RETURN
2050LETT=EXF(Z(1),C,Z(2),Z(3),Z(4),Z(5),Z(6),Z(7),Z(8),Z(9),Z(10),Z(11))
2060RETURN
2070LETA=A(N)
2080FORM=1TO11:LETA=A-2:LETZ(M)=EXF(A,R):NEXTM
2090RETURN
3000PRINT"PARAM OK";:INPUTT:IFT=0THENGOSUB1490
3010FORN=1TON1:LETT=EXF(A(N),T,0):NEXTN
3020RETURN
3030GOSUB440
3040FORN=1TOT(1)-1:LETT=EXF(K,T,0):NEXTN
3050RETURN
3060LETT=EXF(K,T,0):LETA=K:GOSUB2080
3070GOSUB470
3080RETURN
3100GOSUB3030
3110FORN=T(1)TOT(2)
3120GOSUB3060
3130IFLO>Z(7)GOTO3150
3140IFL1>0GOTO3160
3150PRINT"LO,L1";:INPUTLO,L1
3160GOSUB1400
3170PRINT"FOR DATA BETWEEN";LO;"AND";L1;"SEC":GOSUB3250
3175LETRI=(R1-S*S*M)/(M-1)
3180LETY1=0:LETT=0
3190FORM=1TOZ(11):LETT=T+Z(8):IFY1>0GOTO3220
3200IFT>=LOTHENLETY1=M
3220IFT>L1THENLETY3=M-1:GOTO615
3230NEXTM
3240LETY3=Z(11):GOTO615
3250LETS=0:LETRI=0:LETA=A(N)
3260FORM=1TOZ(11):LETA=A-2:LETT=EXF(A,R)/Z(10)/1024*Z(4)

```

3270 LETS=S+T:LETRI=R1+T\*T:NEXTM  
3275 LETS=S/Z(11):RETURN  
3280 LETA=A(N)-2\*Z(11)-2\*M  
3290 LETT=(EXF(A,R)/Z(10)\*Z(4)/1024-S)/R:RETURN  
3300 LETK1=452.1:IFM>4THENLETK1=22.282  
3310 RETURN

## Part 2

### Program PLT

(written in BASIC language)



```

10DATA0,3,9,1,5,10,7,11,4
20DIMA(25),T(2),Z(11)
25LETLO=0:LETL1=0:LETK=16176
30PRINT"PLOT (3-14-74)"
185PRINT"CHOOSE";:INPUT B1
192IFB1=2THENGOSUB240
194IFB1>3THENIFB1<7THENGOSUB1000
197IFB1=7THENGOSUB3100
199IFB1=9THENGOSUB1490
201IFB1=11THENGOSUB3000
202IFB1=12THENGOSUB240
203IFB1=13THENINPUTR
204IFB1=14THENINPUTLO,L1
205GOTO185
240GOSUB3030
250FORV=T(1)TOT(2)
260GOSUB3060
300IFB1>1THENGOSUB1400
310IFB1=12GOTO420
320LETA=A(N):IFB1=2THENPRINT"TIME","VOLTS"
330LETB2=0
340FORM1=1TO2
350FORM=1TOZ(11):LETA=A-2:LETT=EXF(A,R)
360IFB1=2THENPRINTZ(8)*M,T/Z(10)*Z(4)/1024:GOTO390
390NEXTM
400NEXTM1
420FORM=1TO8:PRINT:NEXTM
430NEXTN
435RETURN
440PRINT"BEGIN,END SEG #";:INPUTT(1),T(2)
450IFT(2)>N1THENLETT(2)=N1
460RETURN
470LETM=1:GOSUB530
480LETM=3:GOSUB950
490LETZ(4)=1.25*2*(3-Z(4)/8):LETM=5:GOSUB530
500LETM=7:LETZ(8)=Z(8)-8:GOSUB530

```

```

510LETZ(7)=Z(7)*Z(11):LETM=9:GOSUB950
520LETZ(8)=Z(7)/Z(11):RETURN
530LETT=Z(M):LETZ(M)=T/1E5
540IFZ(M+1)=67THENLETZ(M)=T/1E4
550IFZ(M+1)=69THENLETZ(M)=T/60
560RETURN
615LETY2=(Y1+Y3)/2
620IFABS(Y2-INT(Y2+1E-6))>3E-6THENLETY3=Y3-1:GOTO615
625LETM=Y1:GOSUB3280
630LETY1=T:LETM=Y2:GOSUB3280
635LETY2=T:LETM=Y3:GOSUB3280
640LETY3=T:LETG1=Y1+Y3-2*Y2
645LETG=(Y1*Y3-Y2*2)/G1
650LETS2=(Z(4)/2048)*2
655LETI2=(R1/Z(11)+S2)/R/R
665LETG0=((Y3-G)*2+(Y1-G)*2+4*(Y2-G)*2)/G1/G1
667LETG0=I2+(R1+S2)/R/R*G0
670PRINT:PRINT,"RES CURR","GAMMA"," IO"
675LETP2=0:LETT6=0:LETT7=0:LETY6=0:LETY7=0:LETT(2)=0:LETT5=0:LETT(1)=0
710FORM=1TOZ(11)
720GOSUB3280
730LETT(1)=T(1)+Z(8):IFT(1)<LOGOTO790
740IFT(1)>L1GOTO800
745GOSUB3280
750LETT5=T5+1:LETY=T-G:LETW=Y*Y:LETY=LOG(Y)
760LETT6=T6+W*T(1):LETY6=Y6+W*Y:LETP2=P2+W*T(1)*Y
770LETT7=T7+W*T(1)*2:LETY7=Y7+Y*Y*W:LETT(2)=T(2)+W
790VEXTM
800LETD=T(2)*T7-T6*T6:LETM1=(T(2)*P2-Y6*T6)/D:LETB=(T7*Y6-T6*P2)/D

810LETIO=EXP(B):PRINT,S/R,G,IO
820IFT5<6THENLETS2=0:GOTO840
830LETS2=(Y7-Y6*Y6/T(2)-M1*M1*D/T(2))*(T5-3)/T5/(T5-5)
835IFS2<0THENLETS2=0
840LETS3=IO*2*S2*(1+T6*2/D)/T(2)
845IFS=0THENLETS=1

```

```

850PRINT"STD. DEVS.",SQR(I2)/S*R*100;"%",
855PRINTSQR(G0)/G*100;"%",SQR(S3)/I0*100;"%"
860PRINT:PRINT"    TAU=";-1/M1;"SEC":LETC=(Z(9)/1E3)/(G+I0)
870LETV1=4E-8:LETS3=S3/I0+2
880LETB3=SQR(V1+G0/I0+2+S3)
890PRINT"    RUNC=";C;"OHMS +/-";B3*100;"%"
900LETC3=I0*C/G:LETB3=SQR(S3+B3*B3+G0/G/G)*100
910PRINT"    RFAR=";C3;"OHMS +/-";B3;"%"
920LETC3=-(G+I0)+2/M1/I0/Z(9)*1E3
925LETT=SQR(4*G0/I0+2+S3+S2*T(2)/D/M1/M1+V1)*100
930PRINT"    CAP =";C3"UF +/-"T"%":NEXTN
940RETURN
950GOSUB3300
960LETZ(M)=Z(M)/K1:RETURN
1000IFB1=4THENLETT=EXF(O,G,CURRENT IN UA,TIME IN MS)
1010IFB1=5THENLETT=EXF(O,G,LOG I,TIME IN MS)
1020IFB1=6THENLETT=EXF(O,G,RESIDUAL,TIME IN MS)
1024LETY0=0:LETY1=Z(7)*1E3:LETP=0:GOSUB1110
1026FORM=1TOZ(11)
1028GOSUB3320
1030IFM=1THENLETY0=T:LETY1=T
1055IFT<Y0THENLETY0=T
1058IFT>Y1THENLETY1=T
1060NEXTM
1062LETP=1:GOSUB1110
1065FORM=1TOZ(11)
1067GOSUB3320
1070LETT(1)=M*Z(8)
1075LETD=EXF(INT(T(1)/X3*924*1E3),P,INT((T-Y2)/(Y3-Y2)*680))
1080NEXTM
1090LETY=EXF(O,0):RETURN
1110IFY1-Y0>ABS(Y0+Y1)/1E4GOTO1118
1114IFY1>0THENLETY0=0
1116IFY1<0THENLETY1=0
1118LETS2=Y1-Y0:LETM=0
1120IFS2>1GOTO1180

```

```

1130 LET M=M+1: LET S2=S2*10: LET Y0=Y0*10: LET Y1=Y1*10: GOTO 1120
1180 IF S2<=10 GOTO 1240
1190 LET M=M-1: LET S2=S2/10: LET Y0=Y0/10: LET Y1=Y1/10: GOTO 1130
1240 LET S1=1: IF S2<=4 THEN LET S1=.5
1260 IF S2<=1.5 THEN LET S1=.2
1270 LET Y0=INT(Y0/S1+1E-6)*S1: LET Y1=INT(Y1/S1+1-1E-6)*S1: LET Y=Y0
1325 LET P2=924: IF P=1 THEN LET P2=680
1330 LET S2=INT((Y-Y0)/(Y1-Y0)*P2+.5)
1340 LET S0=Y/10*M
1350 IF P=1 THEN LET D=EXF(S2,Y,S0): GOTO 1370
1360 LET D=EXF(S2,X,S0)
1370 LET Y=Y+S1: IF Y<=Y1 GOTO 1330
1380 LET Y1=Y1/10*M: LET Y0=Y0/10*M: IF P=0 THEN LET X3=Y1: LET X2=Y0
1390 IF P=1 THEN LET Y3=Y1: LET Y2=Y0
1395 RETURN
1400 PRINT "RUN #",N," TIME IN SEC"
1405 PRINT "INIT.",Z(3); "V", "START",Z(1)
1410 PRINT "STEP",Z(9); "MV", "ITER",Z(5)
1415 PRINT "MAX OUT",Z(4); "V", "DECAY",Z(7)
1420 PRINT "RF",R; "OHM": PRINT "NO. ITER.",Z(10), "NO. PTS.",Z(11)
1430 RETURN
1490 PRINT "NO. SETS TO READ": INPUT T(2)
1500 LET A(1)=16154
1510 FOR N1=1 TO T(2): LET T=EXF(K,T,0)
1520 LET A(N1+1)=A(N1)-4*EXF(16154,R)
1530 NEXT N1
1540 RETURN
2080 FOR M=1 TO 11: LET A=A-2: LET Z(M)=EXF(A,R): NEXT M
2090 RETURN
3000 PRINT "PARAM OK": INPUT T: IF T=0 THEN GOSUB 1490
3010 FOR N=1 TO N1: LET T=EXF(A(N),T,0): NEXT N
3020 RETURN
3030 GOSUB 440
3040 FOR N=1 TO T(1)-1: LET T=EXF(K,T,0): NEXT N
3050 RETURN
3060 LET T=EXF(K,T,0): LET A=K: GOSUB 2080

```

```

3070GOSUB470
3080RETURN
3100GOSUB3030
3110FORN=T(1)TOT(2)
3120GOSUB3060
3130IFLO>Z(7)GOTO3150
3140IFL1>0GOTO3160
3150PRINT"LO,L1";:INPUTLO,L1
3160GOSUB1400
3170PRINT"FOR DATA BETWEEN";LO;"AND";L1;"SEC":GOSUB3250
3175LETR1=(R1-S*S*M)/(M-1)
3180LETY1=0:LETT=0
3190FORM=1TOZ(11):LETT=T+Z(8):IFY1>0GOTO3220
3200IFT>=LOTHENLETY1=M
3220IFT>L1THENLETY3=M-1:GOTO615
3230NEXTM
3240LETY3=Z(11):GOTO615
3250LETS=0:LETR1=0:LETA=A(N)
3260FORM=1TOZ(11):LETA=A-2:LETT=EXF(A,R)/Z(10)/1024*Z(4)
3270LETS=S+T:LETR1=R1+T*T:NEXTM
3275LETS=S/Z(11):RETURN
3280LETA=A(N)-2*Z(11)-2*M
3290LETT=(EXF(A,R)/Z(10)*Z(4)/1024-S)/R:RETURN
3300LETK1=464.2446:IFM>4THENLETK1=23.206
3310RETURN
3320GOSUB3280
3330IFB1=4THENLETT=T*1E6:RETURN
3340LETT=LOG(T-G):IFB1=5THENRETURN
3350LETT=T-B-M1*M*Z(8):RETURN

```

### Part 3

#### Program CCPVE

(written in BASIC language)

```

10DATA0,3,9,1,5,10,7,11,4
20DIMA(25),T(2),Z(11)
22DIME(4,25)
25LETLO=0:LETL1=0:LETK=16176
30PRINT"PL0T (3-14-74)"
185PRINT"CHOOSE":INPUT B1
192IFB1=2THENGOSUB240
197IFB1=7THENGOSUB3100
199IFB1=9THENGOSUB1490
201IFB1=11THENGOSUB3000
202IFB1=12THENGOSUB240
203IFB1=13THENINPUTR
204IFB1=14THENINPUTLO,L1
205IFB1=15THENGOSUB3400
206IFB1=16THENPRINT"AREA,ERR":INPUTW2,W1:LETW1=W1*W1/W2/W2
207GOTO185
240GOSUB3030
250FORN=T(1)TOT(2)
260GOSUB3060
300IFB1>1THEVGOSUB1400
310IFB1=12GOTO420
320LETA=A(N):IFB1=2THENPRINT"TIME","VOLTS"
330LETB2=0
340FORM1=1TO2
350FORM=1TOZ(11):LETA=A-2:LETT=EXF(A,R)
360IFB1=2THENPRINTZ(8)*M,T/Z(10)*Z(4)/1024:GOTO390
390NEXTM
400NEXTM1
420FORM=1TO8:PRINT:NEXTM
430NEXTN
435RETURN
440PRINT"BEGIN,END SEG #":INPUTT(1),T(2)
450IFT(2)>N1THENLETT(2)=N1
460RETURN
470LETM=1:GOSUB530
480LETM=3:GOSUB950

```

```

490LETZ(4)=1.25*2*(3-Z(4)/8):LETM=5:GOSUB530
500LETM=7:LETZ(8)=Z(8)-8:GOSUB530
510LETZ(7)=Z(7)*Z(11):LETM=9:GOSUB950
520LETZ(8)=Z(7)/Z(11):RETURN
530LETT=Z(M):LETZ(M)=T/1E5
540IFZ(M+1)=67 THENLETZ(M)=T/1E4
550IFZ(M+1)=69 THENLETZ(M)=T/60
560RETURN
615LETY2=(Y1+Y3)/2
620IFABS(Y2-INT(Y2+1E-6))>3E-6 THENLETY3=Y3-1:GOTO615
625LETM=Y1:GOSUB3280
630LETY1=T:LETM=Y2:GOSUB3280
635LETY2=T:LETM=Y3:GOSUB3280
640LETY3=T:LETG1=Y1+Y3-2*Y2
645LETG=(Y1*Y3-Y2*2)/G1
650LETS2=(Z(4)/2048)+2
655LETI2=(R1/Z(11)+S2)/R/R
665LETG0=((Y3-G)+2+(Y1-G)+2+4*(Y2-G)+2)/G1/G1
667LETG0=I2+(R1+S2)/R/R*G0
675LETP2=0:LETT6=0:LETT7=0:LETY6=0:LETY7=0:LETT(2)=0:LETT5=0:LETT(1)=
710FORM=1TOZ(11)
720GOSUB3280
730LETT(1)=T(1)+Z(8):IFT(1)<LOGOTO790
740IFT(1)>LIGOTO800
745GOSUB3280
750LETT5=T5+1:LETY=T-G:LETW=Y*Y:LETY=LOG(Y)
760LETT6=T6+W*T(1):LETY6=Y6+W*Y:LETP2=P2+W*T(1)*Y
770LETT7=T7+W*T(1)+2:LETY7=Y7+Y*Y*W:LETT(2)=T(2)+W
790NEXTM
800LETD=T(2)*T7-T6*T6:LETM1=(T(2)*P2-Y6*T6)/D:LETB=(T7*Y6-T6*P2)/D

810LETI0=EXP(B)
820IFT5<6 THENLETS2=0:GOTO840
830LETS2=(Y7-Y6*Y6/T(2)-M1*M1*D/T(2))*(T5-3)/T5/(T5-5)
835IFS2<0 THENLETS2=0
840LETS3=I0+2*S2*(1+T6+2/D)/T(2)

```



```

845IFS=0THENLETS=1
847IFB1=0GOTO870
848PRINT:PRINT,"RES CURR","GAMMA","IO":PRINT,S/R,G,IO
850PRINT"STD. DEVS.",SQR(I2)/S*R*100;"%",
855PRINTSQR(GO)/G*100;"%",SQR(S3)/IO*100;"%"
860PRINT:PRINT"    TAU="-1/M1"SEC"
870LETC=(Z(9)/1E3)/(G+IO):LETV1=4E-8:LETS3=S3/IO+2
880LETB3=SQR(V1+GO/IO+2+S3)
890IFB1>0THENPRINT"    RUNC="C"OHMS +/-"B3*100"%"
900LETC3=IO*C/G:LETB3=SQR(S3+B3*B3+GO/G/G)*100
920LETE(3,N)=-(G+IO)+2/M1/IO/Z(9)*1E9
925LETE(4,N)=4*GO/IO+2+S3+S2*T(2)/D/M1/M1+V1
927IFB1=0GOTO935
928PRINT"    RFAR="C3"OHMS +/-"B3"%"
930PRINT"    CAP ="E(3,N)"UF +/-"SQR(E(4,N))*100"%"
935NEXTN
940RETURN
950GOSUB3300
960LETZ(M)=Z(M)/K1:RETURN
1110IFY1-YO>ABS(YO+Y1)/1E4GOTO1118
1114IFY1>0THENLETYO=0
1116IFY1<0THENLETY1=0
1118LETS2=Y1-YO:LETM=0
1120IFS2>1GOTO1180
1130LETM=M+1:LETS2=S2*10:LETYO=YO*10:LETY1=Y1*10:GOTO1120
1180IFS2<=10GOTO1240
1190LETM=M-1:LETS2=S2/10:LETYO=YO/10:LETY1=Y1/10:GOTO1180
1240LETS1=1:IFS2<=4THENLETS1=.5
1260IFS2<=1.5THENLETS1=.2
1270LETYO=INT(YO/S1+1E-6)*S1:LETY1=INT(Y1/S1+1E-6)*S1:LETY=YO
1325LETP2=924:IFP=1THENLETP2=680
1330LETS2=INT((Y-YO)/(Y1-YO)*P2+.5)
1340LETSO=Y/IO+M
1350IFP=1THENLETD=EXF(S2,Y,SO):GOTO1370
1360LETD=EXF(S2,X,SO)
1370LETY=Y+S1:IFY<=Y1GOTO1330

```

```

1380LETY1=Y1/10*M:LETY0=Y0/10*M:IFP=0THENLETX3=Y1:LETX2=Y0
1390IFP=1THENLETY3=Y1:LETY2=Y0
1395RETURN
1400PRINT"RUN #",N," TIME IN SEC"
1405PRINT"INIT.",Z(3);"V","START",Z(1)
1410PRINT"STEP",Z(9);"MV","ITER",Z(5)
1415PRINT"MAX OUT",Z(4);"V","DECAY",Z(7)
1420PRINT"RF",R;"OHM":PRINT"NO. ITER.",Z(10),"NO. PTS.",Z(11)
1430RETURN
1490PRINT"NO. SETS TO READ";:INPUTT(2)
1500LETA(1)=16154
1510FORN1=1TOT(2):LETT=EXF(K,T,0)
1515LETE(3,N1)=0
1520LETA(N1+1)=A(N1)-4*EXF(16154,R)
1530NEXTN1
1540RETURN
2080FORM=1TO11:LETA=A-2:LETZ(M)=EXF(A,R):NEXTM
2090RETURN
3000PRINT"PARAM OK";:INPUTT:IFT=0THENGOSUB1490
3010FORN=1TON1:LETT=EXF(A(N),T,0):NEXTN
3020RETURN
3030GOSUB440
3040FORN=1TOT(1)-1:LETT=EXF(K,T,0):NEXTN
3050RETURN
3060LETT=EXF(K,T,0):LETA=K:GOSUB2080
3070GOSUB470
3080RETURN
3100GOSUB3030
3105PRINT"PRINTOUT";:INPUTB1
3110FORN=T(1)TOT(2)
3120GOSUB3060
3125LETE(1,N)=Z(3):LETE(2,N)=Z(9)/1000
3130IFLO>Z(7)GOTO3150
3140IFL1>0GOTO3155
3150PRINT"LO,L1";:INPUTLO,L1
3155IFB1=0GOTO3172

```

```

3160GOSUB1400
3170PRINT"FOR DATA BETWEEN"LO"AND"L1"SEC"
3172GOSUB3250
3175LETR1=(R1-S*S*M)/(M-1)
3180LETY1=0:LETT=0
3190FORM=1TOZ(11):LETT=T+Z(8):IFY1>0GOTO3220
3200IFT>=LOTHENLETY1=M
3220IFT>L1THENLETY3=M-1:GOTO615
3230NEXTM
3240LETY3=Z(11):GOTO615
3250LETS=0:LETR1=0:LETA=A(N)
3260FORM=1TOZ(11):LETA=A-2:LETT=EXF(A,R)/Z(10)/1024*Z(4)
3270LETS=S+T:LETR1=R1+T*T:NEXTM
3275LETS=S/Z(11):RETURN
3280LETA=A(N)-2*Z(11)-2*M
3290LETT=(EXF(A,R)/Z(10)*Z(4)/1024-S)/R:RETURN
3300LETK1=452.1:IFM>4THENLETK1=22.282
3310RETURN
3320GOSUB3280
3330IFB1=4THENLETT=T*1E6:RETURN
3340LETT=LOG(T-G):IFB1=5THENRETURN
3350LETT=T-B-M1*M*Z(8):RETURN
3400PRINT"COPY":INPUTB2:IFB2=1THENLETD=EXF(-1,0)
3405PRINT,"POT","UF/CM2","% ERR":PRINT:LETT(1)=0
3410FORN=1TON1:IFE(3,N)=0GOTO3475
3420IFT(1)=0THENLETT(1)=N
3430LETT(2)=N
3440LETE(4,N)=SQR(E(4,N)+W1):LETE(3,N)=E(3,N)/W2
3450PRINTN,E(1,N),E(3,N),E(4,N)*100:LETD=E(4,N)*E(3,N)
3460LETE(4,N)=E(3,N)+D:LETE(3,N)=E(3,N)-D
3470LETE(2,N)=E(1,N)+E(2,N)
3475NEXTN
3480IFB2=1THENLETD=EXF(23,0)+EXF(-1,0):GOTO3487
3485INPUTD
3487LETD=EXF(0,G,UF/SQ.CM.,E CELL)
3490LETY1=E(2,T(1)):LETY0=E(1,T(1))

```

```

3500FORN=T(1)+1TOT(2):IFE(3,N)=0GOTO3530
3510IFE(2,N)>Y1THENLETY1=E(2,N)
3520IFE(1,N)<Y0THENLETY0=E(1,N)
3530NEXTN
3540LETP=0:GOSUB1110
3560LETY1=E(4,T(1)):LETY0=E(3,T(1))
3570FORN=T(1)+1TOT(2):IFE(3,N)=0GOTO3600
3580IFE(3,N)<Y0THENLETY0=E(3,N)
3590IFE(4,N)>Y1THENLETY1=E(4,N)
3600NEXTN
3610LETP=1:GOSUB1110
3620LETE=X3-X2:LETD=Y3-Y2
3630FORN=T(1)TOT(2):IFE(3,N)=0GOTO3700
3640LETE(2,N)=INT((E(2,N)-X2)/E*924):LETE(1,N)=INT((E(1,N)-X2)/E*924)
3650LETE(3,N)=INT((E(3,N)-Y2)/D*680):LETE(4,N)=INT((E(4,N)-Y2)/D*680)
3660LETY=EXF(E(1,N),L,E(3,N),E(1,N),E(4,N))
3670LETY=EXF(E(1,N),L,E(4,N),E(2,N),E(4,N))
3680LETY=EXF(E(2,N),L,E(4,N),E(2,N),E(3,N))
3690LETY=EXF(E(2,N),L,E(3,N),E(1,N),E(3,N))
3700NEXTN
3710IFB2=1THENLETD=EXF(23,0):PRINT:LETD=EXF(-1,0):RETURN
3720LETD=EXF(0,0):RETURN

```

#### Part 4

#### Subroutine Package for CAP

(written in PAL-11 assembly language)

```

1      ;CAP--MAY 1975
2      ;
3      ;DEFINE REGISTERS
4      R0=%0
5      R1=%1
6      R2=%2
7      R3=%3
8      R4=%4
9      R5=%5
10     SP=%6
11     R7=%7
12     R6=SP
13     PC=R7
14     R4CT=R4
15     R2VRS=R2
16     ;
17     ;DEFINE PERIPHERALS
18     ADS=176770
19     ADB=ADS+2
20     CSR=172540
21     CBR=CSR+2
22     CTR=CSR+4
23     DA0=176760
24     DA1=DA0+2
25     PS=177776
26     GDIOUT=167772
27     TKB=177562
28     ;
29     ;DEFINE STORAGE
30     LEAVE=37462; ADDRESS OF EXIT ROUTINE
31     NSAVE=24.
32     LSTPTR=LEAVE-2
33     CONDAT=LSTPTR-2
34     IWCBR=LSTPTR-10.
35     IWCSR=LSTPTR-12.
36     DRCBR=LSTPTR-14.
37     DRCSR=LSTPTR-16.
38     .=50;BASIC USES THIS ADDRESS TO FIND EXF
39     .WORD 33400; STARTING HERE SHOULD ALLOW AT
40     .=33400; LEAST 30 TEN-POINT MEASUREMENTS
41     ;HEAD
42     ;SELECTS ROUTINE
43     ;DETERMINES INTEGER VALUE OF FIRST PARAMETER
44     ;MAKES R1 PT. TO NEXT PARAMETER

```

000050 033400

```

45      ;
46 033400 012002 HEAD: MOV (R0)+,R2; GET 1ST VARIABLE INTO R2-R4
47 033402 012903      MOV (R0)+,R3
48 033404 012004      MOV (R0)+,R4
49 033406 104440      TRAP 40; INTEGER OF FIRST VARIABLE IN R0
50 033410 005201      INC R1; PT. TO NEXT VARIABLE
51 033412 012702      MOV >CODES,R2; THE ADDRESS FOR FUNCTION DESIGNATORS
      033436
52 033416 012703      MOV >FUNCT-2,R3; THE ADDRESS LIST FOR THE FUNCTIONS
      033442
53 033422 005723 HEAD1: IST (R3)+; POINT TO NEXT ADDRESS
54 033424 121122      CMPB (R1),(R2)+; DO CODES MATCH?
55 033426 001375      BNE HEAD1; IF NOT, TRY NEW CODE AND ADDRESS
56 033430 122121      CMPE (R1)+,(R1)+; PT. TO NEXT VARIABLE
57 033432 000173      JMP ↓(R3); IF SO, START FUNCTION
      000000
58      ;
59 033436      CODES: .ASCII /CEIMRT/
      042503
      046511
      052122
60      .EVEN
61 033444      FUNCT: CLKSET
      033516
62 033446      ELECT
      034476
63 033450      INIT
      033460
64 033452      MEAS
      033626
65 033454      RETVAL
      034526
66 033456      TAPE
      034554
67      .EOT
68      :
69      :
70      :
71      ;INIT (10-26-73)

```

```

72      ;TO INITIATE THE LIST POINTER FOR CLKSET AND TO CLEAR DATA AREA
73      ;CALLED FROM BASIC THROUGH HEAD BY EXF(0,I)
74      ;USES R0
75      ;REQUIRES ENDPRG TO BE DEFINED AS END OF MAIN SEG OF PROGRAM
76      ;      NSAVE=NO. OF SAVED BYTES BETWEEN LEAVE AND DATA AREA
77      ;      ADDRESS LSTPTR BE DEFINED
78
79      033460 012700 INIT:  MOV ≥LEAVE-NSAVE,R0; ADDR. BEFORE LIST
80      033464 010037      MCV R0,↓≥LSTPTR; SAVE FOR CLKSET
81      033470 005040 INIT1: CLR -(R0); CLEAR A DATA WORD
82      033472 020027      CMP R0,≥ENDPRG; DCNE^
83      033476 003374      BGT INIT1
84      033500 052737      BIS ≥3,↓≥GOIOUT; LEVEL-SHIFTER DISAELED; ELECTRODE UP
85      033506 005037      CLR ↓≥DA1; NO STEP YET
86      033512 000137      JMP ↓≥LEAVE
87      037462
88      .ECT
89
90
91      ;CLKSET (10-26-73)
92      ;CALLED ONCE FOR EACH CAP. TO BE MEASURED
93      ;PUTS CONTROL DATA IN DATA SPACES FOR ACCESS BY EXPT.
94      ;DATA IS STORED AT BEGINNING OF BLCK FOR EACH DATA SET
95      ;IN THE CRDER:
96      ;1. CBR CCNIENTS FOR TIME IO START (C5)
97      ;2. CSR (C6)
98      ;3. DA0 " INIT POT. (Z)
99      ;4. ADS " SENSITIVITY (A0)
100     ;5. CBR CCNIENTS FOR TIME BETWEEN ITERATIONS (C3)
101     ;6. CSR (C4)
102     ;7. CBR " DATA RATE (C1)
103     ;8. CSR " (C0)
104     ;9. DA1 " STEP POT. (Q2)
105     ;10. NO. OF ITERATIONS (Q)
106     ;11. NO. OF PTS. IN DECAY (T4)
107     ;12. NOT STORED; IF PRESENT IN STRING, MEANS TO
108     ;      SAVE JUST TWO WORDS TO STORE RESIDUALS (N)

```



```

109      ;THE BLOCK SIZE IS DETERMINED AS 2*NC. PTS. IN DECAY
110      ;WITH A MINIMUM OF 11 WORDS
111      ;CALLED BY: EXF(C5,C,C6,Z,A0,C3,C4,C1,C0,Q2,Q,T4,N)
112      ;USES: R0,R1,R2,SP
113      ;AT END: R1 PTS. TO 1 PAST RT. PAREN.; SP RESET
114      ;REQUIRES ADDR. LSTPTR BE DEFINED
115      ;NSAVE TO BE DEFINED AS NC. WORDS SAVED BEFORE LEAVE
116      ;
117      033516 012746 CLKSET:MCV ≥11.,-(SP); NO. OF NUMBERS TO LOAD
                000013
118      033522 005301      DEC R1; PT. TO CHAR. BEFORE NEXT VARIABLE
119      033524 013702 CLKST4:MCV ↓≥LSTPTR,R2; PLACE TO LOAD
                037460
120      033530 010042      MCV R0,-(R2); ONE NC. LOADED
121      033532 010237      MOV R2,↓≥LSTPTR; DON'T LOSE IT IN TRAPS
                037460
122      033536 005316      DEC (SP); DONE^
123      033540 003404      BLE CLKST2; QUIT
124      033542 005201      INC R1; PICK UP NEXT VARIABLE
125      033544 104536      TRAP 136; EVAL
126      033546 104440      TRAP 40; FIX
127      033550 000765      BR CLKST4; LOAD IT
128      033552 013737 CLKST2:MCV ↓≥LEAVE-NSAVE-6,↓≥DA0; SET THE FIRST INITIAL POT.
                037424
                176760
129      ;SET LSTPTR FOR NEXT SET OF CONTROLLERS
130      033560 126127      CMPB -1(R1),≥#); DID WE REACH THE END OF STRING^
                177777
                000051
131      033566 001405      BEQ CLKST3; IF YES, WE WANT RESIDUALS
132      033570 122127 CLKST5:CMPB (R1)+,≥#); ARE WE AT END OF STRING+1^
                000051
133      033574 001375      BNE CLKST5; IF NO, GET THERE
134      033576 122020      CMPB (R0)+,(R0)+; SAVE TWO WORDS FOR THE RESIDUAL
135      033600 000401      BR CLKST3+2
136      033602 006300 CLKST3:ASL R0; INCLUDE RESIDUALS
137      033604 162700      SUB ≥11.,R0; THIS MANY WORDS TO SKIP
                000013
138      033610 003403      BLE .+8.; IF NEG., LSTPTR IS OK
139      033612 006300      ASL R0; BYTES TO SKIP

```

```

140 033614 160037      SUB R0,↕LSTPTR; SKIP, PT. TO WORD BEFORE NEXT LIST
      037460
141 033620 005726      TST (SP)++; RESET FOR BASIC
142 033622 000137      JMP ↕LEAVE; GO TO BASIC; R1 IS OK
      037462
143      .EOT
144      ;
145      ;
146      ;
147      ;MEAS (10-27-73)
148      ;DOES A SERIES OF CAPACITANCE EXPTS,
149      ;REAL-TIME-CONTROLLED BY NUMBERS IN DATA SPACE
150      ; (SEE CLKSET FOR ORDER OF NUMBERS)
151      ;PROGRAM IS TTY INTERRUPTIBLE (CNTRL/P)
152      ;USES ALL REGISTERS
153      ;RESETS SP, SAVES R1,R5
154      ;CALLED BY: EXF(N,M)
155      ;WHERE N=0 TO STORE RESIDUALS SEPARATELY
156      ;OR N=1 TO STORE THEM IN A DOUBLE WORD INTEGER
157      ;REQUIRES NSAVE BE DEFINED AS NO. OF BYTES TO SAVE BEFORE LEAVE
158      ;
159 033626 010037 MEAS:  MOV R0,↕LEAVE-NSAVE; RESIDUAL MODE IN LAST SAVED WORD
      037432
160 033632 001412      BEQ MEAS0; FOR ORDINARY
161 033634 012767      MCV ↕5725, WAIT1+2; "TST (R5)++"
      005725
      000212
162 033642 012767      MCV ↕776, WAIT1+4; "BR .-2"
      000776
      000206
163 033650 012767      MCV ↕4, STOP+2; "ADD ↕4, (SP)"
      000004
      000452
164 033656 000411      OR MEAS2
165 033660 012767 MEAS0: MCV ↕776, WAIT1+2; "BR .-2"
      000776
      000166
166 033666 012767      MCV ↕400, WAIT1+4; "BR .+2"
      000400
      000162
167 033674 012767      MCV ↕2, STOP+2; "ADD ↕2, (SP)"
      000002
      000426

```

168	033702	005037 177776	MEAS2:	CLR +2PS; PRIORITY 0
169	033706	010146		MOV R1,-(SP); SAVE THESE FOR BASIC
170	033710	010546		MCV R5,-(SP)
171	033712	012702 000006		MOV 26,R2; SAVE 6 LCCS. FOR BASIC AND REP. CONTENTS
172	033716	012703 034426		MOV 2VECADD,R3; PT. TO LCC. ADDR.
173	033722	012704 034442		MCV 2VECCON,R4; PT. TO NEW CONTENTS
174	033726	017346 000000	MEAS3:	MOV +0(R3),-(SP);SAVE IT
175	033732	012433		MOV (R4)+,+(R3)+; REPLACE IT
176	033734	005302		DEC R2; ANOTHER^
177	033736	003373		BGT MEAS3
178	033740	012705 037432		MCV 2LEAVE-NSAVE,R5; SET FOR FIRST SET, FIRST DATUM
179	033744	042737 000001 167772		BIC 21,+2GDIOUT; DROP THE ELECTRODE IF NOT ALREADY
180	033752	052737 000340 177776		BIS 2340,+2PS; PRIORITY 7
181	033760	010502	NEWP:	MOV R5,R2; PT TO START OF DATA
182	033762	005765 177776		TST -2(R5); IF A ZERC
183	033766	001500		BEQ FINISH; IT'S THE END
184	033770	012703 034456		MCV 2LOADC,R3; ADDRESS LIST
185	033774	012704 000010		MCV 28.,R4; NO. TO LOAD
186	034000	014533	MEAS4:	MOV -(R5),+(R3)+; LOAD IT
187	034002	005015		CLR (R5); COVER UP
188	034004	005304		DEC R4; DONE^
189	034006	003374		BGT MEAS4; NO
190	034010	014500		MCV -(R5),R0; SAVE STEP PCT.
191	034012	005015		CLR (R5)
192	034014	014501		MCV -(R5),R1; NO. ITERATIONS
193	034016	005015		CLR (R5)
194	034020	014504		MOV -(R5),R4; NO. PTS.
195	034022	005015		CLR (R5)

196	034024	012737 034236 000104	NEWITR: MCV ≥CLK1, +≥104; RESET THE VECTOR
197	034032	005737 037432	TST ↓≥LEAVE-NSAVE; RESIDUAL MODE
198	034036	001401	BEQ .+4; IF 0, IGNORE
199	034040	005742	TST -(R2); IF NOT 0, INC PTR. TO LOW WORD OF RESIDUAL
200	034042	010205	MCV R2, R5; PT. TO START OF DATA
201	034044	010403	MCV R4, R3; SAVE THE COUNT
202	034046	005037 177776	CLR ↓≥PS; PRIORITY 0
203	034052	000001	WAIT1: WAIT; FOR CLOCK
204	034054	000776	BR .-2; WAIT SOME MORE
205	034056	000400	BR .+2; CCNTINUE
206	034060	012737 034334 000104	MCV ≥NEWCLK, +≥104; TO START EXPT.
207	034066	000001	WAIT; TO PUT ON STEP
208	034070	010403	MOV R4, R3; RESET COUNT
209	034072	000001	WAIT; TO TAKE DATA
210	034074	000776	BR .-2; SOME MORE
211	034076	000400	BR .+2; NO-OP TO MAKE LIKE WAIT1
212	034100	005037 172540	CLR ↓≥CSR; STOP CLOCK QUICK
213	034104	052737 000002 167772	BIS ≥2, +≥GDIOUT; DISABLE LEVEL-SHIFTING OUTPUT
214	034112	005037 176762	CLR ↓≥DA1; END EXPT.
215	034116	052737 000340 177776	BIS ≥340, +≥PS; PRIORITY 7
216	034124	005301	DEC R1; IF THIS IS LAST ITERATION
217	034126	003407	BLE NEWPOT; START NEW MEASUREMENT
218	034130	013737 037446 172542	MCV ↓≥IWCBR, +≥CBR; OTHERWISE, WAIT FOR NEW ITERATION
219	034136	013737 037444 172540	MCV ↓≥IWCSR, +≥CSR; GC, SINGLE INT.
220	034144	000727	BR NEWITR; GET SET FOR RERUN

```

221 034146 020427 NEWPOT: CMP R4, ≥5; ONLY 10 PTS USED^
      000005
222 034152 003302      BGT NEWP; MORE THAN 10
223 034154 006304      ASL R4; NO. PTS USED WITH RESIDUAL
224 034156 162704      SUB ≥11, R4; NEG. OF PTS TO SKIP
      000013
225 034162 006304      ASL R4; NEG. OF BYTES TO SKIP
226 034164 060405      ACD R4, R5; SKIP DOWN TO NEW SET
227 034166 000674      BR NEWP; A NEW MEASUREMENT
228 034170 005037 FINISH: CLR ↑≥CSR; STOP CLOCK
      172540
229 034174 005037      CLR ↑≥PS; PRIORITY 0
      177776
230 034200 012702      MCV ≥6, R2; REPLACE 6 LOCS. IN BASIC
      000006
231 034204 012703      MCV ≥VECCCN, R3; ADDRESSES IN VECADD BACKWARD
      034442
232 034210 012653 FIN1: MCV (SP)+, ↓-(R3); MOVE ONE BACK
233 034212 005302      DEC R2; DCNE^
234 034214 003375      BGT FIN1
235 034216 012700      MOV ≥7, R0; RING BELL WHEN DCNE
      000007
236 034222 004567      JSR R5, CHOUT
      000072
237 034226 012605      MCV (SP)+, R5; PUT THESE BACK,
238 034230 012601      MCV (SP)+, R1; TCO
239 034232 000137      JMP ↑≥LEAVE; DONE^
      037462
240      ;CLOCK INTERRUPT ROUTINES
241 034236 012737 CLK1: MCV ≥CLK2, ↑≥104; START DATA NEXT TIME
      034270
      000104
242 034244 042737      BIC ≥2, ↑≥GOIOUT; ENABLE LEVEL-SHIFTING OUTPUT
      000002
      167772
243 034252 013737      MCV ↑≥DRGBR, ↑≥GBR; DATA RATE
      037442
      172542
244 034260 013737      MCV ↑≥DRGBR, ↑≥GBR; GC, RPT. INT.
      037440
      172540
245 034266 000002      RTI; AND WAIT
246 034270 005737 CLK2: TST ↑≥ACB; CLEAR DONE BIT

```

247	034274	176772 005237 176770	INC +2ADS; START CATCH
248	034300	005303	DEC R3; LAST PT^
249	034302	002411	BLT STOP; YES, STOP
250	034304	105737 176770	TSTB +2ADS; CONVERSION READY^
251	034310	100375	BPL .-4; NO
252	034312	063745 176772	ACD +2ACB,-(R5); TAKE IT
253	034316	103002	BCC .+6; IF NO CARRY, SKIP
254	034320	005265 030002	INC +2(R5); CARRY TO HIGH WORD
255	034324	000002	RTI; AND WAIT FOR NEXT
256	034326	062716 000004	STOP: ACD +4,(SP); GET PAST THE BRANCH BACK
257	034332	000002	RTI
258	034334	012737 034270 000104	NEWCLK: MCV +2CLK2,+2104; TAKE DATA SOME MORE
259	034342	010037 176762	MCV R0,+2DA1; SET IN STEP
260	034346	000002	RTI
261			;THERE CAN BE ONLY ONE INTERRUPT ON
262			;THE STACK HERE, SINCE THE INTERRUPT
263			;ROUTINES CANNOT BE INTERRUPTED
264	034350	005037 172540	CLERR: CLR +2CSR; STOP^
265	034354	012702 000144	MCV +100.,R2; CTR.
266	034360	012700 000007	MCV +7,R0; BELL TO WARN OPERATOR
267	034364	004567 000530	JSR R5,CHOUT; RING^
268	034370	005302	DEC R2; DONE^
269	034372	003374	BGT .-6; IF NO, DO AGAIN
270	034374	012716 034170	MCV +FINISH,(SP); QUIT
271	034400	000002	RTI

```

272      ;TTY INTERRUPT ROUTINE
273 034402 013746 TTYINT: MCV  $\downarrow$  2KB, -(SP); GET THE BYTE
          177562
274 034406 042716      BIC  $\geq$  177200, (SP); CLEAR OFF EXTRA
          177200
275 034412 022627      CMP (SP)+,  $\geq$  20; CONTROL/PA
          000020
276 034416 001002      BNE TTY2; NO, GO BACK
277 034420 012716      MCV  $\geq$  FINISH, (SP); QUIT WHATEVER
          034170
278 034424 000002 TTY2: RTI
279      ;STORAGE
280 034426 VECA00: .WORD 4,6,60,62,104,106; THE VECTOR ADDRESSES
          000004
          000006
          000060
          000062
          000104
          000106
281 034442 VECCON: .WORD CLERR,300,TTYINT,240,CLK1,300; INTERRUPT DATA
          034350
          000300
          034402
          000240
          034236
          000300
282 034456 LDADD: CBR; CLCCK COUNT
          172542
283 034460 CSR; CLCCK RATE, MODE, STARTS CLCCK IF ODD
          172540
284 034462 DAQ; THE LARGE FCT.
          176760
285 034464 ACS; SENSITIVITY
          176770
286 034466 IWCBR; STORE FOR WAIT BETWEEN ITERATIONS
          037446
287 034470 IWCSP; " " " " "
          037444
288 034472 DRCSR; " " " " " DATA FTS.
          037442
289 034474 DRCSR; " " " " "
          037440
290      .EOT
291      ;
292

```

```

293      ;
294      ;ELECT
295      ;TO RAISE OR LOWER ELECTRODE
296      ;CALLED FROM BASIC THROUGH HEAD BY:  EXF (N,E)
297      ;WHERE N=1 FOR RAISE, 0 FOR LOWER
298      ;FOR OTHER N, NO ACTION
299      ;USES R0
300      ;REQUIRES GOIOUT BE DEFINED AS DR11 OUTPUT REG.
301      ;
302      034476 005700 ELECT: TST R0; 0 OR 1^
303      034500 001003      BNE EL0;  MAYBE A RAISE
304      034502 042737      BIC ≥1, ↓GOIOUT; LOWER IT
           000001
           167772
305      034510 005300 EL0:  DEC R0
306      034512 001003      BNE EL1;  NOT 0 OR 1
307      034514 052737      BIS ≥1, ↓GOIOUT; RAISE IT
           000001
           167772
308      034522 000137 EL1:  JMP ↓≥LEAVE; R1 WAS SET BY HEAD; R5,SP UNTOUCHED
           037462
309      ;EOT
310      ;
311      ;
312      ;
313      ;RETVAL
314      ;MOVES DATUM WHOSE ADDR. IS SPECIFIED TO BASIC
315      ;CALLED FROM BASIC THROUGH HEAD BY
316      ;      EXF(ADDRESS,R)
317      ;USES R0,R1,R6
318      ;RESTORES R1
319      ;R6 IS DECREASED BY 6
320      034526 010127 RETVAL:MCV R1, ≥0; SAVE PTR. HERE
           000000
321      034532 011001      MCV (R0),R1 ; INT(DATA) TO R1
322      034534 162706      SUB ≥6, SP;  LEAVE RCCM FOR RETURN VAL
           000006
323      034540 010600      MCV SP,R0;  SET R0 TO STACK
324      034542 104436      TRAP 36;  FLOAT(DATA) TO STACK
325      034544 016701      MOV RETVAL+2,R1;  RESET R1
           177760
326      034550 000167      JMP 52
           143276
327      ;EOT

```



```

328
329
330
331 ;TAPE 110-30-73)
332 ;READS AND PUNCHES PAPER TAPE TO AND FROM THE
333 ;DATA LOCATIONS (ADDR-1 AND DOWN)
334 ;CALLED FROM BASIC THROUGH HEAD BY
335 ;EXF(ADDR,T,X)
336 ;WHERE X=0 FOR READ OR NO. OF DATA TO PUNCH
337 ;USES BASIC TRAPS: 40,136
338 ;USES ALL REGISTERS
339 ;R1 ADVANCED TO CHAR. FAST RT. PAREN.
340 ;R5,R6 ARE RESTORED
341 ;SPECIAL DEFINITIONS
342 PPS=177554
343 PPB=PPS+2
344 TAPE:   MOV R0,-(SP); SAVE ADDR.
345         TRAP 136; GET
346         TRAP 40; NO. OF DATA WORDS
347         MOV (SP)+,R3; GET ADDR.
348         MOV R1,-(SP); SAVE REGS.
349         MOV R5,-(SP)
350         MOV R3,-(SP); ADDR. ON STACK LAST
351         TST R0; READ OR PUNCH^
352         BEQ TAPR; 0 TO READ
353         ASL R0; BYTES OF DATA TO PUN
354         MOV R0,-(SP); BYTES ON STACK
355         ACD >6,R0; PLUS BYTES IN HEADING
356         MOV R0,TAPHED+2; STORE FOR PUNCHING
357         CLR R3; FOR CKSUM
358         MOV >TAPHED,R2; START OF PUN LIST FOR HEADER
359         MOV >6,R0; NO TO PUN IN HEADER
360         JSR PC, TAPP0; PUNCH HEADER
361         MOV (SP)+,R0; BYTES OF DATA TO PUN
362         MOV (SP)+,R2; ADDR. AFTER DATA

```

363	034634	160002	SUB R0,R2; START OF DATA
364	034636	004767	JSR PC,TAPP0; PUNCH DATA
		000040	
365	034642	005403	NEG R3; PREP CKSUM
366	034644	010367	MOV R3,TAPHED+2; DATA TO FUN
		000060	
367	034650	012702	MCV ≥TAPHED+2,R2; PT TO IT
		034730	
368	034654	004767	JSR PC,TAPP0; PUN CKSUM
		000022	
369	034660	012704	MCV ≥20,R4; NEED 16 NULLS
		000020	
370	034664	105042	TAPTRL:CLRB -(R2); 0 IN TAPHED+3 AND PT TO DATA
371	034666	004767	JSR PC,TAPP0; PUN A NULL
		000010	
372	034672	005304	DEC R4; DONE^
373	034674	003373	BGT TAPTRL; IF NO, REPEAT
374	034676	000167	JMP TAPR5; ALL DONE
		000112	
375	034702	111205	TAPP0: MOVB (R2),R5; ACCUMULATE FOR SUM
376	034704	060503	ADD R5,R3
377	034706	105737	TSTB +≥PPS; READY^
		177554	
378	034712	100375	BPL .-4; IF NO, LOOP
379	034714	112237	MCVB (R2)+, +≥PPB; PUNCH
		177556	
380	034720	005300	DEC R0; DONE WITH LIST^
381	034722	003367	BGT TAPP0; NO, REPEAT
382	034724	000207	RTS PC; R0≤0
383	034726		TAPHED: .BYTE 1,0,0,0,0,0
		000001	
		000000	
		000000	
384			:
385			;THIS IS A TAKEOFF ON ABS LOADER
386	034734	012705	TAPR: MCV ≥TAPR0,R5; PT TO SUBROUTINE
		035024	
387			;LOOK FOR BEGINNING OF BLOCK
388	034740	005000	TAPR1: CLR R0; CKSUM
389	034742	004715	JSR PC,(R5); READ FRAME
390	034744	105303	DECE R3; IS IT A CNE^
391	034746	001374	ONE TAPR1; NO, LOOK MORE
392	034750	004715	JSR PC,(R5); READ THE NULL BYTE

```

393      ;INPUT BYTE CT. AND LOAD ADDRESS
394 034752 004767 JSR PC, TAPR2; GET BYTE CT WORD
          000126
395 034756 010402 MCV R4,R2; SAVE IT
396 034760 162702 SUB >4,R2; 4 BYTES ALREADY READ
          000004
397 034764 004767 JSR PC, TAPR2; GET LOAD ADDRESS
          000114
398 034770 011601 MCV (SP),R1; END ADDRESS, SAVE FOR READ-I ERROR
399 034772 160201 SUB R2,R1; MAKE THE START ADDR.
400 034774 004715 TAPR3: JSR PC,(R5); READ DATA BYTE
401 034776 002402 BLT TAPR4; IF OCNE, BR OUT
402 035000 110321 MOVE R3,(R1)+; STORE BYTE
403 035002 000774 BR TAPR3; GET ANOTHER
404 035004 005726 TAPR4: TST (SP)+; REMOVE THE SAVED ADDR
405 035006 105700 TSTB R0; CKSUM
406 035010 001401 BEQ TAPR5; OK
407 035012 000000 HALT; ERROR IN CKSUM, CONTINUE WILL RESTART
408 035014 012605 TAPR5: MCV (SP)+,R5; RESTORE REGS.
409 035016 012601 MCV (SP)+,R1
410 035020 000137 JMP >LEAVE; THIS SHOULD BE ALL
          037462
411 035024 013703 TAPR0: MOV >37776,R3; DEVICE ADDRESS
          037776
412 035030 005213 INC (R3); START READER
413 035032 005713 TST (R3); ERROR^
414 035034 100411 BMI TAPRER
415 035036 105713 TSTB (R3); DONE^
416 035040 100374 BPL .-6; NO
417 035042 116303 MOVE 2(R3),R3; GET BYTE
          000002
418 035046 060300 ADD R3,R0; CKSUM
419 035050 042703 BIC>177400,R3; MASK OFF JUNK
          177400
420 035054 005302 DEC R2; BYTE CT
421 035056 000207 RTS PC
422 035060 000000 TAPRER: HALT; PLACE TAPE AND PRESS CNT.
423 035062 021627 CMP (SP),>TAPR2; IS TAPR0 CALLED FROM TAPR2^
          035104
424 035066 001403 BEQ TAPR6; IF SC, TAKE 2 WORDS OFF STACK
425 035070 021627 CMP (SP),>TAPR2+4

```

```

426      035074 001001
427      035076 005726   TAPR6: BNE TAPR6+2; IF NOT, JUST ONE WORD CFF
428      035100 005726       TST (SP)+; ONE WORD OFF
429      035102 000714       TST (SP)+; AND ANOTHER
430      035104 004715   TAPR2: BR TAPR; THEN START OVER
431      035106 010304       JSR PC,(R5); GET ONE BYTE
432      035110 004715       MCV R3,R4; SAVE
433      035112 000303       JSR PC,(R5); GET ANOTHER
434      035114 050304       SWAB R3; PUT LAST IN HI BYTE
435      035116 000207       BIS R3,R4; MAKE A WORD
436      .EOT               RTS PC
437      .
438      .
439      .
440      TTKS=      177560
441      TTKB=      177562
442      TTPS=      177564
443      TTPB=      177566
444      .
445      .
446      .
447      .
448      .
449      .
450      .
451      .
452      .
453      .
454      .
455      .
456      .
457      .
458      .
459      035120 105767   CHOUT: TSTB      TTPS      ;CHECK FOR PUNCH READY
460      035124 100375       BFL      CHOUT      ;WAIT FOR READY
461      035126 110067       MCVB      R0,TTPB     ;MOVE IN BYTE
462      035132 000205       .ECT               RTS      R5      ;RETURN
463      .

```

```

464      ;
465      ;
466      ;
467      ENOPRG=.; LABEL THE END OF THE MAIN PROGRAM
468      ; THE EXIT ROUTINE
469      .=LEAVE
470      037462 005046' CLR -(SP); DUMMY VARIABLE
471      037464 005046 CLR -(SP); ON BASIC
472      037466 005046 CLR -(SP); STACK
473      037470 000137 JMP +252; TO BASIC
         000052
474      .END 52

```

Part 5

Subroutine Package for PLT and CCPVE<sup>1/</sup>

(written in PAL-11 assembly language)

---

<sup>1/</sup> Subroutines CHOUT and TPLOT in this package are from Tektronix Document #062-1402-00, copyright Tektronix, Inc. , Beaverton, Oregon, 1971. Used with permission.

```

1      ;DEFINE REGISTERS
2      R0=%0
3      R1=%1
4      R2=%2
5      R3=%3
6      R4=%4
7      R5=%5
8      SP=%6
9      R7=%7
10     R6=SP
11     PC=R7
12     R4CT=R4
13     R2VRS=R2
14     ;
15     ;DEFINE PERIPHERALS
16     ADS=176770
17     ADB=ADS+2
18     CSR=172540
19     CBR=CSR+2
20     CTR=CSR+4
21     DA0=176760
22     DA1=DA0+2
23     PS=177776
24     GDIOUT=177522
25     TKB=177562
26     ;
27     ;DEFINE STORAGE
28     LEAVE=37462; ADDRESS OF EXIT ROUTINE
29     NSAVE=24.
30     LSTPTR=LEAVE-2
31     CONDAT=LSTPTR-2
32     IWCBR=LSTPTR-10.
33     IWCSR=LSTPTR-12.
34     ORCBR=LSTPTR-14.
35     ORCSR=LSTPTR-16.
36     .=50;BASIC USES THIS ADDRESS TO FIND EXF
37     .WORD 33602

```

000050      033602

```

38      . = 33602
39      : HEAD
40      : SELECTS ROUTINE
41      : DETERMINES INTEGER VALUE OF FIRST PARAMETER
42      : MAKES R1 PT. TO NEXT PARAMETER
43      :
44      033602 012002 HEAD: MOV (R0)+,R2; GET 1ST VARIABLE INTO R2-R4
45      033604 012003      MOV (R0)+,R3
46      033606 012004      MOV (R0)+,R4
47      033610 104440      TRAP 40; INTEGER OF FIRST VARIABLE IN R0
48      033612 005201      INC R1; PT. TO NEXT VARIABLE
49      033614 012702      MOV >CODES,R2; THE ADDRESS FOR FUNCTION DESIGNATORS
50      033620 012703      MOV >FUNCT-2,R3; THE ADDRESS LIST FOR THE FUNCTIONS
51      033624 005723      033646
52      033626 121122 HEAD1: TST (R3)+; POINT TO NEXT ADDRESS
53      033630 001375      CMPB (R1),(R2)+; DO CODES MATCH
54      033632 122121      BNE HEAD1; IF NCT, TRY NEW CODE AND ADDRESS
55      033634 000173      CMPB (R1)+,(R1)+; PT. TO NEXT VARIABLE
56      000000      JMP ↓(R3); IF SC, START FUNCTION
57      033640      :
58      046107      : CODES: .ASCII /GLOPRTXY/
59      050117
60      052122
61      054530
62      033650      :
63      034734      : .EVEN
64      034430      : LABAX
65      035020      :
66      034262      : LINPLT
67      033660      :
68      033670      : TEKCON
69      033716      : PTPLT
70      034534      : RETVAL
71      034604      :
72      :
73      :
74      :
75      :
76      :
77      :
78      :
79      :
80      :
81      :
82      :
83      :
84      :
85      :
86      :
87      :
88      :
89      :
90      :
91      :
92      :
93      :
94      :
95      :
96      :
97      :
98      :
99      :

```



```

69      ;MOVES DATUM WHOSE ADDR. IS SPECIFIED TO BASIC
70      ;CALLED FROM BASIC THROUGH HEAD BY
71      ;      EXF(ADDRESS,R)
72      ;USES R0,R1,R6
73      ;RESTORES R1
74      ;R6 IS DECREASED BY 6
75      RETVAL;MOV R1,20; SAVE PTR. HERE
      033670 010127
      000000
76      033674 011001      MOV (R0),R1 ; INT(DATA) TO R1
77      033676 162706      SUB 26,SF; LEAVE ROOM FOR RETURN VAL
      000006
78      033702 010600      MOV SP,R0; SET R0 TO STACK
79      033704 104436      TRAP 36; FLOAT(DATA) TO STACK
80      033706 016701      MOV RETVAL+2,R1; RESET R1
      177760
81      033712 000167      JMP 52
      144134
82      .EOT
83      ;
84      ;TAPE )10-30-73)
85      ;READS AND PUNCHES PAPER TAPE TO AND FROM THE
86      ;DATA LOCATIONS (ADDR-1 AND DOWN)
87      ;CALLED FROM BASIC THROUGH HEAD BY
88      ;      EXF(ADDR,T,X)
89      ;WHERE X=0 FOR READ OR NO. OF DATA TO PUNCH
90      ;USES BASIC TRAPS: 40,136
91      ;USES ALL REGISTERS
92      ;R1 ADVANCED TO CHAR. PAST RT. PAREN.
93      ;R5,R6 ARE RESTORED
94      ;SPECIAL DEFINITIONS
95      PPS=177554
96      PPR=PPS+2
97      TAPE: MOV R0,-(SP); SAVE ADDR.
98      TRAP 136; GET
99      TRAP 40; NO. OF DATA WORDS
100     MOV (SP)+,R3; GET ADDR.
101     MOV R1,-(SP); SAVE REGS.
102     MOV R5,-(SP)
103     MOV R3,-(SP); ADDR. ON STACK LAST
104     TST R0; READ OR PUNCH^
105     BEQ TAPR; 0 TO READ
106     ASL R0; BYTES OF DATA TO PUN
107     MOV R0,-(SP); BYTES ON STACK
108     ADD 26,R0; PLUS BYTES IN HEADING
      010046
      104536
      104440
      012603
      010146
      010546
      010346
      005700
      001457
      006300
      010046
      062700
      000006

```

109	033750	010067 000116	MOV R0,TAPHED+2; STORE FOR PUNCHING
110	033754	005003	CLR R3; FOR CKSUM
111	033756	012702 034070	MOV ≥TAPHED,R2; START OF PUN LIST FOR HEADER
112	033762	012700 000006	MOV ≥6,R0; NO TO PUN IN HEADER
113	033766	004767 000052	JSR PC, TAPP0; PUNCH HEADER
114	033772	012600	MOV (SP)+,R0;BYTES OF DATA TO PUN
115	033774	012602	MOV (SP)+,R2; ACOR. AFTER DATA
116	033776	160002	SUB R0,R2; START OF DATA
117	034000	004767 000040	JSR PC,TAPP0; PLNCH DATA
118	034004	005403	NEG R3; PREP CKSUM
119	034006	010367 000060	MOV R3,TAPHED+2; DATA TO PUN
120	034012	012702 034072	MOV ≥TAPHED+2,R2; PT TO IT
121	034016	004767 000022	JSR PC,TAPP0; PUN CKSUM
122	034022	012704 000020	MOV ≥20,R4; NEED 16 NULLS
123	034026	105042	TAPTRL:CLRB -(R2); 0 IN TAPHED+3 AND PT TO DATA
124	034030	004767 000010	JSR PC,TAPP0; PUN A NULL
125	034034	005304	DEC R4; DCNE^
126	034036	003373	BGT TAPTRL; IF NC, REPEAT
127	034040	000167 000112	JMP TAPR5; ALL DCNE
128	034044	111205	TAPP0: MOV B (R2),R5; ACCUMULATE FOR SUM
129	034046	060503	ADD R5,R3
130	034050	105737 177554	TSTB +≥PPS; READY^
131	034054	100375	BPL .-4; IF NO, LOOP
132	034056	112237 177556	MOV B (R2)+, +≥PPB; PUNCH
133	034062	005300	DEC R0; DONE WITH LIST^
134	034064	003367	BGT TAPP0; NO, REPEAT

135	034066	000207	RTS PC; R0<=0
136	034070	000001	TAPHE0: .BYTE 1,0,0,0,0,0
		000000	
		000000	
137			:
138			;THIS IS A TAKEOFF ON ABS LOADER
139	034076	012705	TAPR1: MOV >TAPR0,R5; PT TO SUBROUTINE
		034166	
140			:LOOK FOR BEGINNING OF BLOCK
141	034102	005000	TAPR1: CLR R0; CKSUM
142	034104	004715	JSR PC,(R5); READ FRAME
143	034106	105303	DECB R3; IS IT A ONF^
144	034110	001374	BNE TAPR1; NO, LOOK MORE
145	034112	004715	JSR PC,(R5); READ THE NULL BYTE
146			;INPUT BYTE CT. AND LOAD ADDRESS
147	034114	004767	JSR PC, TAPR2; GET BYTE CT WORD
		000126	
148	034120	010402	MOV R4,R2; SAVE IT
149	034122	162702	SUB >4,R2; 4 BYTES ALREADY READ
		000004	
150	034126	004767	JSR PC, TAPR2; GET LOAD ADDRESS
		000114	
151	034132	011601	MOV (SP),R1; END ADDRESS, SAVE FOR REAC-I ERROR
152	034134	160201	SUB R2,R1; MAKE THE START ADDR.
153	034136	004715	TAPR3: JSR PC,(R5); READ DATA BYTE
154	034140	002402	BLT TAPR4; IF DCNE, BR OUT
155	034142	110321	MOVB R3,(R1)+; STORE BYTE
156	034144	000774	BR TAPR3; GET ANOTHER
157	034146	005726	TAPR4: TST (SP)+; REMOVE THE SAVED ADDR
158	034150	105700	TSTB R0; CKSUM
159	034152	001401	BEQ TAPR5; OK
160	034154	000000	HALT; ERROR IN CKSUM, CCNTINUE WILL RESTART
161	034156	012605	TAPR5: MOV (SP)+,R5; RESTORE REGS.
162	034160	012601	MOV (SP)+,R1
163	034162	000137	JMP >LEAVE; THIS SHOULD BE ALL
		037462	

164	034166	013703	TAPR0: MOV $\geq 37776, R3$ ; DEVICE ADDRESS
		037776	
165	034172	005213	INC (R3); START READER
166	034174	005713	TST (R3); ERROR^
167	034176	100411	BMI TAPRER
168	034200	105713	TSTB (R3); DONE^
169	034202	100374	RPL -6; NO
170	034204	116303	MOVB 2(R3), R3; GET BYTE
		000002	
171	034210	060300	ADD R3, R0; CKSUM
172	034212	042703	BIC $\geq 177400, R3$ ; MASK OFF JUNK
		177400	
173	034216	005302	DEC R2; BYTE CT
174	034220	000207	RTS PC
175	034222	000000	TAPRER: HALT; PLACE TAPE AND PRESS CONT.
176	034224	021627	CMP (SP), $\geq TAPR2$ ; IS TAPR0 CALLED FROM TAPR2^
		034246	
177	034230	001403	REQ TAPR6; IF SC, TAKE 2 WORDS OFF STACK
178	034232	021627	CMP (SP), $\geq TAPR2+4$
		034252	
179	034236	001001	BNE TAPR6+2; IF NOT, JUST ONE WORD OFF
180	034240	005726	TAPR6: TST (SP)+; ONE WORD OFF
181	034242	005726	TST (SP)+; AND ANOTHER
182	034244	000714	BR TAPR; THEN START OVER
183	034246	004715	TAPR2: JSR PC, (R5); GET ONE BYTE
184	034250	010304	MOV R3, R4; SAVE
185	034252	004715	JSR PC, (R5); GET ANOTHER
186	034254	000303	SWAB R3; PUT LAST IN HI BYTE
187	034256	050304	BIS R3, R4; MAKE A WORD
188	034260	000207	RTS PC
189			.EOT
190			:PTPLT
191			:DRAWS AN "X" AT PT (X,Y).
192			:CALLED THROUGH HEAD FROM BASIC BY EXF(X,P,Y).
193			:USES BASIC FUNCTIONS: EVAL, FIX.
194			:USES SUBROUTINES: DRAW.
195			:USES REGISTERS: R0-R6.
196			:AT END, R1 PTS. TO CHAR. PAST RT. PAREN.
197			:RESTORES R5, R6.
198	034262	062700	PTPLT: ADD $\geq 100., R0$ ; ALLOW FOR THE MARGIN
		000144	
199	034266	010046	MOV R0, -(SP); SAVE X
200	034270	104536	TRAP 136; EVAL(Y)
201	034272	104440	TRAP 40; INT(Y) IN R0
202	034274	062700	ADD $\geq 60., R0$ ; ALLOW FOR MARGIN
		000074	
203	034300	010046	MOV R0, -(SP); SAVE Y

204	034302	012700	MOV ≥COORD1,R0; PTR TO FIRST SET OF COORDINATES
		034370	
205	034306	012702	MOV ≥COORD2,R2; PTR TO 2ND SET OF COORDINATES
		034410	
206	034312	062726	ADD ≥4,(SP)+; INCREASE Y
		000004	
207	034316	062726	ADD ≥4,(SP)+; INCREASE X
		000004	
208	034322	014620	MOV -(SP),(R0)+; X1 COORD1
209	034324	014620	MOV -(SP),(R0)+; Y1 COORD1
210	034326	162726	SUB ≥8.,(SP)+; CHANGE Y, GO TO X
		000010	
211	034332	011622	MOV (SP),(R2)+; X1 COORD2
212	034334	014622	MOV -(SP),(R2)+; Y1 COORD2
213	034336	005726	TST (SP)+; GO TO X
214	034340	162716	SUB ≥8.,(SP); CHANGE X
		000010	
215	034344	011620	MOV (SP),(R0)+; X2 COORD1
216	034346	014620	MOV -(SP),(R0)+; Y2 COORD1
217	034350	062726	ADD ≥8.,(SP)+; CHANGE Y GO TO X
		000010	
218	034354	011622	MOV (SP),(R2)+; X2 COORD2
219	034356	014622	MOV -(SP),(R2)+; Y2 COORD2
220	034360	005726	TST (SP)+
221	034362	005726	TST (SP)+; SP BACK TO ORIG. VALUE
222	034364	004567	JSR R5,DRAW; DRAW FIRST LINE
		000612	
223	034370		COORD1:WORD 0,0,0,0,0,0; DATA AND STOPPERS
		000000	
		000000	
		000000	
		000000	
		000000	
		000000	
224	034404	004567	JSR R5,DRAW; DRAW 2ND LINE
		000572	
225	034410		COORD2:WORD 0,0,0,0,0,0; DATA AND STOPPERS
		000000	
		000000	
		000000	
		000000	
		000000	
		000000	
226	034424	000167	JMP LEAVE
		003032	

227			;LINPLT
228			;DRAW A STR. LINE BETWEEN TWO SPECIFIED PTS
229			; (X0,Y0) AND (X1,Y1).
230			;ADDS ON A MARGIN TO THE COORDINATES.
231			;CALLED FROM BASIC THROUGH HEAD BY:
232			; EXF(X0,L,Y0,X1,Y1)
233			;USES BASIC FUNCTIONS: EVAL, FIX.
234			;USES SUBROUTINES: DRAW
235			;USES REGISTERS: R0-R5.
236			;AT END R1 PTS. TO CHAR. PAST RT. PAREN.
237			;R5 RESTORED.
238	034430	062700	LINPLT:ADD ≥100.,R0; ALLOW FOR THE MARGIN
		000144	
239	034434	010067	MOV R0,X0
		000054	
240	034440	104536	TRAP 136; EVAL(Y0)
241	034442	104440	TRAP 40; INT(Y0)
242	034444	062700	ADD ≥60.,R0; MARGIN FOR Y
		000074	
243	034450	010067	MOV R0,Y0
		000042	
244	034454	005201	INC R1; PT. TO X1
245	034456	104536	TRAP 136; EVAL(X1)
246	034460	104440	TRAP 40; INT(X1)
247	034462	062700	ADD ≥100.,R0; ALLOW FOR THE MARGIN
		000144	
248	034466	010067	MOV R0,X1
		000026	
249	034472	005201	INC R1; PT. TO Y1
250	034474	104536	TRAP 136; EVAL(Y1)
251	034476	104440	TRAP 40; INT(Y1)
252	034500	062700	ADD ≥60.,R0; MARGIN FOR Y
		000074	
253	034504	010067	MOV R0,Y1
		000012	
254	034510	004567	JSR R5,DRAW; DRAW LINE FROM (X0,Y0) TO (X1,Y1)
		000466	
255	034514		X0: .WORD 0
		000000	

256	034516	000000	Y0: .WORD 0
257	034520	000000	X1: .WORD 0
258	034522	000000	Y1: .WORD 0
259	034524	000000	.WORD 0,0; STOPPERS
		000000	
260	034530	000167	JMP LEAVE
		002726	
261			.EOT
262			:XTIC
263			:FILLS IN DATA IN TIC FOR A TIC ON X AXIS
264			:CALLED THROUGH HEAD FROM BASIC BY EXF(S2,X,Y)
265			:WHERE S2=DISTANCE FROM ORIGIN FOR TIC
266			:Y= VALUE OF INDEX
267			:USES REGISTER R0
268			:
269			FTOA00=10716
270	034534	062700	XTIC: ADD ≥100.,R0; X MARGIN
		000144	
271	034540	010067	MOV R0,XTIC1; TIC X COORES
		000150	
272			
273	034544	010067	MOV R0,XTIC2
		000150	
274	034550	162700	SUB ≥28.,R0; SET LABEL BACK
		000034	
275	034554	010067	MOV R0,XTIC0; LABEL X COORD
		000070	
276	034560	012767	MOV ≥39.,YTIC0; LABEL Y COORD
		000047	
		000064	
277	034566	012767	MOV ≥60.,YTIC1; TIC Y COORDS
		000074	
		000122	
278	034574	012767	MOV ≥72.,YTIC2
		000110	
		000120	
279	034602	000420	BR TIC

```

280      ;
281      ;YTIC
282      ;FILLS DATA IN TIC FOR A TIC ON Y AXIS
283      ;CALLED LIKE XTIC BY EXF (S2,Y,Y)
284      ;USES R0 ONLY
285      ;
286      034604 062700 YTIC: ADD ≥60.,R0; Y MARGIN
                000074
287      034610 010067      MOV R0,YTIC0; LABEL Y CCORD
                000036
288      034614 010067      MOV R0,YTIC1; TIC Y COORDS
                000076
289      034620 010067      MOV R0,YTIC2
                000076
290      034624 005067      CLR XTIC0; LABEL X CCORD
                000020
291      034630 012767      MOV ≥100.,XTIC1; TIC X CCORDS
                000144
                000056
292      034636 012767      MOV ≥112.,XTIC2
                000160
                000054
293      ;TIC
294      ;POSITIONS,DEVELOPS ASCII, AND PRINTS AN INDEX
295      ;DRAWS TIC
296      ;R1 MUST PT. TO S0
297      ;USES BASIC FUNCTIONS: EVAL, FTCA00
298      ;USES SUBROUTINS: POSLAB, DRAW
299      ;USES REGISTERS: R1,R5,SP
300      ;AT END: R5,SP RESTORED, R1 PTS. TO CHAR. PAST RT. PAREN.
301      ;
302      034644 004567 TIC: JSR R5,DRAW; POSITION THE LABEL
                000332
303      034650      XTIC0: 0; BY DARK VECTCRING
                000000
304      034652      YTIC0: 0; THEN BACK TO ASCII MCDE
                000000
305      034654      0; STOP
                000000
306      034656      0; STOP
                000000
307      034660 104536      TRAP 136; EVAL S0
308      034662 010146      MOV R1,-(SP); SAVE PTR

```



309	034664	004737 010716	JSR PC,+2FT0A00; S2 IS ASCII-ED
310			;R6 PTS TO ASCII STRING, IS 20. LESS THAN BEFORE
311	034670	010601	MOV SP,R1; R1 PTS TO STRING
312	034672	005301	DEC R1; R1 PTS TO BEFORE STRING
313	034674	004567 000174	JSR R5,POSLAB; WRITE THE LABEL
314	034700		0; POSITIONING ALREADY DONE
		000000	
315	034702	062706 000024	ADD ≥20.,SP; PUT BACK AS BEFORE FTCA00
316	034706	012601	MOV (SP)+,R1; RESTORE PTR
317	034710	004567 000266	JSR R5,DRAW; DRAW TIC
318	034714		XTIC1: 0
		000000	
319	034716		YTIC1: 0
		000000	
320	034720		XTIC2: 0
		000000	
321	034722		YTIC2: 0
		000000	
322	034724		0
		000000	
323	034726		0: STOP
		000000	
324	034730	000167 002526	JMP LEAVE; BACK TO BASIC
325			.EOT
326			:LABAX
327			:DRAWS X AND Y AXES AND LABELS EACH
328			:CALLED THROUGH HEAD FROM BASIC BY
329			: EXF(0,3,LABEL FOR Y, LABEL FOR X)
330			:USES SUBROUTINES: POSLAB,DRAW.
331			:USES REGISTERS: R1,R5.
332			:AT END, R1 PTS. TO CHAR. PAST RT. PAREN.
333			:RESTORES R5.

```

334 034734 005301 LABAX: DEC R1; GO BACK TO COMMA BEFORE LABEL
335 034736 004567 JSR R5,POSLAB; POSITION AND WRITE Y LABEL
      000132
336 034742      .WORD 30,1; ERASE, SOH,
      000030
      C00001
337 034746      .BYTE 40,9.; 9 SPACES
      004440
338 034750      .WORD 0; LABEL
      000000
339 034752 004567 JSR R5,DRAW; MAKE AXES
      000224
340 034756      .WORD 100.,740.,100.,60.,1023.,60.,0,0
      000144
      001344
      000144
      000074
      001777
      000074
      000000
      000000
341      ;COORDINATES OF X, Y AXES AND STOPPERS
342 034776 004567 JSR R5,POSLAB; POSITION AND WRITE X LABEL
      000072
343 035002      .BYTE 1,0,12,38.,40,18.,0,0;SCH,38LF,18SF,LABEL
      000001
      023012
      011040
      000000
344 035012 005201 INC R1; SET TO ONE PAST RT PAREN
345 035014 000167 JMP LEAVE
      002442
346      .EOT
347      .
348      .
349      .
350      ;TEKCON
351      ;FOR SENDING SPECIAL CHARACTERS TO TEK TERMINAL
352      ;CALLED FROM BASIC BY: EXF(N,0)
353      ;WHERE IF N = 0 SENDS AN SOH AND 39 LINE FEEDS
354      ;      N < 0 SENDS ERASE, SOH
355      ;      N > 0 SENDS N
356      ;USES POSLAB, R0, R1, R5
357      ;RESTORES R5
358      ;AT END, R1 PTS TO CHAR PAST RT PAREN
359 035020 124141 TEKCON:CMPB -(R1),-(R1); PT TO BEFORE "-"
360 035022 005700 TST R0

```

```

361 035024 001405      BEQ OFFPAG; 0 MEANS OFFPAG
362 035026 100412      BMI ERASE; NEG IS ERASE, SOH
363 035030 004567      JSR R5, CHOUT; OTHERWISE JUST OUTPUT ASCII R0
                        000226
364 035034 005201      INC R1;PT TO "
365 035036 000413      BR TEKC1; DONE
366 035040 004567      OFFPAG:JSR R5,PCSLAB; OUTPUT
                        000030
367 035044      .BYTE 1,0,12,39.,0,0; SOH, 39 LF, NO LABEL
                        000001
                        023412
                        000000
368 035052 000405      BR TEKC1; DONE
369 035054 004567      ERASE: JSR R5, POSLAB; OUTPUT
                        000014
370 035060      .WORD 30,1,0; ERASE, SOH, STOP
                        000030
                        000001
                        000000
371 035066 005201      TEKC1: INC R1; PT TO AFTER "
372 035070 000167      JMP LEAVE
                        002366
373      .EOT
374      :PSLAB
375      :OUTPUTS A STRING OF ASCII INDICATED AS
376      :CALLING STATEMENT OPERANDS, THEN WRITES
377      :A LABEL INDICATED AS A BASIC EXF OPERAND.
378      :R1 MUST PT. TO CHAR. BEFORE LABEL
379      :LABEL MUST BE TERMINATED WITH COMMA
380      :OR RT. PAREN.
381      :THE CALLING SEQUENCE IS:
382      :      JSR R5,PSLAB
383      :      .BYTE (TYPE OF CHAR.), (NO. OF CHAR.)
384      :      .BYTE (
385      :
386      :
387      :
388      :      .BYTE 0,0; STOPPERS
389      :USES SUBROUTINES: CHOUT.
390      :USES REGISTERS: R0-R5
391      :AT END, R1 PTS. TO CHAR. AFTER LABEL.
392      :RESTORES R5.

```

393	035074	005715	POSLAB: TST (R5); IF WORD ZERO
394	035076	001422	BEQ CODE3; GO TO LABELLING
395	035100	112500	MOVB (R5)+, R0; CODE IN R0
396	035102	112502	MOVB (R5)+, R2; NO. OF TIMES IN R2
397	035104	004567	CODE2: JSR R5, CHOUT; OUTPUT CHAR
		000152	
398	035110	020027	CMP R0, ≥30; IF ERASE
		000030	
399	035114	001010	BNE CODE1; NOT, NEXT CHAR
400	035116	012703	MOV ≥3, R3; NO OF TIMES TC LOAD R4
		000003	
401	035122	012704	CODE0: MOV ≥077777, R4; CT. DOWN MORE THAN 65000 TIMES
		077777	
402	035126	005304	DEC R4; ONE CT
403	035130	100376	BPL .-2; CT AGAIN
404	035132	005303	DEC R3; DONE CTING^
405	035134	003372	BGT CODE0; NO, RELOAD CTR.
406	035136	005302	CODE1: DEC R2; MORE OF SAME CHAR^
407	035140	003361	BGT CODE2; YES, OUTPUT CHAR IN R0 AGAIN
408	035142	000754	BR POSLAB; NO, NEXT CHAR
409			; LABELLING
410	035144	005201	CODE3: INC R1; PT TO LABEL
411	035146	121127	CMPB (R1), ≥54; IF COMMA
		000054	
412	035152	001411	BEQ CODE4; GO TC END
413	035154	121127	CMPB (R1), ≥51; IF RT PAREN
		000051	
414	035160	001406	BEQ CODE4; GO TC END
415	035162	105711	TSTB (R1); IF NULL
416	035164	001404	BEQ CODE4; GO TC END
417	035166	111100	MOVB (R1), R0; CHAR IN R0
418	035170	004567	JSR R5, CHOUT; OUTPUT CHAR
		000066	
419	035174	000763	BR CODE3; NEXT CHAR
420	035176	005725	CODE4: TST (R5)+; PT TC NEXT INSTRUCTION
421	035200	000205	RTS R5
422			.EOT
423			; DRAW
424			; CAUSE BRIGHT VECTOR BETWEEN CCORD. INDICATED
425			; AS CALLING STATEMENT OPERANDS.
426			; CALLING SEQUENCE:
427			; JSR R5, DRAW

428			:		.WORD (X COORD),(Y COORD)
429			:		.WORD (        ),(        )
430			:		
431			:		
432			:		
433			:		.WORD 0,0 ;STOPPERS
434			:		;USES SUBROUTINES: TPLOT, CHOUT
435			:		;USES REGISTERS: R0,R5.
436			:		;RESTORES R5.
437	035202	005000		DRAW:	CLR R0; SET TPLCT INDICATOR FOR VECTOR INITIATE MODE
438	035204	005715		DRAW0:	TST (R5); IF ZERC
439	035206	001005			BNE DRAW1; MIGHT BE END
440	035210	012567			MOV (R5)+,X;LOAD TPLOT OPERAND
		000022			
441	035214	005715			TST (R5);IF ZERC
442	035216	001413			BEQ DRAW5; IS END OF LIST
443	035220	000402			BR DRAW2; NOT END
444	035222	012567		DRAW1:	MOV (R5)+,X; LOAD TPLOT OPERAND
		000010			
445	035226	012567		DRAW2:	MOV (R5)+,Y; LOAD TPLOT CPERAND
		000006			
446	035232	004567			JSR R5,TPLOT; VECTOR TO X,Y
		000040			
447	035236			X:	.WORD 0
		000000			
448	035240			Y:	.WORD 0
		000000			
449	035242	005200			INC R0; BE SURE IN BRIGHT VECTOR MCDE
450	035244	000757			BR DRAW0; GET NEXT COORDS
451	035246	005725		DRAW5:	TST (R5)+;PT TO NEXT INSTRUCTION
452	035250	012700			MOV >37,R0; US--ASCII MCDE
		000037			
453	035254	004567			JSR R5,CHOUT
		000002			
454	035260	000205			RTS R5
455				:	
456				:	

```

457      ;REGISTER DEFINITIONS
458      ;
459      R0=      %0
460      R1=      %1
461      R2=      %2
462      R3=      %3
463      R4=      %4
464      R5=      %5
465      STACK=   %6
466      TTKS=    177560
467      TTKB=    177562
468      TTPS=    177564
469      TTPB=    177566
470      ;
471      ;
472      ;
473      ;
474      ;
475      ;
476      ;
477      ;
478      ;
479      ;
480      ;
481      ;
482      ;
483      ;
484      ;
485      035262 105767 CHOUT:  TSTB      TTPS      ;CHECK FOR PUNCH READY
486      035266 100375      BPL      CHOUT      ;WAIT FOR READY
487      035270 110067      MOVB     R0,TTPB     ;MOVE IN BYTE
488      035274 000205      RTS      R5          ;RETURN
489      ;
490      ;
491      ;
492      ;
493      ;
494      ;
495      ;
496      ;
497      ;
498      ;
499      ;
500      ;
501      ;

```

CHOUT

THIS ROUTINE IS CALLED TO OUTPUT  
AN ASCII CHARACTER TO THE 4002A  
GRAPHIC COMPUTER TERMINAL

TO CALL PUT THE CHARACTER IN REG 0  
AND EXECUTE A

JSR R5,CHOUT

QILL RETURN WITH REG 0 UNCHANGED

TPLOT

THIS ROUTINE IS CALLED TO PLOT  
IN VECTOR, POINT, OR INCREMENTAL  
PLOT MODE DEPENDING ON THE  
VALUE OF REG 0 AS DESCRIBED BELOW.

IF  
A = 0 INITIALIZE AND DARK VECTOR TO X,Y  
A > 0 BRIGHT VECTOR TO X,Y

502						
503					A = -1	POINT PLOT TO X,Y
504						
505					A < -1	INCREMENTAL PLOT X = DIRECTION
506						Y = NUMBER OF POINTS
507						
508					CALLING SEQUENCE	
509					REG 0 = A	
510					JSR R5, TPLOT	
511					VALUE OF X	
512					VALUE OF Y	
513					RETURN POINT	
514						
515						
516	035276	005700	TPLOT:	TST	R0	;CHECK REG R0
517	035300	001476		BEQ	TPTCV	;JUMP IF INIT. AND DARK
518	035302	100002		BPL	TPTNRM	;JUMP IF NORMAL VECTOR
519	035304	004567	TPTXY:	JSR	R5, CHOUT	;SET MODE
		177752				
520						
521	035310	012500	TPTNRM:	MOV	(R5)+, R0	;MOVE X COORD TO REG 0
522	035312	100001		BPL	TPT10	;JUMP IF SEQ 0
523	035314	005000		CLR	R0	;IF NEG SET TC 0
524	035316	020027	TPT10:	CMP	R0, ≥1024.	;CHECK FOR ON SCREEN
		002000				
525	035322	100402		BMI	TPT12	;JUMP IF IN RANGE
526	035324	012700		MOV	≥1023., R0	;SET TO EDGE IF TOO HIGH
		001777				
527	035330	010067	TPT12:	MOV	R0, TPTX	;SAVE X VALUE
		000152				
528						
529	035334	012500		MOV	(R5)+, R0	;GET Y COORD
530	035336	100001		BPL	TPT14	;JUMP IF SEQ 0
531	035340	005000		CLR	R0	;CLEAR REG 0
532	035342	020027	TPT14:	CMP	R0, ≥762.	;CHECK FOR TOO LARGE Y
		001372				
533	035346	100402		BMI	TPT16	;JUMP IF IN RANGE
534	035350	012700		MOV	≥761., R0	;MOVE TO EDGE OF SCREEN
		001371				

535	035354	010067	TPT16:	MOV	R0,TPTY	;SAVE Y VALUE
		000130				
536	035360	006100		ROL	R0	;MOVE UPPER 5 BITS
537	035362	006100		ROL	R0	;TC UPPER BYTE
538	035364	006100		ROL	R0	
539	035366	000300		SWAB	R0	;SWAP UPPER AND LOWER B'
540	035370	042700		BIC	≥177740,R0	;MASK OFF EXTRA
		177740				
541	035374	052700		BIS	≥000040,R0	;SET IN HI Y TAG
		000040				
542	035400	004567		JSR	R5,CHOUT	;OUTPUT HI Y
		177656				
543	035404	016700		MOV	TPTY,R0	;GET Y CCCRD
		000100				
544	035410	042700		BIC	≥177740,R0	;MASK TO LOW 5 BITS
		177740				
545	035414	052700		BIS	≥000140,R0	;AND SET LOW Y TAG
		000140				
546	035420	004567		JSR	R5,CHOUT	;SHIP OUT LOW Y BYTE
		177636				
547						
548	035424	016700		MOV	TPTX,R0	;GET X CCCRD
		000056				
549	035430	006100		ROL	R0	;AND ADJUST LIKE Y
550	035432	006100		ROL	R0	
551	035434	006100		ROL	R0	
552	035436	000300		SWAB	R0	;SWITCH BYTES
553	035440	042700		BIC	≥177740,R0	;MASK OFF EXTRA
		177740				
554	035444	052700		BIS	≥000040,R0	;SET HI X TAG
		000040				
555	035450	004567		JSR	R5,CHOUT	;OUTPUT HI X BYTE
		177606				
556	035454	016700		MOV	TPTX,R0	;GET X CCCRD
		000026				
557	035460	042700		BIC	≥177740,R0	;LEAVE ONLY LOW BITS
		177740				
558	035464	052700		BIS	≥000100,R0	;SET IN LOW X BITS
		000100				
559	035470	004567		JSR	R5,CHOUT	;OUTPUT LOW X BYTE
		177566				
560	035474	000205		RTS	R5	;RETURN
561						
562	035476	012700	TPTDV:	MOV	≥035,R0	;OUTPUT A GS TO INITIAL:
		000035				



```

563 035502 000167          JMP          TPTXY
      177576
564      :
565      :
566      :
567 035506      TPTX:  .WORD 0
      000000
568 035510      TPTY:  .WORD 0
      000000
569 035512      TPTCTR: .WORD 0
      000000
570      .EOT
571      ENDPRG=.; LABEL THE END OF THE MAIN PROGRAM
572      ; THE EXIT ROUTINE
573      .=LEAVE
574 037462 005046      CLR -(SP); DUMMY VARIABLE
575 037464 005046      CLR -(SP); ON BASIC
576 037466 005046      CLR -(SP); STACK
577 037470 000137      JMP ↓≥52; TO BASIC
      000052
578      .END 52

```

## APPENDIX 4

### Program CHARGE

(written in FORTRAN for use on the CYBER 73

computer at the Oregon State University

Computer Center)

PROGRAM CHARGE

73/74 OPT=1

FTN 4.4+REL.

```

1      PROGRAM CHARGE (EC,QOUT,INPUT,OUTPUT,TAPE3=EC,TAPE4=QOUT,
      1TAPE60=INPUT, TAPE61=OUTPUT)
      DIMENSION ECELL(100),CDL(100),CAVG(100),DELQ(100),DQ1DQ(100),
      1Q1(100),Q(100),C2S(100)

5      C
      C INPUT FILE CONTAINS FOLLOWING CARDS:
      C      1: NUMBER OF (E-CELL,C-DL) PAIRS
      C      ROUGHNESS FACTOR
      C      XKM1 FOR CATION AND XKM1 FOR ANION (UF/CM**2)
10     C      XK12 FOR CATION AND XK12 FOR ANION (UF/CM**2)
      C      TOTAL ELECTROLYTE CONCENTRATION (MOL/L)
      C      D. L. CHARGE AT INITIAL POTENTIAL (UC/CM**2)
      C      SPECIFICALLY ADSORBED CHARGE AT INIT. POT.
      C      IPRINT (=1 FOR INTERMEDIATE PRINTING, ELSE 0)
15     C      MAXITR, MAX. NO. ITERATIONS ALLOWED
      C      (ALL IN FREE FORM)
      C 2 THR/ NPTS+1: (E-CELL (VOLTS), C-DL (UF/CM**2)) DATA PAIR
      C      IN 2F6.3
      C      (E-CELL STARTS AT CAP. MIN. AND GOES POSITIVE)
20     C
      C READ INPUT FILE
      C
      READ (3,*) NPTS, R,XKMC,XKMA,XK1C,XK1A,CONC,QINIT,
      1Q1INIT,IPRINT,MAXITR
25     READ (3,100) (ECELL(I),CDL(I), I=1,NPTS)
      100 FORMAT (2F6.3)

      C
      C WRITE OUT HEADING.
      C

```

```

30      WRITE (4,400) R,CONC,XKMC,XK1C,XKMA,XK1A
400  FORMAT (#1ROUGHNESS=      #,1PG10.3/# CONCENTRATION= #,
      11PG10.3//13X,#KM1#,7X,#K12#/# CATION = #,2(1PG10.3)
      2/# ANION      #,2(1PG10.3)/)
C
35  C  CALCULATE CAVG, DELQ, AND Q.  INITIALIZE Q1LAST.
C
      CK=137.8*CONC
      C2S(1)=19.46*SQRT(CK+(QINIT-Q1INIT)**2)
      Q(1)=QINIT
40  Q1(1)=Q1INIT
      CAVG(1)=DELQ(1)=DQ1DQ(1)=Q1LAST=0.
      XKMCIN=1./XKMC
      XKMAIN=1./XKMA
      XK1CIN=1./XK1C
45  XK1AIN=1./XK1A
      DO 2 I=2,NPTS
      CAVG(I)=0.5*(CDL(I-1)+CDL(I))/R
      Q1(I)=0.
      DELQ(I)=CAVG(I)*(ECCELL(I-1)-ECCELL(I))
50  Q(I)=Q(I-1)+DELQ(I)
      2 CONTINUE
      DO 4 J=1,MAXITR
C
C  CALCULATE ESTIMATES FOR C2S, DQ1DQ, AND Q1.
55  C  SELECT XKMC AND XK1C FOR Q1 .GT. 0., ELSE USE XKMA AND XK1A.
C
      DO 3 I=2,NPTS

```

```

      Q2S=0.5*(Q(I)+Q(I-1)-Q1(I)-Q1(I-1))
      C2S(I)=19.46*SQRT(CK+Q2S**2)
50      IF (Q1(I).GT.0.) GO TO 6
      DQ1DQ(I)=1.-(1./CAVG(I)-XKMAIN)/(1./C2S(I)+XK1AIN)
      GO TO 7
5      DQ1DQ(I)=1.-(1./CAVG(I)-XKMCIN)/(1./C2S(I)+XK1CIN)
7      Q1(I)=Q1(I-1)+DQ1DQ(I)*DELQ(I)
65      3 CONTINUE
      IF (IPRINT.NE.0) WRITE (4,200) (ECOLL(I),COL(I),CAVG(I),DELQ(I),
1C2S(I),Q(I),DQ1DQ(I),Q1(I), I=1,NPTS)
200  FORMAT (#1E-COLL      C-DL      C-AVG      DEL Q      DIFFUSE CAP#,4X,1HQ,
70      16X,#DQ1/DQ      Q1#/(1X,F5.3,2F9.2,F8.2,1PG13.4,0PF8.2,F10.4,
      2F8.2))
      IF (ABS((Q1(NPTS)-Q1LAST)/Q1(NPTS)).LT.0.001) GO TO 5
      Q1LAST=Q1(NPTS)
+ CONTINUE
      J=MAXITR
75      5 IF (IPRINT.NE.0) STOP
      WRITE (4,200) (ECOLL(I),COL(I),CAVG(I),
1DELQ(I),C2S(I),Q(I),DQ1DQ(I),Q1(I), I=1,NPTS)
      WRITE (4,300) J
300  FORMAT (#0AFTER#,I3,# ITERATIONS#)
80      STOP
      END

```

## APPENDIX 5

### Program Z2

(written in FORTRAN for use on the CYBER 73

computer at the Oregon State University

Computer Center)

PROGRAM Z2

73/74 OPT=1

FTN 4.4+REL.

```
1      PROGRAM Z2 (PDATA,CDATA,INPUT,OUTPUT,ZOUT,TAPE61=OUTPUT,
      1TAPE60=INPUT,TAPE2=PDATA,TAPE3=CDATA,TAPE4=ZOUT)
      C
      C      TO CALCULATE CELL CURRENT (CURRS) AND CELL IMPEDANCE (ZS) IN
5      C      THE FREQUENCY DOMAIN. CORRECTION IN THE CELL CURRENT IS MADE
      C      FOR THE SLOW RESPONSE OF THE I-V CONVERTER
      C
      C      EQUIP, 2=FILE CONTAINING DATA FOR I-V CONVERTER
      C      LUN 2 HAS:
10     C      (1)  HEADER CARD IN FREE FORM CONTAINING:
      C
      C           NTP, THE NUMBER OF OUTPUT DATA POINTS
      C           RMEAS, THE VALUE OF RU USED TO TEST THE CONVERTER
      C      (2)  NTP DATA CARDS IN E6.6,2(E4.4) CONTAINING TIME, OUTPUT
15     C      VOLTS, AND INPUT VOLTS. INPUT VOLTS MAY BE MISSING FOR
      C      THE LAST CARDS.
      C
      C      EQUIP, 3=FILE CONTAINING DATA FOR TEST CELL.
      C      LUN 3 HAS:
20     C      (1)  HEADER CARD IN FREE FORM, CONTAINING:
      C           NT, THE NUMBER OF DATA POINTS
      C           SHI, THE HIGHEST FREQUENCY TO CONSIDER
      C           SLO, THE LOWEST
      C           RF, THE EFFECTIVE FEEDBACK RESISTOR OF THE CONVERTER
25     C      (2)  NT DATA CARDS OF THE SAME TYPE AS IN LUN 2.
      C
      C      EQUIP, 4=OUTPUT FILE
      C
```

```

30      DIMENSION TP(150),CURP(150),VINP(150),VOUTP(150),CURPS(50),
      1VOUTPS(50),OS(50),T(150),VCELL(150),VOUTC(150),SIGMA(50),
      2VCELLS(50),VOUTCS(50),CURCS(50),ZCS(50)
      EQUIVALENCE (CURP,VINP)
C
C  READ IN POTENTIOSTAT DATA
35  C
      REWIND 2
      READ (2,*) NTP,RMEAS
      READ (2,100) (TP(I),VOUTP(I),VINP(I), I=1,NTP)
      100 FORMAT (3(6PF6.0))
40  C
C  FIND LAST VINP
C
      DO 2 I=1,NTP
      NCURP=NTP-I+1
45  IF (VINP(NCURP).NE.0.) GO TO 3
      2 CONTINUE
C
C  CHANGE VINP TO CURP
C
50  3 DO 4 I=1,NCURP
      CURP(I)=VINP(I)/RMEAS
      4 CONTINUE
C
C  CALCULATE APPARENT RF FROM THIS DATA
55  C
      RFAPP=VOUTP(NTP)/CURP(NCURP)
C

```



```

C   READ IN TEST CELL DATA
C
60   REWIND 3
      READ (3,*) NT, SHI, SLO, RF
      READ (3,100) (T(I),VOUTC(I), VCELL(I), I=1,NT)
C
C   COMPUTE SIGMA VALUES
65   C
      5 WRITE (61,200)
200  FORMAT (* INPUT NUMBER OF S PER DECADE*)
      READ *, PD
      NS=PD*ALOG10(SHI/SLO)+1.00001
70   IF (NS.LE.50) GO TO 6
      WRITE (61,300)
300  FORMAT (* TOO MANY S*)
      GO TO 5
      6 ESINT=10.**(-1./PD)
75   DO 7 I=1,NS
      SIGMA(I)=SHI*ESINT**(I-1)
      7 CONTINUE
C
C   ESTABLISH LAST VCELL VALUE
80   C
      DO 8 I=1,NT
      NVCELL=NT-I+1
      IF (VCELL(NVCELL).NE.0.) GO TO 9
      8 CONTINUE
85   C
C   CALCULATE TRANSFORMS
C
      9 CALL RLPLAC(CURP,TP,NCURP,CURPS,SIGMA,NS)
      CALL RLPLAC(VOUTP,TP,NTP,VOUTPS,SIGMA,NS)
90   CALL RLPLAC(VCELL,T,NVCELL,VCELLS,SIGMA,NS)
      CALL RLPLAC(VOUTC,T,NT,VOUTCS,SIGMA,NS)

```

```

C
C      FIND DS, CURCS, ZCS
C
95      DO 10 I=1,NS
          DS(I)=CURPS(I)*RFAPP/VOUTPS(I)
          CURCS(I)=VOUTCS(I)/RF*DS(I)
          ZCS(I)=VCELLS(I)/CURCS(I)
10      CONTINUE
100     C
C      WRITE OUT RESULTS
C
          WRITE (4,400) (T(I),VCELL(I),VOUTC(I), I=1,NT)
400     FORMAT (#1TIME DOMAIN: #/#0      TIME#,7X,#V-CELL#,6X,#VOUT# /
105      1(3(2X,E10.3)))
          WRITE (4,500) (SIGMA(I),VCELLS(I),VOUTCS(I),DS(I),CURCS(I),
1ZCS(I), I=1,NS)
500     FORMAT (#1FREQUENCY DOMAIN: #/#0  FREQUENCY#,4X,#V-CELL#,7X,
1#V-OUT#,7X,#D(S) #,7X,#CURRENT    IMPEDANCE#/(6(2X,E10.3)))
110     STOP
          END

```

SUBROUTINE RLPLAC

73/74

OPT=1

FTN 4.4+REL.

```
1      C
      C
      C
5      SUBROUTINE RLPLAC(FOFT,T,NT,FOFS,SIGMA,NS)
      C
      C    TO CALCULATE LAPLACE TRANSFORM OF F(T) FOR NS VALUES OF SIGMA,
      C    THE REAL COMPONENT OF THE LAPLACE OPERATOR S.
      C
      C    DIMENSION FOFT(NT), T(NT), FOFS(NS), SIGMA(NS)
10     DO 3 J=1,NS
      C
      C    INITIALIZE AND MAKE THE FIRST TERM OF FOFS(J)
      C
      C    IC=0
15     S=SIGMA(J)
      ST1=S*T(1)
      PRODIM1=EXP(-ST1)
      FUNC=FOFT(1)/ST1/S*(1.-(1.+ST1)*PRODIM1)
      PRODIM1=FOFT(1)*PRODIM1
20     C
      C    DO THE INTEGRAL SUMMATION FROM T=0 TO T=T(NT)
      C
      C    DO 2 I=2,NT
      ST1=S*T(I)
25     C    IF ST1 IS OUT OF RANGE, THE TERM IS NEGLIGIBLE.
      IF (ST1.GT.675.) GO TO 13
      PROD1=FOFT(I)*EXP(-ST1)
      TERM=(PROD1-PRODIM1)*(T(I)-T(I-1))/ALOG(PROD1/PRODIM1)
```

```

C
30 C   IF TERM IS INSIGNIFICANT FOR 3 ITERATIONS, QUIT
C
      IF (TERM.LT.0.0001*FUNC) GO TO 10
      IC=0
      GO TO 11
35 10 IC=IC+1
      IF (IC.GE.3) GO TO 12
11 FUNC=FUNC+TERM
C
C   SET UP FOR NEXT ITERATION
40 C
      PRODIM1=PRODI
      2 CONTINUE
C
C   ADD ON FINAL TERM
45 C
12 TERM=S*T(NT)
      IF (TERM.LT.675.) FUNC=FUNC+FOFT(NT)*EXP(-TERM)/S
13 FOFS(J)=FUNC
      3 CONTINUE
50 RETURN
      END

```

## APPENDIX 6

### Program COMPN

(written in FORTRAN for use on the CYBER 73  
computer at the Oregon State University  
Computer Center)

PROGRAM COMPN

73/74 OPT=1

FTN 4.4+REL.

```
1      PROGRAM COMPN (RXNS,COUT, OUTPUT,TAPE3=RXNS,TAPE4=COUT,  
      1TAPE61=OUTPUT, DEBUG=COUT)  
      C  
      C TO CALCULATE EQUILIBRIUM COMPOSITION OF A SOLUTION IN WHICH A  
5      C NUMBER OF HOMOGENEOUS REACTIONS ARE OCCURRING.  
      C  
      C      DIMENSION CONC(10),ID(2,10),NZ(10),D(10),F(10),XK(10),N(10,10),  
      1ACT(10)  
      C      COMMON CONC,NZ,D,F,XK,N,NI,NJ,SPECZ2,STRENG,ID  
10     C  
      C INPUT NUMBER OF SPECIES, NUMBER OF EQUATIONS, SUM OF (C*Z**2) FOR  
      C SPECTATOR IONS, NDUM, AND MAX. NO. OF ITERATIONS IN FREE FORM.  
      C (NDUM OTHER THAN ZERO CAUSES INTERMEDIATE RESULTS TO BE PRINTED.)  
      C INPUT CHARGE, ID, AND DESIGNATION EFE IF DESIRED TO FIX  
15     C CONCENTRATION, OR EAE TO FIX ACTIVITY, FOR EACH SPECIES IN I2,A19,A  
      C THE CONCENTRATIONS OF SPECIES WITH FIXED ACTIVITIES ARE NOT  
      C USED TO CALCULATE IONIC STRENGTH. IF SUCH SPECIES ARE IONIC  
      C AND IN SOLUTION, THEY SHOULD BE INCLUDED IN SPECZ2.  
      C INPUT DISTANCE OF CLOSEST APPROACH (ANGSTROMS) FOR EACH SPECIES  
20     C IN FREE FORM.  
      C INPUT ESTIMATES OF CONCS FOR EACH SPECIES IN FREE FORM.  
      C INPUT MATRIX OF EQUATION COEFFICIENTS IN FREE FORM, ONE EQUATION  
      C PER LINE.  
      C INPUT THERMODYNAMIC EQUILIBRIUM CONSTANT FOR EACH REACTION.
```

25

C

```

      READ (3,*) NI,NJ,SPECZ2,NOUM,NMAX

```

```

      READ (3,100) (NZ(I),(ID(K,I), K=1,2), I=1,NI)

```

```

100  FORMAT (I2,2A10)

```

```

      READ (3,*)(D(I), I=1,NI), (CONC(I), I=1,NI), ((N(I,J), I=1,NI),

```

30

```

      1J=1,NJ), (XK(J), J=1,NJ)

```

```

      WRITE (4,200) NI, ((ID(K,I), K=1,2), NZ(I),D(I),CONC(I), I=1,NI),

```

```

      1SPECZ2, NJ, (XK(J), NI, (N(I,J), I=1,NI), J=1,NJ)

```

```

200  FORMAT (1H1,9X,2HID,10X,2H NZ,4X,1HD,6X,4HCONC/=(/1X,2A10,I3,0PF6.

```

35

```

      1,1X,1PG11.4)/#0SUM OF C*Z**2 FOR SPECTATOR IONS =#,1PG11.4/1H0,

```

```

      220(2H *)/1H0,5X,1HK,7X,#### N(I,J) #,77(1H*)/=(/1X,1PG11.4,2X,=

```

```

      3I3))

```

```

      CALL EQUILIB (NOUM,NMAX), RETURNS (20)

```

```

      DO 2 I=1,NI

```

```

      ACT(I)=CONC(I)*F(I)

```

40

```

      2 CONTINUE

```

```

      WRITE (4,300) NI, ((ID(K,I), K=1,2), F(I), CONC(I),ACT(I),

```

```

      1I=1,NI), STRENG

```

```

300  FORMAT (1H0,20(2H *)/1H0,9X,2HID,16X,1HF,10X,4HCONC,10X,3HACT

```

```

      1/=(/1X,

```

45

```

      12A10,3(2X,1PG11.4))/#0 IONIC STRENGTH =#,1PG11.4)

```

```

      20 STOP

```

```

      END

```

SUBROUTINE EQUILIB 73/74 OPT=1

FTN 4.4+REL.

```
1      C
      C
      C
      SUBROUTINE EQUILIB (NDUM,NMAX), RETURNS (QUIT)
5      C
      C TO CALCULATE EQUILIBRIUM COMPOSITION OF A SOLUTION IN WHICH
      C SEVERAL HOMOGENEOUS REACTIONS ARE OCCURRING.
      C
      C ALL PARAMETERS EXCEPT NDUM ARE PASSED THROUGH COMMON.
10     C NDUM OTHER THAN ZERO CAUSES INTERMEDIATE RESULTS TO BE PRINTED.
      C
      C DIMENSION CONC(10), NZ(10),NZ2(10),D(10),F(10),DELC(10),
      C 1NORD(2,10),XK(10),N(10,10),ID(2,10)
      C COMMON CONC,NZ,D,F,XK,N, NI,NJ,SPECZ2,STRENG,ID
15     C
      C CALCULATE NZ**2; PUT ZEROES IN NORD
      C
      C DO 2 I=1,NI
      C NZ2(I)=NZ(I)*NZ(I)
20     2 CONTINUE
      C DO 3 J=1,NJ
      C NORD(2,J)=0
      C 3 CONTINUE
      C
```



```

25      C   CALCULATE IONIC STRENGTH AND F(I).
      C
          DO 19 NTIMES=1,NMAX
          STRENG=SPECZ2
          DO 4 I=1,NI
30      IF ((773.AND.ID(2,I)).EQ.1RA) GO TO 4
          STRENG=STRENG+CONC(I)*NZ2(I)
          4 CONTINUE
          STRENG=0.5*STRENG
          STR12=SQRT(STRENG)
35      DO 5 I=1,NI
          F(I)=1.
          IF ((778.AND.ID(2,I)).EQ.1RA) GO TO 5
          F(I)=10.**(-0.51*NZ2(I)*STR12/(1.+0.33*0(I)*STR12))
          5 CONTINUE
40      IF (NDUM.NE.0) WRITE (4,100) STRENG, (F(I), I=1,NI)
100    FORMAT (1H0,20(2H *)/1H0,1PG11.4,2(/5(3X,G11.4)))
      C
      C   FIND AN EQUATION WITH JUST ONE UNKNOWN CONC.
      C
45      DO 13 K=1,NJ
          IS=0
          KLAST=K-1
          DO 6 I = 1,NI
          NVC=778.AND.ID(2,I)
50      IF (NVC.EQ.1RF.OR.NVC.EQ.1RA) GO TO 6
          IF (KLAST.EQ.0) GO TO 7
          DO 8 L=1,KLAST
          IF (NORD(1,L).EQ.I) GO TO 6
          8 CONTINUE
75      IF (IS.EQ.0) GO TO 9
          IF (CONC(I).GE.CS) GO TO 6
55      9 CS=CONC(I)

```

```

        IS=I
60      6 CONTINUE
        DO 33 LOOP=1,NI
        DO 30 J=1,NJ
        IF (N(IS,J) .EQ.0) GO TO 30
        IF (KLAST.EQ.0) GO TO 37
        DO 31 L=1,KLAST
65      IF (J.EQ.NORD(2,L)) GO TO 30
31      CONTINUE
37      DO 32 I=1,NI
        IF (I.NE.IS.AND.N(I,J).NE.0.AND.CONC(I).LE.0.) GO TO 30
32      CONTINUE
        GO TO 34
70      30 CONTINUE
        IF (IS.EQ.NI) GO TO 35
        IT=IS+1
        DO 36 I=IT,NI
75      IF (CONC(I).NE.CONC(IS)) GO TO 36
        IS=I
        GO TO 33
36      CONTINUE
33      CONTINUE
80      35 WRITE (61,600) NTIMES,K,IS,J,I,LOOP,(CONC(I),I=1,NI)
600     FORMAT (#0**** ALL EQUATIONS HAVE AT LEAST 2 CONCS .LE. 0#
        1/1X,6I3,2(/5(2X,1PG11.4)))
        RETURN
34      NORD(1,K)=IS
85      NORD(2,K)=J

```

```

C
C   CALCULATE CCNC(IS) FROM XK(J) AND THE OTHER APPROXIMATE CONC(I)
C
      PRODCF=1.
90      DO 15 I=1,NI
          IF (I.EQ.IS.OR.CONC(I).EQ.0..OR.N(I,J).EQ.0) GO TO 15
          PRODCF=PRODCF*(CONC(I)*F(I))**N(I,J)
15      CONTINUE
          CS=(XK(J)/PRODCF)**(1./N(IS,J))/F(IS)
95      DELC(IS)=CS-CONC(IS)
          CONC(IS)=CS

C
C   CALCULATE THE NEW OTHER CONCS BASED ON THE CHANGE IN CONC(IS)
C
100      DO 12 I=1,NI
          NVC=77B.AND.ID(2,I)
          IF (I.EQ.IS.OR.NVC.EQ.1RF.OR.NVC.EQ.1RA) GO TO 12
          DELC(I)=N(I,J)*DELC(IS)/N(IS,J)
          CONC(I)=CCNC(I)+DELC(I)
105      12 CONTINUE
          IF (NDUM.NE.0) WRITE (4,300) K,IS,J,PRODCF,NI, (DELC(I),
1CONC(I), I=1,NI)
300      FORMAT (1H0,3I3,1X,1PG11.4,=(/2(1X,G11.4)))
13      CONTINUE
110      DO 14 I=1,NI
          IF (ABS(DELC(I)/CONC(I)).GT..001) GO TO 19
14      CONTINUE
          RETURN
19      CONTINUE
115      WRITE (61,400) NMAX
400      FORMAT (1X0**** TERMINATED AFTER#,I3,# ITERATIONS#)
          RETURN
          END

```